Max-Planck-Institut für Meteorologie
Max Planck Institute for Meteorology

MAX-PLANCK-GESELLSCHAFT

The Influence of Vegetation on the Cycling of Persistent Organic Pollutants (POPs) Assessed by a Multi Compartment Box Model

Marin Alan Tomašić

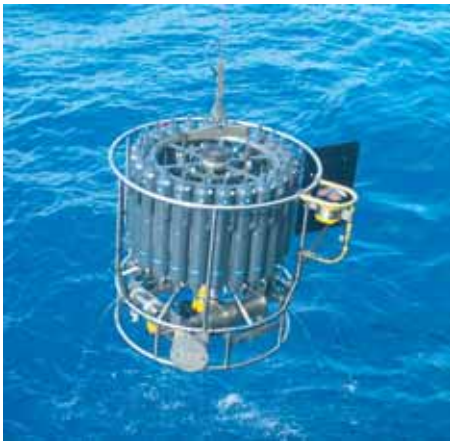

Berichte zur Erdsystemforschung 66/2009

Reports on Earth System Science

Hinweis

Die Berichte zur Erdsystemforschung werden vom Max-Planck-Institut für Meteorologie in Hamburg in unregelmäßiger Abfolge herausgegeben.

Sie enthalten wissenschaftliche und technische Beiträge, inklusive Dissertationen.

Die Beiträge geben nicht notwendigerweise die Auffassung des Instituts wieder.

Die "Berichte zur Erdsystemforschung" führen die vorherigen Reihen "Reports" und "Examensarbeiten" weiter.

Notice

The Reports on Earth System Science are published by the Max Planck Institute for Meteorology in Hamburg. They appear in irregular intervals.

They contain scientific and technical contributions, including Ph. D. theses.

The Reports do not necessarily reflect the opinion of the Institute.

The "Reports on Earth System Science" continue the former "Reports" and "Examensarbeiten" of the Max Planck Institute.

Anschrift / Address

Max-Planck-Institut für Meteorologie
Bundesstrasse 53
20146 Hamburg
Deutschland

Tel.: +49-(0)40-4 11 73-0
Fax: +49-(0)40-4 11 73-298
Web: www.mpimet.mpg.de

Layout:

Bettina Diallo, PR & Grafik

Titelfotos:
vorne:
Christian Klepp - Jochem Marotzke - Christian Klepp
hinten:
Clotilde Dubois - Christian Klepp - Katsumasa Tanaka

Berichte zur Erdsystemforschung 66 2009

The Influence of Vegetation on the Cycling of Persistent Organic Pollutants (POPs) Assessed by a Multi Compartment Box Model

Dissertation zur Erlangung des Doktorgrades der Naturwissenschaften
im Departement Geowissenschaften der Universität Hamburg
vorgelegt von

Marin Alan Tomašić

Baden (CH)

Hamburg 2009

Reports on Earth System Science 66 2009

ISSN 1614-1199

Marin Alan Tomašić
Max-Planck-Institut für Meteorologie
Bundesstrasse 53
20146 Hamburg
Germany

Als Dissertation angenommen
vom Department Geowissenschaften der Universität Hamburg

auf Grund der Gutachten von
Prof. Dr. Hartmut Graßl
und
Dr. Sebastian Rast

Hamburg, den 3. Februar 2009
Prof. Dr. Jürgen Oßenbrügge
Leiter des Departments für Geowissenschaften

ISSN 1614-1199

The Influence of Vegetation on the Cycling of Persistent Organic Pollutants (POPs) Assessed by a Multi Compartment Box Model

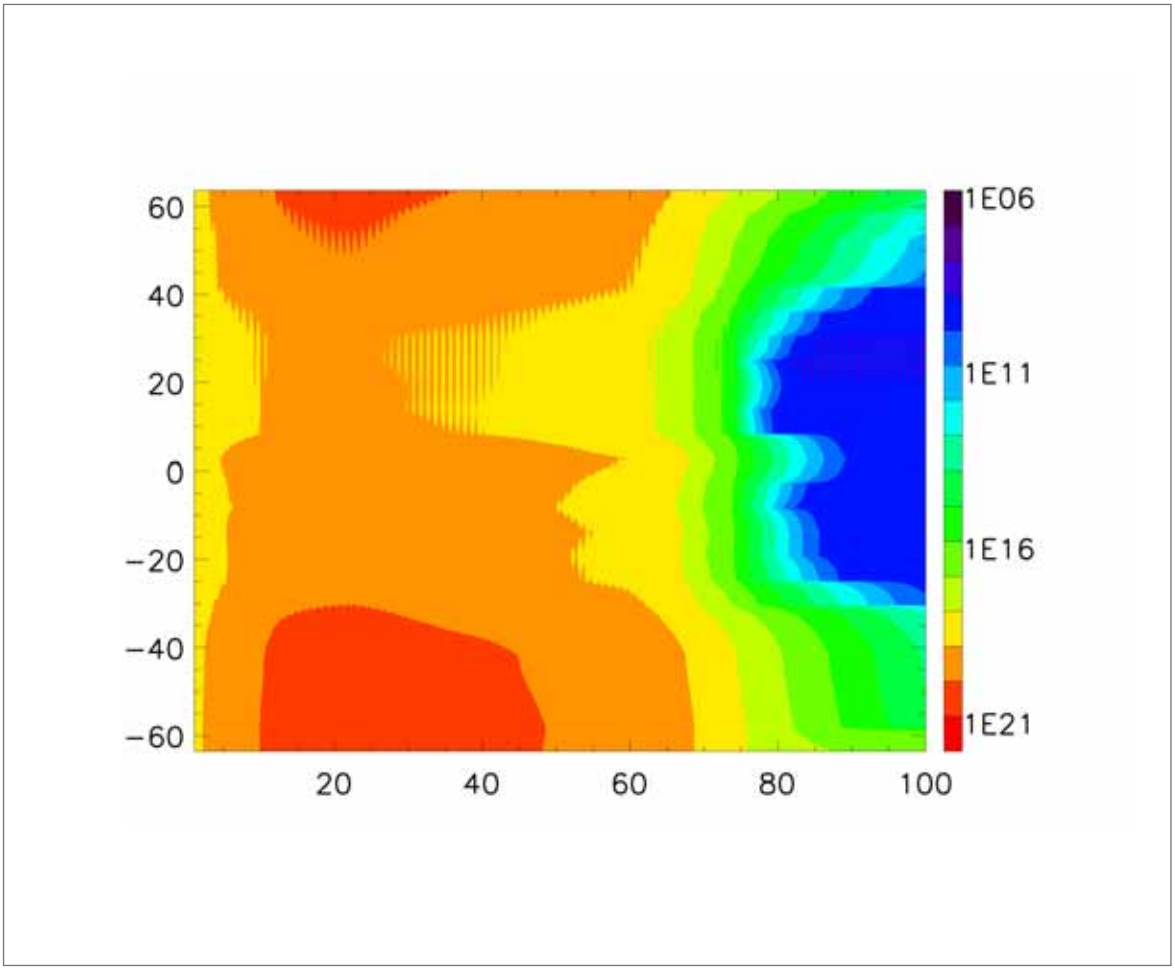

Marin Alan Tomašić

Hamburg 2009

Abstract

Because of its potential impact on human health, awareness of chemical pollution has been rising in the last decade. Especially the group of bioaccumulative organic xenobiotics is under suspicion to cause serious health problems. These substances usually have a long life cycle and the ability to biomagnify throughout the food chains. Due to their chemical properties, they are characterized by semivolatility, have a long-range transport potential (LRTP) and are also capable to distribute among different compartments in nature. Transport mechanisms of these substances include ocean currents, rivers and especially the atmosphere. In particular the colder higher latitudes are affected by pollution although the initial point of release is located typically thousands of kilometers away in temperate climate zones. Many of those compounds are released either from the industry or as agrochemicals.

Among important mechanisms of atmospheric transport, vegetation plays a key role on the overall cycling and distribution in nature. The large canopy surface on the continent has an accumulation effect for chemicals in the atmosphere and is a preferred place for deposition. Many factors influence the overall deposition process at the canopy. Persistent organic pollutants (POPs) can settle either in the gas phase, attached to particles or by gas exchange reaction of leaves. To investigate different processes for the overall fate of these compounds, a multi media box model was developed and tested against increasing levels of vegetation complexity. This study concentrates on two different POP-chemicals (PCB-52 and DDT).

Significant differences of overall contamination and compartment distribution are detected depending on the deposition process considered. Gas deposition of DDT and PCB-52 shows a strong dependence on the calculation method leading to a variation of chemical allocation and thus causing different contamination levels. Particle deposition causes further reduction of overall burden of DDT, but not for PCB-52. Large uncertainties of air-vegetation partitioning are found in quantifying the gas diffusion reactions. Both chemicals show a very similar behaviour for the tested partitioning factors although their compound properties are very different.

Defoliation and the introduction of an additional vegetation soil causes reduction of the overall burden compared to a big leaf approach. It is obvious that the litter fall cycle leads to a faster reduction of POPs because a higher revolatilization with the atmosphere reduces significantly the overall contamination level. The accumulation effect of the canopy and the revolatilization from its soil induces an additional atmospheric cleaning. An overall POP filter effect of the vegetation depends to a large extend on the vegetation phenology. Simulations with a more detailed canopy wind profile indicate that big leaf canopies most likely underestimate the real overall contamination levels of DDT and PCB-52. A higher wind speed in the canopy top of a big leaf approach also means more turbulence, less deposition on the canopy and thus more atmospheric OH-radicals removal.

Vegetation types are an essential factor in the overall fate of both chemicals. Differences between the vegetation types can have a significant impact on the overall

distribution, as well as on the overall burden. Experiments with different canopy setups also reveal that the canopy characteristics and different climatic conditions have significant impact on the overall cycling of POPs.

Contents

Chapter 1

Introduction

1.1 Raising the awareness for chemical pollution

During the last decades, many products, which have been introduced on the global market by the chemical industry, were released prior analysis of the consequences for the environment. Many of those substances are still in commercial use today. Concerns about chemical exposure of humans were for a long time either not understood or simply ignored. Reservations against the usage of problematic compounds increased in the 1960's, primarily by individual and later scientific observation. Chemical pollution activated growing public interest. Among the first consequences observed were egg shell thinning and reduced bird life expectancy in the Polar region. Concentrations found in the tissues of birds and mammals in this pristine area generally demonstrated a high exposition to chemicals, although often no climate specific contamination source was found. The environmental damage came to the attention of Rachel Carson (*Carson* (1962)), a popular writer, scientist, and ecologist. Carson, who wrote about this problem in her book 'Silent Spring' was attacked by people in the chemical industry and the government as an alarmist. POPs came more and more under the scientific spotlight in the 1970's and 1980's. The increasing damage reported from the Arctic circle led to the general affirmation of a transboundary chemical pollution caused by the industry. Chemicals can have very complex effects on health. For many compounds, a screening of the potential damage to human health caused by chemical pollution is still not accomplished to a satisfactory level. Depending on their compound properties, chemicals can have very different overall behaviour. Dispersion, transport mechanisms and the grade of potential harm are still not investigated properly for many chemical categories. Among toxic chemicals of concern, persistent organic pollutants (POPs) were identified as a group of very hazardous substances are linked to severe damage to humans and animals. They are held responsible for the disruption of endocrine, reproductive, and immune systems; neurobehavioral disorders; and cancers possibly including breast cancer. They are often halogenated organic compounds, which, to a varying degree, resist photolytic, biological and chemical degradation (*Ritter et al.* (1995)). Although the usage of some POPs is restricted or banned since years, they continue to be detected in

considerable concentrations in the environment, even far from their point of initial release (*Wania* (1999)). A lot of damage caused to the environment by POPs is legacies from decades ago. Even breakdown products often persist for years or decades and still harm the environment. POPs have been associated and linked to problems of human health, sometimes even at very low concentrations.

1.2 Health impact of POPs

Effects of POPs on humans however can be difficult to be proven conclusively. Humans can be exposed to POPs through diet (aquatic and terrestrial food chains), accidents, inhalation or even indoor exposure by products containing POPs (*Ritter et al.* (1995)). No matter whether the exposure is acute or chronic, the effects on health can be irreversible. Acute exposure to POPs can cause even death. However, most of the harm is due to chronic pollution at lower levels. Such a contamination may not be lethal, but chronic weakening of the immune system can be a consequence. The potential impairment by POPs has to be taken seriously (*WHO* (2005a)). The most significant observations made in correlation with POPs are their potential to cause serious body dysfunctions. POPs are suspiciously linked to an increase of cancer and tumors, neurobehavioral impairment including learning disorders, immune system dysfunction, blood, liver and kidney disorders and reproductive disorders. Even the risk of diabetes can increase by even more than a factor of ten (*Ritter et al.* (1995)) because of POPs. POPs cause also a great threat to babies, because these chemicals can be transmitted to other humans via breast feeding (*AMAP* (2004), *AMAP* (1997)).
Arctic and marine wildlife is exposed to POPs to a very high level. In polar regions high lipid levels are pivotal for animal adaptation, energy storage, isolation and reproduction in the cold climate (*AMAP* (1998), *AMAP* (1997)). The effects described on whales or polar bears include immune dysfunction, handicapped reproduction, subtle neurobehavioral effects or immune suppression (*Stow* (2005)). Observations in seabirds showed symptoms like for the fish predators and additionally egg shell thinning, impairment of mating behavior (*Fry and Toone* (1981)); malformation and complete failure of reproduction followed by a population decline (*Faber and J.J.* (1970)) were additionally documented (*AMAP* (1997)). Lipophilic substances like POPs, are resistant to the metabolism and are selectively accumulated in the food chain (*AMAP* (2002)). Most POPs are soluble in fat and have the ability to get stored in the fatty tissues of animal species.

1.2.1 Bioaccumulation and Biomagnification of POPs

Bioaccumulation and biomagnification are the two main mechanisms of POPs that threaten humans and wildlife. Biomagnification describes the transfer of a chemical substance in the food chain from one trophic level to another. Bioaccumulation is the increase in the concentration of a pollutant in an organism compared to its direct environment or food (*Mörner et al.* (2002)).
Studies in both temperate and Arctic ecosystems have shown that the accumu-

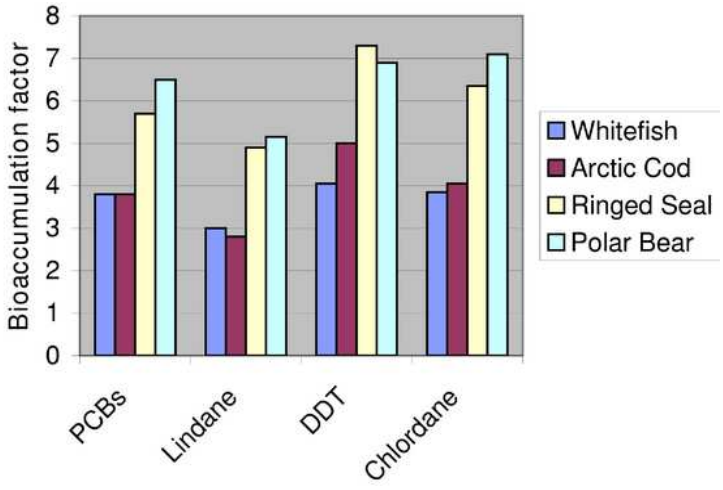

Figure 1.1: Bioaccumulation occurs when the absorption of a persistent (toxic) substance occurs in biological tissues. Predators at the end of the food chain (seal, ice bear) are more vulnerable due to biomagnification and the usually fatty nutrition. Data compiled from *Schindler et al.* (1995)

lation depends on the length of the food chain. Particularly in the marine environment, the transfer of lipids is evident and the complexity of lipid-based food chains additionally contributes to high levels of POPs (*AMAP* (1998)). Fish can occupy several trophic levels. Due to the different accumulation potential in the food pyramid, they are susceptible to biomagnification of POPs (*Stow* (2005)). In the case of trout, Rasmussen (*Rasmussen et al.* (1990)) found that PCBs increase by a factor of 3.5 per trophic level. Marine predators like shark, tuna (*Ueno et al.* (2003)) or swordfish bear much more risk of bioaccumulation. But also mammals like orcas, ice bears and seals show as well very high levels of POP concentration. All of them are at a higher rank in the trophic pyramid and are long-lived. The transfer of POPs to higher trophic levels of the marine food chain occurs over many years. This induces automatically a higher concentration (see also the bioaccumulation levels in figure 1.1).
As a consequence, even low environmental concentration of POPs can cause high POP levels in animals at the end of the food chain. Due to the shorter terrestrial food chains the problem of bioaccumulation is less dramatic compared to the marine counterpart (*Stow* (2005)). The main concern in the terrestrial environment is that contaminants of vegetation are carried through the food chain, as the plants become food for grazing mammals, live stock and birds. Many of the POPs are applied directly on vegetation canopies as pesticides, rodenticide or against fungal decay. Contamination of the vegetation can be considered as one of the main threads to human and animal health. Therefore research on the role of vegetation for the dispersion of POPs is crucial for understanding the global proliferation.

1.3 Production and usage of POPs

Sources of POPs can be anthropogenic as well as natural (*Ritter et al.* (1995)). Anthropogenic release of POPs includes intended industrial or farming application as well as by-products of combustion. Pollution happens in all the compartments of the environment (air, water, soil, vegetation). The agricultural usage of POPs is basically found worldwide in all areas with intensive agriculture. Chlorinated agrochemicals such as DDT, Toxaphene, $\alpha-$HCH, $\gamma-$HCH, Chlordane, Aldrin, Mirex and Dieldrin belong to this category (*AMAP* (2002)). Today, some of these agrochemicals have been substituted by other less toxic chemicals or they are restricted in usage (e.g. DDT for malaria vector control).
Main production sites of industrial POPs are in developed countries of the northern hemisphere, including the countries of the former Eastern block. The usage of POPs in the industry is manifold. Capacitors, hydraulic installation, softeners for lacks are only a limited selection of usage area where POPs can be found.
POPs or POP like substances are often produced as unintended by-products. This kind of natural synthesis can take place in forest fires as well as through industrial combustion. PCDD's[1], PCDF's[2], HCB's[3] and PAH's[4] are examples for such unintentional by-products (*Selin and Eckley* (2003)). Today, modern methods allow us to filter POPs from industrial combustion effectively. These technologies may be standard in rich countries; however, developing nations either do not have the financial resources or do not have the legal enforcement yet. Protection from chemical pollution is often sacrificed in the favor of faster industrial development with all its negative global consequences.

1.4 Political agenda and safety of POPs

Environmental health is today part of the official political agenda of international organizations. POPs started to get restricted and regulated at national level since the early 1970's. In western countries risk assessments of substances like DDT and PCBs revealed environmental effects which are so severe that it was necessary to restrict their production and usage. Many of the discoveries including the health implication on the local population were related to the Arctic region (*Selin and Eckley* (2003)). Preventive actions led to a general belief in many industrialized countries that the problem of hazardous chemicals was under control. In the 1980's new scientific findings revealed the transboundary nature of POPs. It was clear that regulating the usage of hazardous chemicals like POPs had to be raised above the national level.
Based on this new awareness several political initiatives were launched. Canada was one of the first countries seeking international support for a better control of

[1] polychlorinated dibenzo-p-dioxins
[2] polychlorinated dibenzofurans
[3] Hexachlorobenzenes
[4] polyaromatic hydrocarbons

POPs. Pressure for a better safety control of POPs came also from non government organizations (NGO's) such as the Pesticide Action Network (PAN) or the International Pesticide Elimination Network (IPEN). International organizations such as the OECD[5], FAO[6], UNEP[7] or the WHO[8] did not yet deal with POPs on their agenda until the late seventies (*Selin and Eckley* (2003)). UNEP established in 1987 (together with FAO) the London Guidelines for the Exchange of Information on Chemicals in International Trade.
Canada joined forces with the other circumpolar countries and after preparatory meetings the Arctic Environment Protection Strategy (AEPS) was established in June 1991. The strategies of AEPS include the Arctic Monitoring and Assessment Programme (AMAP) to monitor the pollution levels and assess the effects of anthropogenic pollutants (such as POPs, heavy metals etc.) in all compartments.
The Governing Council of UNEP started at the Washington Conference in 1995 together with other organizations (IPCS[9], ILO[10], IFCS[11] and WHO) to work on a priority list for the scientific inventory of POPs. The aim was to collect more scientific information and criteria (e.g. bioaccumulation potential, toxicity etc.) and screen substances about their transport potential, sources, risk assessments and (if necessary) define the special economic needs to eliminate the POP usage. An additional goal was to adopt a global program for the protection of the marine environment from land-based pollution such as POPs. The conference recognized the fact of long-range transport of POPs via atmosphere and ocean currents resulting in high concentrations far away from the initial point of release.
In 1997 UNEP started together with IPCS, IFCS and IOMC [12] with negotiations resulting in a priority list of problematic chemicals. The final aim was a legally binding instrument for international action, initially beginning with twelve substances 'for immediate action', the so-called 'dirty dozen'[13] of POPs. The short list included eight organo-chlorine pesticides: aldrin, chlordane, DDT, dieldrin, endrin, heptachlor, mirex and toxaphene; two industrial chemicals hexachlorobenzene (HCB) and the polychlorinated biphenyl (PCB) group; and two industrial by-products: dioxins and furans. In the same year UNECE [14] negotiated a climate specific convention for countries surrounding the Arctic Circle, which was ratified by 2002.
In 2001 the UNEP Stockholm Convention was signed (*UNEP* (2003b)) which is in force since May 2004. Until today, it is the most important achievement concerning the regulation, production, import, use and/or ban of POPs. So far the regulation encompasses only the 12 chemicals targeted, because the choice was taken in a broader consensus for key countries. Most of the substances were

[5]Organization for Economic Co-operation and Development
[6]Food and Agricultural Organization
[7]United Nations Environment Program
[8]World Health Organization
[9]International Programme on Chemical Safety
[10]International Labour Organization
[11]Intergovernmental Forum on Chemical Safety
[12]Inter-Organization Programme for the Sound Management of Chemicals
[13]source: http://ipen.ecn.cz/handbook/html/index.html
[14]United Nations Economic Commission for Europe

already restricted or banned in these countries, hence agreeing on this list was relatively easy (*Selin and Eckley* (2003)). New chemicals that fulfill the criteria for being a POP can be included in the list after a submitted proposal and evaluation process through the POPs Secretariat and the POPs Review Committee (*Weber* (2001)). The treaty opens the possibility of a strictly regulated use of some POPs for disease and vector control. For example: DDT is a highly efficient pesticide to fight the malaria vector. The transmitting female anopheles mosquito transmits protozoan parasites to millions of people every year all over the world.
According to the recommendations of WHO, DDT can be sprayed inside a house to prevent the spreading of the disease. Every country that uses DDT for vector control is obliged to report this to the WHO and the POPs Secretariat.
Although the awareness has grown, developing countries are still using especially older POPs. These chemicals may already be prohibited in industrialized countries, but are still exported to developing nations. The Stockholm convention includes measures against obsolete stockpiles of POPs that still exist in some third and second world countries. The reason is that a significant part of these may find their way on the illegal market (*Mörner et al.* (2002)).

Other conventions regulating hazardous chemicals Export of chemical waste to poorer countries is another topic related to this problem. The first convention developed under the auspices of UNEP concerning hazardous chemicals was the Basel Convention in 1989. It was adopted in response to concerns about toxic waste from industrialized countries being dumped in developing countries[15]. It also implies that dangerous waste has to be disposed as close to the production site as possible (*Weber* (2001)). The Rotterdam Convention (PIC Convention) in 1998 was another added regulation to focus the trade with specific hazardous chemicals. Chemicals that are part of this convention are not to be exported to another country without its explicit, previous informed consent (PIC) (*Weber* (2001)).
World health and environment protection organizations insist that the only way to solve the problem of POPs can be via the rise of public information and awareness. Reduction and/or elimination of POP pesticides, as mandated by the Stockholm Convention, provide an opportunity to re-think strategies used in pest and vector control (*Mörner et al.* (2002)).
During the last 10 years the international environmental safety agenda is focusing increasingly on the determination of preventing long-term damages of chemicals. Many potentially problematic compounds are still not screened on their health impact. The need for a more detailed risk assessment of chemical pollution is an evolving necessity for further regulations. The complexity of processes, and the number physical-biological compartments involved in the overall transport, are the two main issues for estimating the dispersion, exposure and degree of damage caused by POPs. Scientific understanding of the overall behaviour is essential for the prediction of contamination pathways of these chemicals.

[15]http://www.POPs.int/documents/background/hcwc.pdf

1.5 The problem of tracking POPs

POPs are distributed ubiquitously around the world and they persist in every climate zone. Geographical distribution of contamination includes areas without industrialization or sources of contamination. They have been found even in deserts (*Ritter et al.* (1995)), remote polar regions (*Halsall et al.* (1998), *AMAP* (1998), *Cotham and F.* (1991), *Lohmann et al.* (2001)) and global high mountain ranges (*Blais et al.* (1998), *Villa et al.* (2003), *Vilanova et al.* (2001)). Due to the larger landmass and industrialization level, the northern hemisphere is basically a more intensively polluted environment. Investigations confirmed the presence of POPs in air (*Lohmann et al.* (2001), *Ockenden et al.* (1998), *Agrell et al.* (1999), *Meijer et al.* (2003b)), lake sediments (*Muir et al.* (1996)), soils (*Meijer et al.* (2002), *Meijer et al.* (2003a)), tree bark (*Simonich and Hites* (1995)) and in all water media (*OSPAR* (2000), *Theobald et al.* (1996), *Sapozhnikova et al.* (2004), *Nhan et al.* (1998), *Hollert et al.* (2002), *Gustafsson et al.* (2001)). Coastal areas are more contaminated than the open sea due to riverine and estuarine inflow (*Basheer et al.* (2003)).

The wide geographical and compartmental distribution of POPs discloses that tracking must be approached on the global scale as well as in different environmental media. Because of the potential complexity and diversity, approaches of understanding the overall distribution of POPs cannot include all the possible compartments where they can be found. The necessity for a simplified representation of overall processes is evident. POPs are affected directly or indirectly by several environmental variables like temperature, rain, wind and sea currents. But also convective mixing of the atmosphere, resuspension by snow and dust particles cause variability in the transport and distribution path of POPs. The transport of POPs towards higher latitudes is made possible through the following main paths: Atmospheric transport, oceanic transport and large rivers.

Atmospheric transport is recognized as the most important long-range transfer route (*Wania and Mackay* (1993), *Strand and Hov* (1996)). POPs are moved either in the vapor phase or adsorbed on atmospheric particles which is the main reason for their long-range transport potential (LRTP). Removal from the atmosphere can occur via deposition or breakdown reactions. Deposition includes: washout via rain, fog, snow, dry particle deposition or dry gas deposition into the water column, sediment, vegetation or soil (*Ritter et al.* (1995), *AMAP* (2002)). Another special case of deposition is the exchange of POPs in the gas phase with the vegetation canopy.

POPs transport by ocean circulation is driven by a combination of various forces. In particular tidal forces, wind stress, mixing of water masses may dominate in some areas. Atmospheric transport is usually much faster than the oceanic analogue, which may take years (*AMAP* (2002)) to reach the higher latitudes. Additionally to the physical transport patterns, there is evidence for a minor biological transport. Birds, Cetaceans (beluga, bowhead whales, minke whales), pinnipeds, salmon or arctic cod are all migratory and are capable to transfer chemicals towards other ecosystems (*AMAP* (2002)).

1.5.1 Semivolatility and Grasshopping of chemicals

POPs follow thermodynamic principles and a change of temperature can cause a change of aggregate as well as a possible compartment change from soil/ocean to the atmosphere. Physico-chemical properties of many POPs also allow them to bind and reside on organic fractions in soil, dust or sediment particles (figure 2.2). Such semivolatility explains why chemicals can reside and coexist in different compartments. As many POPs are semivolatile organic compounds (SVOCs), their ubiquitous presence in the environment is driven by several factors. Temperature is certainly the most important one that defines in which aggregate state and medium a chemical is found in the environment. It can have significant effects on the ability how often a POP molecule can change the compartment. Temperature influences the partitioning equilibrium, which can lead to changes from the gaseous state to the liquid state (plus attaching to aerosols) and vice versa. The POP half-life in the atmosphere can change with temperature (*Beyer et al.* (2003)). As temperature drops below the freezing point the cycling of POPs will be influenced in several ways. Precipitation mainly falls as snow; the snow and ice cover on the other hand is retarding volatilization (*Beyer et al.* (2003)).
One decade ago, the concept of 'cold condensation' was formulated to understand the global occurrence of POPs. Wania and Mackay referred to the chemical fractionation and suggested that the global distribution of many organic pollutants will largely depend on the volatility of the compound and the ambient temperature (figure 1.2). They predicted the partitioning properties that allow POPs to accumulate in higher latitudes. Mainly those substances which both are either very volatile (*Wania and Mackay* (1993)) and water soluble or semivolatile and hydrophobic will most likely accumulate in the polar ecosystems *Wania* (2003). Depending on their properties, chemicals can behave very differently in their movement through the environment. POPs can be subdivided by their behaviour into several types: no hop, no-hop required, single-hop and multi-hop substances.

No-hop required substances are substances that do not need the frame of volatilization for their transport. They are very water-soluble and are transported mainly in their dissolved phase through riverine and oceanic currents. Agrochemical pesticides such as HCH's and Atrazine are examples for this class of compound (*UNEP* (2003a)).

No-hop substances No hop substances are so volatile that they do not deposit substantially on the Earth's surface and therefore remain in the atmosphere. Chlorofluorocarbons are such a class of chemicals (*UNEP* (2003a)).

Single hop substances Single-hop pathways describe the movement of compounds that are emitted to the atmosphere, transported, and then deposited to the surface, but never return to the atmosphere. Single-hop pollutants are lead, cadmium, benzo(a)pyrene [B(a)P], black carbon particles, and many radionuclides.

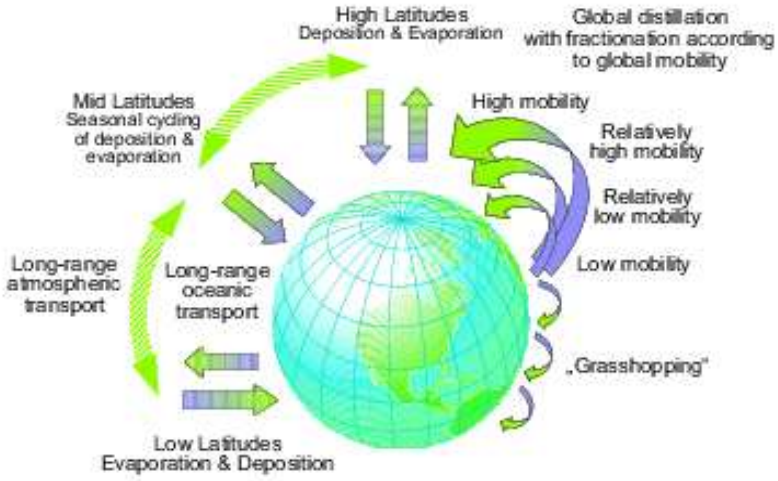

Figure 1.2: 'Grasshopping effect': Depending on the compound properties, a chemical can undergo atmospheric transport, be deposited and revolatilized again. Such a 'chemical hitchhiking' implies a further transport towards the poles where chemical mobility is reduced due to lower temperature. The chemical properties determine the mobility of a chemical. Highly mobile chemicals will be transported faster towards the higher latitudes. Picture adapted from *Wania and Mackay* (1996)

Multi hop substances Multi-hop substances get airborne again after initial deposition to the Earth's surface and continue to move through the environment in more than one cycle. This phenomenon of multiple hopping was described as the 'Grasshopper-Effect' (*Wania and Mackay* (1996)). This kind of chemical 'hitchhiking' tends to deposit in higher latitudes driven by the general circulation of the atmosphere, especially using air-currents in summertime. However also daily cycles occur to have influence on the cycling path. For multi-hop compounds, the source region affecting the Arctic is not only defined by atmospheric transport; removal, circulation but also surface processes are criteria that control its re-entry into the atmosphere. Concentration data collected from various environmental samples in remote areas confirmed the assumption that many persistent SVOCs fulfill the criteria of multiple hopping and thus also having LRTP. The list of multi-hop substances includes the organochlorine (OC) pesticides (*Kallenborn et al.* (1998), *Calamari et al.* (1991), *Wania* (1999), *Thurman and Cromwell* (2000), *Hung et al.* (2002), polychlorinated biphenyls (PCBs) (*Stern et al.* (1997), *Meijer et al.* (2002)) polybrominated diphenyl ether (PBDEs) (*Ikonomou et al.* (2002)), polycyclic aromatic hydrocarbons (PAHs), dioxin and furans (*Cohen et al.* (2002)).

For many reasons it is important to understand the partitioning of contaminative xenobiotics in the miscellaneous physical-biological compartments. Health and environment protection goals can only be achieved with a clear scientific knowledge in which media toxic chemicals will be accumulated in the future.

Many chemicals are still to be screened and investigated whether they are candidates for the black list according to the regulations of the Stockholm convention. This work focuses mainly on substances, which are characterized by their 'multihop' behaviour. Multihopping chemicals show the strongest interaction with different compartment media. It is essential to estimate the influence of different processes, which could have significant impact on the LRTP of these substances. Multihopping of POPs includes transport, deposition on different surfaces (continent, ocean, vegetation) as well as possible sedimentation and degradation. POPs cycling can be heterogeneous in terms of pathways due to many influences on local as well as on global scale.

1.6 The influence of the vegetation on the cycling of POPs and their representation in models

Many POPs are used in agriculture and it is evident that the vegetated land mass often serves as a starting point for the cycling of these chemicals. But not only because of application, vegetation is important: Vegetation structures are ideal to filter and accumulate large amounts of air-borne pollutants (*Riederer* (1990)). Studies and field measurements (*Tremolada et al.* (1993)) have shown that vegetation can be a main reason for a disproportional large increase of net atmospheric deposition to the terrestrial environment, and thus reducing the LRTP of POPs. Global vegetation has a large surface exchange area. Depending on the climate zone and the vegetation type the leaf area index can reach values of almost $10\frac{m^2}{m^2}$. The large exchange surface between canopies and the atmosphere leads to the question how vegetation can buffer the further condensation and transport towards higher latitudes. This is especially important for the more land bound Northern hemisphere where large areas of the continents are covered with leaves and needles and the main sites of chemical pollution are situated. Canopies have very diverse physiological and phenological characteristics which could have influence on the overall cycling of POPs: roughness length, canopy height, amount of leaf stomata available, LAI, leaf physiology, leaf phenology, cuticular structure (*Kerler and Schönherr* (1988)), vegetation surface roughness, terpene variation (*Kylin et al.* (2002)), leaf-volume ratio (*Boehme et al.* (1999)) cause a relatively unclear picture about what are the main processes of the compounds vegetation-air exchange. Additionally, different climate conditions may favour different interactions for similar vegetation types.
POPs can accumulate in the waxy tissue of leaves. E.g. leaves are covered with hydrophobic lipid layers, which make an accumulation in the cuticula possible. POPs are found on the canopy surface (e.g. cuticula) as well as within the leaf interior and they even move from one leaf cell to the next one. Processes that take place on or within a leaf are the volatilization ('hopping'), degradation, photolysis, and removal by phloem transport or dilution growth. Different exchange

of POPs with the atmosphere may occur even on the same vegetation type due to physiological reasons. Leaves exposed to the sun most likely cause higher degradation and volatilization rates than their counterparts in the shadow. Additionally, wind speed and surface roughness could play another important role in the overall distribution of POPs.
A lot of ambiguities prevail on the role of vegetation, although it may have feedback effects on the cycling pattern of POPs. The consequences would be a different overall pollution level or/and accumulation of POPs in different compartments. Vegetation and its processes may even influence the half-life time of chemicals.

1.6.1 Atmospheric exchange with the vegetation canopy

Vegetation exchanges POPs directly with two other media in the environment, namely the atmosphere and the soil underneath the vegetation. Vegetation emits POPs into the atmosphere as well as POPs get deposited on the canopy. Emission or volatilization of POPs occurs either attached on mainly organic particles or in the gas phase. Deposition of POPs on the vegetation canopy follows basically the same mechanisms as for other particles and gases. Deposition is influenced by the physico-chemical properties of the compound and the surface. Deposition of POPs on the vegetation canopy occurs via gas and particle atmospheric settling, as well as diffusive gas exchange with the vegetation canopy.

Gas deposition: Gas deposition of POPs on vegetation canopies can be described by two different methods. It has been measured empirically (*McLachlan et al.* (1995)) and used in other models (MPI-MBM *Lammel et al.* (2007)). Another possibility would be by calculating the overall resistance R_T which a gas molecule has to overcome to settle on the vegetation canopy.

Particle deposition: Particle deposition of POPs depends on partitioning ratios between the air and the aerosol (*Junge* (1977)). One has to distinguish between the particle wet and dry deposition. Dry deposition of particles follows a resistance mechanism R_{T_p} similar to the already mentioned gas deposition.

Diffusion: The diffusive gas exchange of POPs with the leaf interior is based on the laws of fugacity, which describes the tendency of a chemical to prefer one phase (solid, liquid, gaseous) over another . The leaf-air exchange does not only include the vegetation surface. This is a process, which involves the leaf interior, and thus is accompanied by many uncertainties concerning the partitioning between the air and vegetation medium. A discussion about how many leaf compartments are necessary for the accurate description of POP gas diffusion process is needed. The reason is that POPs are able to change their locations in leaves (see also figure 3.3). The accumulation mechanism and the role of leaf anatomy are still not properly understood and can be an important detail for the re-emission from canopy back into the atmosphere.
The intensity of all the canopy-atmosphere exchange processes depends on several

influential factors. Wind speed, surface temperature and aerosol type are probably the most important criteria to investigate in relation with vegetation.

1.6.2 Soil exchange with the vegetation

Soil vegetation exchange of POPs takes place basically via periodical litter fall. Beside this mechanism, dripping from the canopy top is another indirect atmospheric wet deposition pathway. Gas and dry deposition on the soil underneath the vegetation soil are probably not as efficient and depend also on the LAI and vegetation type.

Phenology: Vegetation cycles change the overall cycling of POPs. The defoliation process could cause essential changes for the filter effect of vegetation canopies. Soil storage is enhanced by litter fall. Thus vegetation soil processes require an additional vegetation sub compartment for the display of the interactions between the atmosphere, canopy and soil. Defoliation cycles are very different for every vegetation type and climate zone. It is thus useful to know whether vegetation soil is a threshold or a storage compartment of POPs and what its long-term consequences for the overall cycling would be.

Chapter 2

Objectives and procedures

Lab experiments with vegetation are difficult to accomplish because of the persistence of the compounds. Multi-compartment monitoring of POPs in the environment is very costly and requires a large network of sampling stations. Applied mathematical models thus offer an alternative to address questions of the dispersion and exposure patterns of SVOCs. This work has the aim to investigate the complexity of POP exchange processes with the vegetation and will focus on the following questions.

- What are the main vegetation processes for the overall cycling of POPs and how can they be quantified?
- Which processes have to be included in an accurate description of atmospheric deposition of semivolatile organic compounds on plants? What are other important criteria for the deposition?
- How does phenology and other factors influence the overall cycling of POPs. Do we need a sophisticated modelling tool for the processes involved (leaf decomposition, soil storage and revolatilization)?
- Are vegetation types important for the overall cycling of POPs?
- How do other factors influence the overall cycling of POPs and what are the different effects of these factors in different climate zones?

To address all the questions and to advance in the overall understanding of the influence of vegetation on POPs cycling (figure 2.3), a multimedia nonsteadystate and nonequilibrium box model (see also table 2.1) was designed. Box models can have different levels of complexity. Level IV POP box models tend to an unsteady state. They are zero dimensional tools, where POP exchange processes with the different environmental media are simulated. Such a model is mass conservative and all the processes take place inside a fixed Eulerian cell (*Seinfeld and Pandis* (1998)).
Box models are based on mass balance equations of a predefined number of chosen compartments. The minimum of compartments in a multicompartment POP box model are three, namely; atmosphere, ocean, soil. Additional compartments (such

as vegetation, land- or sea ice, snow layers etc.) can be considered depending on the scientific question addressed. Many factors have to be represented in a very simplified manner. Heterogeneous and complex environmental factors that may have influence on the partitioning of substances such as vorticity, divergence, humidity, cloud water or albedo are usually not incorporated.
According to the question addressed and vegetation process investigated, different box model complexities were designed to experiment with the influence of each single vegetation process (figure 2.3).

	level I	level II	level III	level IV
Steady state	yes	yes	yes	no
Degradation	not allowed	allowed	allowed	allowed
System is with resp. to mass	closed	open	open	open
Antropogenic emissions	no	mode of entry not important	mode of entry needed	mode of entry needed
Advection	no transport	allowed (no resistance)	allowed (with resistance)	allowed (with resistance)
Sinks	No	Included	Included	Included
Residence time	One overall residence time	One overall residence time	Potentially more than one	Potentially more than one

Table 2.1: Several types of Box models were developed to investigate the fate of POPs. Levels of complexity are increasing with additional processes considered. Level I was the first type of models used while level IV models are state of the art box models.

2.1 Experiment and Model Design

The aim of this work is to study the influence of the different vegetation processes on a global as well as on a more climate specific scale for the overall cycling of POPs. Experimental and model designs are made to address several processes of the POPs-vegetation interaction. Complexity of the vegetation description and its exchange mechanisms with the environment are one of the main fields of this investigation. Four different ways of atmosphere-vegetation canopy exchange processes are investigated and validated in this work, namely :

- prescribed gas deposition of POPs
- calculated (including surface roughness and canopy characteristics) deposition of POPs in the gas phase
- deposition of POPs attached to aerosol particles

- diffusive gas exchange with leaf interior

The other important compartment exchange of POPs addressed is the interaction between the vegetation canopy and the vegetation soil underneath. This process includes the defoliation, as well as indirect atmospheric deposition on the canopy and further transport to the soil (e.g. dripping from leaves during rain). Canopy architecture and its influence on the overall cycling is investigated in an additional experiment.
Two different approaches are taken for the simulation of the vegetation processes. In a first 'global' approach, the influences of the several vegetation processes mentioned is simulated on global scale. The global experiments focus on describing several deposition mechanisms and vegetation processes and its global impact for a simple 'unit vegetation type', which has the same biological-physical characteristics in every grid point. Only three input values are allowed to vary in every grid point. They are: the area of continent with vegetation cover, the LAI and the ratio of continent and ocean. The climate specific approach focuses on the influence of different vegetation types on the overall cycling of POPs. Studies of the impact of different vegetation types on the overall cycling of POPs are mainly performed in only one climate zone. The reduction of the investigation area is due to practical reasons (potentially a large dataset has to be investigated for every climate zone and vegetation type). The process study of the different vegetation-atmosphere and vegetation-vegetation soil interactions is applied for both, global and climate specific approaches.
Four different process setups are designed for addressing several vegetation processes (see also figure 2.1). They are: The big leaf canopy model (setup 1), the big leaf vegetation volume model (setup 2), the big leaf canopy model with defoliation (setup 3) and the multilayer canopy setup with defoliation as well (setup 4). In step 1, a big leaf model only with vegetation surface is applied to model gas- and particle deposition (figure 2.1, table 2.3). For the inclusion of the gas diffusion process, an additional leaf interior vegetation sub compartment was added (setup 2). Both of the setups are big leaf model setups without any kind of vegetation soil. The defoliation process is represented with an additional simple soil compartment underneath the vegetation canopy (setup 3), while the multilayer compartment requires a 2-layer canopy split (setup 4).

2.1.1 Setup 1: Big leaf vegetation

The compartments considered are a one-column boundary layer atmosphere, a big leaf vegetation, a bare soil compartment and a simplified ocean without seafloor (figure 2.1). The big leaf vegetation area covers the whole vegetation canopy surface and is assumed as $1m^2$ leaf per $1m^2$ bottom surface. The influence of the LAI is not considered with such a setup. The burden of POPs in each compartment is calculated in $\left[\frac{molec}{m^2}\right]$. This setup will be used for simulating the gas- and particle deposition processes. Processes included (1-11) can be seen on the in figure 2.1. All the mentioned processes are also found in the next setups.

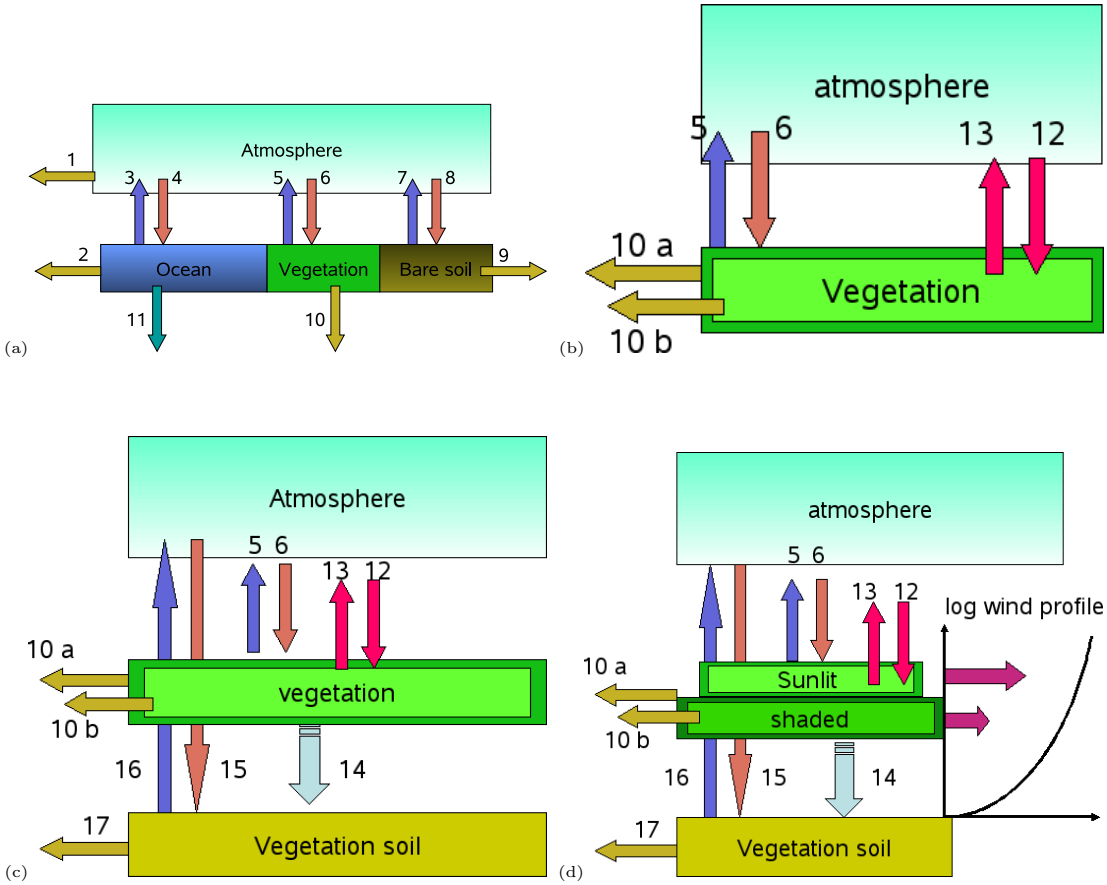

Figure 2.1: Schematic representation of the multi compartment exchange processes of the box model. The ocean and bare soil compartment processes are shown only in the first diagram because no further changes are made in the other 3 setups. Process 1-11 is calculated in every setup and thus only the model extensions are displayed for the further setups. Diagram a) represents the big leaf surface vegetation (setup 1) of the total box model, b) the big leaf vegetation (setup 2) with leaf volume, c) introduction of the defoliation (setup 3) and d) the 2-layer vegetation approach with vegetation soil (setup 4). The processes are: 1: OH-radicals daytime degradation G_A, 2: Oceanic removal G_O, 3: Volatilization from ocean surface V_O, 4: Deposition (wet, dry and particle) on the ocean surface D_O, 5: Volatilization from the vegetation surface V_V, 6: Deposition (wet, dry and particle) on the vegetation surface D_V, 7: Volatilization from bare soil V_B, 8: Deposition (wet, dry and particle) on bare soil D_B, 9: Degradation on bare soil G_B, 10 a: Degradation on the leaf surface G_V, 10 b: Removal in the leaf interior by Phloem L_{V_V} (b_{V_V}), 11: Oceanic removal to the deep sea as final sink L_O, 12: Gas diffusion from the atmosphere to vegetation $F_{A \to V_V}$, 13: Gas diffusion vegetation to atmosphere $F_{V_V \to A}$, 14: Litter fall to the vegetation soil T_{V_V} (b_{V_V}), 15: Deposition (wet, dry and particle) through the canopy on the vegetation soil (including the indirect deposition) D_{V_S}, 16: Volatilization from the vegetation soil V_{V_S} (b_{V_S}), 17: Degradation on the vegetation soil G_{V_S} (b_{V_S})

	Re-emission	Degrad	Depos	Loss or Litter	Burden	Surface fractions
Bare soil	V_B	G_B	D_B		b_B	a_B
Ocean	V_O	G_O	D_O	L_O	b_O	a_O
Veg can	V_{V_C}	G_{V_C}	D_{V_C}	$T_{V_C}(b_{V_C})$	b_{V_C}	a_V
Veg soil	$V_{V_S}(b_{V_S})$	$G_{V_S}(b_{V_S})$	D_{V_S}		b_{V_S}	a_V
Veg vol	$F_{A\to V_V}$		$F_{A\to V_V}$	$L_{V_V}(b_{V_V})$ $T_{V_V}(b_{V_V})$	b_{V_V}	a_V

Table 2.2: Display of process nomenclature all the processes above have the unit $\left[\frac{molec}{m^2 s}\right]$. The burden is given in $\left[\frac{molec}{m^2}\right]$ while the surface fraction are dimensionless. The re-emission includes volatilization as well as gas diffusion. Deposition can also include gas diffusion from atmosphere to vegetation.

This setup is the base from which all the other setups are developed from. All the processes of this setup can be found in all the other setups too. The processes of this box model are: application (emission) $\frac{d\,M_a}{d\,t}$, deposition D, chemical degradation G, volatilization V, diffusion F, transport by litter fall T and loss processes in the compartments L (see also table 2.2). D, G, V, F, T, L depend on the actual burden in the compartments.

Atmosphere: $\left[\frac{molec}{m^2 \cdot s}\right]$

$$\begin{aligned}\frac{d\,b_A}{dt} =& E_A + V_V\left(b_V\right) \cdot a_V + V_B\left(b_S\right) \cdot a_B \\ &+ V_O\left(b_O\right) \cdot a_O - D_O\left(b_A\right) \cdot a_O \\ &- D_B\left(b_A\right) \cdot a_B - D_V\left(b_A\right) \cdot a_V \\ &- G_A\left(b_A\right)\end{aligned} \tag{2.1}$$

Bare Soil: $\left[\frac{molec}{m^2 \cdot s}\right]$

$$\frac{d\,b_S}{dt} = D_B\left(b_A\right) \cdot a_B - V_B\left(b_S\right) - G_B\left(b_S\right)$$

Vegetation: $\left[\frac{molec}{m^2 \cdot s}\right]$

$$\frac{d\,b_{V_C}}{dt} = D_V\left(b_A\right) \cdot a_V - G_V\left(b_{V_C}\right) - V_V\left(b_V\right)$$

Ocean $\left[\frac{molec}{m^2 \cdot s}\right]$

$$\begin{aligned}\frac{d\,b_O}{dt} =& = D_O\left(b_A\right) \cdot a_O - G_O\left(b_O\right) \\ &- V_O\left(b_O\right) - L_O\left(b_O\right)\end{aligned} \tag{2.2}$$

2.1.2 Setup 2: Big leaf with vegetation volume

Gaseous leaf-air-exchange is supposed to play a major role in the cycling of POP's. Information for the gas exchange moldel study was collected either from experiments in combination with model data (*Tolls and McLachlan* (1994), *McLachlan et al.* (1995)) or air/vegetation measurements (*Bacci et al.* (1990) *Tremolada et al.* (1993) *Tremolada et al.* (1996) , *Eriksson et al.* (1989) *Jensen et al.* (1992) *Hellström et al.* (2004), *Kylin and Sjödin* (2003)). Here the process of gas diffusion with the leaf interior requires an additional vegetation compartment, which will be called the vegetation volume. The total leaf exchange area for this process can be much larger than the soil surface below (figure 2.1 b), hence the leaf area index can have values higher than $1\frac{m^2}{m^2}$. Gas diffusion is a process with 2 directions: from the atmosphere into the vegetation volume (process 12) and vice versa (process 13). Additional removal from the vegetation canopy (process 10, figure 2.1) occurs with the vegetation volume removal of the phloem (process 10 b). The bare soil and the ocean compartment do not change neither in this nor in the other setups. Hence, only the interaction between the vegetation compartments and the

atmosphere will be displayed here. The full description of all the compartment processes in all the setups can be found in the equation chapter of the appendix. The implementation of gas exchange of POPs requires the implementation of the processes 10b to 13 and the new vegetation volume compartment. The affected compartments are displayed as

Atmosphere:

$$\begin{aligned}\frac{d\,b_A}{dt} =& E_A + V_V\left(b_V\right)\cdot a_V + V_B\left(b_S\right)\cdot a_B \\ &+ V_O\left(b_O\right)\cdot a_O - D_O\left(b_A\right)\cdot a_O \\ &- D_B\left(b_A\right)\cdot a_B - D_V\left(b_A\right)\cdot a_V \\ &- G_A\left(b_A\right) + F_{V_V\rightarrow A}\cdot a_V\end{aligned} \tag{2.3}$$

Vegetation Volume:

$$\frac{b_{V_V}}{dt} = F_{A\rightarrow V_V} - L_{V_V}\left(b_{V_V}\right)$$

2.1.3 Setup 3: Big leaf with defoliation

Litter fall requires an additional compartment: A new vegetation soil compartment includes processes that are the result of defoliation (figure 2.1 c). New processes in this setup are: defoliation (process 14), degradation on the vegetation soil (process 17), volatilization from vegetation into the atmosphere (process 16), indirect deposition from the atmosphere either via vegetation canopy (leaf dripping wet deposition), or direct deposition when the LAI is smaller than $1\frac{m^2}{m^2}$ (process 15). For simplification reasons, immediate leaf decomposition and revolatilization is assumed to take place. Processes 14 to 17 require changes for the atmosphere and all the vegetation compartments as well as the new vegetated soil compartment. They are written as

Atmosphere:

$$\begin{aligned}\frac{d\,b_A}{dt} =& E_A + V_V\left(b_V\right)\cdot a_V + V_B\left(b_S\right)\cdot a_B \\ &+ V_O\left(b_O\right)\cdot a_O - D_O\left(b_A\right)\cdot a_O \\ &- D_B\left(b_A\right)\cdot a_B - D_V\left(b_A\right)\cdot a_V \\ &- G_A\left(b_A\right) + F_{V_V\to A}\cdot a_V \\ &+ V_{V_S}\left(b_{V_S}\right)\cdot a_V\end{aligned} \tag{2.4}$$

Vegetation Surface:

$$\begin{aligned}\frac{d\,b_{V_C}}{dt} =& = D_{V_C}\left(b_A\right)\cdot a_V - G_V\left(b_{V_C}\right) \\ &- V_V\left(b_V\right) - T_{V_C}\left(b_{V_C}\right)\end{aligned} \tag{2.5}$$

Vegetation Volume:

$$\frac{b_{V_V}}{dt} = F_{A\to V_V} - L_{V_V}\left(b_{V_V}\right) - T_{V_V}\left(b_{V_V}\right)$$

Vegetation Soil:

$$\begin{aligned}\frac{d\,b_{V_S}}{dt} =& D_{V_S}\left(b_A\right)\cdot a_V - V_{V_S}\left(b_{V_S}\right) \\ &- G_{V_S}\left(b_{V_S}\right) + T_{V_C}\left(b_{V_C}\right) \\ &+ T_{V_V}\left(b_{V_V}\right)\end{aligned} \tag{2.6}$$

2.1.4 Setup 4: Two leaf layer vegetation

Setups 1-3 considered vegetation as a simple one single layer big leaf. Influences of different wind speed and canopy temperature at different canopy height are not considered in those setups. In this setup, the leaf canopy is segregated between the crown part exposed to the sunlight and the canopy layer in the shadow (figure 2.1 d). Processes in both canopy layers are the same like in the single vegetation layer of setup 3. Both layers also consider the differences in wind speed and canopy temperature. The deposition arriving at the canopy is distributed according to the fraction of sun/shaded leaves. No new processes are added in this setup, however, the split into a multi-vegetetation layer setup requires that processes need to be calculated with two separate equations (shaded/non shaded). They are summed up in our system as

Atmosphere:

$$\begin{aligned}\frac{d\,b_A}{dt} =& E_A + \sum V_V\left(b_V\right)\cdot a_V + V_B\left(b_S\right)\cdot a_B \\ &+ V_O\left(b_O\right)\cdot a_O - D_O\left(b_A\right)\cdot a_O \\ &- D_B\left(b_A\right)\cdot a_B - \sum D_V\left(b_A\right)\cdot a_V \\ &- G_A\left(b_A\right) + \sum F_{V_V\to A}\cdot a_V \\ &+ V_{V_S}\left(b_{V_S}\right)\cdot a_V\end{aligned} \tag{2.7}$$

Vegetation Surface:

$$\begin{aligned}\frac{b_{V_C}}{dt} =& \sum D_{V_C}\left(b_A\right)\cdot a_V - \sum G_V\left(b_{V_C}\right) \\ &- \sum V_V\left(b_V\right) - \sum T_{V_C}\left(b_{V_C}\right)\end{aligned} \tag{2.8}$$

Vegetation Volume:

$$\begin{aligned}\frac{b_{V_V}}{dt} =& \sum F_{A\to V_V} - \sum L_{V_V}\left(b_{V_V}\right) \\ &- \sum T_{V_V}\left(b_{V_V}\right)\end{aligned} \tag{2.9}$$

Vegetation Soil:

$$\begin{aligned}\frac{d\,b_{V_S}}{dt} =& D_{V_S}\left(b_A\right) - V_{V_S}\left(b_{V_S}\right) - G_{V_S}\left(b_{V_S}\right) \\ &+ \sum T_{V_C}\left(b_{V_C}\right) + \sum T_{V_V}\left(b_{V_V}\right)\end{aligned} \tag{2.10}$$

model setup	tested process	sensitivity experiment vegetation		focus on
		global effects	zonal effects and Vegetation type	
Setup 1	1. gas deposition (I)	influence of wind speed on vegetated and non vegetated surfaces	- aerosol type	- overall burden b_{tot}
	2. gas deposition (II) 3. particle deposition		- wind speed	- compartment burden - τ_{ov} residence time
Setup 2	4. gas exchange of POPs	1. influence of wind speed on vegetated surface 2. influence of plant air-partitioning coefficient K_{PA}	- aerosol type - K_{PA} - wind speed	- compartmental residence time - flux into or out of compartment
Setup 3	5. defoliation	- leaf turnover	leaf turn over veg-type - K_{PA} - Wind speed	
Setup 4	6. 2-layer canopy	comparison how detailed process		

Table 2.3: Test strategy of the several setups. In the first global experiments focus rather on the overall influence of the different setups, while the climate specific experiments investigate the influence of other environmental parameters.

2.2 Model environment

Box models can encompass a certain geographic region, even the whole world can be assumed as one box. The typical spatial scale of box models covers areas from 10^4 to 10^6 square kilometers (*MacLeod et al.* (2001)). Several type of box models with different compartments have been developed for studying the fate of POPs. Some examples are: CHEMRANGE[1], ELPOS [2], BETR[3] (*MacLeod et al.* (2001)), GLOBOPOP[4], ClimoChem [5], SIMPLEBOX [6]. An approach in-between simple box and 3-dimensional models are so called 'connected boxes'. These models (*Mackay et al.* (1992), *Wania and Mackay* (1995)) use measured dispersion data of chemicals to simulate the long-range transport of POPs (*Scheringer and Wania* (2003)).
Transport models were developed to study POP transport on different scales. They can contain the whole globe (*Koziol and Pudykiewicz* (2001), *Semeena and Lammel* (2005)), only one hemisphere or just regions (*Van Jaarsveld et al.* (1997) *Prevedouros et al.* (2004), *Wania et al.* (2000)). Usually the temporal and spatial resolution is very high which requires a lot of input data and CPU power. Especially long-term trends are very costly to obtain.

2.2.1 Global vegetation forcing

Our model is a meridian fictional North-South cross-section from 63° N to 63° S, with a grid point every 4.5 degrees representing a box. This is the most contiguous N-S landmass with vegetation. All the chosen grid points represent a calculation box and all the boxes are not connected with each other (thus no mass exchange takes place between the 'grid point boxes'). The climate and vegetation data are taken on the 28E because this basically represents the largest connected North-South surface on the globe. Grid points between 34S and 54S are added as there is also global land mass.
The Arctic and Antarctic circle are not included because neither land-, nor sea ice processes are considered. For every latitude the sea fraction is according to the total latitude land-ocean distribution. The amount of the continental vegetation cover depends on the latitudinal zone. Zones without vegetation are deserts. The vegetation forcing is changed depending on the requirements for the individual experiment setup. For the global experiments, a climate specific unit shrub vegetation type is applied. The climate zones differ in terms of leaf area index (LAI), temperature but do all have the same roughness length and vegetation height. The data applied for vegetation, surface temperature and roughness length are mostly from model outputs (e.g. LPJ (Lund, Potsdam, Jena), JSBACH) and missing data is completed with published climate diagrams in the literature. All

[1] M. and F. Wegmann, ETH Zurich, Switzerland
[2] M. Matthies, University Osnabrück, Germany
[3] M. MacLeod et al. (Berkeley Lab,Trent University)
[4] K. Breivik on behalf of F. Wania, NILU, Norway
[5] M. Scheringer and F. Wegmann, ETH Zurich, Switzerland
[6] D. van de Meent and A. van Pul, the Netherlands

the areas chosen correspond to a certain climatic zone and latitude.

2.2.2 Climate specific forcing

Vegetation types (e.g. grass, deciduous forest, coniferous forest) sensitivities are studied in dependence of other environmental factors (e.g. different aerosols, wind speeds etc.) in only one climate zone for this second experiment. These sensitivity studies are made under stable conditions with an impulse application in the first year and a total runtime of 7 years (approximately 2500 days).

2.3 Emission scenarios

Information about emission sources of POPs is often lacking. Main reasons for such a poor information density either are that countries did not document and report their historical usage of POPs, or due to political reasons, some governments are simply not interested to report the real amount of POP usage. One of the biggest problems concerning the modeling is the uncertainty of contamination levels, and very hypothetical emission scenarios have been assumed. The emission path of POPs is via atmosphere only because some latitudes do not have larger emission sources or are not centres of agricultural activities. Hence, for standardization reasons, atmospheric pollution is assumed as the only source of input to the system. Such a pollution scenario can be interpreted as the input to one box via LRTP from sources.

2.3.0.1 Realistic application

A qualitative comparison of long-term trends under the inclusion of important environment variables such as (e.g.) seasonal cycles is the frame of the global scenario runs. All these runs are performed for a period of 100 years and are applied on every climatic zone. The current experimental setup assumes a 60-65 years market lifetime of the substance of concern (figure 2.3). Strong growth occurs in the first 20 years to its peak, around 25 years after the market introduction, followed by a nonlinear decrease to almost zero emission towards the end of the market life. In the period from 80 to 100 years, only remainders would be responsible for further emissions. This scenario should hypothetically give an outlay what could be expected in the future.

2.3.0.2 Impulse application

The application scenario of this experiment is a one-year continuous air emission impulse. The runtime is is 2500 days for this simulation. The non-spatial resolution and the simplified setup could give hints about the influence of factors like e.g. canopy structure, canopy height and LAI. The experimented setup includes stable environmental conditions. Temperature is not changing throughout

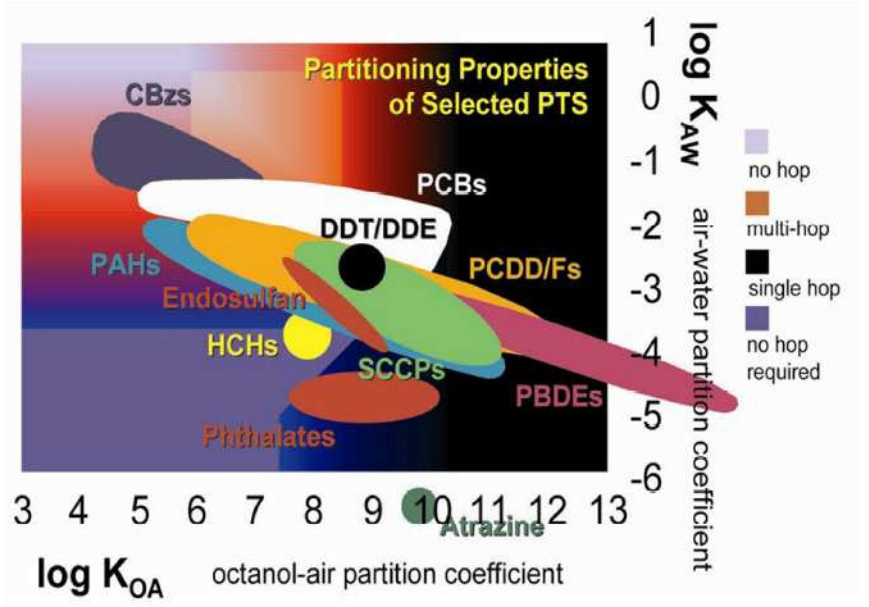

Figure 2.2: Selective categorization of chemicals and their transport path as a function of distribution characteristics. The most important ones are the octanol-air partitioning (log K_{OA}) and the air-water (log K_{AW}) coefficients. POPs are basically categorized in four main categories of compartment behaviour: with log K_{OA} higher than 10 the chemical is so involatile that it stays deposited irreversibly. Chemicals with log K_{OA} less than 7 or 8 are in general strongly water-soluble and undergo oceanic LRT. Chemicals with positive values of log K_{AW} are too volatile to deposit even in cold regions. Chemicals with K_{OA} and K_{AW} between these extremes are able to change compartments.

the whole year without any daily cycles and also the depletion rates of POPs are linear.

2.4 Compound selection

Environmental behaviour of chemicals strongly depends on their physico-chemical properties (see also figure 2.2). The most important ones are: water solubility, vapour pressure, degradation rates and partitioning coefficients. Partitioning can include air-water partitioning K_{AW}, octanol-air K_{OA} or other liquids. It is thus important to know the compound properties as well, as its distribution mechanism across the different media. This information helps to indicate whether a chemical is prone to reside in the air, water or on the continent. These properties also indicate whether a chemical is considered as single-hop, multi-hop or no-hop at all compound. They also indicate the LRTP of a compound.
This work included experiments with two compounds. The first one is DDT, an organochlorine pesticide very heavily applied in the last century. The second compound PCB-52 is an industrial chemical out of a group of 209 chemicals. A more detailed overview of invention and historical usage of both chemicals can be

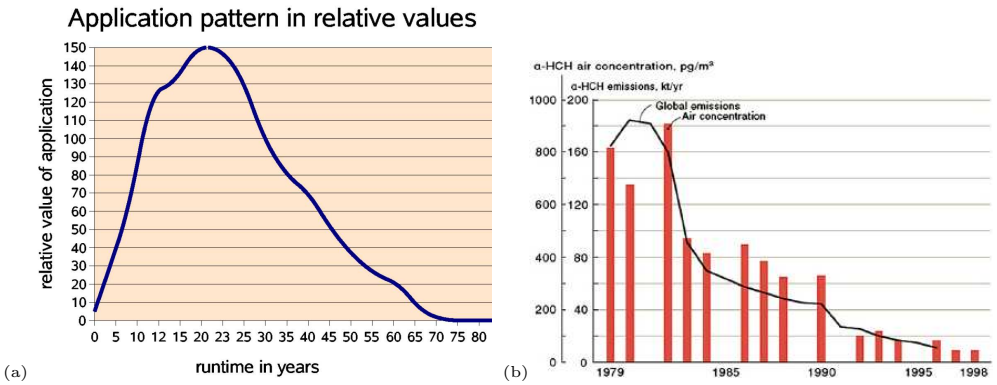

Figure 2.3: a) Application index used in this study for the long term simulations. b) Global emissions of $\alpha - HCH$ (*Li* (1999)) and its mean concentration from 1979 to 1996 assembled from published data (*de Wit et al.* (2002))

found in the appendix. DDT is prone to reside in several compartments and is treated as a chemical with a very high half-life. It has an extremely low water solubility and is often preserved in soil organic matter at the surface (although, more mobile metabolites of DDT have also been detected). PCB's have a larger variation in terms of degradability, vapour pressure and water solubility. PCB's are generally hardly soluble in water due to high $logK_{OW}$ values. The grade of chlorination is also a very important chemical property of PCB's. The general rule is that the higher the grade of chlorine substitution the lower is the water solubility.

2.5 Synopsis

Two different blocks of vegetation processes are investigated in the following chapters. Chapter 3 deals with the deposition on the canopy. Gas- and particle deposition are described as well as a discussion and description of the gas exchange process. Chapter 4 deals with canopy removal processes and also includes the description of the two-layer canopy structure. The outcome of the experiments with the two chemicals are described in separate chapters. The main criteria for the analysis of the chemicals in this work are: the overall burden b_{tot}, the compartment distribution, the latitudinal distribution, the sensitivity of fluxes and the overall residence time τ_{ov}. Chapter 6 summarizes the overall findings for both chemicals. It concludes with an outlook about future research questions concerning POPs and vegetation.

Chapter 3

Deposition of POPs on vegetation

The canopy-atmosphere interface has a very large surface for exchange with the atmosphere. The often high values of the LAI underline the importance of plant communities for the interception and accumulation of air-borne pollutants. The main processes occurring at the vegetation surface are the different types of deposition on the leaf and diffusive gas exchange into the leaf interior. Pollutants arrive at the vegetation surface in the vapour phase, dissolved in droplets or in particulate form (*Riederer* (1990)). Because of their high carbon content, leaf surfaces may act either as permanent sinks or buffer media for air-borne pollutants, depending on the equilibrium and kinetics of the phase transfer (*Tao and Hornbuckle* (2001)). Studies with chemical visualization techniques (Two-Photon Excitation Microscopy) have shown that there is even a sub cellular compound movement within the leaf[1] (figure 3.3).
Physico-chemical properties determine whether POP are deposited as gas or attached on aerosols. Environmental factors (e.g. temperature, wind speed, humidity and light conditions), plant characteristics (e.g. species type, surface area, cuticle structure and surface morphology) and habitat can also have its effect on the flux between air and vegetation. Other interactions with the vegetation canopy can have indirect influence on the deposition of POPs. Possible processes are: Photochemical degradation, leaf surface volatilization and removal by the plant transport processes (mainly through the phloem), translocation of POPs to other parts of the plant (root, stem), dilution by growth potentially can occur too (*Simonich and Hites* (2003)). As one can see, there are many uncertainties about the complex behaviour of chemicals on or inside the leaf, and some processes are still not properly understood. A POP molecule could get deposited on the leaf surface and getting absorbed into the canopy leaf. Sorption of POPs on leaves can be considered as a function of an equilibrium distribution between phases and kinetics of the phase transfer (*Tao and Hornbuckle* (2001)). It is thus very difficult to segregate the processes or even define the different compartments necessary for the POP modeling in leaves.
This approach simplifies the canopy uptake of POPs into two main compartments: the leaf surface and the leaf interior without considering additional sorption. The

[1] http://www.lec.lancs.ac.uk/ccm/research/visualisation/index.htm

leaf interior in our model is defined as all the processes that would include an accumulation on or within the cuticula or other leaf interior compartments (apoplast, mesophyl, phloem etc.). So far, it was commonly supposed that the cuticle route of entry is the only important for accumulation in leaves. However, recent works (*Barber et al.* (2004)) pay also much more attention to the stomata uptake mechanism. And thus in this model, there are two main deposition pathways how a gaseous POP molecule enters the leaf interior, namely via the stomata and/or the lipophilic cuticula. So far the uptake dynamics of POPs with the leaf interior via diffusive gas exchange with the leaf interior and its effects have not been studied to a satifactory extent. Other leaf mechanisms like litter fall, leaf decomposition, removal by the phloem stream and further distribution to the other parts of a plant or dilution by growth (*Duyzer and van Oss* (1997)) are not considered either. Soil-vegetation interactions will be discussed in the next chapter.
This work tests the deposition paths with an increasing level of complexity and additional inclusion of processes.
In a first step, the model is run with prescribed gas deposition values D_{g_p} from literature. In a second step, a developed calculated gas deposition parameterization D_{g_c} is compared with the original one. A similar deposition scheme is developed for the particle deposition D_p. Wet deposition D_w is set as constant in every climatic zone and will not be discussed further in this work. Hence, the total deposition D_t has to be changed depending on the overall scheme chosen:

$$D_t = D_w + D_g \longrightarrow D_t = D_w + D_g + D_p \tag{3.1}$$

3.1 Setup 1: gas deposition

Instead of being calculated with only one deposition velocity like in the case of D_{g_p}, the new scheme takes into account the different deposition surface conditions. Aerosol and gas deposition are based on the gas-particle partitioning theory by Junge-Pankow (eq. A.8). This section describes the resistance scheme for gas- and particle deposition. They follow the Kirchhoff rules for electric resistances.
The general assumption takes into account that three main resistances restrict the mass transport from the atmosphere. They are: the aerodynamic resistance R_a, the quasi-laminar layer resistance R_b and the canopy or surface layer resistance R_c, whereby canopy or surface resistance includes several sub-resistances. Resistances formulations of R_a and R_b for the gas and the particle deposition differ though. The total deposition resistance R_T is the sum of all the three main serial resistances, which is also considered as the reciprocal of the deposition velocity v_d, namely

$$\frac{1}{v_d} = R_T = R_a + R_b + R_c \tag{3.2}$$

3.1.1 Aerodynamic resistance R_a

Deposition fluxes from the atmosphere are determined by turbulent processes that also define the deposition resistance. The intensity of turbulence depends on the stability of the atmospheric boundary layer and the surface characteristics. Hence, R_a is dependent on the atmospheric conditions. We assumed neutral atmospheric stability and thus aerodynamic resistance R_a can be written as (*Seinfeld and Pandis* (1998)):

$$R_a = \frac{1}{\kappa \cdot u_*} ln \cdot \left(\frac{z_{ref}}{z_0} \right) \tag{3.3}$$

where κ is the Karman constant taken from values in literature, and u_* is the friction velocity. The equation can be further simplified as (*Monteith and Unsworth* (1990))

$$R_a = \frac{u(z)}{u_*^2} \tag{3.4}$$

The reference height z for wind speed u_z was set to $z_{ref_L} = 30m$ over land and $z_{ref_S} = 10m$ over sea.

3.1.2 Quasi laminar boundary layer resistance R_b

The boundary layer resistance for gaseous deposition is described by the well-known formula (*Wesely and Hicks* (1977), *Hicks et al.* (1987)).

$$R_b = \frac{2}{\kappa \cdot u_*} \cdot \left(\frac{S_c}{P_r} \right)^{\frac{2}{3}} \tag{3.5}$$

with the dimensionless Schmidt number S_c and Prandtl number P_r. For the quasi laminar boundary layer resistance over sea, the Schmidt number was calculated (see also eq.A.21) as

$$S_c = \frac{\upsilon_a}{\kappa_D} \tag{3.6}$$

with kinematic viscosity of air $\upsilon_a = 17.4 \cdot 10^{-6} \, [Pa \cdot s]$, while the diffusivity coefficient κ_D is different for gas and particles.

3.1.2.1 Diffusion coefficient for gas κ_{D_g}

There are several ways of calculating κ_{D_g}. Here we use a formula for the binary diffusive gas exchange coefficient of a gas in $\left[\frac{m^2}{s} \right]$ as already given by *Fuller et al.* (1966).

$$\kappa_{D_g} = 10^{-7} \cdot T_{at}^{1.75} \cdot \frac{\sqrt{\frac{1}{M_{mol_{air}}} + \frac{1}{M_{POP}}}}{p_{air} \left[\left(\sum_{air} \nu_i \right)^{\frac{1}{3}} + \left(\sum_{POP} \nu_i \right)^{\frac{1}{3}} \right]^2} \tag{3.7}$$

where ν_i are diffusive gas exchange coefficients depending on the molecular structure of the gas. They are to be summed up over the atoms, molecules of the diffusing species (*Fuller et al.* (1966)). p_{air} is the pressure of air which in this case is supposed to be constant. $M_{mol_{air}}$ and M_{POP} are the molecular weight of air and the POP while T_{at} is the temperature of the atmosphere.

3.1.3 Surface or canopy resistance R_c

Many factors play a role in the vegetation canopy resistance R_c and due to lack of input data, only a limited resistance scheme could be used for the model. The resistance scheme follows the Kirchoff's rules of resistance. The approach taken here is based mainly on works of *Wesely* (1989) for climate models. It was adopted to different land use types and also seasons. The canopy surface resistance R_c is calculated using different resistances. The vegetation leaf R_{cf} with its sub-resistances, namely the surface resistance of the upper canopy R_{lu} and the resistance of the ground R_{gs}. This should be just a reasonable approach to face the difficulty of modeling the deposition on the vegetation canopy.

$$R_c = \left(\frac{1}{R_{cf}} + \frac{1}{R_{lu}} + \frac{1}{R_{gs}} \right)^{-1} \tag{3.8}$$

3.1.4 Resistances of the vegetation leaf R_{cf}

Once the gaseous molecule has overcome the resistances at the canopy surface, there are two main pathways into the leaf compartment. POPs can enter the plant either via the stomata or the cuticula and depending on the time of the day, the resistance scheme changes from serial to parallel. The foliar resistance R_{cf} comprises the stomata R_s , mesophyllic R_m and cuticle resistance R_c depending on the LAI and the daily cycle. The laminar leaf boundary layer resistance R_{lbl} acts as a serial resistance above the leaf surface. During daytime, when the stomata are open, the resistances of the leaf act in parallel. During nighttime, the resistance scheme changes and the stomata-mesophyllic pathway is closed. Thus this resistance cannot be overcome.

$$R_{cf} = \begin{cases} \left(R_{lbl} + \frac{1}{R_s + R_m} + \frac{1}{R_{cut}} \right)^{-1} \cdot (LAI)^{-1} & daytime \\ R_{lbl} + R_{cut} \cdot (LAI)^{-1} & nighttime \end{cases} \tag{3.9}$$

3.1.4.1 Stomata resistance R_s

Plants are often exposed to environmental stresses, especially drought, light, high and low temperature that force the plant to protect itself. Stomata is the main

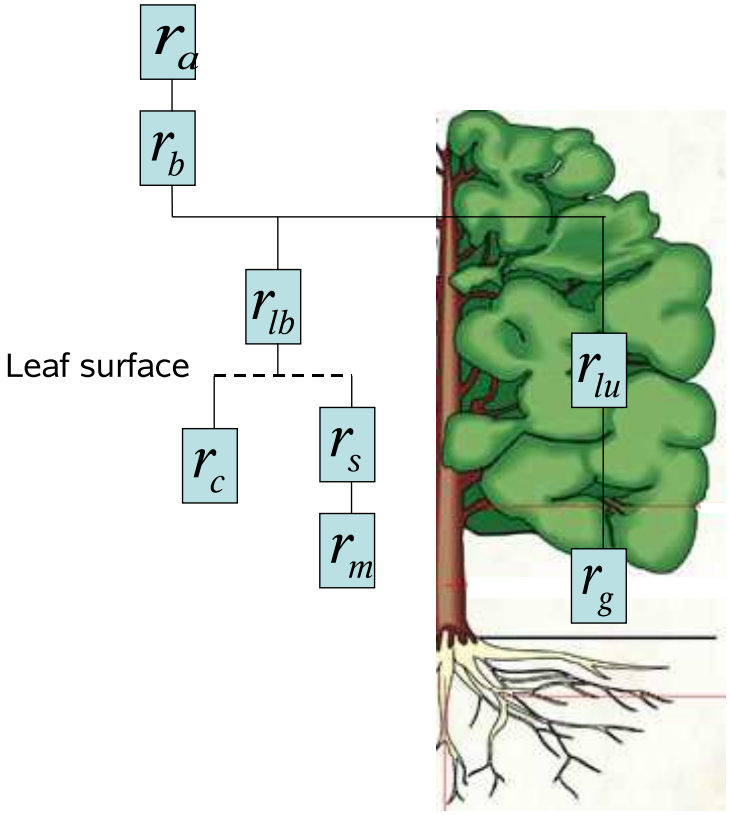

Figure 3.1: Resistance scheme used for the vegetation canopy: r_a aerodynamic resistance,r_b the boundary layer resistance, r_{lbl} leaf boundary layer resistance, r_c cuticle resistance, r_s stomata resistance, r_m mesophyllic resistance, r_{lu} upper layer canopy resistance, r_g ground and soil resistance

photosynthesis organ of leaves which regulates the water potential to a great extent and controls the plant response to drought. Stomata resistance responds unambiguously to soil humidity and humidity in general. It is clear that without data about humidity one has to choose a simpler approach to model this resistance in our case. The stomata resistance R_s of the leaf was therefore calculated with an equation used by *Duyzer and van Oss* (1997)

$$R_s = R_{s_{H_2O}} \sqrt{\frac{M_{POP}}{M_{H_2O}}} \tag{3.10}$$

where $R_{s_{H_2O}}$ is the stomata resistance of water vapour and has been measured in the laboratory and ranges in values between $750 - 5000 \frac{s}{m}$. M_{POP} is the molecular weight of the substance exchanged, while M_{H_2O} is the molecular weight of water (*Duyzer and van Oss* (1997)).

3.1.4.2 Mesophylic resistance R_m

When stomata are open, the leaf/air interface includes the pore interior, lined with mesophyl cells. Each mesophyl cell is covered with a thin wax layer. Since

the intercellular air space forms a continuous system connected with the stomata, these wax layers constitute a continuation of the cuticle on the outer surface epidermis (*Faun* (1990)). When the stomata are open, the ratio of mesophyl surface area to the leaf projected surface area is generally between 10-40. This system of intercellular air space facilitates rapid gas exchange of oxygen, carbon dioxide, water, and air pollutants (*Tao and Hornbuckle* (2001)). Due to lack of data like e.g. solar radiation and in order to represent the effect of the mesophyl resistance, we thus write a combined serial resistance for the stomata as well as for the mesophyl formulated as (*Seinfeld and Pandis* (1998)).

$$R_{sm} = R_s + \frac{1}{3.3 \cdot 10^{-4} H_i^* + 100 \cdot f_i^0} \tag{3.11}$$

f_i^0 is a reactivity factor for the gas and is set to zero here, H_i^* is the effective Henry laws constant of the chemical.

3.1.4.3 Cuticle resistance R_{cut}

The predominant initial site of interception of atmospheric contaminants by vegetation is the plant cuticle. It is a lipophilic polymer membrane with associated cuticle waxes (*Schönherr and Riederer* (1989), *Trapp and McFarlane* (1995)). The biopolymer cutin consists of hydroxylalkanoic acid monomers and associated wax like lipids. The high affinity of cuticle material for lipohilic compounds have been extensively investigated (*Schönherr and Riederer* (1989)). The leaf areas present in most types of vegetation suggest that substantial amounts of organic compounds will be removed from the atmosphere by plants. Riederer and Welke (*Riederer* (1990), *Welke et al.* (1998)) point to the cuticula having a strong impact on the distribution of POPs in the overall vegetation compartment. Because of its structure they proposed to look at the exchange processes with the cuticle matrix separately.
Cuticle/air partitioning coefficients characterize the role of plant surfaces as lipohilic sinks which may also influence the atmospheric residence times of POPs (*Welke et al.* (1998)). The cuticle resistance R_{cut} is an estimation given by *Kerler and Schönherr* (1988) as

$$R_{cut} = \frac{H}{R \cdot T_{at}.} \cdot K_{CW}^{-0.734} \cdot 10^{11.26} \tag{3.12}$$

where R is the gas constant, H is as Henry's coefficient given in $\left[\frac{Pa \cdot m^3}{mol}\right]$ and K_{CW} is the dimensionless cuticula-water partitioning coefficient. K_{CW} is found to be related to the octanol/water partitioning coefficient K_{OW}, which is a well-known chemical property for POPs (*Sabljić et al.* (1990)).

$$K_{CW} = 10^{0.057} \cdot K_{OW}^{0.97} \tag{3.13}$$

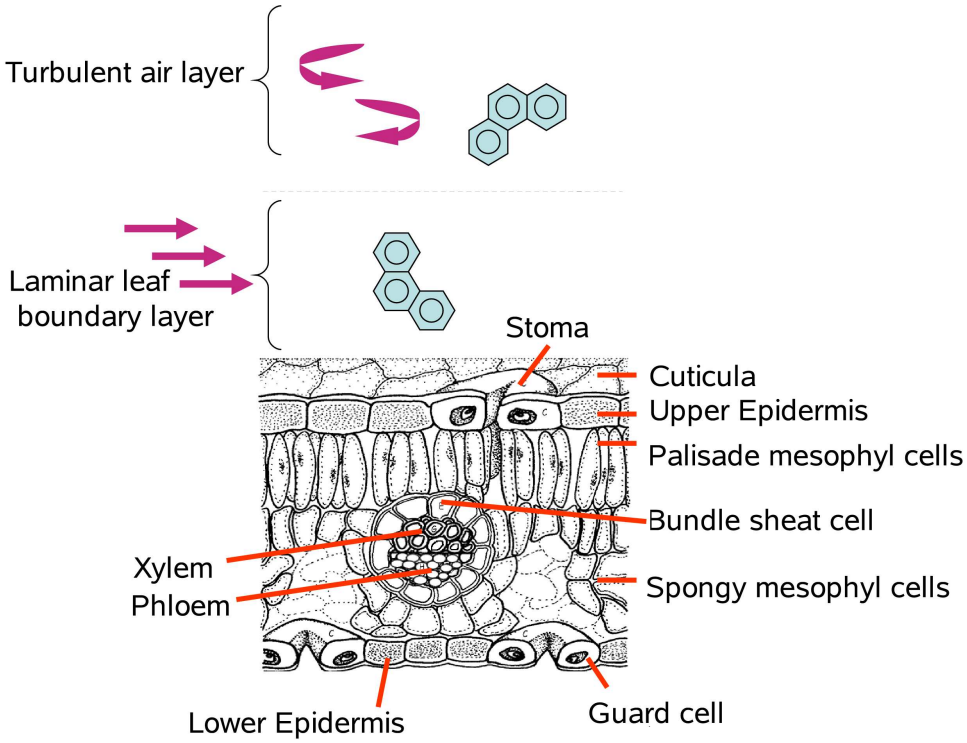

Figure 3.2: Display of the deposition path of chemicals at the laminar leaf boundary layer with the anatomy of an average leaf.

3.1.4.4 Laminar leaf boundary layer R_{lbl}

Recent work on the deposition on leaves (*Barber et al.* (2004)) suggests that the leaf surface is surrounded by another very thin laminar boundary layer, through which the gas or particle has to overcome before deposition. The leaf boundary layer (R_{lbl}) limits the deposition scheme towards the leaf interior as well as the leaf surface. It embraces only the area above the leaf where the flow is no longer turbulent but laminar. Tests including R_{lbl} showed a significant effect for the partitioning of the POPs. The leaf boundary layer resistance (*Ganzeveld and Lelieveld* (1995)) considers the effect of diffusive gas exchange through the thin laminar layer adjacent to the vegetation surface with the approach of (*Hicks et al.* (1987)).

$$R_{lbl} = \frac{1}{4C_{sto}\kappa_{D_g}\alpha} \tag{3.14}$$

where an empirical value of $\alpha = 180$ is used, C_{sto} is the number of stomata open per unit area with $250mm^{-2}$, and κ_{D_g} is the already mentioned gas diffusive gas exchange coefficient.

3.1.4.5 Ground and inner canopy resistances R_{g_s}

The resistance scheme within vegetation canopies is very complex. Many factors influence the deposition. In addition R_c is assumed to be zero for particles hence

only gases are considered for the calculations. Other factors that can influence the deposition are changes in the surface such as snow, rain and dew. The two main resistances R_{lu} and R_{g_s} include the canopy drag and depend on the Henry coefficient H of the chemical. R_{g_s} and R_{lu} vary during the year and both depend on the vegetation type cover. In our model, we follow the approach of *Seinfeld and Pandis* (1998) for the ground and soil resistance $R^i_{g_s}$. The resistance is changing over the year and varies for each land use category.

$$R_{g_s} = \left(\frac{10^{-5} \cdot H}{R_{gs}} \right)^{-1} \tag{3.15}$$

For the upper canopy layer resistance R_{lu} one can write a formulation which changes with the seasonal value of R_{lu_s} the surface and the Henry coefficient.

$$R_{lu} = R_{lu_s} \left(\frac{1}{10^{-5} \cdot H} \right) \tag{3.16}$$

3.2 Setup 1: Dry deposition of particles

Particle deposition can be divided into two main categories, namely the dry and wet particle deposition. Dry particle transport is caused by gravitational settling, the diffusive gas exchange and turbulence causing changes in eddies and fluxes. The probably most important variable for the deposition of particles are its size. It determines all the other factors as well and the deposition velocity. Similar to the gaseous deposition, the dry deposition of particles can be related to the resistance scheme already mentioned. Additionally one has to consider the settling velocity of particles v_s.

$$v_{d_p} = \frac{1}{R_t} = \frac{1}{R_a + R_b + R_a R_b v_s} + v_s \tag{3.17}$$

Including the Junge-Pankow relation (eq. A.8), equation 3.17 can be now written as

$$D_p = \frac{(1-\theta) \cdot v_{d_p}}{h_{mix}} \tag{3.18}$$

The dry deposition velocity of particles v_s depends on many factors and also on the surface onto which the aerosol is falling on. Gravitational settling of the particle is also depending on other forces besides gravity such as the drag force F_{drg} and viscosity ν of the medium through which the particle is falling. We make the assumption that the aerosols in our model are spherical and take into account that falling through a viscous medium is characterized by the Reynolds number Re. It also defines the ratio between the inertial and viscous forces within the fluid.

$$R_e = \frac{r_p \cdot u_\infty}{\nu} \approx \frac{|\overrightarrow{u} \cdot \nabla \overrightarrow{u}|}{|\nu \nabla^2 \ \cdot \overrightarrow{u}|} \tag{3.19}$$

r_p is the particle radius (which is calculated from aerosol input data), $\overrightarrow{u}$ is the velocity, ν is the kinematic viscosity of the medium (in this case air) and u_∞ is the terminal velocity. If Re is small, the viscous forces are dominant. The Stokes law for the drag force originates from the Navier Stokes and the continuity equation.

$$F_{drg} = 6\pi\rho_a \nu r_p u_\infty \tag{3.20}$$

The derivation of this assumes:

- incompressible flow with $\frac{dp}{dt} = 0$
- incompressible fluid with $\nabla \cdot \overrightarrow{u} = 0$
- spherical particles
- flow is continuous and laminar
- conservation of mass, momentum and energy is given
- Reynolds number is very small ($Re << 1$)

3.2.1 Stokes law

Equation 3.20 for the drag force F_{drg}, thus we write

$$F_{drg} = C_D A_p \rho_a \frac{u_\infty^2}{2} \tag{3.21}$$

where C_{D_p} is the drag coefficient, and the particle cross section A_p can be calculated from

$$A_p = \pi r_p^2 \tag{3.22}$$

while the drag coefficient C_{D_p} is depending on the Reynolds number Re

$$C_{D_p} = \begin{cases} \frac{24}{Re} & (Re < 0.1) \quad Stokes \\ \frac{24}{Re} \cdot \left[1 + \frac{3}{16} Re + \frac{9}{160} Re^2 ln\left(2Re\right)\right] & (0.1 < Re < 2) \\ \frac{24}{Re} \cdot \left[1 + 0.15 Re^{0.687}\right] & (2 < Re < 500) \\ 0.44 & Re > 500 \end{cases} \tag{3.23}$$

For the settling velocity v_s of particles we can also write (*Seinfeld and Pandis* (1998))

$$v_s = \frac{2\rho_p g}{9\nu\rho} r_p^2 \tag{3.24}$$

3.3 Setup 2: Vegetation volume

Deposition onto vegetation can also be driven by other factors than the usual settling of gases or particles. Diffusion is considered as one of the main processes at the canopy of a plant. Studies about flux exchange between leaves and their local environment are central for understanding plant-atmosphere interactions. For the exact mechanisms of interactions of the leaf interior with the atmosphere, one has to understand that POPs are found within different locations of leaves.
The conventional knowledge about accumulation of POPs on plants was assuming that a hydrophobic substance would be accumulated by the plant lipids. The conclusion was that plant uptake of POPs would accumulate within the most hydrophobic parts such as the cuticula (*Barber et al.* (2004)). The plant cuticle is a lipophilic polymer membrane with associated cuticle waxes (*Schönherr and Riederer* (1989), *Trapp and McFarlane* (1995)). The high affinities of cuticle material for organic substances and the extensive leaf area in most types of vegetation suggest that substantial amounts of semivolatile organic compounds (SOCs) such as POPs will be absorbed from the atmosphere by this mechanism. Cuticle/air partitioning coefficients characterize lipohilic sinks, which influence the behaviour of lipophilic organic pollutants (*Welke et al.* (1998)).

3.3.1 Tracking POPs within plants

Earlier works (*Riederer* (1990), *Tolls and McLachlan* (1994)) indicated that the partitioning of POPs in the plant is not only related to one single leaf compartment. Today technologies allow us to track chemicals even in plants (figure 3.3). Hence the view of the cuticle as being the main accumulation spot is currently revised. Studies and experiments with PAHs (Anthracene) (*Wild et al.* (2005)) have shown the ability of POPs to be found in very different parts of the leaf. Anthracene was identified in the diffusive section of the epicuticular wax layer, the cell walls of the epidermis, on the external surface of the epidermal cell walls and also within the cytoplasm of the epidermal cells. Apart from the location in several leaf locations, *Wild et al.* (2005) showed that POPs are even able to move inside the leaf compartment from one leaf organ to the other. Metabolism of leaves are not to be neglected when it comes to POP transport within leaves. Earlier the common opinion was that POPs do not interfere with the aqueous medium of plants. Hence, vegetation could get even a more important role in storing and re-emitting (hopping) of POPs. The question how many compartments in a leaf are necessary to represent POP transport needs a complex answer.

One generic overall vegetation compartment *Trapp and Matthies* (1995) used one vegetation compartment to describe the uptake. One-compartment models have been common especially in the beginning of POP box modeling. It consists out of one equation for the calculation of uptake into the vegetation canopy.

Two vegetation compartments *Su* (2005) and *Tolls and McLachlan* (1994) used a second vegetation compartment to better describe the partitioning in the

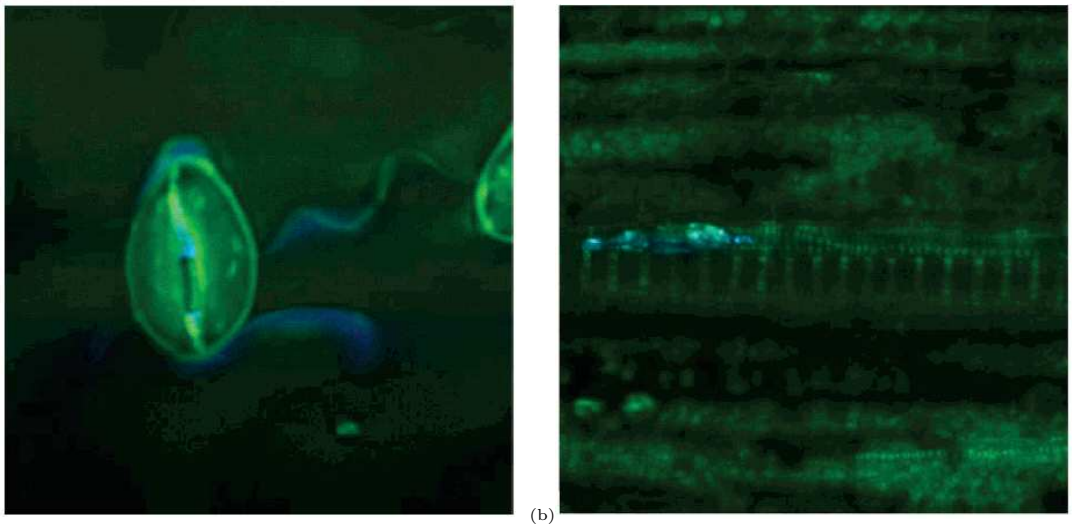

Figure 3.3: Visualization of the air to leaf and within leaf movement of a POP (Phenanthrene) with a two-photon excitation microscopy. a): Phenanthrene (blue) within the stomata and the cuticle cells of a spinach leaf. b): Phenanthrene (blue) within maize xylem walls (green) (*Wild et al.* (2006)).

vegetation interior.

Three vegetation compartments Because of the lipophilic cuticula, partitioning with the outer leaf could be again a too simple representation of processes in/at the leaf canopy. A three vegetation compartments approach would include the surface of a leaf, the aqueous leaf interior and the cuticle matrix and would require more knowledge about the partitioning between the mentioned compartments.

3.3.2 Modeling approach

Our model uses the approach with two vegetation compartments for the diffusive gas exchange mentioned above. The two compartments are the leaf interior and the leaf surface. Uptake into the leaf interior can be via the stomata as well as the cuticula (see figure 3.2). The diffusive gas exchange with the leaf interior is modeled with a fugacity approach and thus the equation for the exchange of POPs from the atmosphere to the leaf interior is (*Duyzer and van Oss* (1997)):

$$\frac{\partial C_L}{\partial t} = \frac{S_L}{R_T} \cdot \left(C_A - \frac{C_L}{K_{PA}} \right) \tag{3.25}$$

C_A is the concentration in the atmosphere (in the gas phase) C_L is the concentration in the leaf-interior. Both are given in $\left[\frac{molec}{m^3}\right]$. S_L is the fraction between the leaf area and the volume of the leaf given in m^2/m^3. R_T is the total resistance for a gas molecule to be deposited on the canopy. R_T is in principle similar like the one for gas deposition on a leaf.

Other works (*Paterson et al.* (1991), *Trapp and Matthies* (1995), *Riederer* (1990)) developed an approach to model the vegetation exchange of POPs based on the knowledge of fugacity. Fugacity describes the tendency of leakage from a compartment of a chemical. Fugacity follows the equation

$$C = f \cdot Z \tag{3.26}$$

where C is the concentration in the media $\left(\frac{mol}{m^3}\right)$, f the fugacity of the chemical (Pa) and Z the capacity of a compartment to uptake the chemical $\left(\frac{mol}{m^3 Pa}\right)$. The advantage of fugacities is that they are comparable.

3.3.3 Reformulating the vegetation compartment

As the box model is defined in burden. The concentration in equation (eq. 3.25) is rewritten and the concentration in the atmosphere C_A is rewritten as atmospheric burden b_A.

$$C_A = \frac{b_A}{h_{mix}} \tag{3.27}$$

The concentration in the leaf is now given as burden in the leaf including the leaf area index (LAI) as

$$C_L = \frac{1}{2}\frac{S_L}{LAI} b_{V_V} \tag{3.28}$$

Furthermore we assume that only POPs in the gas phase interact for the gas diffusive gas exchange with the vegetation. b_{A_g} is the atmospheric burden in the gas phase and follows the aerosol-gas partitioning by Junge-Pankow (*Junge* (1977), *Pankow* (1994a), *Pankow* (1994b), see also A.8) as

$$b_{A_g} = b_A(1-\theta). \tag{3.29}$$

Hence, equation 3.25 can now be written as

$$\frac{\partial C_L}{\partial t} = \frac{S_L}{R_T}\left[\frac{b_{A_g}}{h_{mix}} - \frac{1}{2}\frac{S_L}{LAI}\frac{b_{V_V}}{K_{PA}}\right] \tag{3.30}$$

or also as

$$\frac{1}{2}\frac{S_L}{LAI}\frac{db_{V_V}}{dt} = \frac{S_L}{R_T}\left[\frac{b_{A_g}}{h_{mix}} - \frac{1}{2}\frac{S_L}{LAI}\frac{b_{V_V}}{K_{PA}}\right]. \tag{3.31}$$

From 3.30 and 3.31 we can write for the diffusive gas exchange flux $F_{A\rightarrow V_V}$ from the atmosphere to the vegetation surface

$$\frac{db_{V_V}}{dt} = \frac{1}{R_T}\left[\frac{2LAI}{h_{mix}} b_{A_g} - S_L\frac{b_{V_V}}{K_{PA}}\right]. \tag{3.32}$$

Now, the burden in the gas phase is given by

$$\frac{db_{A_g}}{dt} = -A_V \cdot \frac{db_{V_V}}{dt}, \tag{3.33}$$

thus we obtain

$$\frac{db_{A_g}}{dt} = A_V \cdot \left[\frac{S_L}{R_T \cdot K_{PA}} \cdot b_{V_V} - 2 \cdot \frac{LAI}{R_T \cdot h_{mix}} \cdot b_{A_g}\right] \tag{3.34}$$

Leaf area per volume S_L

The ratio between leaf-surface and leaf-volume S_L was given by *Boehme et al.* (1999). Values vary between $14700\frac{m^2}{m^3}$ for ryegrass and $4000\frac{m^2}{m^3}$ for the creeping thistle. A typical value used as S_L for our calculations is $8000\frac{m^2}{m^3}$.

3.3.4 Leaf-air partitioning coefficient K_{PA}

K_{PA} is a key parameter in the whole air-vegetation exchange. Because there is still uncertainty how to parameterize the leaf-air partitioning coefficient K_{PA}, varying formulations can be found in the literature; even the naming of this partitioning coefficient is sometimes very different. Some authors call it bioconcentration factor, grass-air partitioning coefficient or plant-atmosphere partitioning coefficient. The factors included in the calculation of K_{PA} depend on the complexity of the leaf model and the authors' calculation method.
This work emphasizes the differences between the calculation methods of K_{PA}. Some methods are more based on chemical properties, others focus on plant characteristics. The complexity of the calculation also depends on the plant anatomy and the leaf compartments included.

Method 1 This approach uses for the calculation the octanol-air partitioning coefficient of a POP and the plant specific regression parameters m and n.

$$K_{PA_1} = m \cdot K_{OA}^n \tag{3.35}$$

McLachlan et al. (1995) used also this approach for a two compartments vegetation model. Table (3.2) shows some data for typical vegetation types included in the calculations. This method to calculate K_{PA} as function of K_{OA} has been applied by several authors (*Tolls and McLachlan* (1994), *Paterson et al.* (1991), *Hiatt* (1999)). K_{OA} is the octanol-air partitioning coefficient which can be calculated from the octanol-water partitioning coefficient K_{OW}, the gas constant R, the Henry's law constant H of the compound and the temperature on the vegetation surface T_{veg}.

$$K_{OA} = K_{OW} \cdot \frac{R \cdot T_{veg}}{H} \tag{3.36}$$

Method 2 Temperature has a crucial influence on K_{PA} (*Horstmann* (1990)). For the second method, K_{PA} is modified with a van t' Hoff-type temperature dependence. It is expressed in an integrated form with dependence on the vegetation temperature T_{veg} (*Kömp and McLachlan* (1997)) as

$$K_{PA_2} = 0.003 \cdot K_{OA}^{1.0928} \cdot e^{\left[\left(\frac{1}{T_{veg}} - \frac{1}{T_{ref}}\right) \cdot \frac{\Delta H_{pa}}{R}\right]} \tag{3.37}$$

ΔH_{pa} is the enthalpy given in $\left[\frac{J}{mol}\right]$. ΔH_{pa} is calculated with the Clausius-Clapeyron equation (*Mortimer* (1987))[1].

Method 3 Although the primary site for chemical accumulation appears to be in the cuticle waxes of a leaf (*Paterson et al.* (1991)), a typical leaf composition includes type specific volume fractions of water V_W, air V_A, glycerin V_G, cuticle V_C, proteins V_P, cell lipids V_L. Experiments (*Tolls and McLachlan* (1994)) with azalea leaves and ryegrass, which have different leaf architecture, showed consistently the influence of these factors on the partitioning of chemical components in plants. This K_{PA} method includes five subcompartments and is estimated with the equation by *Riederer* (1990) as

$$K_{PA_3} = V_A + \frac{R \cdot T_{veg}}{H} \cdot (V_W + V_C \cdot K_{CW} + V_G \cdot K_{OW}) \tag{3.38}$$

The volume fractions were assumed to be stable. The cuticula water-partitioning coefficient K_{CW} is derived from the equation (*Sabljić et al.* (1990))

$$logK_{CW} = 0.057 + 0.97 \cdot logK_{OW} \tag{3.39}$$

Method 4 This method is based on the physico-chemical properties and the octanol-air partitioning coefficient of the substance studied (*Paterson et al.* (1991)).

$$K_{PA_4} = 0.19 + \frac{H}{0.7 \cdot R \cdot T_{veg}} + 0.05 \cdot K_{OA} \tag{3.40}$$

Method 5 *Bacci et al.* (1990) considered only the volumetric amount of lipids in the leaf and the octanol partitioning coefficient for the calculation of K_{PA}

$$K_{PA_5} = V_L \cdot K_{OA} \tag{3.41}$$

Method 6 This is the most complicated method to calculate K_{PA}. In addition to the other components mentioned in the previous methods, K_{PA} includes also the major volume of carbohydrates V_F and proteins V_P (*Müller et al.* (1994)).

$$\begin{aligned} logK_{PA} = \quad & \left(\tfrac{R \cdot T}{H}\right) \cdot [V_C \left(1.11 \cdot K_{OW}^{0.097}\right) + V_W \\ & + V_L \cdot K_{OW} + V_F \left(0.0372 \cdot K_{OW}^{0.95}\right) \\ & + V_P \cdot \left(86.2 \cdot K_{OW}^{-1} + 3.7\right)] \end{aligned}$$

[1] $log\left(\frac{p_1}{p_2}\right) = \frac{\Delta H_{pa}}{2.303 \cdot R} \cdot \left(\frac{T_2 - T_1}{T_1 \cdot T_2}\right)$

3.3.5 Canopy removal processes

The degradation process within the canopy involves photolyis and/or biological degradation (*Su* (2005)). POP breakdown processes within the vegetation compartment remain very unclear. Although there is experimental evidence for the degradation reactions of dioxins and DDT-like substance within the vegetation compartment, the uncertainty is still very high because measurements are very sparse. Even the type of leaves (deciduous or coniferous) may influence the degradation of SOCs as measurements indicate (*Niu et al.* (2003), *Niu et al.* (2004)). *Wild et al.* (2005) assumed that the difference between the photolytic and metabolic degradation might be found in the nature of the leaf anatomy. The amount that is residing within and around the lipophilic cuticle matrix is likely been decomposed by light while the compound in the aqueous phase is potentially rather exposed to metabolic degradation. Other factors like UV absorption by wax and lipids may be limiting the breakdown processes too.
It is obvious that photochemical degradation also depends on the substrate the chemical of concern is attached to. Experiments made with polycyclic aromatic hydrocarbons (PAHs) on aerosols, silica, and black carbon found that the behaviour strongly depends on the nature of the surface (*Behymer and Hites* (1985), *Dabestani et al.* (1995), *Barbas et al.* (1996), *Reyes et al.* (2000), *Matsuzawa et al.* (2001) and *Wang et al.* (2005)).

Plant	V_W	V_L	V_C	V_F	V_P	$t_p h$
Spruce needles	58	3.7	2.7	21.6	2.4	2000
Azalea leaves	62	1.3	1.9	9.0	4.2	2000
Grass	62	0.3	0.4	7.8	3.9	2000

Table 3.1: Percentage of volume fractions of the plant specific parameters taken from *Müller et al.* (1994). t_{ph} is the flow time for the phloem removal.

A POP in aqueous phase can undergo various processes such as photoionization, self-sensitized oxidation and attacks by hydroxide radicals (*Miller and Olejnik* (2001). Another result from experiments was the very short half-life cycle of PAHs in the aqueous phase (*Zepp et al.* (1979), *Mill et al.* (1981), *Miller and Olejnik* (2001), *Sabate et al.* (2001)).
This would question again the approach of *Wild et al.* (2005) and demands a more precise definition of such a metabolism. On the other hand the traditional knowledge of POPs accumulating in the lipophilic wax structure would become also plausible due to differences of the degradation. For this model two kinds of removal processes in vegetation canopy were considered. The first one is degradation at the leaf canopy, and the second one removal by transport inside the vegetation medium.

3.3.5.1 Degradation on leafs k_l

Many open questions concerning degradation of POPs the plant surface still exist.Hence, one has to assume degradation processes like in the atmosphere or a degradation like the one chosen for the soil or ignore it. The last option should be

avoided. We assume higher degradation than on the bare soil and thus adopt here a best guess degradation rate, namely the one from the soil surface k_b by three

$$k_l = 3 \cdot k_b \tag{3.42}$$

from which the amount of degradation G_V is calculated as

$$G_V = k_l \cdot b_{V_C} \tag{3.43}$$

3.3.5.2 Removal of POPs by phloem L_{V_V}

	Grass	Forest canopy	
		coniferous	deciduous
m	22.91	38	14
n	0.445	0.69	0.76

Table 3.2: m and n values for the K_{PA} calculation taken from *Thomas et al.* (1998) and *McLachlan and Horstmann* (1998)

The removal rate τ_{ph} of POPs within the vegetation volume is calculated with the equation given by the reciprocal of the removal time scale τ (*Duyzer and van Oss* (1997)) as:

$$\tau_{ph} = \frac{t_{ph}}{V_{ph}} \frac{H}{R \cdot T_{veg}} K_{PA} \Longrightarrow L_{V_V} = \frac{1}{\tau_{ph}} b_{V_V} \tag{3.44}$$

t_{ph} is the removal flow time of the phloem and given with $2000s$, while the V_{ph} is the phloem volume fraction of the leaf (taken as $6 \cdot 10^{-3}$). T_{veg} is the temperature of the leaf given with the canopy temperature. H is the Henry coefficient while R is the gas constant. Other possible removal processes like the dilution by growth were not included. Generally a dilution by growth leads to a decrease of concentration in the leaf.

Chapter 4

Vegetation cycles and canopy structures

The inclusion of defoliation and the soil under the vegetation canopy as additional compartment requires the implementation of several new processes. New cycles introduced beside the defoliation are: Degradation on the soil under the vegetation canopy, volatilization back to the atmosphere and/or accumulation in the soil under the vegetation canopy. With the additional process of litter transport, one has to consider that so far the soil was interpreted as a bare soil not interacting with the vegetation but only the atmosphere. At this point one must change the box setup since now interactions between the vegetation and soil take place. The area of total soil $a_{S_{tot}}$ gets the size of vegetation a_V area plus the surface not covered with plants a_B, or more simple: the whole land mass in the model will from now on be assumed as soil. However, processes on the soil under the vegetation canopy and bare soil are also temperature driven and thus they will be distinguished. Beside that, defoliation takes place only on the soil under the vegetation canopy.

$$a_{S_{tot}} = a_V + a_B \tag{4.1}$$

The change of surface has effects in formulating the flux from and to the soil. Due to the temperature difference, several processes as volatilization or degradation on the two soil compartments are calculated with two different formulae.

4.1 Setup 3: Litter fall

In our model we assume that litter fall takes place only if $\frac{d\,LAI}{dt} < 0$. This approach may fit for a deciduous forest with annual change of canopy but could lead to an oversimplification of processes for evergreen canopies without an pronounced vegetation cycle. Both vegetation compartments are involved in the defoliation and as a first order approach one can write for both canopy compartments

Vegetation Canopy: $\left[\frac{molec}{m^2 \cdot s}\right]$

$$T_{V_C} = \begin{cases} 0 & if\ \frac{d\,LAI}{dt} \geq 0 \\ \frac{d\,LAI}{dt} \cdot b_{V_C} & if\ \frac{d\,LAI}{dt} < 0 \end{cases}$$

Leaf volume: $\left[\frac{molec}{m^2 \cdot s}\right]$

$$T_{V_V} = \begin{cases} 0 & if\ \frac{d\,LAI}{dt} \geq 0 \\ \frac{d\,LAI}{dt} \cdot b_{V_V} & if\ \frac{d\,LAI}{dt} < 0 \end{cases}$$

The soil under the vegetation canopy compartment gets the full amount of burden released from the vegetation compartments. b_{V_C} and b_{V_V} are the burden of the vegetation canopy and vegetation volume subcompartments.

4.1.1 Soil processes

Root-uptake from contaminated soils may be translocated in the plant or better into the stem of the plant. However many things are still not understood how the distribution within the plant and its possible remission functions. To which extent a lipophilic substance can enter into the vegetation root compartment from contaminated soil depends mainly on the water solubility, the octanol water partitioning coefficient K_{OW} and factors such as organic content of the soil and the plant species (*Simonich and Hites* (1995)). It is therefore unlikely for most of the organic pollutants of concern that they would enter to a larger extent via the inner root and xylem of a plant (*Meneses et al.* (2002)). In a first assumption one can say that lipophilic pollutants are not translocated within the plant and the metabolism is not significant (*Simonich and Hites* (1995)). Thus this process has not been included.

Volatilization from the vegetated soil compartment In our approach, the vegetation canopy does not represent a resistance for the flux back to the atmosphere. No boundary layer resistance is involved in the revolatilization back into the atmosphere. For the volatilization from the vegetated soil V_{V_S}, we assume the same process like for bare soil volatilization V_B. The only significant difference is the inclusion of the vegetated soil temperature T_{V_S}

$$V_{V_S} = V_B\left(T_{V_S}\right) \tag{4.2}$$

Leaves falling on the surface are not hindering the volatilization of the chemicals on the ground either. They are currently considered as part of the soil compartment. An instantaneous decomposition and mineralization and further volatilization is assumed.

Dry deposition on soil under the vegetation canopy The big leaf model assumes that the dry deposition process encompasses the top of the vegetation canopy. As follows, a particle or gas molecule that arrives at the canopy will be caught by the vegetation canopy unless the LAI is smaller than 1 m^2/m^2. Deposition of gases and particles on the soil under the vegetation canopy is only possible and linear if the LAI gets smaller than one.

$$D_{V_{S_d}} = \begin{cases} 0 & if\ LAI \geq 1 \\ (1 - LAI) \cdot (D_g + D_p) & if\ LAI < 1 \end{cases} \left[\frac{molec}{m^2 s}\right] \tag{4.3}$$

and as consequence the vegetation canopy would get a similar value.

$$D_{V_{C_d}} = \begin{cases} D_g + D_p & if\ LAI \geq 1 \\ LAI \cdot (D_g + D_p) & if\ LAI < 1 \end{cases} \left[\frac{molec}{m^2 s}\right] \tag{4.4}$$

Soil atmosphere interaction Defoliation causes a larger area of soil exposed to the atmosphere. A possibility to describe indirectly the area of soil under the vegetation canopy could be via a modified Lambert-Beer extinction coefficient I_z, which describes the decrease of shortwave radiation underneath the canopy (*Monsi and Saeki* (1953)). This extinction coefficient will be used to simulate the amount of wet deposition under the vegetation canopy.

$$I_z = I_0 \cdot e^{-k_p \cdot LAI} \tag{4.5}$$

I_z is the radiation that arrives at the surface of a soil under the vegetation canopy which is also called the photosynthetic photon flux density (PPFD) (*Hirose* (2005)), while I_0 is the radiation in the atmosphere and I_s the ratio in percent of the total light namely $I_s = \frac{I_z}{I_0}$. k_p describes the attenuation coefficient valid for the plant type. In agricultural fields, meadows (grass land) more than $\frac{3}{4}$ of the leaves are erectile (with a leaf direction more than 45^0) so that the attenuation coefficient is between $k_p = 0.3 - 0.5$. Vegetation with more planophile and plagiophile leaves is described with a factor of $k_p = 0.7$. Deciduous and also tropical rain forests with very dense canopies (LAI >7) intercept most of the light and rain in the crown height. The leaf density is nevertheless just $2.5 - 3.5 m^2 m^3$ because of the decline in the stem space (*Yoda et al.* (1978)). Their attenuation factor is usually very high ($k_p = 0.8 - 1.0$) (*Larcher* (1994)).

Canopy	k_p
meadows	0.4
agricultural plants	0.4
planophile deciduous forest	0.8

Table 4.1: attenuation factors k_p for different plant types taken from *Larcher* (1994)

Wet deposition on the vegetation covered soil Neglecting the effects of turbulence, the case of wet deposition has been described with the Lambert extinction coefficient by Glydekaerne (*Glydekaerne et al.* (1999)) who tested the

ratio of pesticides that arrived on the soil under the vegetation canopy. Thus the wet deposition on the soil under the vegetation canopy $D_{V_{S_w}}$ is the fraction of total wet deposition D_w which can also be used to describe the wet deposition process occurring on and underneath the canopy.

$$D_{V_{S_w}} = I_s \cdot D_w \tag{4.6}$$

Wet deposition D_w contains an additional dripping from leaves f_L and the stem f_S, which is an indirect deposition process. Following the water budget of plants, one can define the dripping ratio f_T (*Schnock and Duvigneaud* (1971)). The rain which is first intercepted by the canopy and drips off the leaf surface or that runs down the stem, is formulated as transfer from the vegetation surface to the soil under the vegetation canopy. We reformulate the dripping rate

$$f_T = f_L + f_S \tag{4.7}$$

as a direct removal from the atmosphere. f_S is given with 4 to 10 percent according to the amount of vegetation cover while f_L is depending on the vegetation type and the amount of rain and the LAI (74%). For our calculation the total values taken from the dripping from tree top and stem flow were varying with LAI between 78 and 90 percent (*Schnock and Duvigneaud* (1971)). No threshold value for the canopy dripping is included; this means that all the wet deposition arriving at the canopy top will start to drip. The total fraction of wet deposition arriving at the soil under the vegetation canopy f_D can now be written. The interception ratio f_C of the vegetation canopy is the amount of rain that remains on the vegetation canopy and/or gets re-volatilized.

$$f_D = (I_s + (1 - I_s) \cdot f_T) \tag{4.8}$$

and thus we define

$$f_C = 1 - f_D \tag{4.9}$$

and eventually the wet deposition onto soil under the vegetation canopy $D_{V_{S_w}}$ and on the canopy $D_{V_{C_w}}$ is written as

$$D_{V_{S_w}} = D_w \cdot f_D \longrightarrow D_{V_{C_w}} = D_w \cdot f_C \tag{4.10}$$

4.1.2 Leaf longevity ϑ

So far, the phenology of our model is based on the change of temperature and leaf defoliation due to variation of leaf area index throughout one year. Litter fall also occurs without the change of LAI. Some vegetation types (such as the evergreen ones) renew their canopies regardless to seasonal cycles.
Patterns of leaf production and leaf senescence vary among species (table 4.2). For the case of decidous trees, it can differ between a simultaneous canopy production without a later leaf renewal at the beginning of the growing season and the evergreen leaf production independent of seasonality. Needle trees usually keep their needles longer than one year. Annual herbs and many tropical trees produce their

leaves continuously during the vegetative growth (*Ackerly et al.* (1996)). Many deciduous trees and shrubs have a simultaneous canopy production at the beginning of the growing season without later leaf turnout (*Kikuzawa* (2003)). Neglecting the fact of leaf senescence would be problematic.
To calculate the annual leaf turn over fraction in our model, one can refer to the annual carbon mass of leaves c_{m_l}. The carbon mass of leaves is defined as the fraction between the LAI and the specific leaf area (SLA)[1]. SLA defines leaf area per unit of leaf carbon mass $(\frac{m^2}{kg})$. With this method we assume

$$c_{m_l} = \frac{LAI}{SLA} \Longrightarrow \frac{dc_{m_l}}{dt} = \left(\gamma - \frac{1}{\vartheta}\right) \cdot c_{m_l}. \tag{4.11}$$

The growth rate γ may be compensated by the litter fall which is represented by $1/longevity$. In nature γ is basically larger than $1/\vartheta$ during the growth period of the plant. Due to lack of further knowledge we assume that the leaf growth compensates the litter fall at every time.

$$\gamma = \tfrac{1}{\vartheta} \tag{4.12}$$

Otherwise the total annual overproduction and removal of leaves from the vegetation canopy would be taken into account by

$$\frac{dLAI}{dt} = \left(\gamma - \tfrac{1}{\vartheta}\right) \cdot LAI \tag{4.13}$$

The litter fall due to leaf senenscence introduces some additional transport of POPs from the canopy to vegetated soil, even if the leaf area index is constant in time. The total burden in the leaf mass is given by

$$b_{V_V} + b_{V_C} = c_{\mathrm{POP}} \cdot \frac{LAI}{SLA}, \tag{4.14}$$

where c_{POP} is the total mass of POPs divided by the total leaf mass. Differentiating with respect to time yields

$$\frac{d(b_{V_V} + b_{V_C})}{dt} = \frac{dc_{\mathrm{POP}}}{dt} \cdot \frac{LAI}{SLA} + \frac{c_{\mathrm{POP}}}{SLA} \cdot \frac{dLAI}{dt} \tag{4.15}$$

Hence, the equation for the plant renewal consists of two terms: the leaves that still grow and take up POPs and the ones that are being removed. In order to take this transport into account we assume that the concentration of POPs in leaves is independent of leaf age. In addition, we neglect the first term of the right hand side of the above equation. This equation can then be simplyfied to

Vegetation soil:

$$R_V = -\frac{1}{\vartheta}\left(b_{V_V} + b_{V_C}\right)$$

[1]The implementation may slightly differ from these definitions

The approach to model leaf senescence is basically a very primitive one and that the leaf dynamics depend on many other factors which we cannot represent in our model (e.g. nitrogen concentration, nitrogen fixing, nitrogen resorption proficiency, light availability (*Killingbeck* (1996), *Hikosaka* (2005)). Including the litterfall transfer from both vegetation leaf compartments T, the vegetation renewal rate R, the different dry and wet deposition fluxes D the additional volatilization V and degradation G the change rates for the different compartments become:

Vegetation Soil:

$$\frac{d\,b_{V_s}}{dt} = D_{V_{S_w}} + D_{V_{s_d}} - V_{V_S} - G_{V_S} + T_{V_C} + T_{V_V} + R_V \tag{4.16}$$

Atmosphere:

$$\frac{d\,b_A}{dt} = a_V \cdot V_{V_S}$$

Vegetation Canopy:

$$\frac{d\,b_V}{dt} = \left(D_{V_{C_w}} + D_{V_{C_d}}\right) \cdot a_V - T_{V_C}$$

Vegetation Volume:

$$\frac{d\,b_V}{dt} = -T_{V_V}$$

4.2 Setup 4: Multilayer vegetation

Vegetation canopies are complex structures with many factors influencing the exchange of gases and particles. The light environment and the particular leaf properties in a hard wood forest (or in vegetation in general) influence indirectly the exchange flux of POPs significantly. Profiles of multilayer canopies may be necessary because multiple environmental variables could then be incorporated into estimation of the canopy POP net flux. In a next step a two layer vegetation configuration is tested versus the conventional one layer big-leaf layout. Because there is no radiation included in the model, one must use simplified assumptions (fig. 2.1). Distinctions are made between the shade and sunlit parts of the vegetation canopy. The assumption is that the sun is in the zenith and we use the Lambert-Beer extinction coefficient. The sun/shade fraction of the vegetation surface for the canopy depth x is written as (*Dai et al.* (2004)).

$$f(x)_{Sun} = e^{-k_p \cdot x} \tag{4.17}$$

and the amount of leaf area index in the sun L_{Sun} is given with the formulation

$$L_{Sun} = \int_0^{LAI} f(x)_{Sun} dx = \frac{1}{k_p} \cdot \left(1 - e^{-k_b \cdot LAI}\right) \tag{4.18}$$

and the shadow part of the plant L_{Sha} is described as

$$L_{Sha} = LAI - L_{Sun} \tag{4.19}$$

As a consequence we calculate now 2 different temperatures of vegetation The sunlit and the shaded fractions are given with.

$$F_s = \frac{L_{Sun}}{LAI}; \qquad \Longrightarrow F_c = \frac{L_{Sha}}{LAI} \tag{4.20}$$

Vegetation temperatures In the big leaf model only one temperature is applied (which is the sunlit temperature on the top of the canopy). The multilayer model distinguishes a sunlit and a sunshade temperature. For reasons of simplification and no further available information the temperature of leaves in the shade is also the temperature of the vegetation covered soil.

4.2.0.1 Wind profile of the canopy

An idealized air flow through the canopy was suggested by *Cionco* (1965) and adopted here. The wind profile becomes then

$$u(z) = u_H \cdot exp\left[a\left(\frac{z}{H} - 1\right)\right] \tag{4.21}$$

The attenuation coefficient of a can be derived for different vegetated surfaces from table (4.1). $u(z)$ represents the horizontal wind speed at height z within the canopy. u_H is the horizontal wind speed at the canopy top; H represents the canopy height.

The coefficient a is just a conservative measure of response of the air flow to the various types of vegetation and helps to classify the density, flexibility and general structure of a canopy. Although, it may be too simple to calculate the wind speed with such a formula because if the leaf area density would increase with the depth of the canopy the attenuation coefficient would increase aswell. For the 2-dimensional leaf setup, the assumption is made that the leaves are distributed all over the leaf area equally. The canopy height for the wind speed calculations is estimated by the fraction of LAI in the shadow L_{Sha}, respectively in the sun L_{Sun}.

Canopy	ϑ
Deciduous Broadleaf Forest	1.0
Deciduous Needleleaf Forest	1.0
Evergreen Broadleaf Forest	0.5
Evergreen Needleleaf Forest	0.26
grasses C3 and C4	1.0
evergreen shrubs	0.26

Table 4.2: Values taken for the annual leaf turnover fraction values taken from the BIOME-BGC model

Assumptions Due to lack of further knowledge, only a limited amount of vegetation processes are split up into this 2-layer vegetation setup. Several simplifying assumptions are made for the calculations of the multi-layer vegetation.

The deposition processes at the vegetation surface (gas deposition, particle deposition, wet deposition) are assumed to be equal on both parts of the vegetation canopy. Volatilization, degradation and gas-diffusion into the vegetation volume is proportional to the given LAI fraction. They are also in dependence to the appropriate temperature and wind speed of the canopy layer. The processes of volatilization (V_V), degradation (G_V), litter fall (T_V), gas diffusion ($F_{V_V \to A}$, $F_{A \to V_V}$) and phloem removal (L_{V_V}) are split into shaded and sunlit fractions. For the different compartments the change rates then become:

Canopy	Investigator	*a*-value
Immature Corn	Wright :1965	2.82
Oats	Allen :1965	2.80
Wheat	Inoue et al. 1963	2.45
Rice	Nakagawa :1965	1.62
Larch Trees	Ohmstede :1964	1.06

Table 4.3: Values for the attenuation coefficient from *Cionco* (1972)

Atmosphere:

$$\frac{d\,b_A}{dt} = +\sum V_V \cdot a_V - \sum D_V \cdot a_V + \sum F_{V_V \to A} \cdot a_V$$

Vegetation Surface:

$$\frac{d\,b_V}{dt} = \sum \left(D_{V_{C_w}} + D_{V_{C_d}} \right) \cdot a_V - \sum G_V - \sum V_V - \sum T_{V_C}$$

Vegetation volume:

$$\frac{b_{V_V}}{dt} = \sum F_{A \to V_V} - \sum L_{V_V} - \sum T_{V_V}$$

Vegetation Soil:

$$\frac{d\,b_{V_s}}{dt} = D_{V_{S_w}} + D_{V_{s_d}} - V_{V_S} - G_{V_S} + \sum T_{V_C} + \sum T_{V_V} \tag{4.22}$$

Chapter 5

DDT box model study

5.1 Global Process study for DDT

The process study for DDT is split in two major blocks. The first block which includes all the big leaf vegetation processes, does not contain phenological processes. The simulation experiment was run with the same 'global' shrub type vegetation characteristics for all the latitudes (with the exception of zones assumed to be deserts). Important variables like e.g. canopy structure, canopy height, annual leaf turnover are supposed to be the same all over. LAI was the only canopy factor which was allowed to vary in different climate zones. Big leaf vegetation setups (setup 1) include the prescribed gas deposition, calculated gas deposition and the calculated particle deposition. For the representation of the diffusive gas exchange process (setup 2), the vegetation compartment is the sum of two vegetation subcompartments, namely the vegetation surface and volume. The first three setups with big leaf surface are compared, followed by a sensitivity study of the diffusive gas exchange process. As an additional experiment the global processes are run without any vegetation cover at all. The goal of this experiment was a general quantification of the influence of vegetation.
In the second part of the experiments, the phenological processes like litter fall, vegetation renewal (setup 3) and the canopy structure (setup 4) are investigated. The goal of such an evaluation is to study the sensitivity to physical factors (aerosols, wind speed etc.) and to make a qualitative comparison of overall sensitivity and predictions for long term trends. Also validation and ranking of the described processes is attempted.

5.1.1 Application pattern

For the 100 year simulations a market life time of 70 years of both DDT and PCB-52 was assumed (see also 2.3). A steep increase of DDT usage simulates the market introduction and followed by a peak level of application after 25 years. This high application period follows a slow decrease of DDT usage until year 70. The usage of year 70 to 100 simulates a reduced usage of both POPs after their ban.
The vegetation type simulations are 7 year (ca. 2500 days) runs under stable

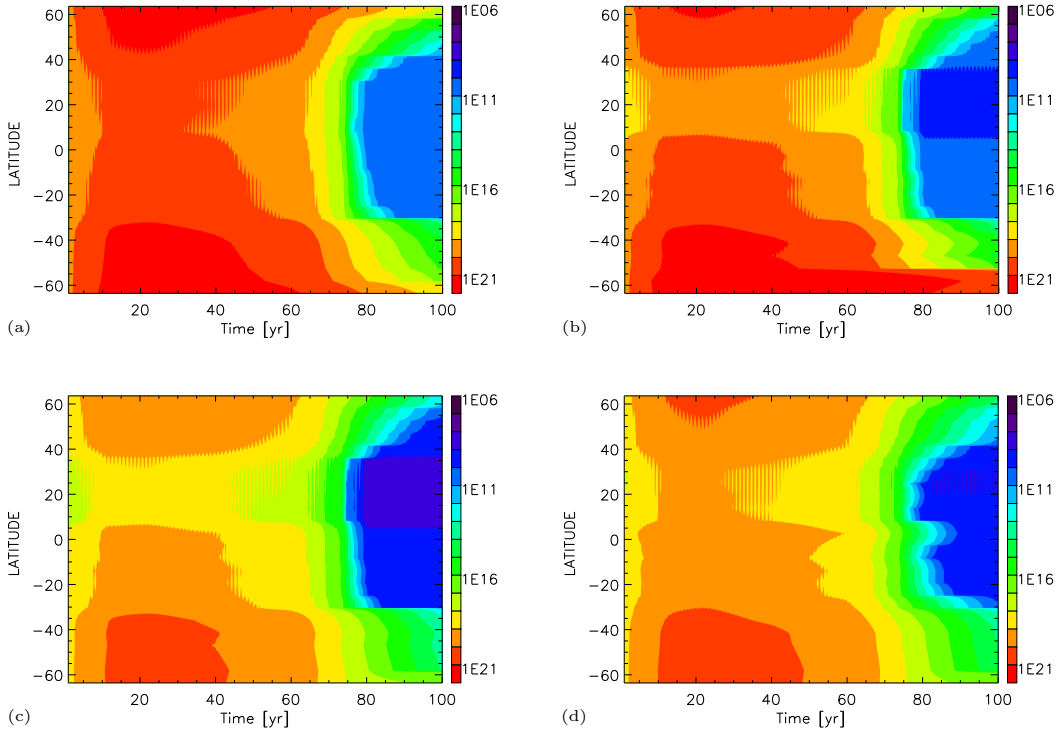

Figure 5.1: Box model run 100 years with setup 1, Fig. a) Overall burden b_{tot} of DDT gas deposition prescribed. b) Overall burden of DDT gas deposition calculated. c) and d) Overall burden of DDT particle deposition at high ($13\frac{m}{s}$) and low ($2.5\frac{m}{s}$) wind speed. All values are given in $\frac{molec}{m^2}$

climatic conditions and a one year impulse application. After this first year the application is shutdown to zero.

5.1.2 Setup 1: Gas and calculated particle deposition

5.1.2.1 Global overall burden b_{tot}

Deposition schemes studied with DDT manifest that each deposition process has influence in terms of b_{tot} in the environment. Beside the deposition process, the different georeferenced physical and meteorological conditions have a major impact on the overall contamination b_{tot} (figure 5.1). Several factors are to be held responsible for the differences of b_{tot} across the 'global box'. Temperature, variation of land fraction and the differences of day length (leading to changes in the OH-radical degradation cycles) can all influence b_{tot}.

Larger differences of b_{tot} between the different deposition parametrizations are obtained around the equator, as well as in the temperate northern latitudes. In both areas the highest values for b_{tot} are simulated with the prescribed gas deposition setup (figure 5.1 a). Differences of b_{tot} between the two gas deposition schemes in the cold northern areas with a large continental fraction are not large. The calculated gas deposition has similar values like the test with prescribed gas

deposition. Obviously the influence of temperature must be the dominant factor in cold latitudes. The same can be seen in the high latitudes of the southern hemisphere with its larger water surface.
Differences between the calculated and the prescribed gas deposition are smaller than between particle and gas deposition. This is observed for both wind speeds. Particle deposition has the effect of a large reduction of b_{tot} (figure 5.1 c). Compared to the version of calculated gas deposition the amount of reduction is in the range of about one order of magnitude at every grid point. The reasons for a lower b_{tot} of the particle deposition are probably related to the aerosol-gas partitioning of DDT.
Differences between the prescribed and the calculated gas deposition are rather small (figure 5.3, and 5.4), but the ratio volatilization flux/b_{tot} is higher by at least one order of magnitude. The degradation of DDT is obviously faster attached on aerosols than only in the gas phase. The effect of different wind speeds is seen especially in areas with more land fraction. Wind speed is an important factor concerning b_{tot} and its sensitivity is visible in all the climatic zones. Higher wind speed could be the reason for a longer residence of DDT in the atmosphere and thus degradation is enhanced (figure 5.1 d). However, in the cold higher latitudes this effect is attenuated and this process probably is only important during the summer period. It is evident that vegetation is especially in large cold continental areas an important factor for the overall distribution of DDT. Runs without vegetation cover show for both wind speeds a strong drop of the land fraction and switch of POP burden to the atmosphere (figure 5.2). Areas with smaller continent fractions (e.g. in the tropics and in southern latitudes) do not have such an large difference between vegetated and non vegetated surfaces. This is seen especially for low wind speed. The relationship between the land surface fraction, the wind speed and temperature is complex and no definite rule can be applied.
The various setups are not equally sensitive to changes in wind speed. E. g., the setups using a prescribed deposition velocity of DDT are sensitive to changes in the wind velocity only because of changes in volatilization leading to an overall small sensitivity to wind velocity (figure 5.2). Despite its lower overall contamination level, the land fraction of b_{tot} in the more continental northern hemisphere is higher with high wind speed. The filtering effect of the canopy is also correlated with temperature and is more pronounced in the northern hemisphere. Higher wind speed also means less transport towards the ocean and more potential accumulation on the continent. This is certainly partly explained by the larger vegetation fraction in this area.
In the southern hemisphere even the opposite trend can be the case. A higher overall land contamination is reached without vegetation. In this case, the influence of vegetation is more ambiguous, and could be related to the temperature and the higher ocean fraction. If one compares b_{tot} in relation to the land mass available, one gets a higher land fraction of b_{tot} of DDT in the mid latitudes, especially for high wind speed (figure 5.2).
In all runs non vegetated simulations have larger fractions in the ocean for the northern hemisphere. In the southern latitudes, differences between vegetated and non vegetation runs are very small, mainly because of the small land fraction.

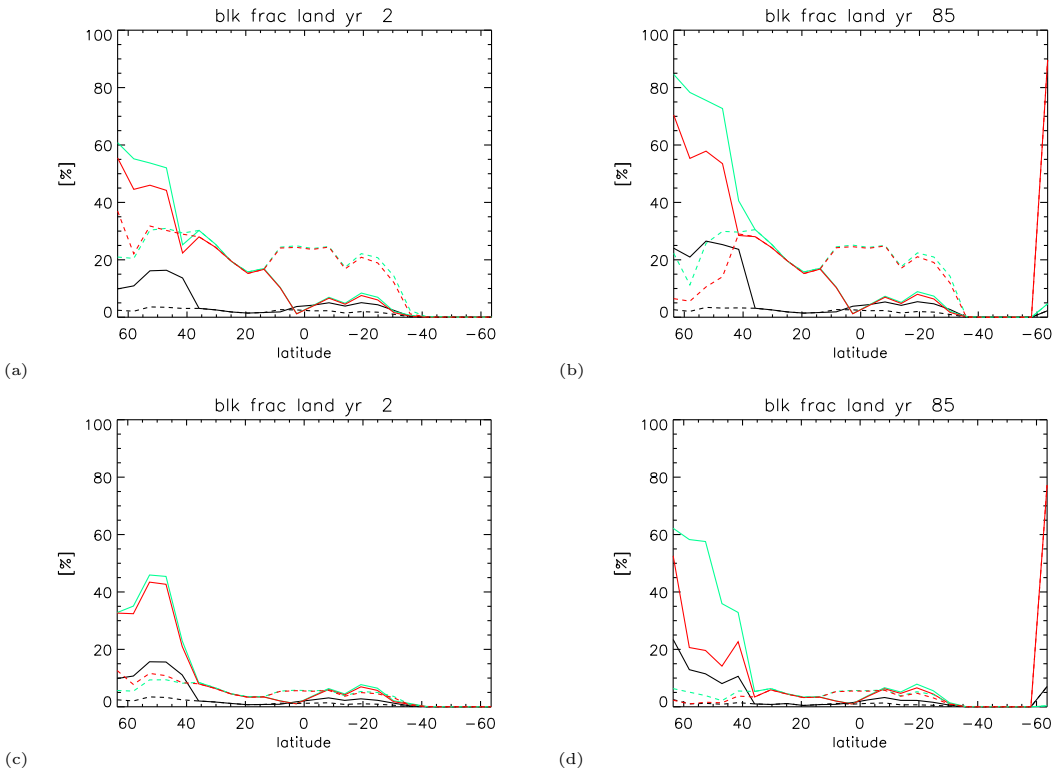

Figure 5.2: Box model setup 1, meridional section for the annual average DDT fractions on land of the overall contamination at high (fig a and b) and low (figure c and d) wind speed for the years 2 and 85. Black lines: prescribed deposition, green lines: calculated gas deposition, red lines: calculated particle deposition. The dashed lines are the non-vegetation runs.

The ocean fraction is higher towards the end of all the simulation period and a final deposition of DDT into the ocean must be assumed (figure 5.5). Therefore the land compartment can be considered as a storage before the final transport towards the ocean. The influence of the wind speed must be seen as an important factor the rapid transfer of DDT into the ocean.

5.1.2.2 Global compartment distribution DDT

The results of the different deposition processes reveal a clear interaction between the distribution among compartments and the deposition processes (figure 5.2, 5.5). For strong wind the land fraction of b_{tot} is in general higher. However, the influence of zonal surface fraction and temperature cannot be neglected. The lowest values of the DDT overall fraction on the continent are found for the (first) prescribed gas deposition method, while values of the other two schemes are relatively similar. This is valid for both wind velocities simulated and also remains relatively stable over time. For the calculated gas deposition and the included particle deposition, vegetation increases the land fraction of DDT North of 35N to almost 30 to 40% compared to only 20 to 25% with prescribed deposition (figure 5.2).

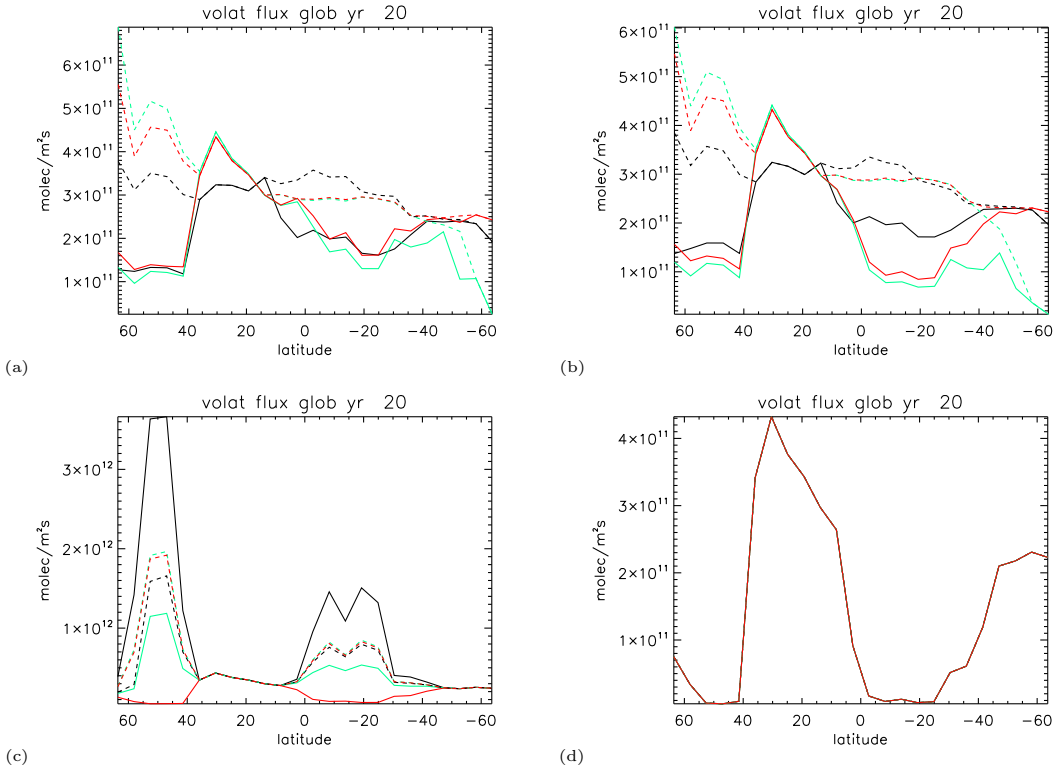

Figure 5.3: Box model setup 1: Meridional section of the 100 years simulations. Annual Mean volatilization flux of DDT in $\frac{molec}{m^2 s}$ for big leaf vegetation (setup 1) with high (a) and low wind (b) speeds at year 20. Black lines: prescribed deposition case, green lines: calculated deposition case, red lines: particle deposition case. Dashed lines: Annual mean volatilization flux without vegetation. c) and d) are sensitivity studies for setup 2 c) and 3 d) with different K_{PA} values. Full lines: K_{PA_1}: black, K_{PA_2}: green, K_{PA_3}: red dashed lines: K_{PA_4}: black, K_{PA_5}: green, K_{PA_6}: red

5.1.2.3 Global flux analysis

Explanations for the importance of processes can also be found by studying the fluxes between the compartments. All the tested box model setups have a much higher volatilization without a vegetation canopy (figure 5.3). This is consistent for the whole North-South section. As there is more volatilization, more DDT is being removed by OH-radicals (figure 5.3).
Correlations between fluxes, compartment distributions and b_{tot} are difficult to establish. For the case without vegetation, a proportional relationship between land fraction and volatilization may be estimated, while there is no such ratio for the case with vegetation (figure 5.2 and 5.3). An assumption could be that the differences of b_{tot} for different speeds are mainly not caused by volatilization. Volatilization flux differences between the three studied methods are not too large, and neither are the discrepancies between the wind speed. Surface degradation could be more important than it is assumed so far.
Unlike the volatilization, deposition fluxes are more related to the choice of parametriza-

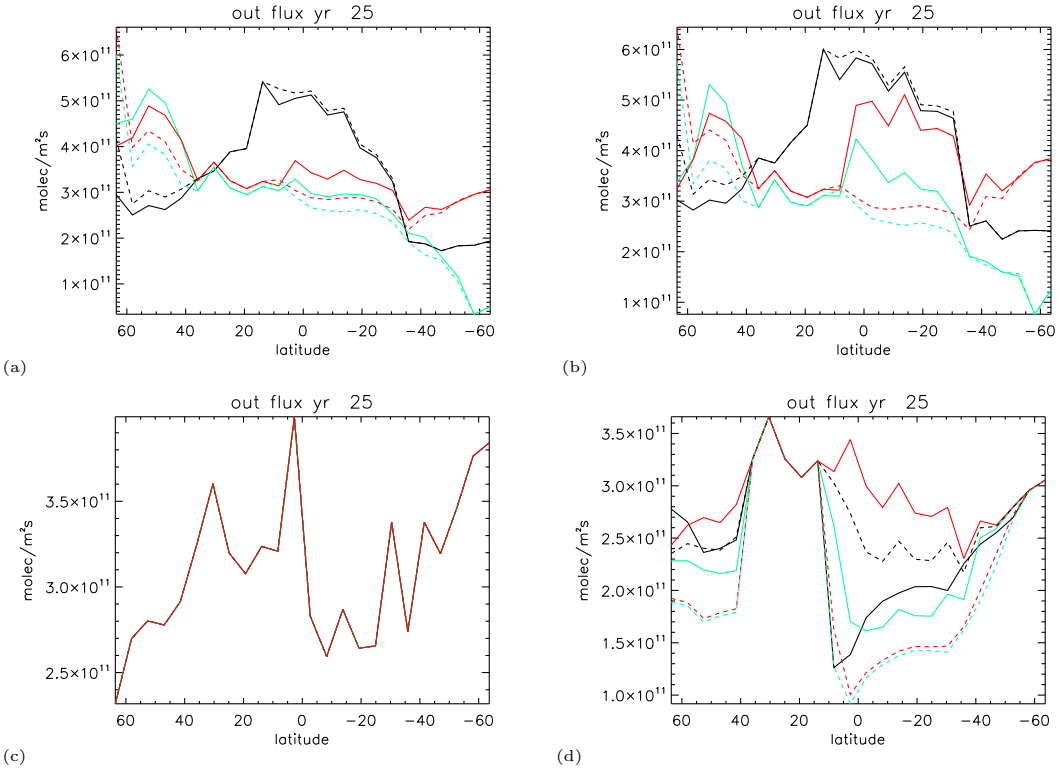

Figure 5.4: Annual mean deposition flux of DDT for setup 1 with high (a) and low wind (b) speeds. Prescribed deposition: black line, Calculated deposition: green lines, Particle deposition: red lines. c) and d) Annual Mean deposition flux (setup 3 and 4) for DDT with different K_{PA} coefficients; full lines: K_{PA_1}: black, K_{PA_2}: green, K_{PA_3}: red Dashed lines: K_{PA_4}: black, K_{PA_5}: green, K_{PA_6}: red

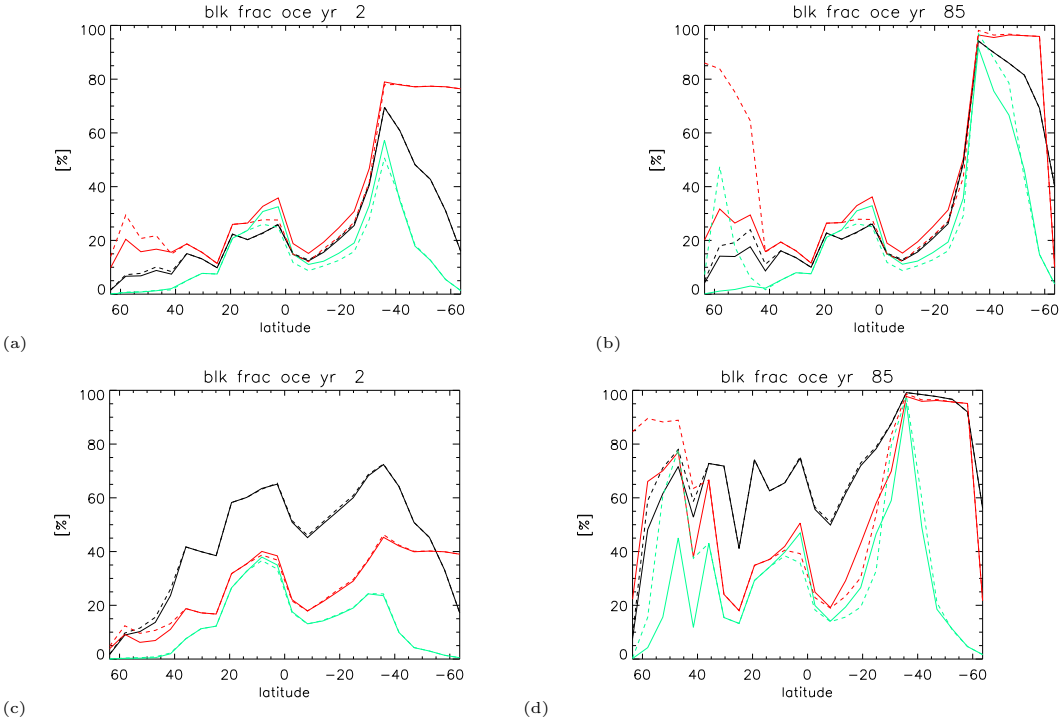

Figure 5.5: Fraction in the ocean compartment for setup 1 in percent. Dashed lines represent the case without vegetation: (a,c): Bulk fraction in the atmosphere and the ocean after 2 yrs, (b,d): Bulk fraction atm and oce after 85 yrs. The colors are used like (figure 5.4)

tion. Differences with or without vegetation are rather small no matter which wind speed is considered (figure 5.5). The overall pattern is very similar. Significant meridional variation can be observed for every deposition scheme. It seems that temperature, land fraction and surface roughness of the continent are an evident factor for the deposition flux. However, no clear and consistent meridional trend is observed (figure 5.5). In the more land dominated northern latitudes the deposition of all the parametrization is mirrored in comparison to the flux in the tropical latitudes. Prescribed deposition is the highest in the mid latitudes, followed by particle deposition and calculated gas deposition.
Both wind speeds lead to similar of deposition fluxes (figure 5.2). A strong drop of overall deposition and volatilization occurs in the ocean dominated southern hemisphere. Obviously a much slower exchange between atmosphere and ocean is taking place at lower water temperature, which enhances the ocean accumulation. Another effect of a larger land compartment is that DDT cycles faster in comparison with the overall burden. In the ocean dominated southern hemisphere the volatilization is perhaps 50% higher than in the land dominated north (5.3). However b_{tot} in the south is in general higher by the order of one order of magnitude for most of the setups.
The box model experiments also predict that the global DDT accumulation in colder zones works with different accumulation mechanisms in both hemispheres. In the South a stronger transport into the ocean takes place, while the continent in the North works as a threshold for further transport.

5.1.3 Setup 2: Gas diffusion

5.1.3.1 Global overall burden b_{tot}

Gas diffusion is the third possible deposition pathway beside gas deposition on the canopy leaf and calculated particle deposition. It can also be considered as the second gas deposition process on the canpoy. Because of several calculation methods for the partitioning factor K_{PA}, diffusive gas exchange is a sensitivity study for the vegetation influence and its consequence for the overall cycling of POPs. Strong variations of b_{tot} are the result of using different K_{PA} parameterizations (figure 5.7). For K_{PA_3} the highest b_{tot} of DDT follows for both wind speeds. Partitioning fractions vary in the range of one order of magnitude for the different K_{PA} parameterizations. Lower wind speed results in higher values of b_{tot}.
Especially for K_{PA_3} the vegetation serves as a major sink because revolatilization takes place at much lower pace than for the other partitioning coefficients (figure 5.3). Such a low level of revolatilization is mostly the reason for high b_{tot} in the vegetation canopy. Removal processes in the leaf volume compartment are obviously not very effective. The degradation within the leaf interior and the phloem removal are minor processes and not effectively reducing b_{tot}. This can be seen especially after the shut down of application, where the contamination level of K_{PA_3} remains very high (figure 5.7) and revolatilization is the only reduction process in the leaf volume.
A factor that should not be underestimated is the available leaf surface. The in-

fluence of the LAI is seen in the northern hemisphere where a strong drop occurs for areas with very low vegetation canopy surface. But also the mid latitudes the contamination levels are in proportion with the vegetation surface available (figure 5.7).
Other factors that have an influence on the process of diffusive gas exchange are certainly the land fraction, as well as temperature. Tropical zones and the large continental areas have very large capacity of DDT storage for K_{PA_3}. Results of the other partitioning coefficients are on the other hand not too different from the previous vegetation setup, and thus one cannot not give a definite answer on the question what are the effects of diffusive gas exchange for b_{tot}.

5.1.3.2 DDT fractions in different compartments

The distribution among different compartments reflects the finding of b_{tot}. Runs with the method K_{PA_3} reveals a stronger affinity of DDT to reside in the land compartment. Values of up to more than 90% are simulated for this run (figure 5.9). However, also here a very large difference between land fraction and K_{PA} choice is found. In mid latitudes the different K_{PA} parameterizations lead to a span of less than 10% in the land compartment to more than 95% (figure 5.9). The higher northern latitudes do not have such a strong variation concerning the land compartment. This is related to the higher overall land mass and/or the lower temperatures whereby the latter reduce the volatilization flux.
The ocean fraction is affected less by this variation of land compartment fraction. With the exception of K_{PA_3}, values of the ocean fraction for the several K_{PA} parameterizations are relatively similar at the beginning of the run (figure 5.6). At high wind speed, the ocean fraction increases. In the northern latitudes the ocean fraction rises from less than 20% to values up to almost 70% after the stop of DDT. This finding is exactly opposite to the big leaf vegetation deposition scenarios. Low wind speed leads to a lower ocean DDT fraction. Hence, the effect of diffusive gas exchange is much stronger at low wind speed. It leads to a weaker flux from the land towards the ocean.

DDT fractions on land in equatorial latitudes are not changing with such a strength no matter which K_{PA} is taken. Reasons could be the influence of the higher temperature or the LAI in this area, which may have an indirect effect on the K_{PA} and overall distribution.

5.1.4 Setup 3: Defoliation and introduction of vegetation covered soil

The main topic in this experiment is to find out whether an introduction of an additional soil compartment would have effects on the overall cycling and fate of DDT. A simplified leaf phenology is simulated with an annual litter fall for the unit vegetation type in all the zones. Recycling of POPs with the atmosphere would be done through litterfall, its immediate decomposition and revolatilization.

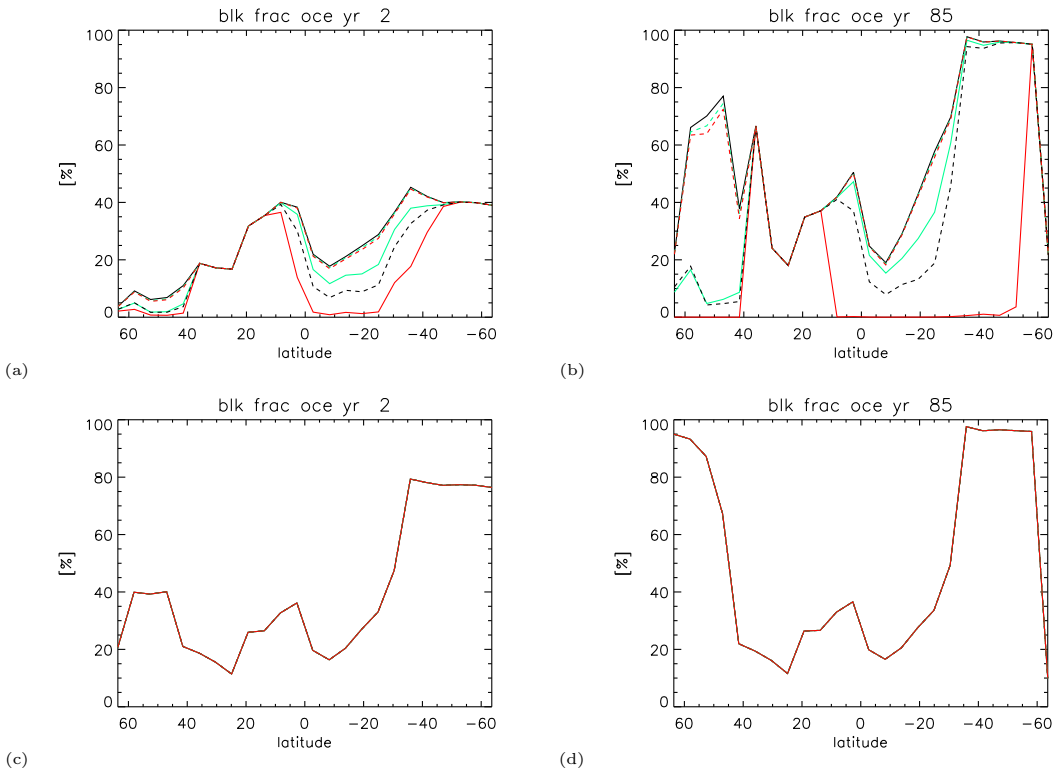

Figure 5.6: DDT fraction in the ocean compartment as a function of latitude for a) and b) show a sensitivity study for diffusive gas exchange. c) and d) include the vegetated soil (setup 3). Full lines: K_{PA_1}: black, K_{PA_2}: green, K_{PA_3}: red Dashed lines: K_{PA_4}: black, K_{PA_5}: green, K_{PA_6}: red

5.1.4.1 Global overall burden b_{tot}

Vegetation soil processes obviously have large effects on the partitioning coefficients as well as on b_{tot}. Defoliation and phenology must be considered as major factors for DDT cycling. This test also reveals that the K_{PA} has less influence compared to the defoliation and subsequent volatilization to the atmosphere. However one must also consider that the defoliation scheme is followed by an immediate POP release. The process of leaf decomposition is accompanied with many uncertainties and thus the results shown with this simple vegetation scheme are preliminary.
The speed of litter fall may also lead to a variation in b_{tot} and overall cycling. In addition leaf phenologies can be very different according to the climatic zone. Results performed with such a basic annual change of canopy, without biodegradation and a very simple soil and revolatilization model are meaningful only to a limited extent.
The overall burden b_{tot} is lower for at least one order of magnitude in the northern hemisphere, while the desert part is not affected at all (figure 5.7). The tropical part also shows about one order of magnitude lower values b_{tot}. With this calculation method, the highest of b_{tot} values occur in the oceanic southern hemisphere, but are in general much lower than without the inclusion of a vegetation covered

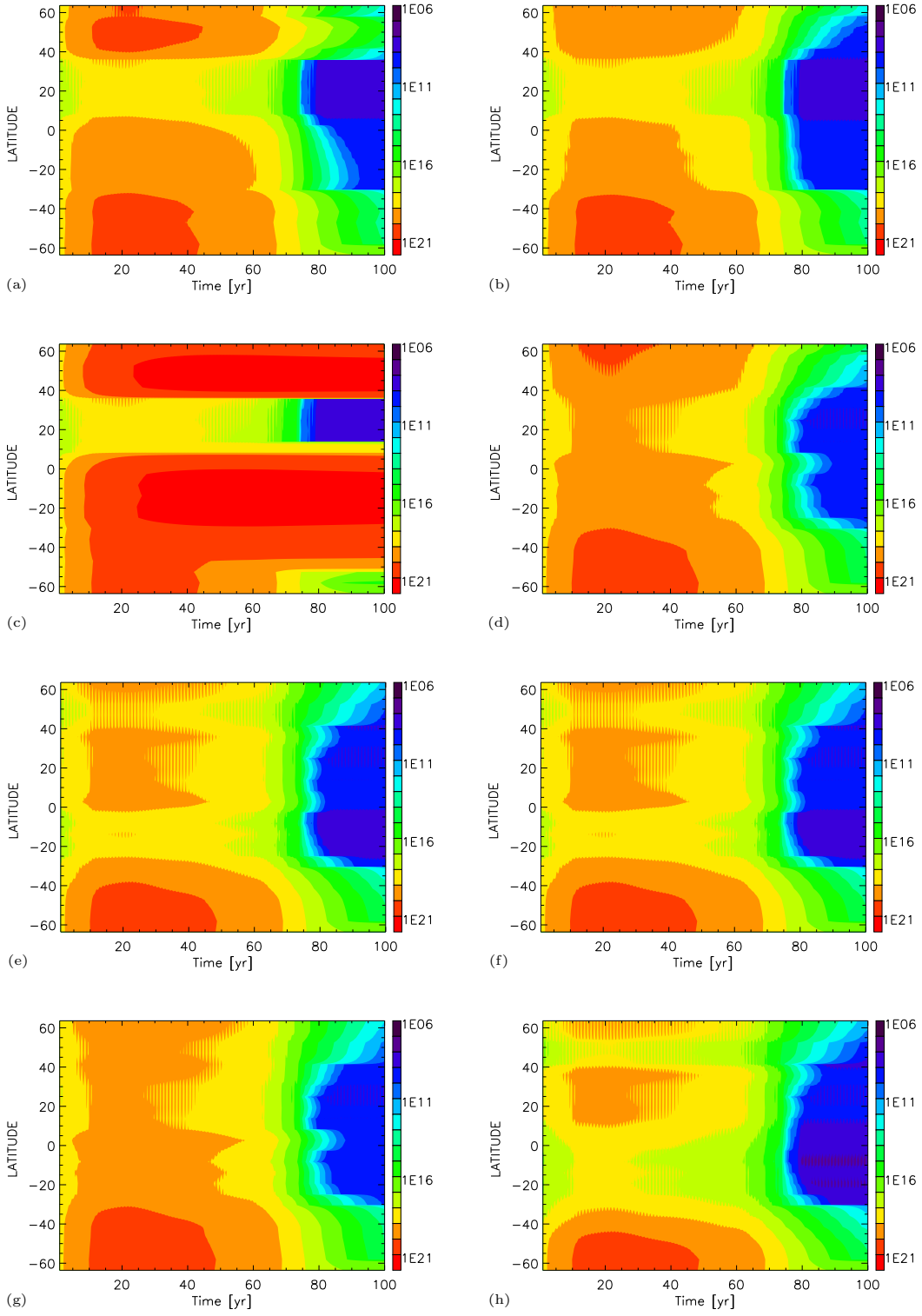

Figure 5.7: Time series of overall burden of DDT (in $\frac{molec}{m^2 s}$) as a function of latitude for different leaf and multilayer vegetation setups. a),b) and c) Big leaf diffusive gas exchange (setup 2) calculated with K_{PA_4}, K_{PA_5}, K_{PA_3} respectively at high wind speed ($13\frac{m}{s}$). d) Big leaf K_{PA_5} at low wind speed. e) and f) K_{PA_3}, K_{PA_5} with the inclusion of soil under vegetation and defoliation at low wind speed (setup 3). g) and h) K_{PA_3}, K_{PA_5} with the multi-layer canopy setup at low wind speed (setup 4).

soil. Defoliation (as simulated here) can be considered as a cleaning of the environment (figure 5.7). The soil compartment thus is a de facto accelerator of the overall degradation of POPs via the atmosphere.

5.1.4.2 Flux analysis and compartment distribution

This faster overall cleaning is documented by the reduction of volatilization and overall deposition. Fluxes between the compartments are related with b_{tot} and thus volatilization is in general lower about one order of magnitude. A higher atmosphere compartment fraction is one of the consequences for the introduction of the soil under vegetation. Especially tropical latitudes are affected by a proportionally higher revolatilization. In the northern cold latitudes a change of flux direction can be seen and the additional volatilization is accompanied by a stronger pumping into the ocean compartment. Equatorial latitudes do not have such a sensitivity. Differences between the several volatilization fluxes and the partitioning coefficient are not documented. Reasons for such a model behaviour remain unclear. Defoliation is clearly a strong process and can marginalize the diffusive gas exchange with its different partitioning coefficients.
Much smaller DDT fractions of the land compartment are obtained with the introduction of vegetation covered soil compared to the calculations hitherto. No larger differences can be seen concerning the choice of the partitioning factor. Highest values of the DDT land fraction are found in areas without an annual leaf phenology. The reasons for the overall smaller land fraction is mostly related to the faster overall revolatilization process via the soil under vegetation. However this process must be subject to further discussions. Especially the diminishing importance of different K_{PA} parameterizations leaves open questions.

5.1.5 Setup 4: Multi layer vegetation setup

5.1.5.1 Global overall burden b_{tot}

Compared to the big leaf vegetation the 2-layer vegetation is a more detailed resolution of processes within the canopy compartment. No larger differences are observed in the general trend of the signals compared to setup 3. However, the coefficient K_{PA} is more important for a multi-layer approach of vegetation. Higher b_{tot} values are reached in most cases with this more detailed phenological description. Depending on the calculation method and latitude, differences of b_{tot} of a factor 5 up to one order of magnitude for b_{tot} are achieved in every latitude zone with vegetation (figure 5.7).
Like in the big leaf vegetation runs, the K_{PA_3} simulation has the highest b_{tot} whilst K_{PA_1} had the lowest overall contamination. The significance of the partitioning coefficient is higher than for the big leaf canopy test. Explanations for the importance of K_{PA} could be the different influx in the vegetation compartment caused by the multi canopy layer. Resistance scheme, wind speed, roughness length, vegetation height and temperature are the main factors of influence for b_{tot}.
Big leaf diffusive gas exchange setups with defoliation are assumed to be calcu-

lated only in the canopy top and do not show such a sensitivity. It is thus possible that low wind speed in the lower canopy sublayer does have a higher b_{tot} as consequence (figure 5.7). This would be in accordance with the finding of the big leaf defoliation tests. Wind speed in these layers is calculated according to the logarithmic wind profile, the canopy roughness and the different height of the vegetation. The crown canopy in the top layer is exposed to higher overall wind speed than in the case of the second layer below (all the big leaf runs are assumed to be calculated on the top level of vegetation). Canopy surface temperature is another factor that influences the cycling and b_{tot}. Tests with different vegetation types and either fixed vegetation temperature or wind speed did not answer the question which is the more important factor for b_{tot} (figure 5.24). Both factors probably have adding effects on the atmosphere-vegetation volume interaction, giving the factor of K_{PA} a higher grade of sensitivity for the overall fate of DDT.

5.1.5.2 Global compartment distribution

The overall allocation to the different compartments remains in a similar range as the simple leaf defoliation calculation (setup 3). Main compartment interactions takes place between the ocean and atmosphere. This test also shows that the vegetation compartment and especially the defoliation act as a catalyzer for the further transport into the ocean.
Slight variations of the compartment distribution are obtained in comparison with the big leaf vegetation setup (figure 5.8). Temperature is a driving factor for the overall distribution of POPs within this setup. The ocean compartment in the high latitudes takes up with time most of the DDT. This trend has been observed also for setup 3 (figure 5.6). The ocean compartment in the tropics remains similar for both setups and is rather independent of time.

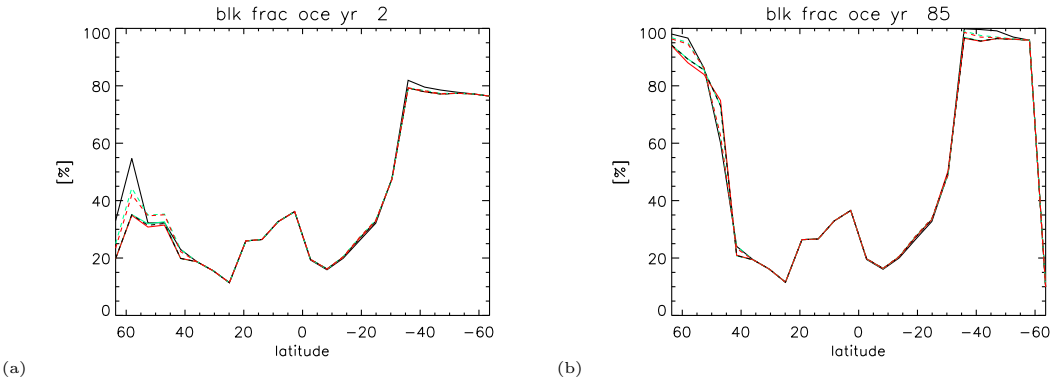

Figure 5.8: Meridional section of DDT proportion in the ocean comparmtent for the vegetation 2-layer approach (setup 4). a) and b) stand for 2 and 85 years of the 100 years simulation. Slight variations of the ocean fraction compared to figure 5.6 can be observed. Full lines: K_{PA_1}: black, K_{PA_2}: green, K_{PA_3}: red Dashed lines: K_{PA_4}: black, K_{PA_5}: green, K_{PA_6}: red

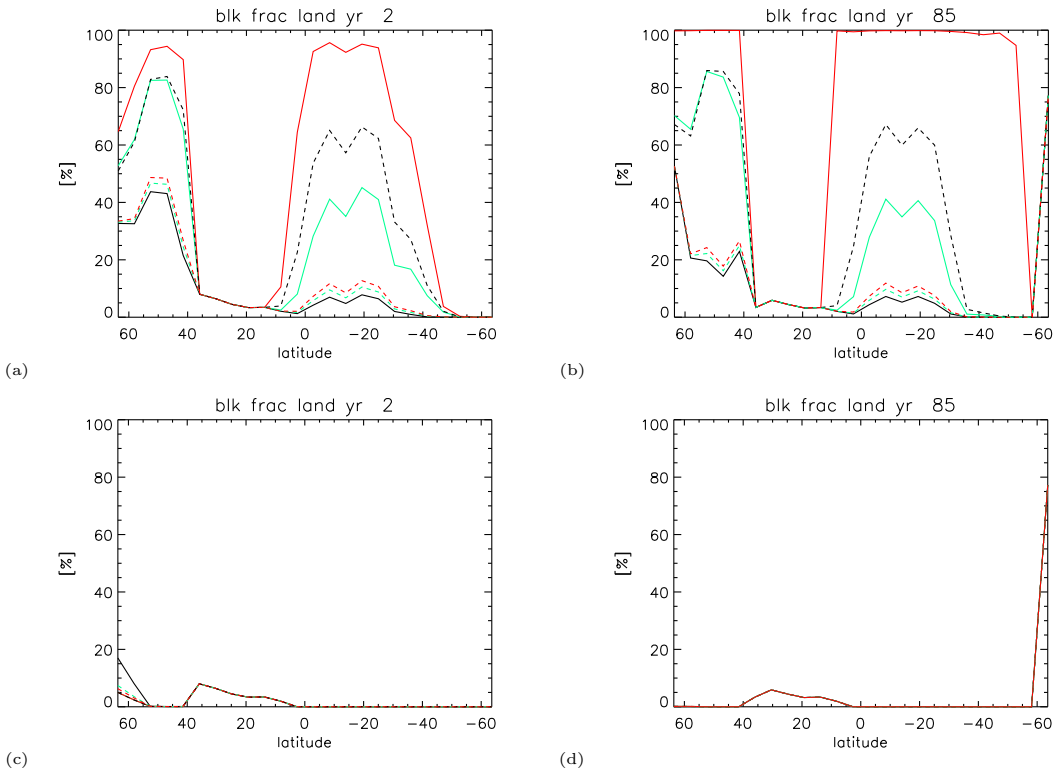

Figure 5.9: Meridional section of the bulk fraction of land for the big leaf diffusive gas exchange setup 2 at (figure a and b). Figure c and d show the annual mean fractions after the inclusion of the soil under vegetation compartment for the multi layer vegetation (setup 4).Full lines: K_{PA_1}: black, K_{PA_2}: green, K_{PA_3}: red Dashed lines: K_{PA_4}: black, K_{PA_5}: green, K_{PA_6}: red

5.1.6 Conclusions

The introduction of the soil under vegetation and the defoliation process has large effects on the overall cycling of DDT. Leaf phenology is a very important factor for the overall cycling and the role of vegetation needs to be reconsidered for further simulations with DDT. The overall burden b_{tot} as well as compartment fractions of DDT are both affected by the additional cycling of DDT via soil under vegetation. The introduction of the litter fall process leads to a strong reduction on the annual overall land fraction and a faster transport back into the atmosphere, where the chemical decomposition takes place at higher pace.
The tests confirm that overall cycling and b_{tot} strongly depending on wind speed. Furthermore the wind profile plays a key role too. Defoliation and revolatilization (as far as they could be represented in such model setup) can be understood as major vegetation activities. The effects of different leaf phenology, decomposition and other processses are still to be investigated. Indirect cleaning the environment of POPs via the vegetation is accelerated via the diffusion and defoliation process (setup 3 and 4). Vegetation must be considered as a important buffer compartment for the followed atmospheric removal of DDT. Life cycles of leaves are critical factors for the overall fate of DDT. The perhaps most unanticipated

effect of litter fall (setup 3) is the elimination of the differences between the different K_{PA} parameterizations. The defoliation process and the revolatilization are more important than the choice of leaf-air partitioning coefficient.
A 2-layer vegetation canopy (setup 4) provides variations of b_{tot} and increase the importance of K_{PA}. Results of b_{tot} differ up to one order of magnitude in some latitudes. However, most of the trends of setup 4 are very similar to the findings of the big leaf defoliation approach (setup 3). The single vegetation type is tested is probably not sufficient for an accurate display of canopy processes.

5.2 Vegetation Type Testing

Vegetation cycles are an important factor in the complex overall cycling and fate of POP's. So far the leaf phenology is accounted for only a limited and not representative standard canopy model. Effects of leaf phenology, LAI, canopy roughness though are expected to play an important role for the overall fate of DDT. The main focus of the following vegetation type testing is on the prominence of certain processes and the quantification of the influence of canopy structures on the overall cycling of DDT. The prescribed deposition scheme is not considered in the vegetation type study, because it does not take any vegetation characteristics into account.
This approach will focus mainly on three different vegetation types (grassland, coniferous and deciduous forest) in a temperate mid latitude zone (47^0 N). To exclude external effects (temperature, day length, seasonal oscillation etc.) the climatic parameters are set to average conditions. An impulse application (1 year of full constant atmospheric release of POPs) is assumed, and the box model runtime is set to seven years. The only annual variation allowed in the model is the annual leaf phenology (change of LAI) of each vegetation type. The analysis follows the same scheme like for the global tests.

5.2.1 Setup 1: Gas and calculated particle deposition

5.2.1.1 Overall burden

Previously observed general trends about the behaviour of vegetation for b_{tot} and the dependence of wind are also valid for the vegetation types. Also for vegetation type testing, b_{tot} is higher at low wind speed. Different vegetation types cause a different b_{tot} and change their behaviour with the deposition schemes simulated (figure 5.11).
In both cases (gas and calculated particle deposition) b_{tot} of the grassland vegetation has the highest b_{tot} at low wind velocity, while the other two vegetation types do not differ too much (figure 5.11). A possible explanation for such an effect is that low wind speed favours slow volatilization and overall degradation in the compartments. The effects on b_{tot} for different vegetation types show less wind sensitivity also with particle deposition. Under high wind speed, the values b_{tot} for the several vegetation types are almost the same.

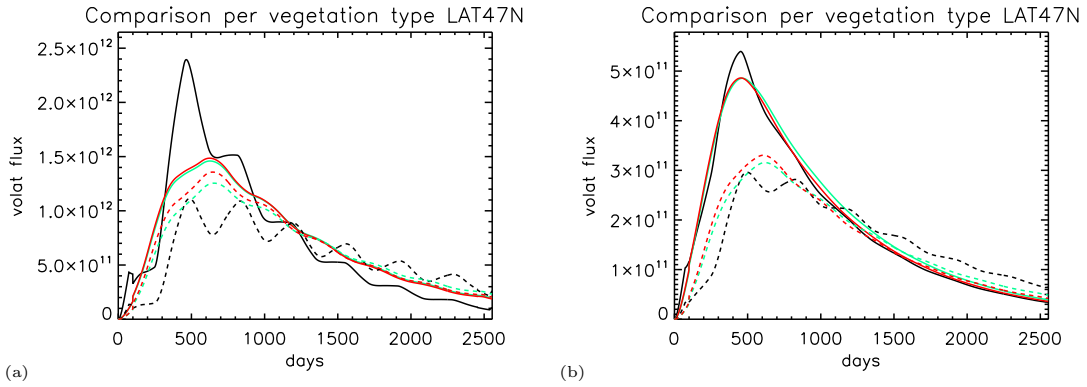

Figure 5.10: Time dependent DDT volatilization flux ($\frac{molec}{m^2 s}$) for the calculated gas deposition (setup 1) and background aerosols. a) and the calculated particle deposition b). Dashed lines are the low wind speed case. Black: grassland, green: deciduous and red: coniferous vegetation.

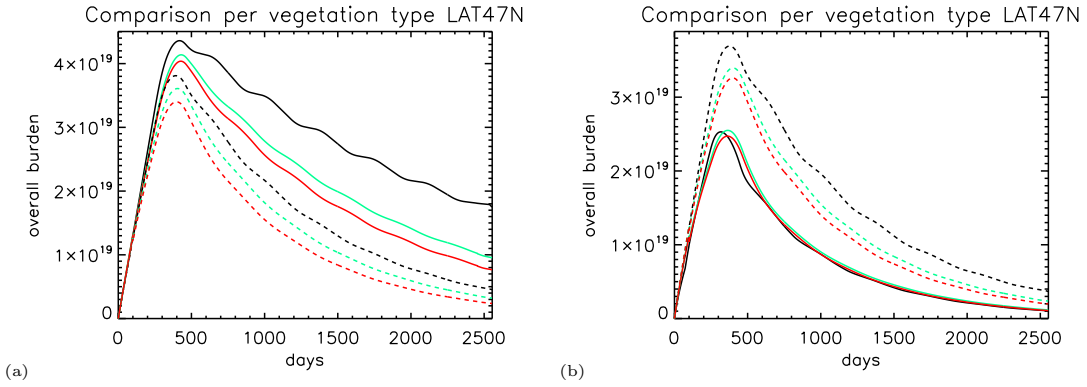

Figure 5.11: Time dependent Total DDT burden b_{tot} a) for gas deposition (full lines), particle deposition (setup 1) flux and different vegetation types. b) Comparison of b_{tot} for two wind speeds (full line: high wind speed ($13 m/s$), dashed lines low wind speed $2.5 m/s$) for background aerosols and calculated particle deposition of setup 1 . Vegetation types: Black: grassland, green: deciduous forest, red: coniferous forest

Reasons for such small difference are possibly reduction of the importance of the canopy roughness. Above a certain level of turbulence, the influence of the vegetation characteristics on the on the overall cycling are probably reduced.

5.2.1.2 Flux Analysis

Differences in the overall values of volatilization are directly related to b_{tot}. The inclusion of particle deposition decreases volatilization fluxes by about a factor 5. Different volatilization behaviour for the different vegetation types can be seen for both parameterizations (figure 5.10). One has also to mention that the volatilization fluxes and b_{tot} strongly depend on the type of aerosol. In the model, differences in the aerosol type can be characterized by either different volatilization values or different behaviour of all the vegetation types.

5.2.1.3 Compartment fractions

The distribution among the compartments for DDT is driven by several factors. Aerosol types influence the overall distribution of DDT to a large extent. Very unequal overall trends for DDT in different compartments are obtained for the calculated gas and gas plus particle deposition. For all the aerosol types of the gas deposition method, the main fraction of DDT is on the land and in the atmosphere (figure 5.12). After the initial one year DDT application, the amount of DDT on land remains stable in the post application period. Depending on the aerosol type, the fraction can differ remarkable and the atmosphere takes a larger burden for urban aerosol.
The seasonality of the LAI can be very distinct for the different vegetation types (figure 5.12). However, the relationship between vegetation type, wind speed, compartment distribution, aerosol type, leaf area index (LAI) and b_{tot} is not really a linear one, and thus it is not possible to establish a generally valid rule. All variables can contribute to distinct distribution variability of the compartment allocation. The results of these tests have to be considered as only valid for the distinct climatic zone at $47N^0$. Vegetation type tests with the same deposition schemes in other climate environments do not give the same pattern at all (figure 5.13).

5.2.2 Setup 2: Gas diffusion

5.2.2.1 Overall burden

The sensitivity tests of this diffusive gas exchange setup were run with all the six vegetation-air partitioning coefficients K_{PA}. However, because there is a very large amount of data, only a limited selection of the overall runs is presented in this section. As it was shown before, diffusive gas exchange can be (depending on the choice of K_{PA}) an essential factor for the cycling and fate of DDT. Similar to the general vegetation global tests, the highest b_{tot} is calculated with K_{PA_3} (figure 5.14) while other K_{PA} values do not have such a strong effect on b_{tot}. Gas diffusion onto different vegetation types also depends on other factors like the aerosol type (figure 5.14) and the interactions between these different factors are nonlinear.
Low wind speed has in every run the higher value of b_{tot} for all vegetation types no matter which K_{PA} is taken. Wind speed is a very decisive factor concerning b_{tot} for both, the gas and calculated particle deposition scheme. The behaviour of the different vegetation types on the other hand depends strongly on the K_{PA}. No general trend can be observed. It is thus not clear which are the most important factors of the diffusive gas exchange into the vegetation volume. Influential elements are: the surface roughness, wind speed, the diffusive gas exchange resistance scheme and the LAI. Probably the aerosol-gas partitioning in relation with all the mentioned factors is another criterion which has to be taken into account for b_{tot}.

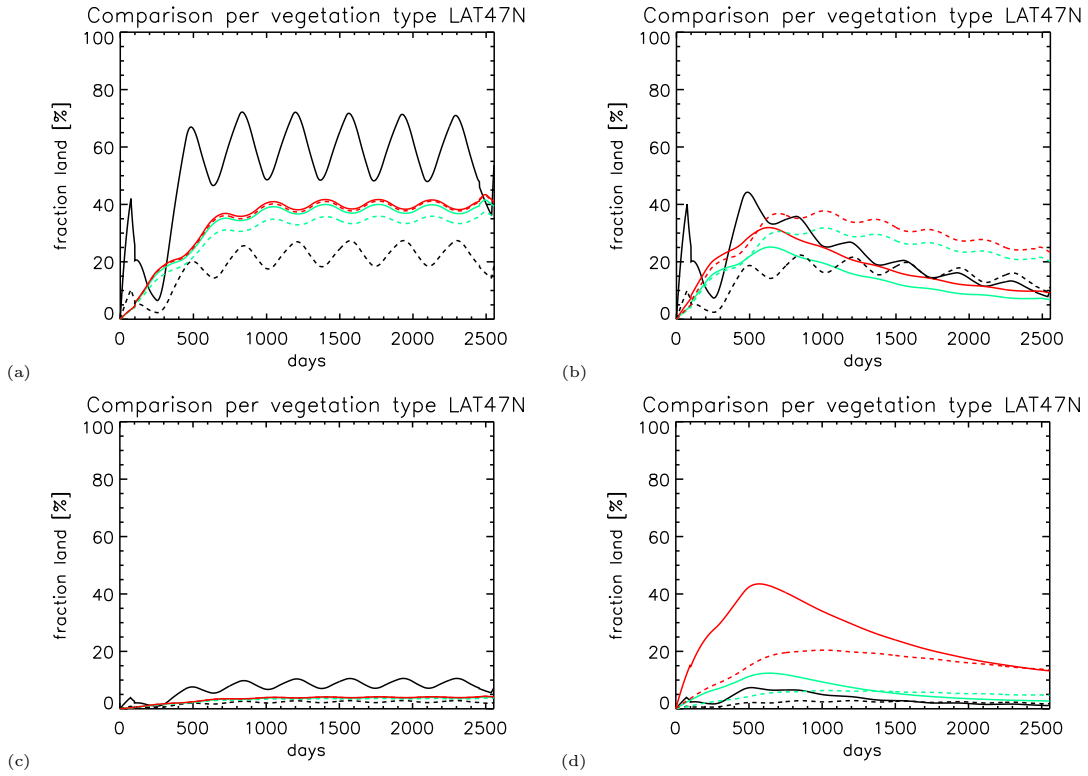

Figure 5.12: Time dependent compartment DDT fraction in % for calculated gas deposition (setup 1) (a,c) and calculated particle deposition (b,d) for three different vegetation types. The calculations show results for two different aerosol types, namely the background aerosol (a,b) and the urban type aerosol (c,d). Grassland (black), deciduous forest (green), coniferous forest (red). The full lines stand for high wind speed, the dashed ones for low wind speed.

5.2.2.2 Compartment fractions

Beside the ocean, vegetation has to be considered as the second largest sink of DDT. At higher wind velocity, the ocean fraction is proportionally higher than in the low wind speed case. Obviously the high wind speed leads to revolatilization from vegetation and further transport towards the ocean. This is exactly the opposite effect than seen for setup 1. However, this trend also depends on the leaf-air partitioning coefficient. Some K_{PA} parameterizations do not show a different behaviour than in the case of particle deposition. It is thus apparent that the subject of compartment distribution and leaf air-partitioning cannot be concluded with a simple statement. The results of the different calculations are too different to provide a definite answer.

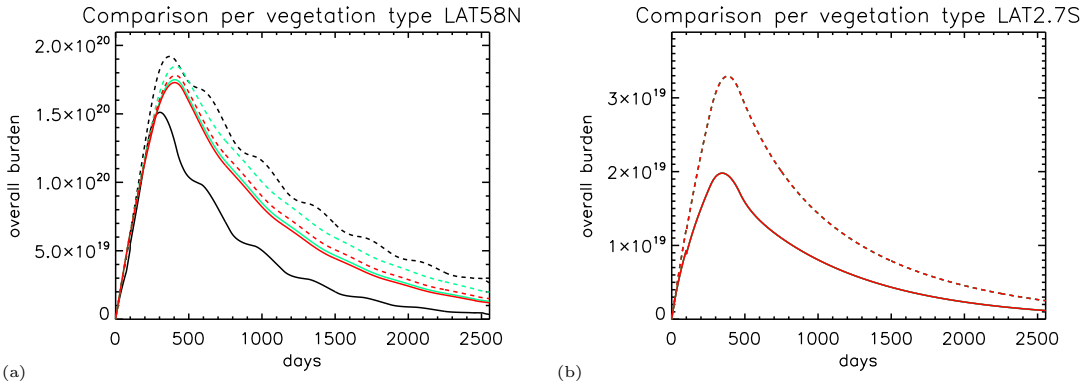

Figure 5.13: Comparison of overall burden b_{tot} for different vegetation types at different latitudes (58^0N (a) and 2.7S (b)) for setup 1 at high (full lines) and low wind speed (dashed lines). Vegetation of latitude 58^0N: Grassland (black), deciduous forest (green), coniferous forest (red). Vegetation of latitude 2.7^0S: red lines: tropical rain forest

5.2.3 Setup3: Defoliation

5.2.3.1 Overall burden b_{tot}

Phenology is an important factor concerning the overall cycling and burden of DDT. In the previous experiments in section 4.1, the vegetation type was a shrub canopy with an implemented annual canopy change. The inclusion of soil underneath the canopy causes changes in the flux scheme of the box model, as well as it leads to a reduction of b_{tot}. The focus here is on the leaf longevity of each canopy to understand its interaction with the overall cycling. For this experiment, grass changes its leaves on an annual base. The coniferous forest vegetation in the model renews its needles once in four years, while the deciduous forest vegetation has an average leaf turnover ϑ of about 1.5 years. All of them also include an annual canopy renewal but do not loose all of their leaves at the end of the year. Results of the different calculation methods indicate that K_{PA} is much less influential (or not at all) if defoliation is included. Other environmental factors become more important than the leaf-air paritioning coefficient K_{PA}. Aerosol types for example, are very relevant for the change of b_{tot} (figure 5.15). Wind speed is another influential parameter for setup 3. Trends of the different vegetation types are in most cases in agreement with the findings of the big leaf deposition setups. Grass causes also here the highest level of overall contamination b_{tot}.

5.2.3.2 Effects of leaf longevity

One of the main findings of this box model experiment is certainly that phenology has a different influence on b_{tot} and compartment distribution than expected. Leaf turnover does not enhance accumulation of POPs in the vegetation canopy and neither does it the soil under vegetation (figure 5.15, 5.16). The effects of leaf longevity for b_{tot} are ambiguous. The cyclic defoliation of the vegetation enhances the further accumulation in the ocean compartment. A shorter cycle of

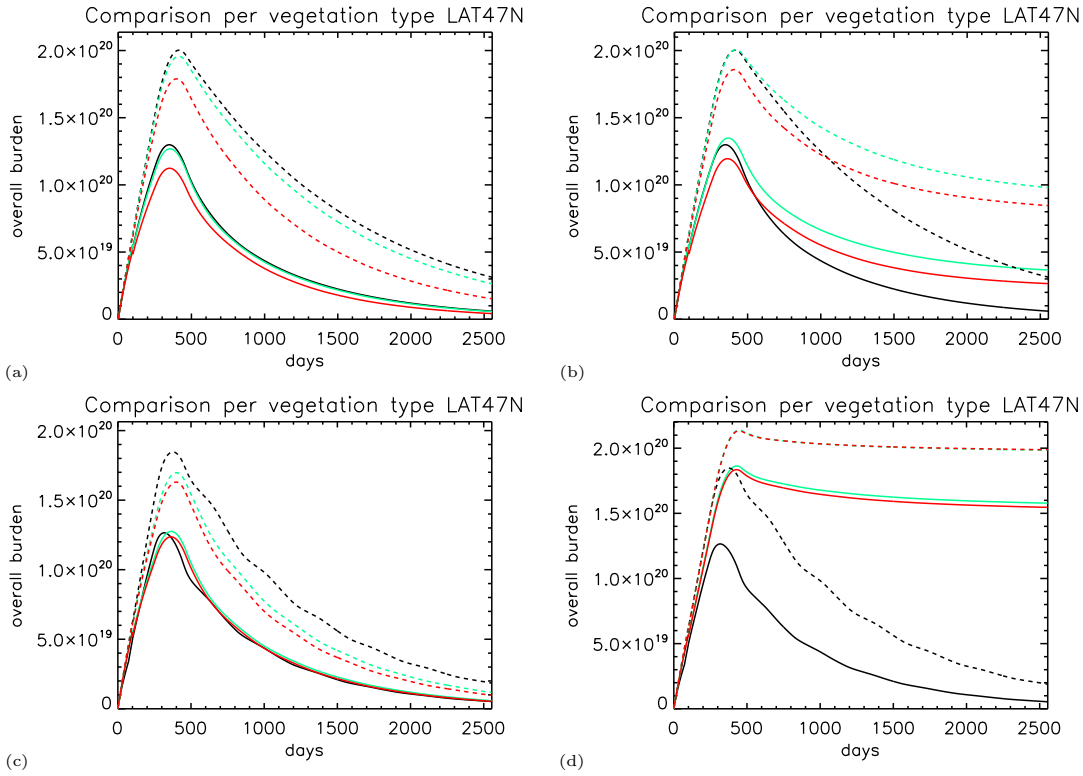

Figure 5.14: Total DDT burden b_{tot} for the diffusive gas exchange onto different vegetation types (setup 2): Here tests for different aerosol types: a) and b) for urban aerosols with K_{PA_1} and K_{PA_3}. c) and d) continental background aerosols. Dashed lines: low wind speed test. Vegetation types: Grassland (black), deciduous forest (green), coniferous forest (red).

defoliation contributes to a faster transport of DDT into the ocean. The overall effect of the longevity is best seen because land leads to b_{tot} higher by a factor 2-3 (figure 5.15). The influence of the aerosol on b_{tot} is probably even bigger than the phenology factor. One can conclude that the influence of the phenological cycle of the different vegetation types is probably rather secondary compared to other factors.

5.2.3.3 DDT distribution in different compartments and flux analysis

The additional influx on the soil under vegetation does not initiate a further accumulation on the continent. Maximum values of land fraction do not reach more than 30% of b_{tot} during the first two years. For all the aerosols, coniferous forest has the highest capacity to accumulate on the land compartment, followed by the deciduous forest and grassland (figure 5.16). Though one can observe a strong decrease of the land fraction after the stop of application and allmost all of the DDT ends up in the ocean compartment. All the studied K_{PA} lead to very similar land compartment burdens. Such a burden of the land compartment is largely due to the phenology of needle type canopies.
All the tests confirm that with the inclusion of defoliation, the grassland vegeta-

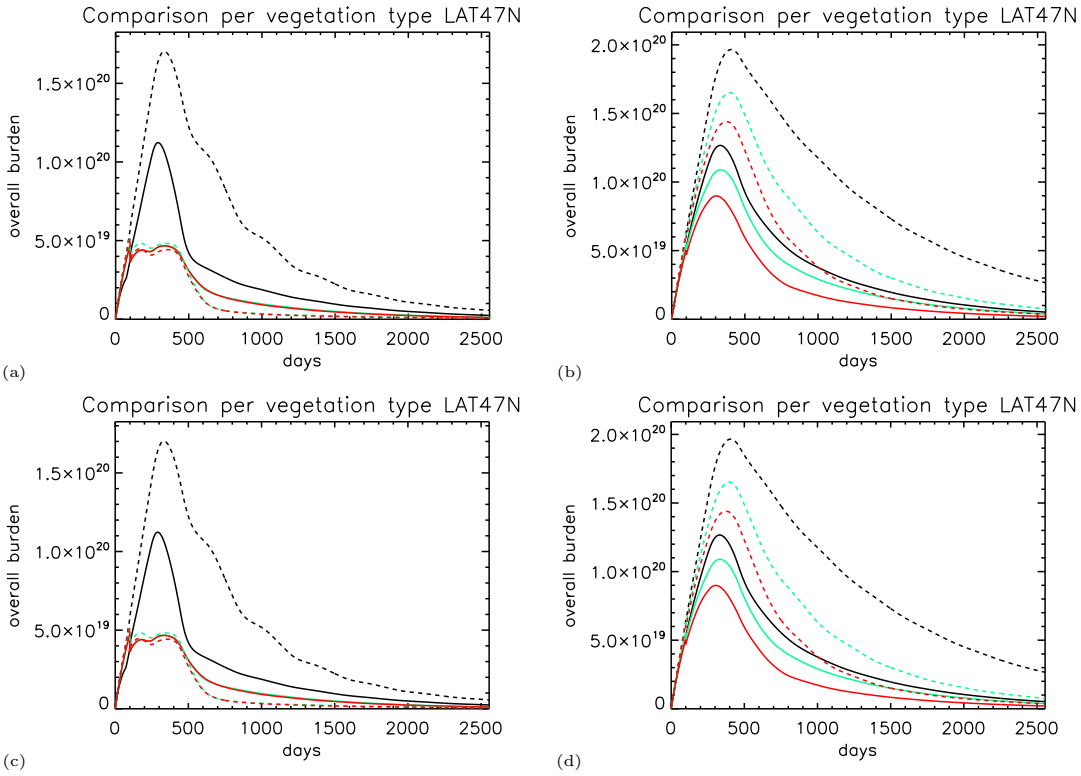

Figure 5.15: Time dependent total burden of DDT b_{tot} for two different wind speeds for setup 3 and different vegetation types. Two different types of aerosol and K_{PA} factors are displayed here: a) and c) background aerosols, b) and d) urban aerosols. Grassland (black), deciduous forest (green), coniferous forest (red). The full lines high wind speed, dashed lines: low wind. All simulations are made for latitude 47^0N.

tion has the highest values of b_{tot} (figure 5.15), although the grassland vegetation is assumed to be renewed every year. The findings of the defoliation process illustrate that there could be a saturation level in the atmosphere where a higher pace of degradation is not possible. A stronger deposition into the ocean is the consequence, followed by less strong volatilization in the following years. Wind speed is very important for the compartment shift, and the main interaction takes place between the atmosphere and the ocean. For all the K_{PA}, high wind speed causes a larger ocean fraction because of the proportionally higher volatilization and simultaneous decomposition by OH-radical in the atmosphere.
The aerosol type influences on the overall distribution and the annual oscillation of compartment distribution in relation to the LAI are remarkable. While urban aerosol types indicate quite little seasonality, the background aerosols react with stronger oscillation (figure 5.16). Reasons for this behaviour are quite unknown. Obviously a stronger allocation of DDT in the land compartment means also a lower b_{tot}. As a general rule, the introduction of litter fall enhances degradation on the soil.
The correlations between the vegetation type and the volatilization flux do not

show a regularity. It is clear though that the volatilization flux would be much stronger steered by the aerosol type than by K_{PA}. However, the interplay between wind speed, canopy type and annual cycles remains rather unclear (figure 5.17). Lower wind speed allows in general stronger seasonality in case of defoliation. Especially the grassland vegetation influence depends on the annual cycle, while the multi annual defoliation process of coniferous canopies allows less seasonality. Seasonality can sometimes only be seen in the first two or three years.

5.2.4 Setup 4: Multilayer canopy and vegetation type

5.2.4.1 Overall burden b_{tot}

Runs with a two layer vegetation disclose that b_{tot} can, but must not vary compared to the single big-leaf vegetation (figure 5.15, 5.18). Albeit this multi-layer vegetation setup is based on very simplyfied assumptions of canopy mechanisms. The multi-layer canopy concept must be seen as preliminary. Results just confirm the previous 'global box' testing. The influence of the K_{PA}-factor is more important than in the experiments with setup 3 (figure 5.18).
b_{tot} for the different vegetation types vary very strongly also with K_{PA}. Some K_{PA}-values are obviously not sensitive to the change towards a multi layer vegetation (e.g. K_{PA_3}), while others (e.g. K_{PA_5}) are. The impact of the vegetation type can be seen in the display of b_{tot} and there are considerable differences between the calculation methods of K_{PA}. In most of the runs the grassland vegetation is regarded as the test with the highest amount of b_{tot} DDT.
It is though not clear whether the wind speed profile or the temperature difference are more important for b_{tot}. Tests with fixed wind profile or fixed canopy temperature do not identify which factor is more important (figure 5.24).

5.2.4.2 DDT fractions in compartments distribution fluxes between them

The findings for b_{tot} are also reflected in the compartment distribution. Values of the overall land fraction of DDT are in a range similar to the single leaf case (figure 5.19). As K_{PA}-values are obviously important for multi-layer vegetation, no general conclusion for the allocation of DDT can be made (see also figure 5.20). Similar to the single leaf vegetation, the coniferous forest canopy accumulates the most DDT in the land compartment (figure 5.19).
An influence of LAI in the DDT distribution pattern is found in most of the mentioned multi-layer tests. The annual cycles of the compartment fraction is stronger at low wind speed. Differences which are related to the aerosol type are visible in the pattern as well as the decrease of the land fraction of DDT with time.
Differences in the volatilization flux are either related to the aerosol type or the choice of K_{PA} (figure 5.17). Depending on K_{PA}, volatilization can change up to one order of magnitude and strong differences are also found in the shape of the curves.

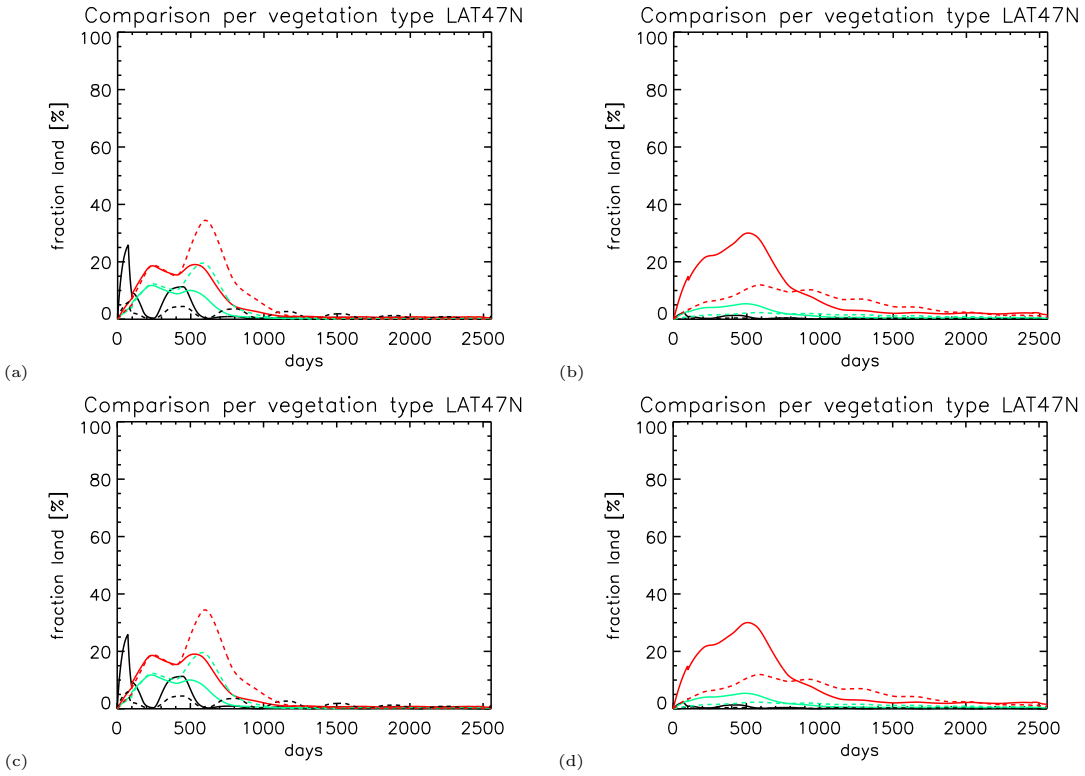

Figure 5.16: Relative burden on land for different vegetation and aerosol types. a) and c) are the background aerosol type b) and d) are the urban aerosol simulation. Figure a) and b) are calculated with K_{PA_3} while c) and d) is the same for K_{PA_5}. The full lines are high wind speed, dashed lines: low wind. All simulations are at 47^0N (grassland (black), deciduous (green), coniferous forest (red))

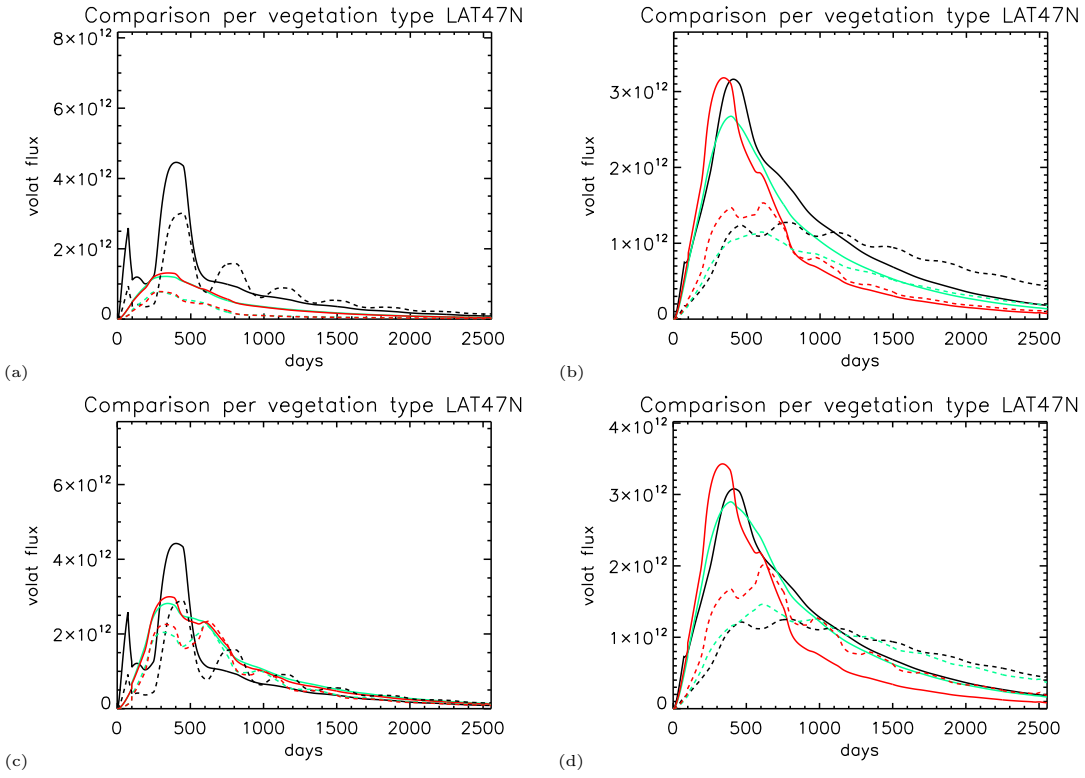

Figure 5.17: Volatilization flux in $\frac{molec}{m^2 s}$ for setup 3 with defoliation (figure a,b) and setup 4 (c,d) with two different aerosol types (background figure (a,c) and urban (b,d)) for K_{PA_3}. Lines are like in 5.16

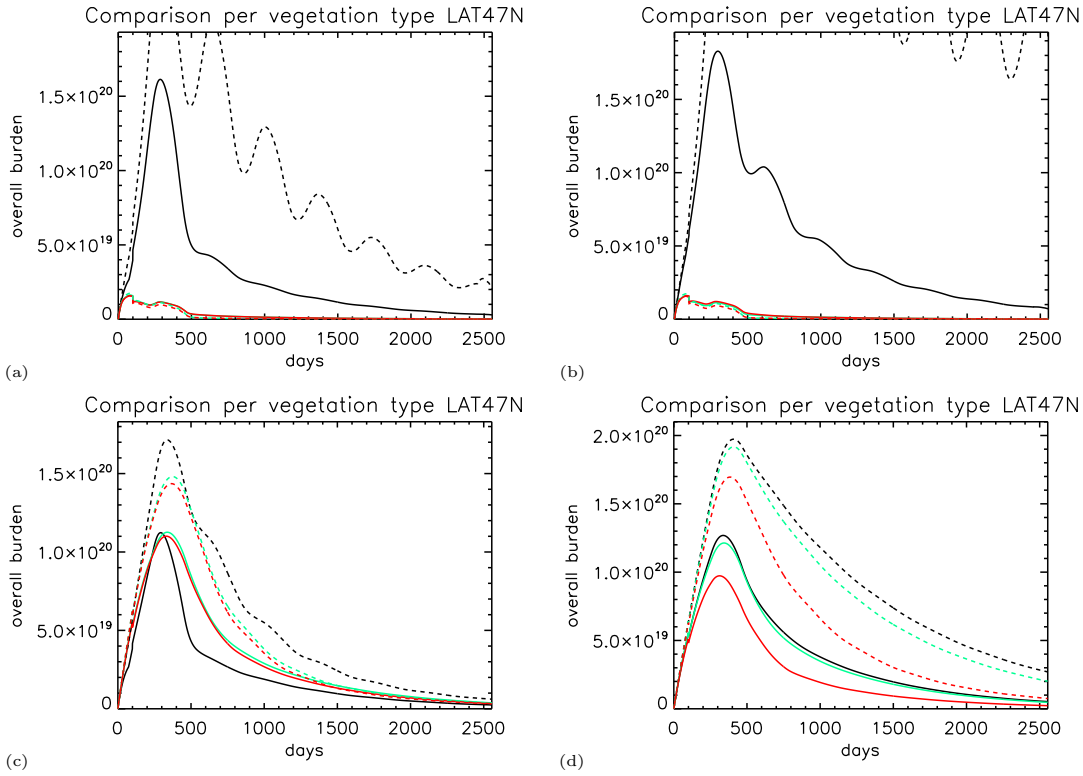

Figure 5.18: Time dependent total DDT overall burden b_{tot} of DDT of setup 4 with runtime 2500 days. a) and c) stand for background aerosols, b) and d) are the same for urban type aerosols. a) and b) simulate the case with K_{PA_5}, c) and d) are the same with the value of K_{PA_3} at high (full line) and low wind speed (dashed lines). Grassland (black), deciduous forest (green), coniferous forest (red).

5.3 Validation with model data and measurements

The assumptions and scenarios used in this model are partly hypothetical and a comparison with outputs from other models remains challenging. These other models may also be very hypothetical, however, a reasonable comparison is hard to establish because of the differences in the calculation methods, the DDT application pattern, land surface fraction, general assumptions, setup and runtime. This section is an attempt to discuss differences to other model results and to compare with measurements, though it is evident that it can be considered only as a preliminary comparison with other model data and results.
Collected data are often not compatible with the model results, because measurements can be strongly influenced by specific regional variabilities. We compared our model results with data from an intercomparison study of several POP models. Differences in the application pattern, reference data set and process complexity are main problems for a more detailed study. The models called Simplebox 2.0 (*Brandes et al.* (1996))and Chemrange (*Scheringer et al.* (2001)) are two steady-state level III (see table 2.1) multimedia mass balance box models, while the

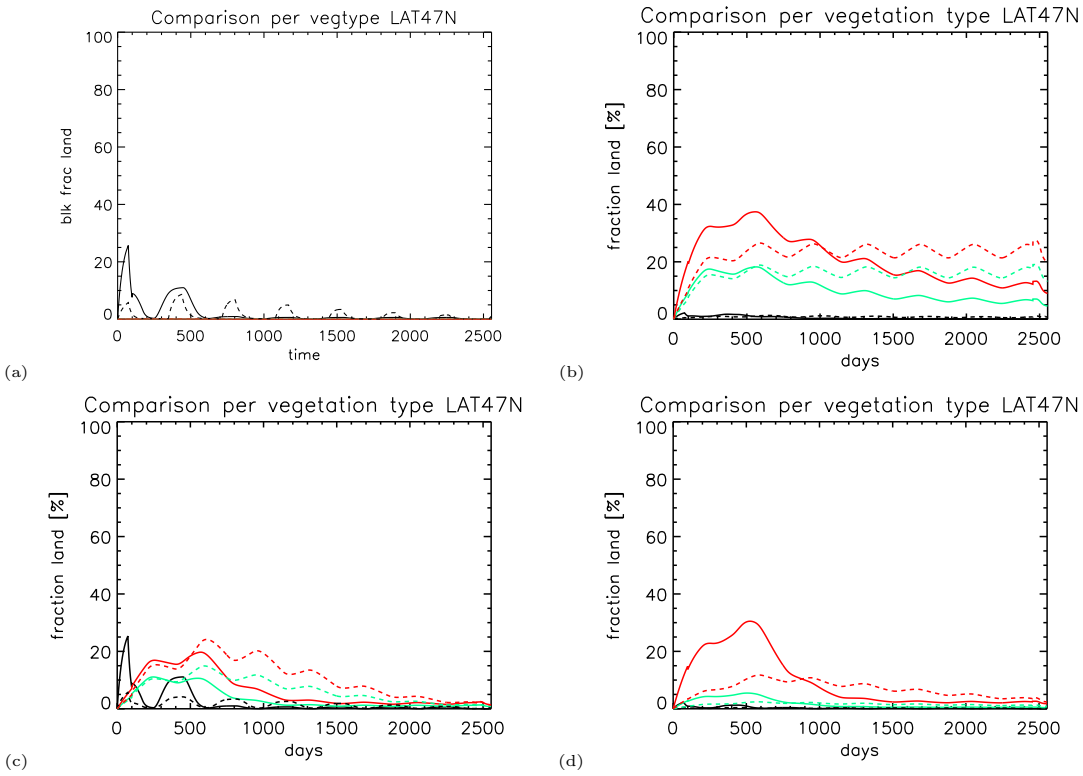

Figure 5.19: Time dependent total burden of DDT on land 47^0N for setup 4 and 2 different aerosols and 2 different K_{PA} values. Background aerosols are simulated in a) and c), the effects for urban type aerosols are displayed in b) and d)). K_{PA_4} is shown in a) and b), K_{PA_3} values can be seen in b) and c). The full lines are the case of high wind speed ($13\frac{m}{s}$) while the dashed lines represent the low wind speed case ($2.5\frac{m}{s}$)Grassland (black), deciduous forest (green), coniferous forest (red).

MPI-MBM model(*Lammel et al.* (2007)) is a non-steady state box model with one box simulating the whole world. Simplebox 2.0 uses various boxes to display the different climate conditions (arctic/temperate/tropic/continental), while Chemrange 1.0 is a setup of latitudinal belts around the globe. MPI-MBM consists of one box with 4 compartments (air, soil, vegetation, ocean) while the multi compartment transport model (MCTM) is a general circulation model. Like in the case of MPI-MBM, the MCTM is a non-steady state model.
Most of these predict that a large portion of DDT will be accumulated in the soil compartment followed by the ocean compartment. The parametrizations used in this work are far from reaching the amount of soil contamination predicted by the other models. Every model setup of this study predicts a much higher atmospheric pollution level and a very small overall fraction of contamination on the continent. This can be partly explained by the different application pattern used (see table 5.1). Most DDT is directly applied to vegetation or soil, while our study only applied it to air. The MCTM model has the highest fraction of DDT in the atmosphere and thus simulates a similar compartment shift as in our model setup.

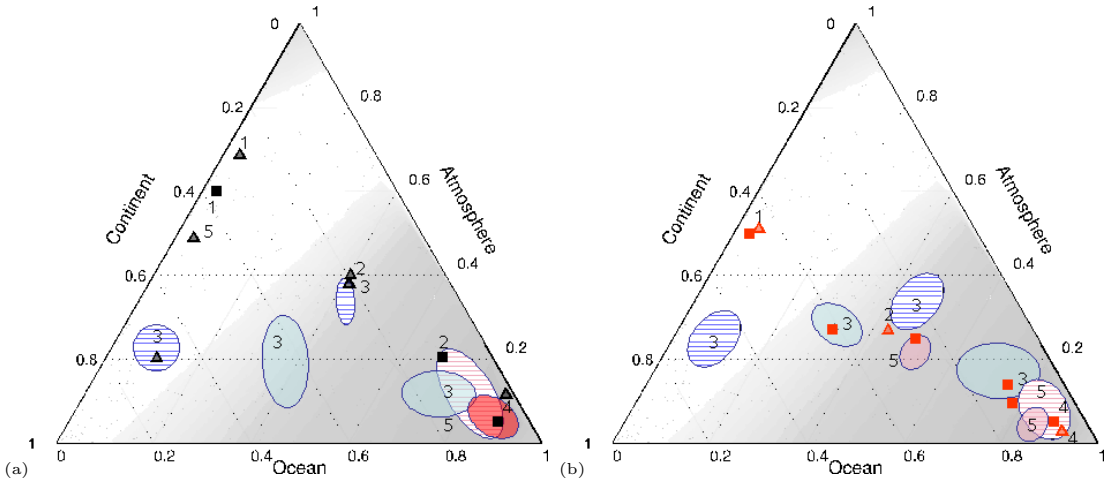

Figure 5.20: a) and b): Ternary plots of the compartment distribution for grassland (a) and coniferous forest (b) at the end of the simulation period (2500 days). The numbers represent different simulation setups, while the symbols are stand for different wind speed. 1) setup 1 with gas deposition (II), 2) setup 1 with particle deposition, 3) setup 2 with diffusive gas exchange, 4) setup 3 with defoliation single layer vegetation 5) setup 4 with multi-layer vegetation. The triangles represent the low, the square the high wind speed. The blue (setup 3) and red areas (setup 4) represent the uncertainty range caused by the different parameterization methods of K_{PA}. The striped area stands for the uncertainty of setups 3) and 4) at low wind speed ($2.5\frac{m}{s}$).

In addition, we compared our impulse application scenario simulation with a similar experiment with the level III steady stated model ClimoChem by *Wegmann et al.* (2004) where also an air pollution impulse of DDT was released in an area close to the equator. Although it is only approximately the same latitudal zone, the decrease of DDT in the atmosphere compartment is for both model experiments very similar. The differences of DDT fraction in the atmosphere was in the range of 10 to 15% (fig. 5.22). *Wegmann et al.* (2004) also showed that the decrease of atmospheric concentration depends on the organic fraction in soils. Organic fraction in the soil serves as a reservoir and buffer compartment for the further cycling of DDT.

The overall residence time τ_{ov} is in general agreement with most of the other model outputs (table 5.3). Especially the two steady state results do not differ substancially from most of the modeled setups in this work. All the residence times calculated here are higher than for the other model tools. Differences of τ_{ov} to other runs range from factor 1.2 to 4. An explanation for our higher τ_{ov}-values is the higher ocean fraction, which reduced atmospheric cycling, causing less degradation and thus a longer lifetime.

	SimpleBox 2.0	Chemrange	MPI-MBM	MCTM	This study
Application pattern (air/soil/veg)	0 /20/80	0/20/80	0/20/80	0/20/80	100/0/0
Area fraction ocean assumed in the model experiment (ca. 57^0N)	60	n.d.	73.2	73.2	53
DDT burden after 10 yrs of simulation time (air/oc/cont))	0.05/17/83	0.3/1/98	0.1/0.6/99	3-23/3-17/63-95	see table5.2

Table 5.1: Comparison of experiment setups and average distribution patterns from different model studies. Comparison of the cross model study with DDT after 10 years of simulation time. The study outline is taken from *Lammel et al.* (2007). All the models show a strong affinity to reside in the continent compartment.

5.4 Long term trends for vegetation types

The results of the impulse application tests are documented as well in longer model runs. The importance of vegetation types for b_{tot}, compartment fraction etc. can be found over longer periods. 100 year runs with the global box application scenario follow the findings of the previous signal tests. The various vegetation types have an impact on the overall fate of DDT, but they also depend on other factors in the environment. Differences of b_{tot} between the several vegetation types are in the same range like for the impulse application experiments. Coniferous type vegetation is for setup 3 and 4 here the canopy with the lowest b_{tot} while the grass canopy values are higher by factor $2-3$. The aerosol type and the choice of partitioning K_{PA} are among the most important factors for b_{tot} and compartment fraction changes with vegetation type over time (figure 5.21).
Wind speed is as before an important factor resulting in a higher contamination at lower atmospheric turbulence. For almost all the tests provided with the single leaf defoliation, the grassland vegetation has the highest b_{tot} of DDT over a run period of 100 years. The multi-layer vegetation tests on the other hand confirm the uncertainty and difference of b_{tot} (figure 5.21). Some tests have a very similar behaviour like the big leaf type vegetation, while other K_{PA} calculations are not comparable with the single big leaf setup. This additional test just proves the previous assumptions that the multi-layer setup is not fully developed.

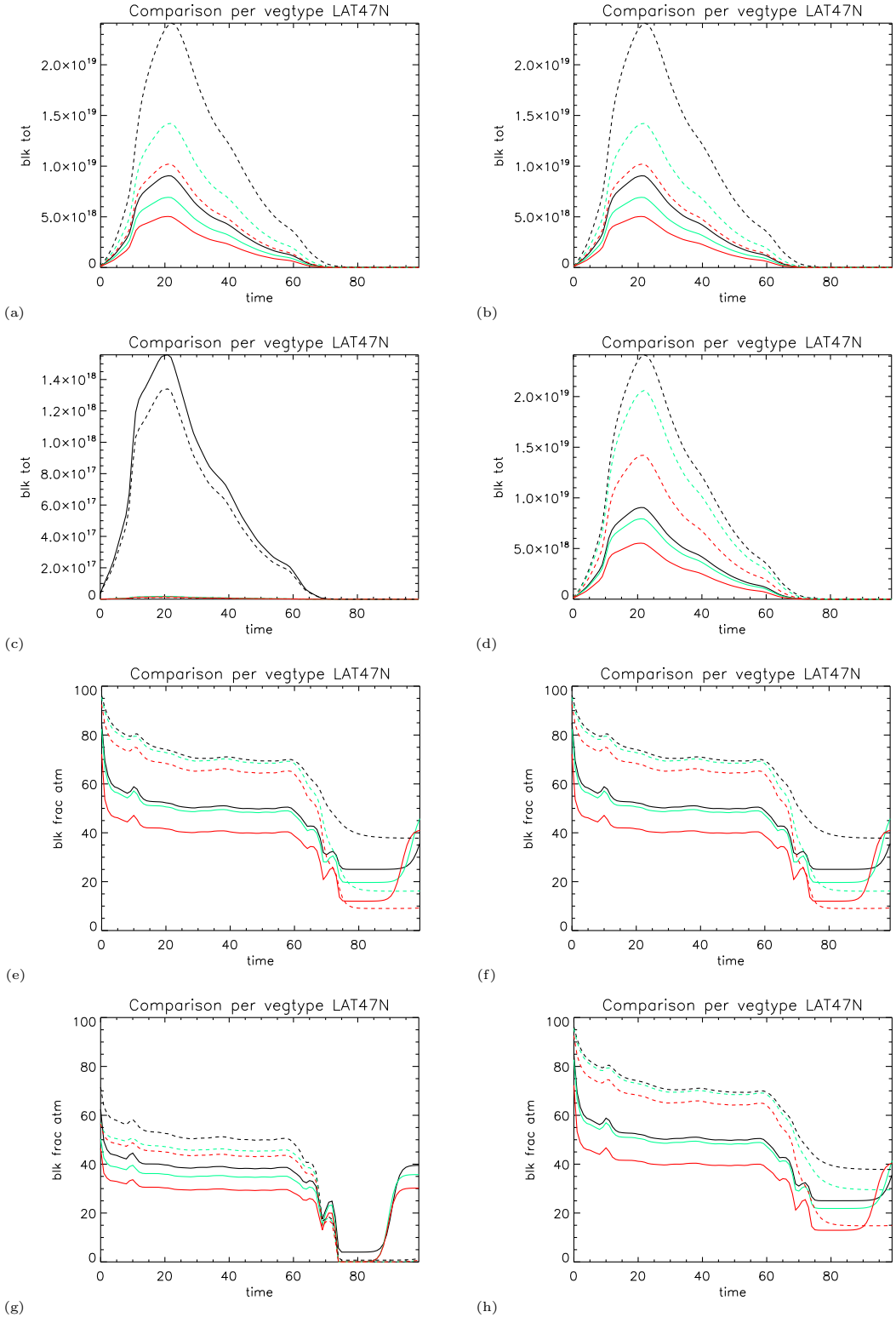

Figure 5.21: Long term trend of total DDT burden and atmospheric fraction given in $\frac{molec}{m^2}$ for different vegetation types in a 100 year run comparing setup 3 and setup 4. Overall burden b_{tot}: a) and c) are for K_{PA_1}, b) and d) are for K_{PA_3}. Atmospheric fraction: e) and g) are for K_{PA_1}, f) and h) are for K_{PA_3}. Both partitioning coefficients are calculated with an urban type aerosol. Grassland (black), deciduous forest (green), coniferous forest (red). The full lines stand for high wind speed, the dashed ones for low wind speed.

high wind					
Setup 1			Setup 2	Setup 3	Setup 4
gas presc	gas calc	part calc	GDF	Defoliation	Multi
69/25/6	65/16/19	47/37/16			
K_{PA_1}			59/30/11	52/41/7	52/42/6
K_{PA_3}			28/17/55	52/41/7	54/40/6
K_{PA_5}			57/30/13	52/41/7	53/41/6
low wind					
Setup 1			Setup 2	Setup 3	Setup 4
gas presc	gas calc	part calc	GDF	Defoliation	Multi
48/47/5	74/14/12	59/30/11			
K_{PA_1}			47/37/16	65/33/2	63/34/3
K_{PA_3}			20/23/57	65/33/2	67/32/1
K_{PA_5}			46/37/17	65/33/2	65/33/2

Table 5.2: Comparison with table 5.2 meridional mean of compartment allocations (air/ocean/continent) DDT after 10 years with several process setups. The compartment distribution of the overall burden b_{tot} is compared with the 10 years simulation results of the model inter comparison study (*Lammel et al.* (2007)). Our model setups show a less strong affinity to reside in the land compartment than other model tools. A major factor for this different results of compartmental distribution is most likely our different application pattern (100% air pollution).

5.5 Climte zone and vegetation type testing

Vegetation type tests are so far performed only for one climate zone with a very limited selection of input parameters. Other influential factors like temperature and land distribution have not been investigated in relationship with the vegetation type either. The findings for this mid latitude environment cannot be transferred simply to other climate zones. Tests with other climate zones confirm the importance of climate zone dependent model runs and influence of the vegetation type (figure 5.13).
Runs with the same vegetation type setup in higher latitudes find a similar pattern for b_{tot}, the overall distribution in comparments and residence time. Tropical areas on the contrary are not similar at all with the findings for mid latitudes. Almost no vegetation type difference between the deciduous rain forest and a grassland vegetation could be detected (figure 5.13). It seems that the behaviour of vegetation and vegetation types are influenced by the temperature pattern to a very high extent. Vegetation can thus have a very different impact depending on the latitude and climate.

5.6 Summary

Tests with the three different deposition schemes and a big leaf vegetation canopy revealed that both gas- and calculated particle deposition processes have extensive

			SimpleBox 2.0	Chemrange	MPI-MBM	MCTM
Overall residence time τ_{ov} in days			2307	2670[1]	132	317-1527[2]
high wind $\left(13\frac{m}{s}\right)$						
Setup 1				Setup 2	Setup 3	Setup 4
gas presc	gas calc	part calc		GDF	Defoliation	Multi
5126	6235	2931				
K_{PA_1}				3334	3238	3234
K_{PA_3}				8996	3238	3211
K_{PA_5}				3465	3238	3247
low wind $\left(2.5\frac{m}{s}\right)$						
Setup 1				Setup 2	Setup 3	Setup 4
gas presc	gas calc	part calc		GDF	Defoliation	Multi
2769	7463	3400				
K_{PA_1}				2882	4043	4018
K_{PA_3}				8415	4043	3963
K_{PA_5}				2949	4043	4093

Table 5.3: Comparison of global averages of τ_{ov} DDT with data taken from a comparative study of simulation runs (*Lammel et al.* (2007)) with several modelling tools. All the residence times were estimated after 10 years of simulation time.

impact on DDT cycling. Differences of up to one order of magnitude for b_{tot} are the result of various calculation methods. The prescribed deposition in setup 1 has the highest b_{tot} values no matter at which wind speed and latitude investigated. Calculated gas deposition and prescribed gas deposition do not have such a strong difference in b_{tot}, and their trends are depending on the latitude characteristics and thus are more difficult to interpret. Particle deposition decreases DDT b_{tot} (figure 5.1). The influence of wind speed on b_{tot} and compartment distribution should not be underestimated (figure 5.23). At low wind speed, the ocean can be considered as a preferred sink of DDT causing generally higher b_{tot}. More atmospheric turbulence at high wind speed is reflected by a less strong shift of DDT into the ocean compartment. Land distribution and b_{tot} do not necessarily correlate, though results tend towards a higher land fraction with lower b_{tot}. The lowest fraction of land contamination is reached with the prescribed deposition in setup 1.

Ocean and atmosphere do not have such a clear trend. The influence of wind speed is very important for the distribution though (figure 5.20). Combined with the high wind speed, a faster cycling in the atmosphere means a stronger removal of DDT by OH-radicals. Whether the diffusive gas exchange is reducing or increasing b_{tot} depends mainly on the choice of the partitioning coefficient K_{PA}. Although there would be an additional pathway to the compartment, diffusive gas exchange has a lot of uncertainties and one cannot make a final conclusion. It can however play a important role in the overall distribution and further cycling.

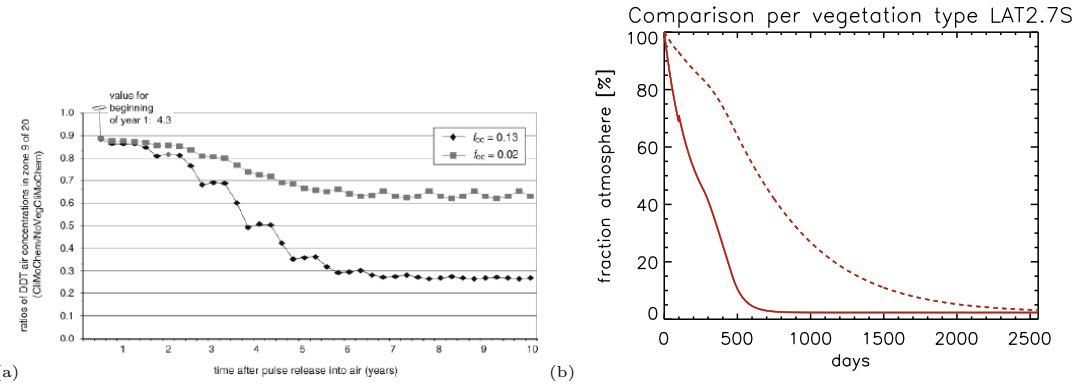

Figure 5.22: Comparison of the fraction of the atmospher for the overall burden b_{tot} with gas and particle deposition (setup 1) and the impulse experiment by *Wegmann et al.* (2004).

Some K_{PA} yield a higher land contamination than for the first three big leaf deposition paths. This could on the other hand point to a stronger storage in the vegetation compartment before overall transfer towards the ocean. Wind speed has a very different role compared to the first three deposition schemes in setup 1.

The last two vegetation setups 2 and 3 have shown that the box model simulation of vegetation processes is limited to a critical extent. The multi-layer vegetation approach highlights that a more complicated model setup has many uncertainties and could lead to errors. All the mentioned simulations with a defoliation process scale down the discrepancy of K_{PA} calculation. The different types of aerosols and vegetation have a stronger influence on the behaviour of DDT than the choice of the partitioning coefficient.

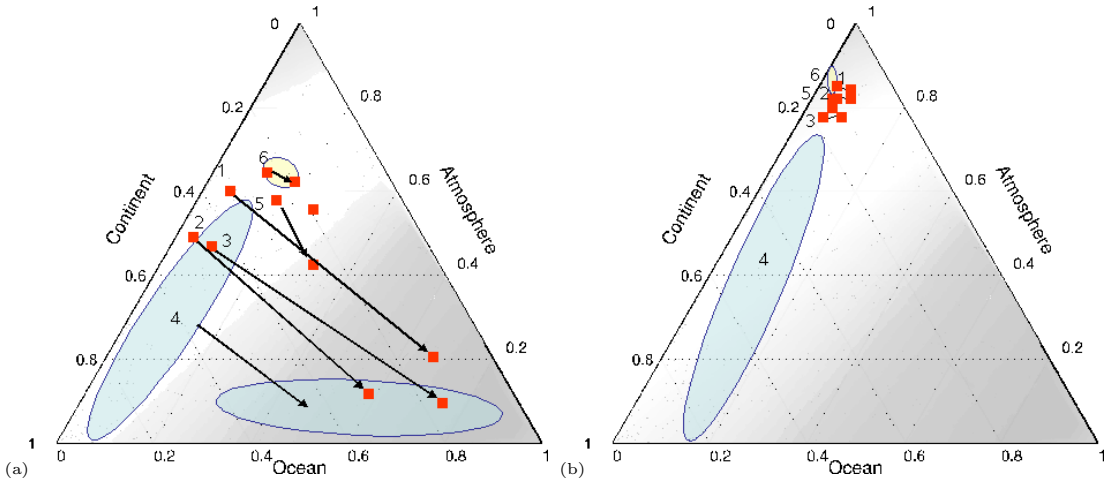

Figure 5.23: Trends for DDT fractions in different compartments over a 100 year run. The numbers represent the different processes and setups tested: 1) setup 1 gas deposition (I), 2) setup 1 gas deposition (II), 3) setup 1 particle deposition, 4) setup 2 diffusive gas exchange, 5) setup 3 defoliation single layer 6) setup 4 multi-layer vegetation. a): Ternary plot for the unit type vegetation in temperate latitudes (47 N). The arrows show what the direction of compartment switch is for during the simulation period of 100 years. b): Ternary plot for the tropics. No larger compartment switch can be seen in most case. The blue areas are the area of uncertainty caused by the different calculation methods for K_{PA} values. All the runs were performed with a shrub type vegetation.

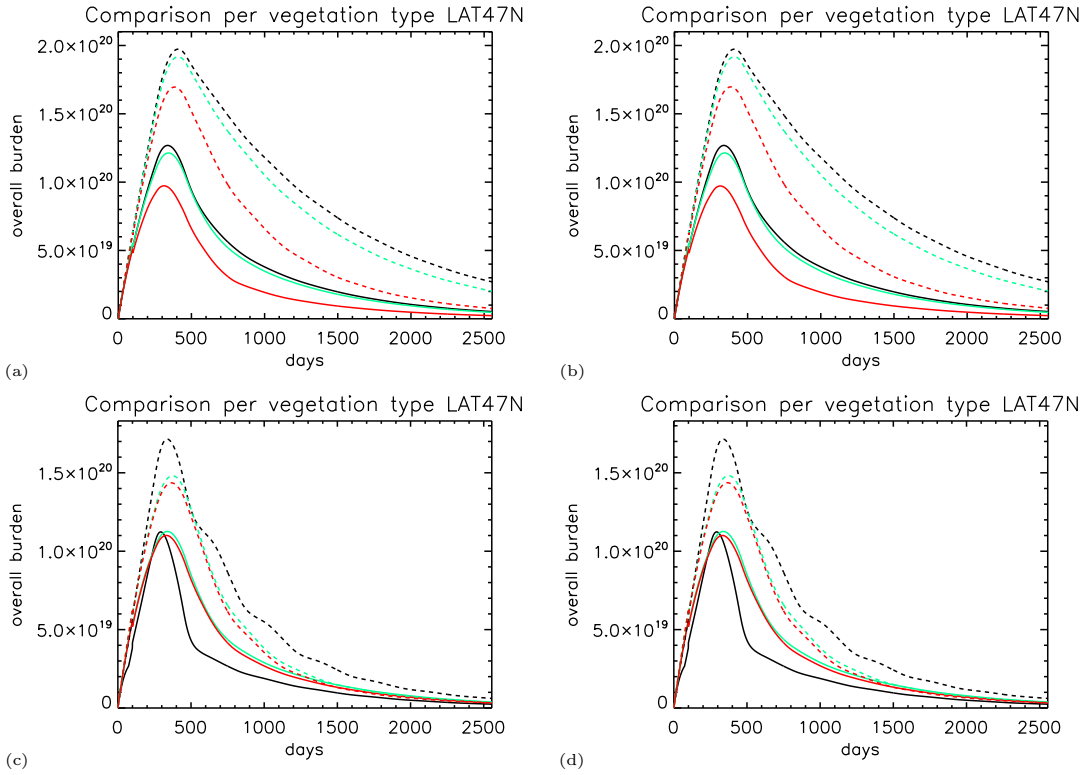

Figure 5.24: Time dependent overall DDT burden b_{tot} in $\frac{molec}{m^2}$ for the multi-layer vegetation types for DDT with K_{PA_3}. a) and c) are the case wind speed of both canopy layers is the same. b) and d) temperature of both canopy layer is the same. This figure is best compared with (figure 5.18). Grassland (black), deciduous forest (green), coniferous forest (red). The full lines stand for high wind speed, the dashed ones for low wind speed.

Chapter 6

Box model study for PCB-52

6.1 Global process study PCB-52

PCB-52 is the second compound to be simulated with the same box model scheme like DDT. The three big leaf deposition process studies (setup 1) are performed and validated. The same shrub type vegetation is used for the latitude dependent experiments. The experiments include also the big leaf canopy model with the addition of the gas diffusion process (setup 2) followed by the defoliation (setup 3) and multi-layer canopy (setup 4). Also in this latter case, only one latitude has been chosen.

6.1.1 Setup 1: Gas and particle deposition study

Global overall burden b_{tot} of PCB-52

The process studies with PCB-52 reveal that chemical properties have an influence on the overall behaviour in the environment. Different temporal and meridional trends of b_{tot} are found between the two simulated chemicals (figure 6.1). The three different (setup 1) deposition parameterizations of PCB-52 vary by one order of magnitude for b_{tot} (figure 6.1).

The prescribed gas deposition is the parametrization with the lowest b_{tot} for this simple vegetation type approach. Though, it has the highest values of b_{tot} in areas with a high ocean fraction. The cold ocean in the southern latitudes is the area with higher PCB-52 accumulation potential in this deposition scheme (figure 6.1). Differences between the two gas deposition calculation methods are in the range of factor $5 - 10$ (figure 6.1), however they also depend on latitude. An explanation for such a discrepancy of b_{tot} may be found in the different compartment distributions (figure 6.3) of the two calculation methods. The land fraction of the prescribed gas deposition is higher than than for the other deposition parameterizations. Calculated gas deposition is not as effectively degraded on the continent as it is for the prescribed gas deposition (figure 6.3). The role of the ocean in this case is different than in the case of DDT.

Unlike in the case of DDT, vegetation has a weaker influence on b_{tot}; levels of b_{tot} between non vegetated and vegetated surfaces are in general very similar (figure

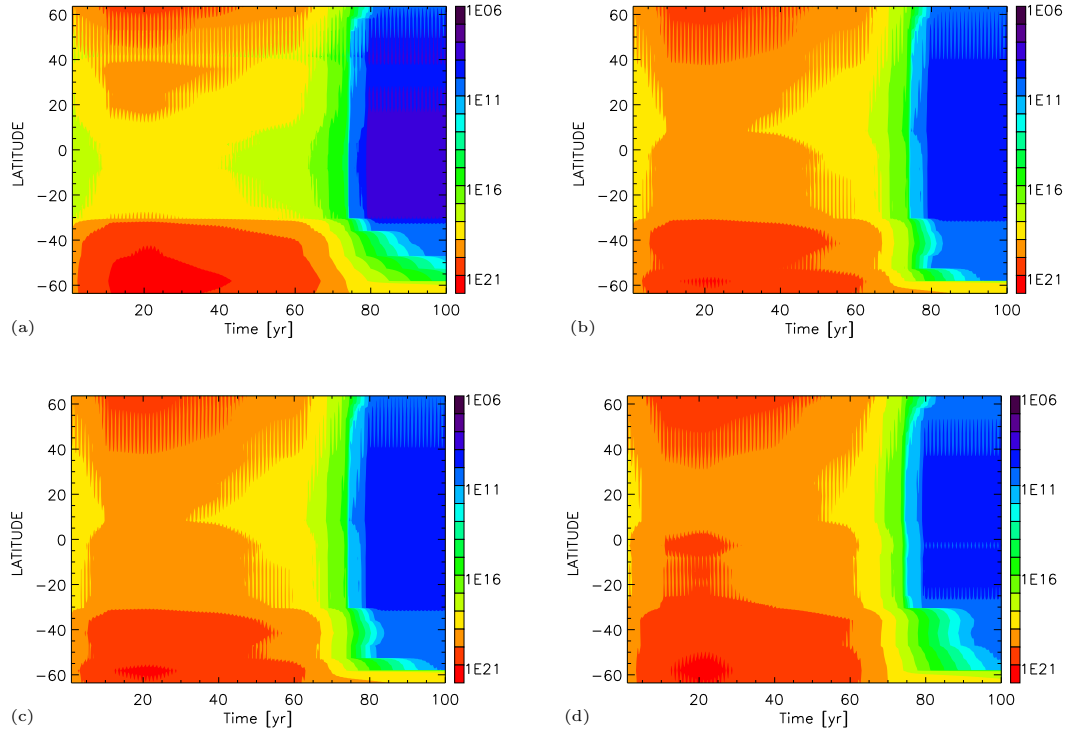

Figure 6.1: Time dependent total burden b_{tot} of PCB-52 given in $\frac{molec}{m^2}$ for 100 years runs. a) is setup 1 with gas deposition prescribed. b) b_{tot} setup 1 PCB-52 gas deposition calculated. c) and d) b_{tot} setup 1 PCB-52 particle deposition at high ($13\frac{m}{s}$) and low ($2.5\frac{m}{s}$) wind speed. All the calculations are made with the uniform shrub type vegetation. A clear seasonality is displayed in the plots where b_{tot} is higher in the winter period in the range of one order of magnitude.

6.2). However the compartment distribution of vegetated and non vegetated surfaces are not in agreement (figure 6.3).
Almost no impact on b_{tot} is observed for the added particle deposition process. Very similar values like for the calculated gas deposition are found. Properties of PCB-52 are most likely the main reasons for such a behaviour. PCB-52 is categorized either as single or multiple gaseous hopper. The lower vapour pressure as well as the lower molecular weight of PCB-52 could be the main reason why it resides mostly in the gaseous phase and thus does not attach easily to organic particles. Volatilization and deposition fluxes of gas deposition (I) and particle deposition are very similar.

Distribution of PCB-52 different compartments

The overall burden differences are also reflected in the distribution pattern. Depending on the parameterization process, different ocean-land interactions take place. Prescribed gas deposition has the highest land fraction of the studied parametrizations, as well as the largest proportional amount of ocean contamination in the northern hemisphere. Land and ocean together account for almost

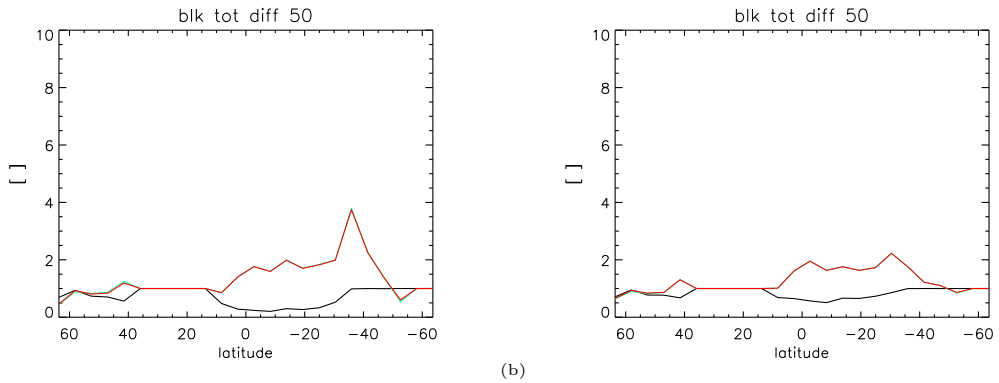

Figure 6.2: Comparison of the ratio vegetated run/nonvegetated run meridional cross section of the relative difference of the overall burden b_{tot} at high (a) and low wind speed (b) for PCB-52 for the year 50. All simulations are for setup 1: prescribed deposition (black), calculated gas deposition (green), calculated particle deposition (red).

90 percent of the total burden. The land and ocean compartments of the northern hemisphere take up most of the PCB-52 (figure 6.3 and 6.4). A higher land fraction results in a stronger volatilization flux, hence stronger degradation in the atmosphere and redeposition (figure 6.6). This indicates that the degradation on the land must be a stronger factor for the prescribed calculation method.

Compared to the other methods, the prescribed gas deposition leads to a higher ratio of volatilization/b_{tot}. This explains why the compartment fraction in the atmosphere is much smaller than in the case of the gas deposition setups. The removal by reaction with OH-radicals is probably larger. Vegetation decreases the PCB-52 fraction on land for every calculated deposition scheme. This could be an indirect effect of cleaning the land compartment from PCB-52, though not from the total environment, because the degradation in the atmosphere seems to be less effective.

Higher volatilization is observed in the northern hemisphere for simulations without vegetation (figure 6.6). Differences of b_{tot} or media allocation are rather marginal between calculated gas deposition and calculated particle deposition. More PCB-52 resides in the atmosphere or in the terrestrial environment at medium or lower temperatures (figure 6.3). Particle deposition is obviously not an additional path for removal from the atmosphere. Very similar results like for the calculated gas deposition are the consequence.

Removal of PCB-52 by OH-radicals in the atmosphere is in general less efficient than in the case of DDT. The compartmental fractions of PCB-52 also remain relatively stable with time (unlike for DDT). An open question remains about the influence of the temperature on the overall distribution. Due to the surface distribution, all the runs have an expected North-South increment of ocean fraction (figure 6.4). The by far highest ocean fraction is calculated for the prescribed deposition, while the other two simulations are similar. Ocean storage depends on the continent fraction in a latitude belt.

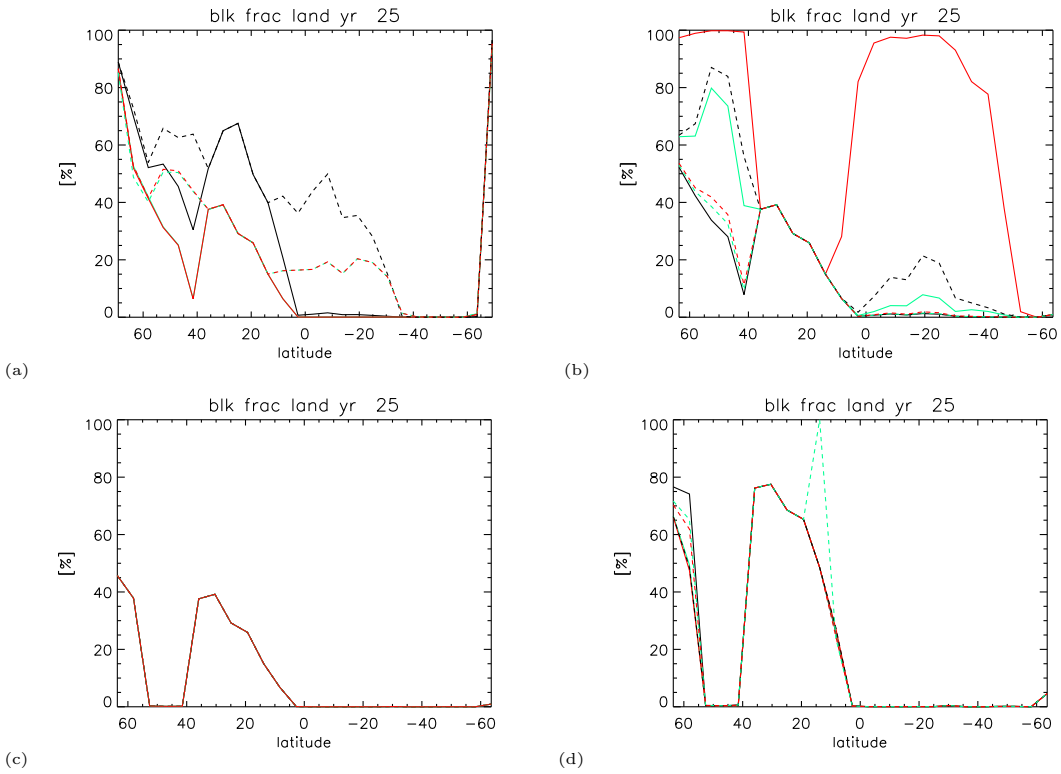

Figure 6.3: Land fractions of PCB-52 in a meridional N-S section for the annual average PCB-52 at simulation year 25 land fractions for setup 1 (a), setup 2 (b), setup 3 (c) and setup 4 (d). Setup 1: prescribed deposition (black), calculated gas deposition (green), calculated particle deposition (red). The dashed lines, without vegetation effects. For setup 2-4: Full lines: K_{PA_1}: black, K_{PA_2}: green, K_{PA_3}: red. Dashed lines: K_{PA_4}: black, K_{PA_5}: green, K_{PA_6}: red

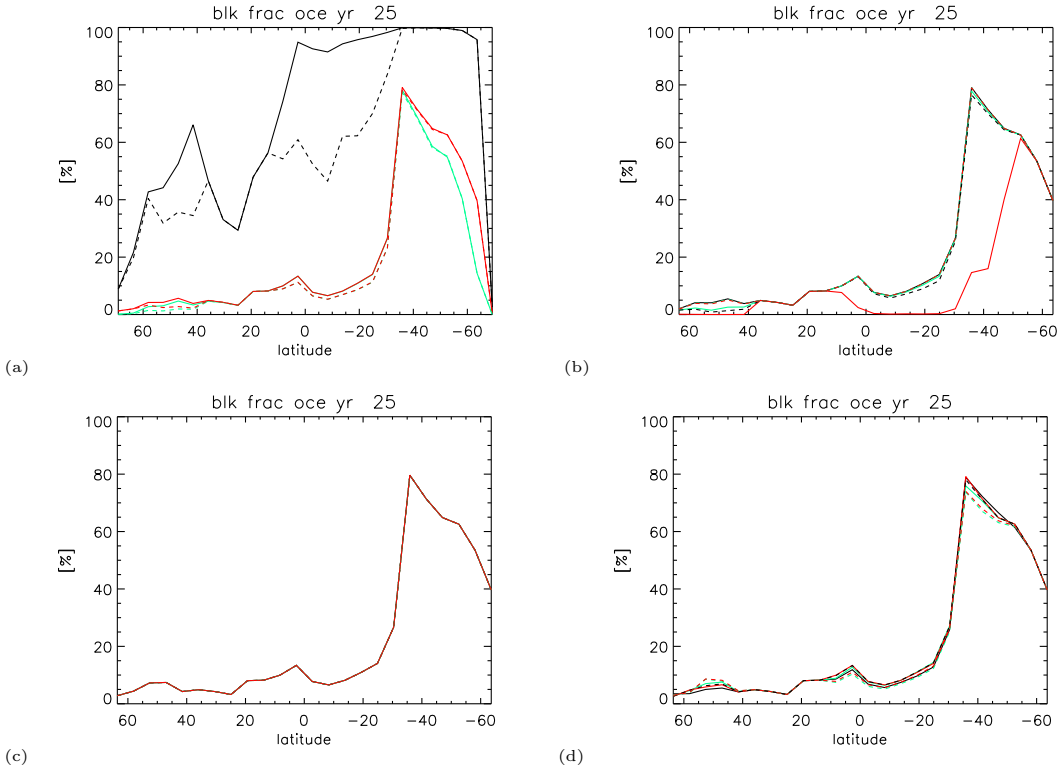

Figure 6.4: Ocean fraction of PCB-52 in a meridional N-S section for the annual at simulation year 25 for setup 1 (a), setup 2 (b), setup 3 (c) and setup 4 (d). Colours and curves see also figure 6.3

However, the ocean fraction and b_{tot} are related differently than in the case for DDT. Other factors that influence the overall distribution are temperature and wind speed. For the land fraction, all the deposition setups have a very similar amount of volatilization and deposition (figure 6.6. Higher overall cycling is not necessarily reducing b_{tot}, because the atmospheric removal process is less strong for PCB-52. The role of the vegetation can be described as inhibition of volatilization.

6.1.2 Setup 2: Gas diffusion

Global overall burden b_{tot}

The gas diffusion exchange onto vegetation reveals very similar findings like for the case of DDT. Gas diffusion is a very substantial process for the overall cycling and the canopy filter effect (figure 6.5). b_{tot} does less depend on the chemical properties than the choice of K_{PA}. Similar to DDT, a large variability for the different partitioning coefficient K_{PA} is found. Differences of b_{tot} vary up to more than one order of magnitude (figure 6.5). K_{PA_3} tests have also here the highest values of b_{tot}. b_{tot} for K_{PA_1}, K_{PA_5} and K_{PA_6} are very similar, while for K_{PA_2} and K_{PA_4} values are slightly higher.

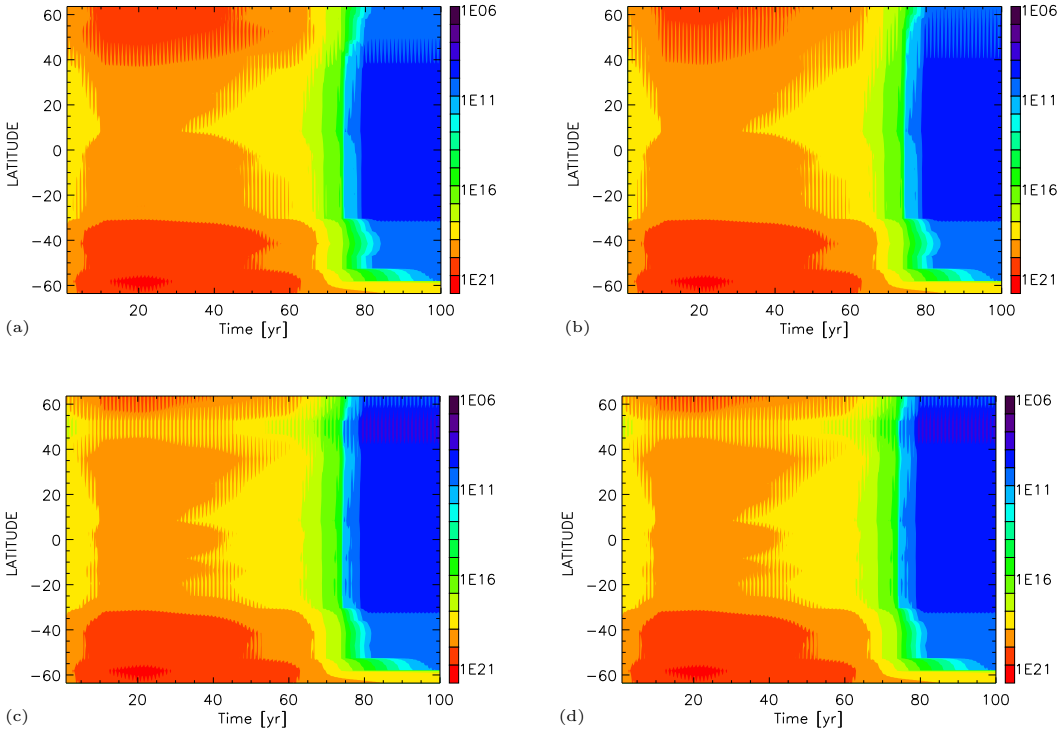

Figure 6.5: b_{tot} for PCB-52 and setup 2. a) and b) Big leaf gas diffusion setup calculated with K_{PA_2} and K_{PA_1}, respectively at high wind speed ($13\frac{m}{s}$). b_{tot} for PCB-52 and setup 3 (defoliation). a) and b) Big leaf gas diffusion setup calculated with K_{PA_2} and K_{PA_1}, respectively at high wind speed ($13\frac{m}{s}$)

Several important factors can be detected for all the gas diffusion runs. The b_{tot} has a quite large land fraction throughout all the latitudes. In temperate continental areas of the mid latitudes with large land fractions, the LAI is more important than temperature. Differences between the K_{PA_3} method and the other calculations are growing with the land surface fraction and LAI (figure 6.3 b).
Gas diffusion, temperature and LAI show very distinct relationships between each other. Although the higher latitudes are colder and could accumulate PCB-52 there, one can observe a decrease of b_{tot} compared to the mid latitudes. The reason is most likely the lower LAI which makes accumulation on and in leaves less strong for the uniform vegetation type (figure 6.6). The higher b_{tot} in the southern hemisphere is related to the larger water surface fraction of the colder ocean and not to the gas diffusion onto vegetation on land.

Compartmental distribution of PCB-52 in setup 2

Several factors are important for the correlation between ocean-continent ratio, compartment distribution of b_{tot} and K_{PA}. The influence of K_{PA} is reflected also in the compartment distribution pattern (figure 6.3, 6.4). However, also temperature is very important for the accumulation rate on land.
The biggest shift in the overall distribution of PCB-52 is seen between atmosphere and land, while the ocean compartment fraction remains almost unchanged (figure 6.3, 6.4). K_{PA_3} has the by far highest overall values for the land fraction followed by K_{PA_4} and K_{PA_2}. This is related to the lower temperatures and and the larger continental surface which obviously enhance stronger land accumulation for these parameterizations of partitioning. Volatilization is the driving factor of the distribution pattern (figure 6.6) which is exactly the opposite to the land fraction of overall burden (figure 6.6, 6.3).
The influence of the LAI is also an important factor for the volatilization and must be correlated with the temperature. Lower temperature favors accumulation in the leaf. The influence of different K_{PA} is stronger at lower annual mean temperature.
Although PCB-52 resides to a large extent in the atmosphere, one can see that the process of gas diffusion influences its ability to remain in this compartment. Compared to DDT, the compartmental fractions of PCB-52 remains almost stable with time. The ocean fraction is almost not changed with the implementation of gas diffusion (figure 6.4). A reason could be that the ocean fraction has reached its maximum capacity where additional accumulation is rather unlikely. This is explained with the K_{AW} coefficient of PCB-52. Unlike DDT, PCB-52 is not such a good 'swimmer'.

6.1.3 Setup 3: Inclusion of defoliation

Defoliation is a major process for b_{tot} and the further cycling of PCB-52. It also outrivals the gas diffusion process (figure 6.5). Like in the runs with DDT, the partitioning factor K_{PA} is not sensitive for big leaf vegetation setups with defoliation. Very similar effects are observed for both chemicals, despite its differences in

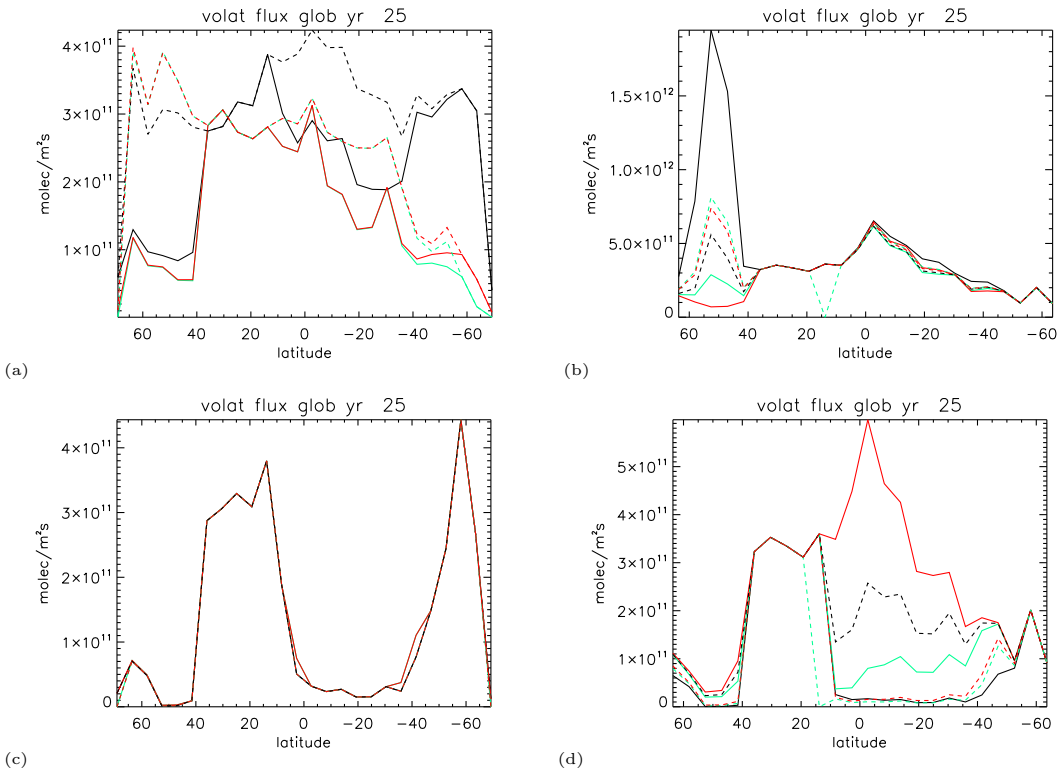

Figure 6.6: Annual mean PCB-52 volatilization flux ($\frac{molec}{m^2 s}$) at year 25. a), setup 1: Black line for prescribed deposition, green line: calculated for gas deposition, red line for particle deposition. b), c) and d) are sensitivity test of K_{PA}; b) setup 2, c): setup 3, d) setup 4. Full lines: K_{PA_1}: black, K_{PA_2}: green, K_{PA_3}: red, dashed lines: K_{PA_4}: black, K_{PA_5}: green, K_{PA_6}: red

chemical properties. Overall reduction of contamination levels by approximately one order of magnitude in land dominated areas is another consequence of this additional process (figure 6.5).
Most of PCB-52 is in the atmosphere, especially in areas with high vegetation fraction. Vegetation defoliation is not pumping PCB-52 into the ocean and the compartment shift ends with accumulation in the atmosphere. Different log K_{AW} values are most likely the reason for such a behaviour. However, atmospheric accumulation is also achieved by some of the K_{PA} parameterizations without the inclusion of litterfall, which also reflects the uncertainty caused by these coefficients.
The North-South ocean fraction distribution is very similar to the previous deposition processes (figure 6.4). PCB-52 accumulates more in the land compartment of areas with high continent fraction and for very low temperature (figure 6.3). These areas do not have a larger vegetation canopy (e.g. deserts or tundra). It is thus not clear to which extent this would be related to this additional process.
The compartment fractions are similar to the particle deposition, as well as there are similarities to some runs of the gas diffusion tests. Due to the different log K_{AW} of PCB-52, setup 3 with defoliation has smaller impact on the allocation

pattern than for DDT.

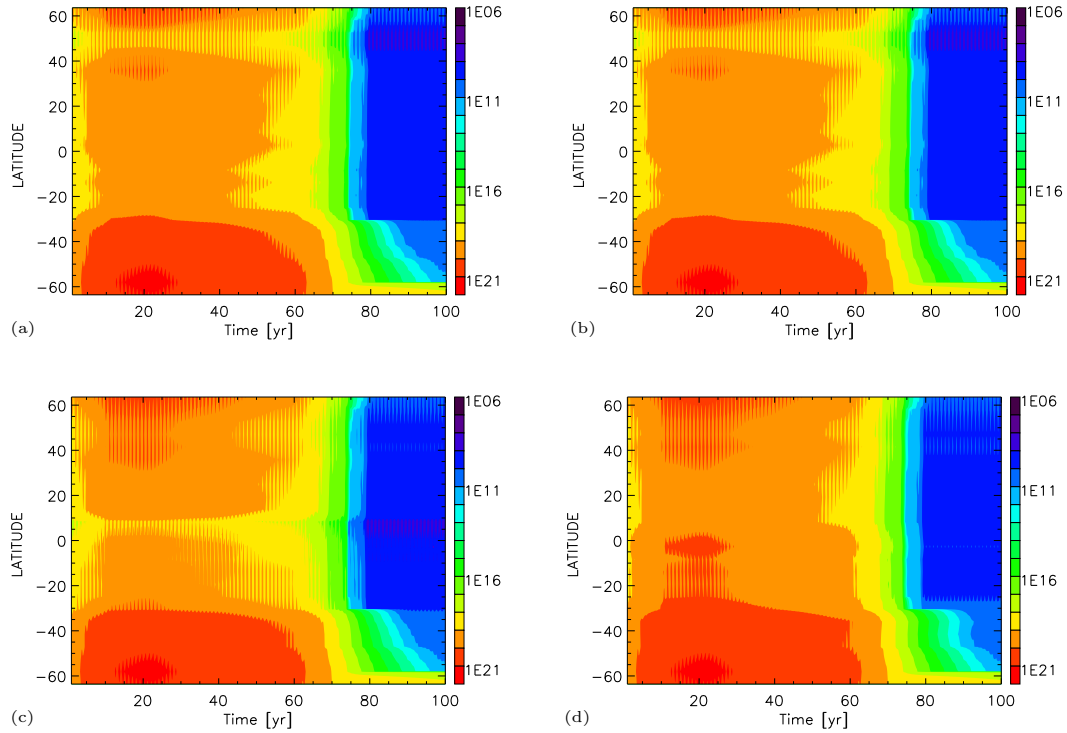

Figure 6.7: Time dependent burden b_{tot} PCB-52 for setups 3 (a and b) and 4 (c and d) at low wind speed ($2.5\frac{m}{s}$). a) and c) are calculated for K_{PA_4} while b) and d) stand for K_{PA_3}.

6.1.4 Setup 4: Multi-layer vegetation tests

Two different trends are obtained with the canopy split. Multi-layer vegetation runs tend to either be very similar to the results achieved with setup 3 or look completely different. The influence of the leaf-air partitioning is evident. K_{PA} changes introduces a lot of variability, similar to DDT (figure 6.7).
Values for b_{tot} reflect the uncertainty very well. They either are in the same range like 3, or differ up to two orders of magnitude. Differences of b_{tot} between setup 3 and setup 4 also vary with the climate zone. Even less b_{tot} can be found for setup 4 for some K_{PA} parameterizations (figure 6.7). It is obvious that setup 4 has an even higher level of uncertainty than setup 3. Differences for K_{PA} show up more strongly in the overall burden b_{tot} in the compartment distribution. The overall partitioning between air, land and ocean remains nearly the same as in setup 3 (figure 6.3, 6.4). Volatilization on the other hand is stronger affected by setup 4 and larger differences of K_{PA} calculations to setup 3 are found especially in mid latitudes (figure 6.7). Effects of the adaptation of the logarithmic wind profile and the canopy temperature difference are evident. Similar to DDT, the different K_{PA} values are more important for setup 4 than for setup 3.

6.2 Influence of vegetation type on PCB-52 cycling

Additional vegetation type model experiments are performed for a single latitude ($47N^0$). The setups chosen are basically the same as in the DDT runs and thus this section highlights the effects on PCB-52 for the different deposition parameterization and vegetation specific phenologies. The focus is on the overall effects of the canopy filter effect with different aerosols and vegetation life cycles.

6.2.1 Setup 1: Big leaf deposition

Test with two different aerosol types reveal that the inclusion of particle deposition does not have large effects on b_{tot} for each vegetation type simulated (figure 6.8). Differences between the vegetation type depend on the aerosol type. However they are in general small because the impulse application is decreasing at a rapid pace. The urban type aerosol leads to a higher peak of b_{tot} in the first year. The vegetation type pattern for both aerosol types looks very similar and differences between the vegetations are rather marginal. Calculated gas and particle deposition both have a peak followed by a minor drop in the application year. Because these tests are performed under stable conditions for temperature, application etc., this drop is related to the influence of LAI and volatilization from soil (figure 6.8). Further sensitivity tests with aerosols reveal that particle deposition can have a great influence on volatilization (figure 6.9). Particle deposition reduces the overall volatilization for the urban aerosols to about half the values of calculated gas deposition (figure 6.9).

The relationship between volatilization and wind speed and vegetation type is difficult to interpret. While one can detect an annual oscillation for grassland vegetation during the first few years (which is mostly related to the annual change of LAI) at low wind speed, for high wind speeds and other vegetation types such a behaviour is absent. Grassland vegetation has the highest volatilization rates, but there is no clear evidence to what extent this would be related to wind speed (figure 6.9). Additionally this does not have any consequences for b_{tot} (figure 6.8). Both canopy types have almost similar values of volatilization, which is an indication for the influence of roughness length or canopy height on this process.

6.2.2 Setup 2: Big leaf gas diffusion

Overall burden b_{tot}

The interactions of aerosol type, wind speed and leaf air partitioning factor K_{PA} affect the overall burden b_{tot} (figure 6.10). The influence of the leaf partitioning factor K_{PA} is also relevant for b_{tot}. The other important parameter for gas uptake are roughness length, LAI and wind speed. However, it is not clear which of the mentioned factors is the most important one. Grassland vegetation is the canopy with a similar range of b_{tot} for all the K_{PA} values. In addition, grass is perhaps

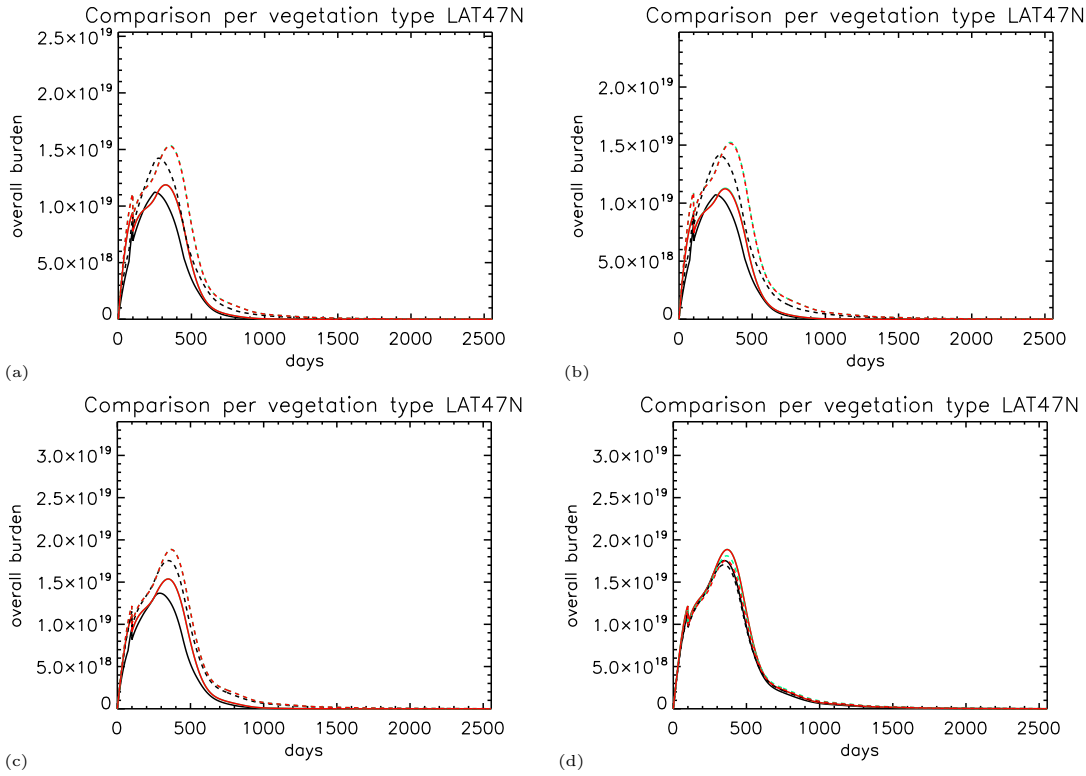

Figure 6.8: Time dependent total burden b_{tot} in $\frac{molec}{m^2 s}$ setup 1 with different aerosol types: a) and b) are for background aerosol, c) and d) is for the urban type aerosol; a) c): setup 1 with calculated gas deposition, b) and c): setup 1 for particle deposition. Grassland (black), deciduous forest (green), coniferous forest (red). The full lines stand for high wind speed ($13\frac{m}{s}$), the dashed lines for low wind speed ($2.5\frac{m}{s}$).

less sensitive to the change of aerosol. The other two vegetations react with a much larger variation of b_{tot} (figure 6.10). This is most likely due to the wind profile or the canopy roughness of the different vegetation types.
Degradation and outgassing from the leaf volume subcompartment works faster for grassland vegetation and K_{PA_3}. K_{PA_3} tests indicate that the forest type vegetation tends to use litter as long term sink. Unlike the runs with DDT, grassland vegetation shows for both wind speeds the lowest b_{tot} for gas diffusion. Differences for b_{tot} with the deciduous and coniferous canopy are not large in all the variations of K_{PA} (except K_{PA_3}). This indicates that surface roughness is less important than LAI for the process of gas diffusion.
Similar remarks can be made for the gas diffusion process for PCB-52 as for DDT. K_{PA} can be considered as a major factor for b_{tot} and overall fate of POPs. Compound properties are less influential on the process of gas diffusion.

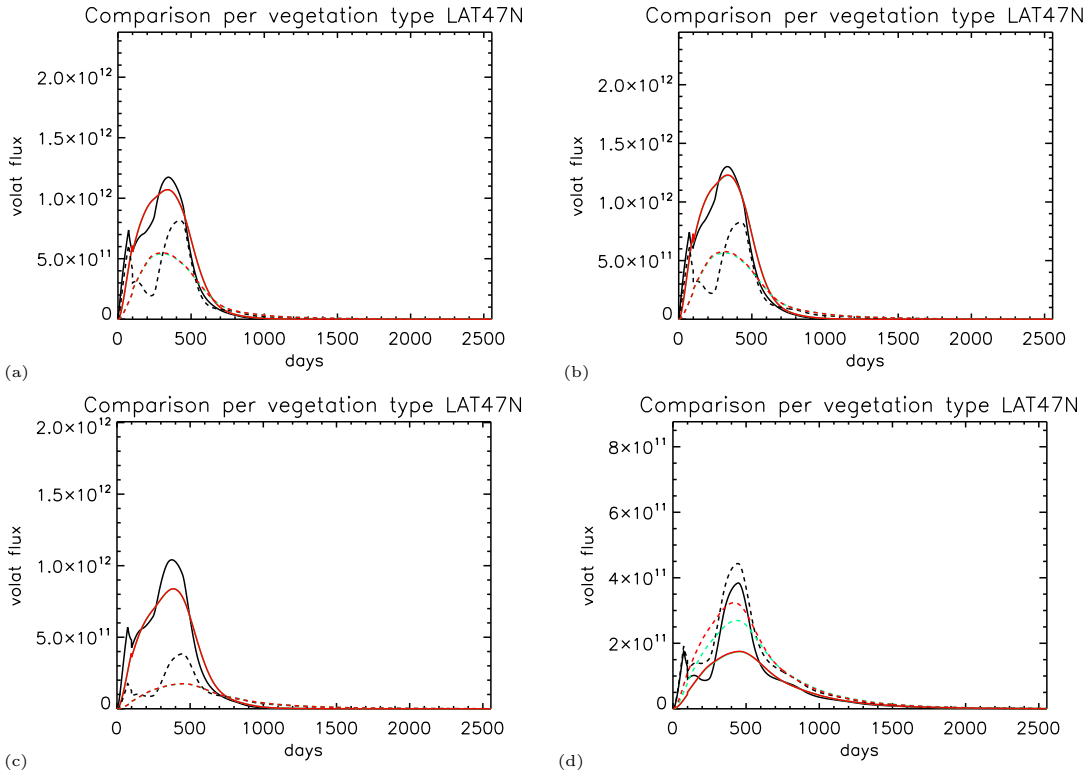

Figure 6.9: Volatilization flux setup 1. Figure a,b: Background aerosols, figure c,d: Urban type aerosol. Figure a,c: gas deposition calculated, Figure b,d: particle deposition. Grassland (black), deciduous forest (green), coniferous forest (red). The full lines stand for high wind speed ($13\frac{m}{s}$), the dashed lines for low wind speed ($2.5\frac{m}{s}$).

Compartment distribution

It is evident that differences of the overall compartment distribution are related to the plant air-partitioning coefficient. Depending on the choice of K_{PA}, changes in the burden on land are very remarkable (figure 6.11). Though, also vegetation type specific criteria have an influence on the overall allocation of PCB-52. Tests show that for K_{PA_3} and every vegetation type the land compartment would increase to a maximum value. Differences in the land fraction also depend on the aerosol type (figure 6.11).
The annual cycles are due to LAI change during the year and can be found in every K_{PA} test and compartment. In most cases, PCB-52 would be very sensitive to wind speed; differences between the vegetation types are in general very small. Low wind speed means a higher b_{tot} and higher ocean fraction of PCB-52. Calculations with K_{PA_3} show that with grassland vegetation a higher overall fraction in the ocean must be expected. This is probably related to two factors: the annual LAI cycle and the higher volatilization rate from grass followed by rather low volatilization from the sea.

Volatilization fluxes depend strongly on K_{PA} as well as on wind speed and aerosol type. No clear trend is documented which vegetation type is the one most

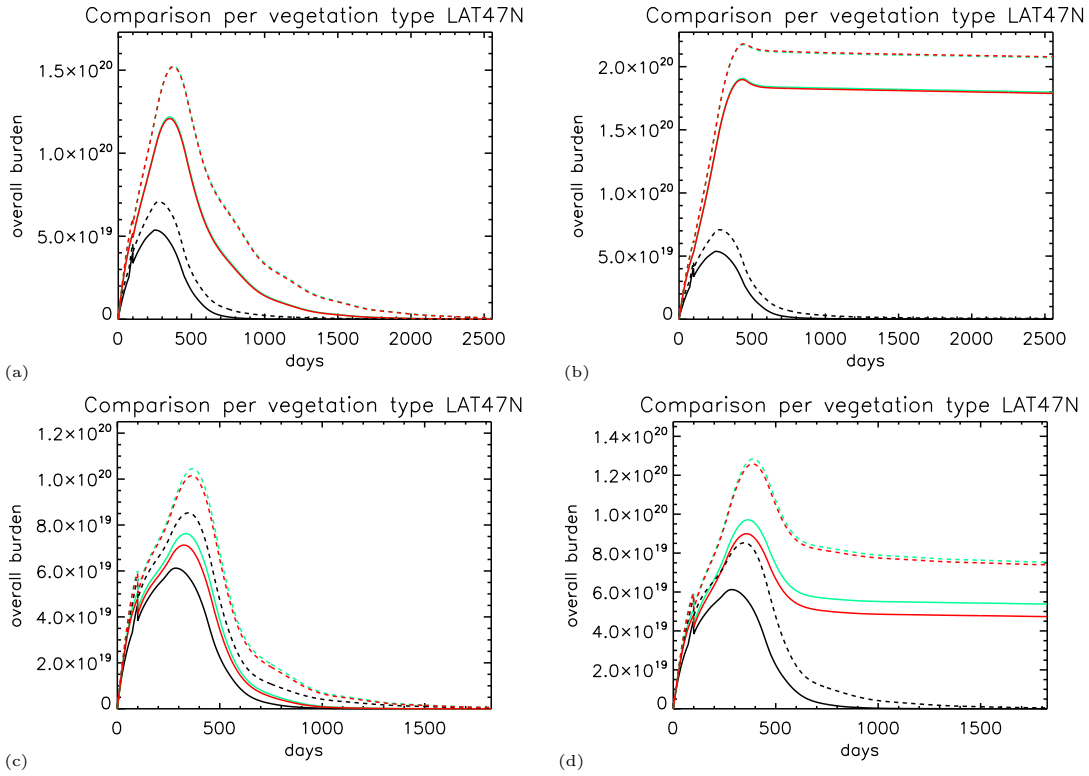

Figure 6.10: Time dependent total burden b_{tot} in $\frac{molec}{m^2 s}$ for PCB-52 setup 2 at $47^0 N$. Figure a and b: background aerosols, figure c and d:urban type aerosols. Figure a,c:K_{PA_2}, figure b,c: K_{PA_3}. Grassland (black), deciduous forest (green), coniferous forest (red). The full lines stand for high wind speed ($13\frac{m}{s}$), the dashed lines for low wind speed ($2.5\frac{m}{s}$).

exposed to volatilization. Depending on the wind speed value, K_{PA} or the aerosol type the vegetation type with most exposition is changing. Seasonality of LAI is seen in many cases though as a clear oscillation of compartment fraction. Also the wind speed can influence the overall distribution on seasonal scale.

6.2.3 Setup 3: Big leaf defoliation

Very similar results are found for the defoliation tests with PCB-52 as for DDT. It can also here be assumed that the process of defoliation is probably more important than the differences in the chemical characteristics of both compounds. The choice of the partitioning coefficient K_{PA} is less important after the introduction of defoliation and the vegetation soil (figure 6.16). However this is only valid for our model setup with immediate revolatilization from soil under the vegetation. All the tests show a very strong decrease of b_{tot} after the impulse application year. Depending on the vegetation type, the defoliation runs do not depend on seasonality of LAI for b_{tot}. Probably the application interval is too short. Differences are difficult to track after the application stop. Low wind speed leads in general to higher b_{tot} no matter which vegetation or aerosol type is selected. The ratio

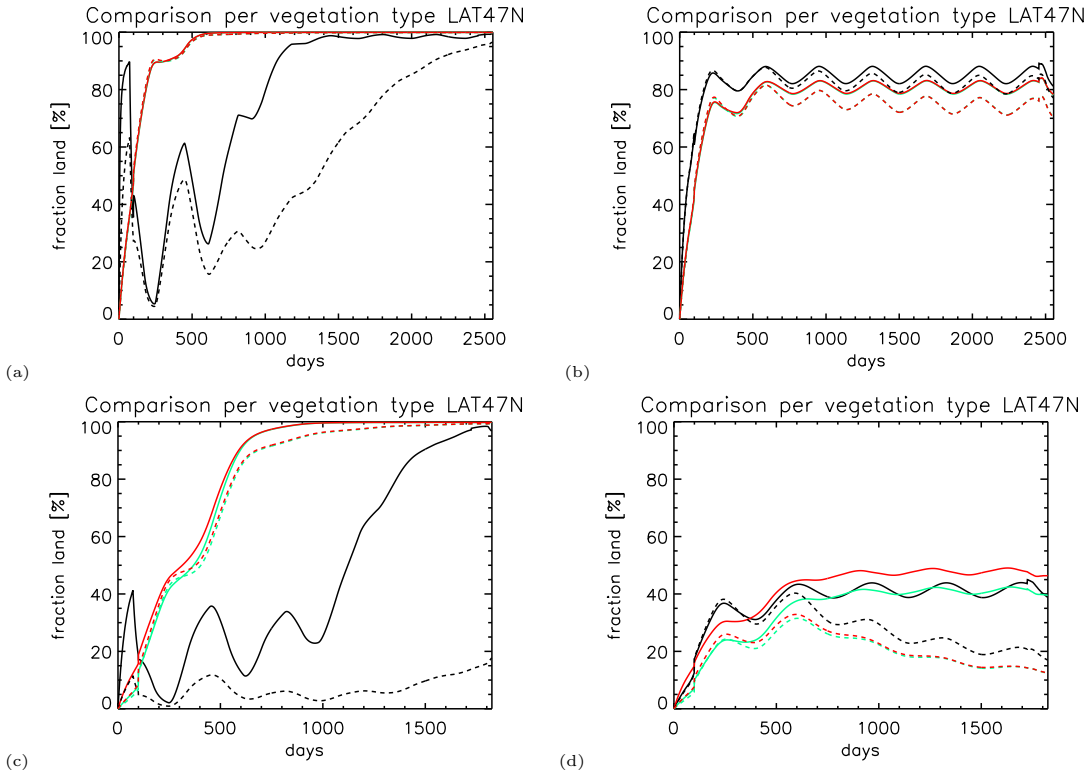

Figure 6.11: Time dependent (2500 days run) land fraction of PCB-52 at 47^0N in percent. a) and b) are for background aerosols, c) and d) are the same case for urban type aerosol. a) and c) are for K_{PA_3}, figure b) d) is the same calculation for K_{PA_4}. Grassland (black), deciduous forest (green), coniferous forest (red). The full lines stand for high wind speed ($13\frac{m}{s}$), the dashed lines for low wind speed ($2.5\frac{m}{s}$).

volatilization/ b_{tot} is higher at high wind speed. Thus this additional cycling leads to stronger degradation by OH-radicals while for low wind speed the accumulation in the ocean is higher. Differences between the vegetation types are not too large. b_{tot} of the various vegetation types are in a similar range after year one. In general the grassland vegetation has the highest b_{tot} at low wind speed, which is due to the combined effects of wind speed, canopy profile, annual cycle and the subsequent faster deposition in the ocean compartment (figure 6.16). The main deposition process into the ocean compartment takes place in the first year and remains stable afterwards. Defoliation is not leading to additional accumulation in the soil compartments. Compared to the big leaf gas diffusion tests, the land fraction remains in the most cases stable over time (figure 6.11, 6.12) and resembles to the big leaf compartment fraction without gas diffusion or defoliation. Aerosol types do not have such a strong effect on the overall distribution like in the big leaf vegetation model. Lower wind speed reduces the overall land fraction extensively (figure 6.12) after the first year of application. Pointing to the rapid volatilization from land is taking place very fast. A growth of the atmosphere fraction and later the ocean fraction is the consequence.

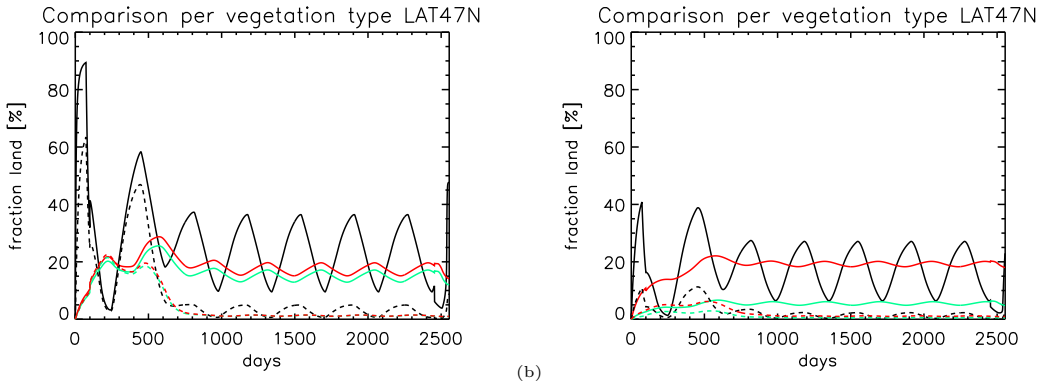

Figure 6.12: Time dependent land fraction for PCB-52 and setup 3 at 47^0N. a) is the case of K_{PA_3}, b) stands for K_{PA_4}. Grassland (black), deciduous forest (green), coniferous forest (red). The full lines stand for high wind speed ($13\frac{m}{s}$), the dashed lines for low wind speed ($2.5\frac{m}{s}$).

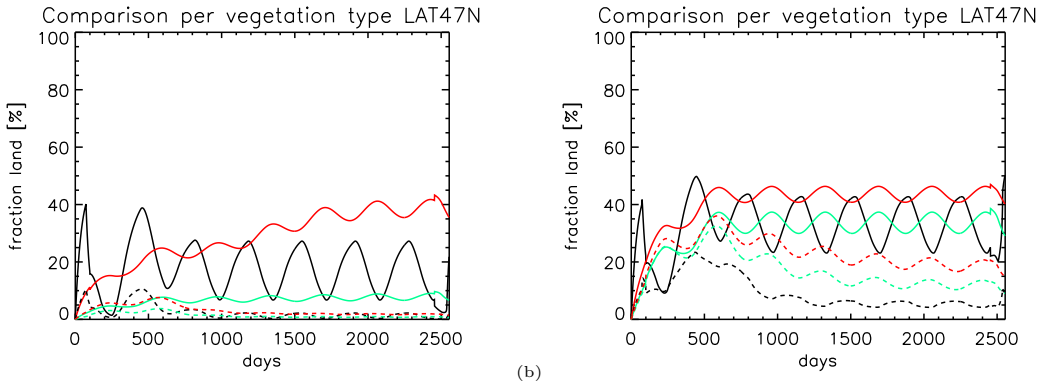

Figure 6.13: Time dependent land fraction for PCB-52 and setup 4 at 47^0N. a) is for K_{PA_3}, figure b) for K_{PA_4}. Grassland (black), deciduous forest (green), coniferous forest (red). The full lines stand for high wind speed ($13\frac{m}{s}$), the dashed lines for low wind speed ($2.5\frac{m}{s}$).

When including defoliation, differences between vegetation types are more relevant than the choice of K_{PA}. Land fractions for different vegetations vary from 10-30 percent. At low wind speed the overall fraction of ocean is higher although the ocean is not the main residence compartment for PCB-52.

6.2.4 Setup 4: Multi-layer canopy and vegetation type

Compared to the single big leaf vegetation, multi-layer vegetation box model results are rather inconsistent. Especially the partitioning factors give no clear evidence and it is thus not definite what the exact effects of a two layered vegetations are. As already mentioned for DDT, different K_{PA} values also lead to distinct changes of b_{tot}. Depending on the K_{PA} chosen, the results of b_{tot} are difficult to interpret. Effects of the seasonality of LAI for vegetation types are sometimes absent or small (figure 6.16). b_{tot} is in general within the same range as

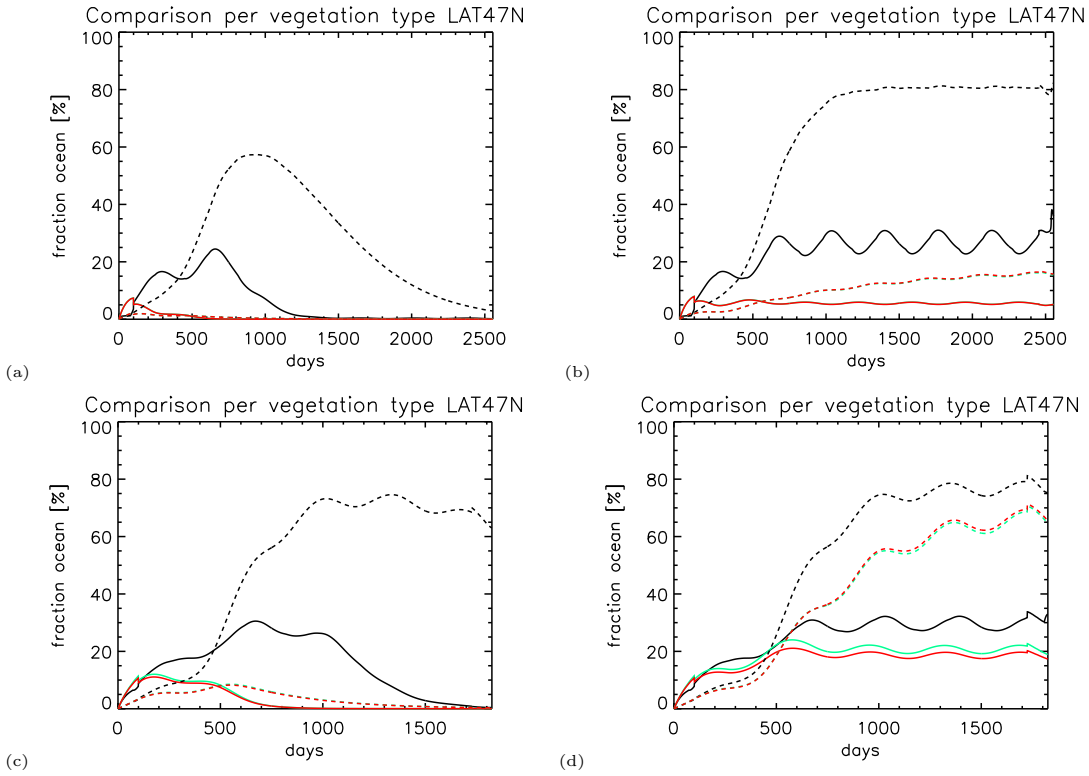

Figure 6.14: Time dependent land fraction for PCB-52 and setup 2 at 47^0N. a) and b) are with background aerosols, c) and d) are the fractions for the urban type aerosol. a) and c) are for K_{PA_3}, figure b) and d) is for K_{PA_2}. Grassland (black), deciduous forest (green), coniferous forest (red). The full lines stand for high wind speed ($13\frac{m}{s}$), the dashed lines for low wind speed ($2.5\frac{m}{s}$).

for setup 3. However, for some K_{PA} values b_{tot} varies by one order of magnitude, probably related to the different wind speeds within the two vegetation layers. This may also have an influence on the further cycling process.

The higher b_{tot} could be the consequence of a slower degradation in the atmosphere. The land compartment holds back the further recycling of PCB-52, and thus a higher b_{tot} is the consequence. This test setup shows much stronger dependence of the land fraction on K_{PA} than with a single layer of vegetation. While the big leaf vegetation approach with defoliation has a no land fraction, the two layer vegetation approach can lead to a higher or lower overall land fraction (figure 6.13). For low wind speed a lower overall land fraction results in all the simulated cases. It is though not clear whether temperature or wind speed have a larger effect on the comparmtent distribution and b_{tot}. Runs with fixed wind in both canopy layers and fixed temperature did not clarify this question (figure 6.17).

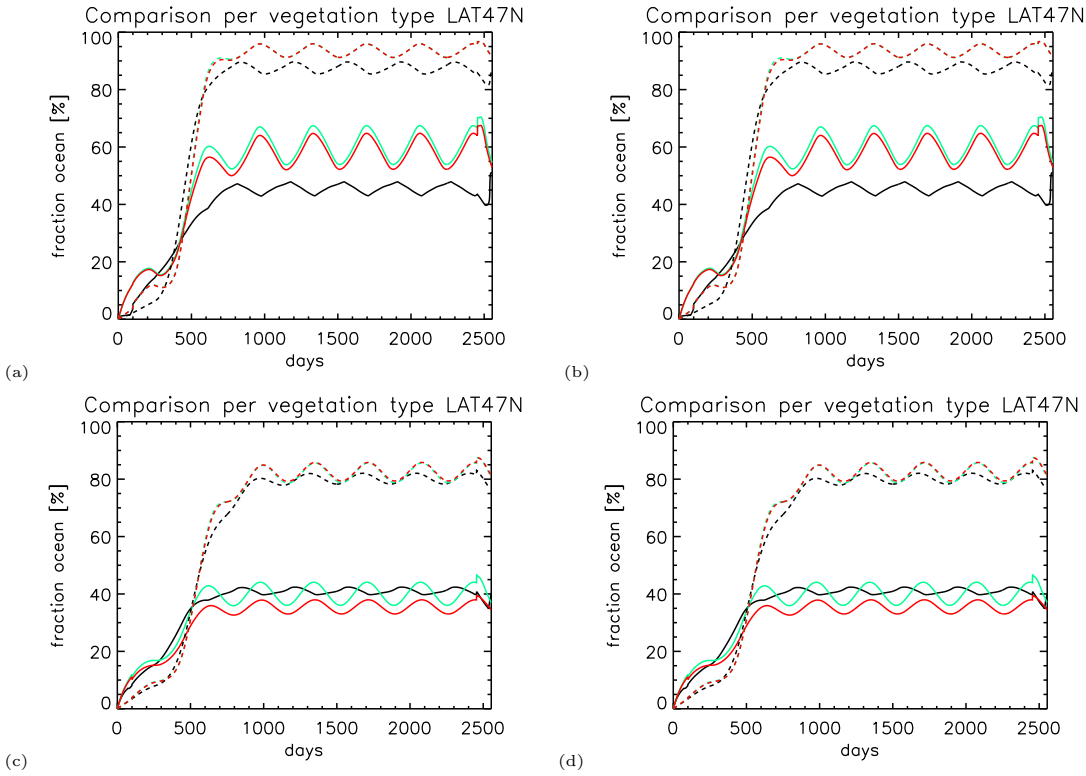

Figure 6.15: Time dependent ocean fraction for PCB-52 and setup 3 at 47^0N. a) and b) background aerosols, figure (c, d) urban type aerosol. b) and c) is for K_{PA_2} , a) and c) for K_{PA_3}. Grassland (black), deciduous forest (green), coniferous forest (red). The full lines stand for high wind speed ($13\frac{m}{s}$), the dashed lines for low wind speed ($2.5\frac{m}{s}$).

6.3 Comparison with measurements

The calculated deposition fluxes of the impulse experiment were compared with data from different measurement campaigns in the Italian Alps (Lys valley) (*Nizzetto et al.* (2006)) at around 45^0N, near the Great Lakes in Ontario,Canada (*Su et al.* (2007)) (unknown exact geographical location), and a PCB 12 month sampling in a forest (*Horstmann and McLachlan* (1998)) near the German city of Bayreuth (at around 55^0N 37^0E). *Nizzetto et al.* (2006) collected data from April till November in 2003. The sampling sites were situated in 3 different altitudes at 1100, 1400 and 1800 metres above sea level. Most of the vegetation in this area of the Lys Valley is composed of the coniferous deciduous species Larix decidua Miller. The Lys Valley is a remote region without any industry and thus advected air pollution is probably the only source of contamination. The Ontario measurement campaign took place from October 2001 untill December 2002 and the most predominant tree species found in this area were the red maple (Acer rubrum L.) and large tooth aspen (Populus grandidentata Michx.). The Bayreuth vegetation is given as coniferous forest.
Results of the modelling study are in general in good agreement with the mea-

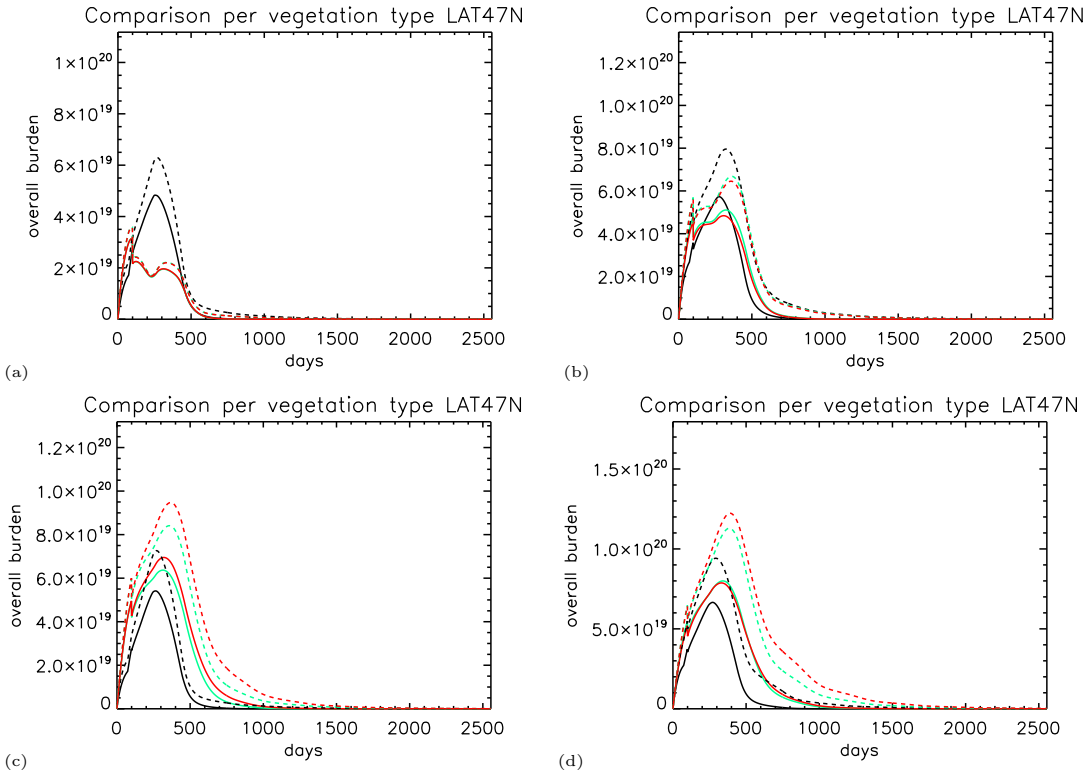

Figure 6.16: Time dependent (2500 days run with impulse application scenario) ocean fraction for PCB-52 and setup 3 (a and b) and 4 (c and d) at 47^0N. a) and c) are the simulations for background aerosol, figure (b, d) for urban type aerosol. All the runs are simulated with K_{PA_2}. Grassland (black), deciduous forest (green), coniferous forest (red). The full lines stand for high wind speed ($13\frac{m}{s}$), the dashed lines for low wind speed ($2.5\frac{m}{s}$).

surements (table 6.1). Differences between the measurement campaign and the model results differ depending on the setup chosen. Especially the gas and particle deposition values are in very good agreement with the field data (differences are in the range of factor 1-4). With the higher model development steps 2, 3 and 4 the discrepancies grow (up to factor 20). It is thus likely that the setups 2, 3 and 4 are overestimating the overall deposition. However, deposition fluxes of the different setups are total deposition fluxes to all the compartments and include also the flux into the ocean. It is thus not possible to make a direct comparison with the campaign. The Ontario site is probably located near the Great Lakes while neither the Lys Valley nor the City of Bayreuth are close to any larger water body.

6.4 Comparison with other Model Results

The results for the PCB-52 were compared with another fugacity based model (*Wania* (1999)) which used a similar application pattern for a time period of 60 years, however latitudinal pollution differences were considered. This study also

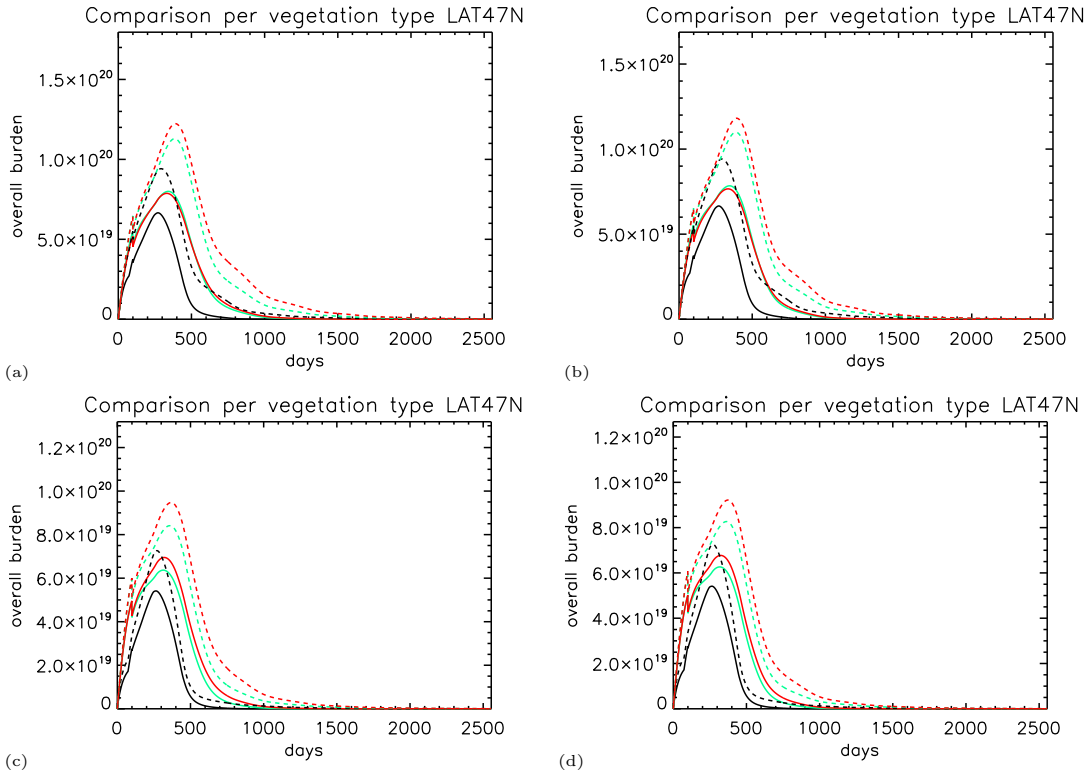

Figure 6.17: Time dependent overall PCB-52 burden b_{tot} in $\frac{molec}{m^2}$ for the multi-layer vegetation types for PCB-52 with K_{PA_3}. a) and c) are the case wind speed of both canopy layers is the same. b) and d) temperature of both canopy layer is the same. This figure is best compared with (figure 5.18). Grassland (black), deciduous forest (green), coniferous forest (red). The full lines is for high wind speed $\left(13\frac{m}{s}\right)$, the dashed ones for low wind speed $\left(2.5\frac{m}{s}\right)$.

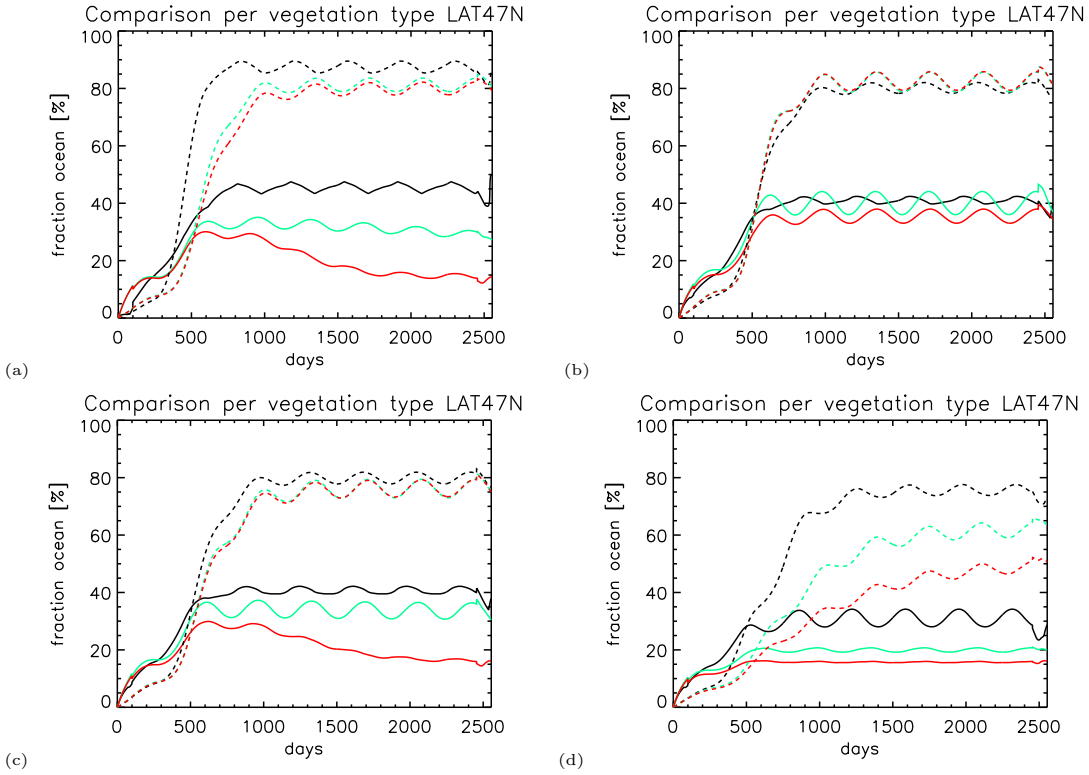

Figure 6.18: Time dependent ocean fraction of PCB-52 for setup 4 at 47^0N for setup 4. a,b: background aerosols, c) and d) urban type aerosol. b) and d) are simulations for K_{PA_2}, figure a) and c) are for K_{PA_3}.

Deposition flux in $\left[\frac{ng}{m^2 \cdot month}\right]$			
Nizzetto et al. (2006)	1800F	1400F	1100F
Spring	12.2	10.8	9.5
Early summer	2.3	4.3	6.6
Late summer		17.7	41.4
Autumn	44.6	61.4	58.6
Su et al. (2007)	87.5		
Horstmann and McLachlan (1998)	31		

background aerosols					
Setup 1			Setup 2	Setup 3	Setup 4
gas dep	calc	part dep calc	Gas diffusion	Defoliation	Multi-layer
	18-51	42-51			
K_{PA_1}			202-242	200-230	166-190
K_{PA_3}			67-72	200-230	226-265
K_{PA_5}			202-247	200-230	191-241
urban type aerosols					
Setup 1			Setup 2	Setup 3	Setup 4
gas dep	calc	part dep calc	Gas diffusion	Defoliation	Multi-layer
	18-44	18-26			
K_{PA_1}			66-102		166-203
K_{PA_3}			49-83	146-232	126-234
K_{PA_5}			66-102	146-232	154-196

Table 6.1: Comparison of deposition flux (in $\frac{molec}{m^2 s}$) mean values of the coniferous vegetation type with data obtained from a measurement campaign in the Italian Alps (*Nizzetto et al.* (2006)). The other measurement campaign is from the field sampling campaign in Ontario (Canada) and represents a boreal deciduous forest (*Su et al.* (2007)) and a coniferous forest in Germany (*Horstmann and McLachlan* (1998))

includes a forest canopy and the global environment is 'described with ten latitudinal bands, each of which is divided into a set of well mixed compartments, representing environmental phases such as the atmosphere, the terrestrial, the fresh water and the marine environment' *Wania* (1999). The descriptions of the model and equilibrium partitioning and the chemical transfer kinetics are given in *Wania and Mackay* (1995) and *Wania et al.* (1999).
The simulation results of this model study (fig 6.19) do not agree with latitudinal the compartmental distribution of our model study. However, land fractions of PCB-52 in both models increased in both model studies. The model study of *Wania* (1999) also showed a decrease of land fraction of PCB-52 with time while the land fraction in our model approach remains almost stable. Similarities are observed for the ocean with both model calculations. Both compartment fractions remain stable with time (fig. 6.4, 6.19). Differences can be seen in the comparison

of the overall fractions where the model of *Wania* (1999) has in most cases (except the prescribed gas deposition setup 1) higher overall fractions (in most cases more than 15%) of PCB-52 in the ocean. There are many possible reasons for such a different chemical behaviour: *Wania* (1999) used a model with exchange mechanisms between the different latitudes. In addition, the polar circle is included in the calculations, other compartment were included (e.g. fresh water sediment) in their study and different surface fractions than in our model were chosen for the PCB calculations. It is thus very difficult to compare the studies because the input parameters differ to a large extent.

6.5 Summary

Recapitulating, the big leaf vegetation tests with PCB-52 have shown that the chemical properties are an important factor to estimate the behaviour in the environment. Most of the differences between DDT and PCB-52 can be attributed to different K_{OA}, K_{OW} and other compound properties. Also here the deposition process and the vegetation type are important to estimate the overall behaviour. Vegetation serves in general as a reservoir compartment for the slower recycling back into the atmosphere. One of the most important differences to the tests with DDT are the results of PCB-52 for the calculated gas and particle deposition (figure 6.3). The removal process by OH-radicals in the atmosphere seems to have a slower pace than in the case of DDT, and more PCB-52 resides in the atmosphere. The gas diffusion process on the other hand is very similar for the overall behaviour like DDT. The chemical properties of a compound is less important for this process than the partitioning factor K_{PA}.
Comparative tests between setup 3 and setup 4 show in many parts similar results between single layer and multi-layer vegetation approach. Values of b_{tot}, residence time and ocean compartment distribution are in general in a similar range for this shrub type vegetation test. Effects are obtained for b_{tot} where the influence of wind speed and temperature causes changes in the atmosphere-vegetation partitioning. Defoliation in the single layer canopy approach was considered as a dominant process diminishing the importance of the partitioning coefficient K_{PA} of gas diffusion. Multi-layer vegetation is on the other hand emphasizing again the findings of the big leaf canopy setup.
The largest differences in terms of K_{PA} between setup 3 and setup 4 are observed for the volatilization fluxes (figure 6.6). However, because the volatilization and deposition fluxes have relatively small values, these effects do not influence b_{tot} or the compartment distribution considerably (figure 6.3 and 6.3). The results of multi-layer vegetation in setup 4 are uncertain because of the multitude of assumptions.
Although b_{tot} is in a very similar range, the multi-layer approach yields changed compartment distributions. K_{PA} has been shown to be a driving factor for the gas uptake and media allocation of PCB-52, but of less importance when introducing defoliation. The combined gas diffusion plus defoliation processes cause an enhancing fraction of the ocean compartment (figure 6.15 and 6.18). A high wind

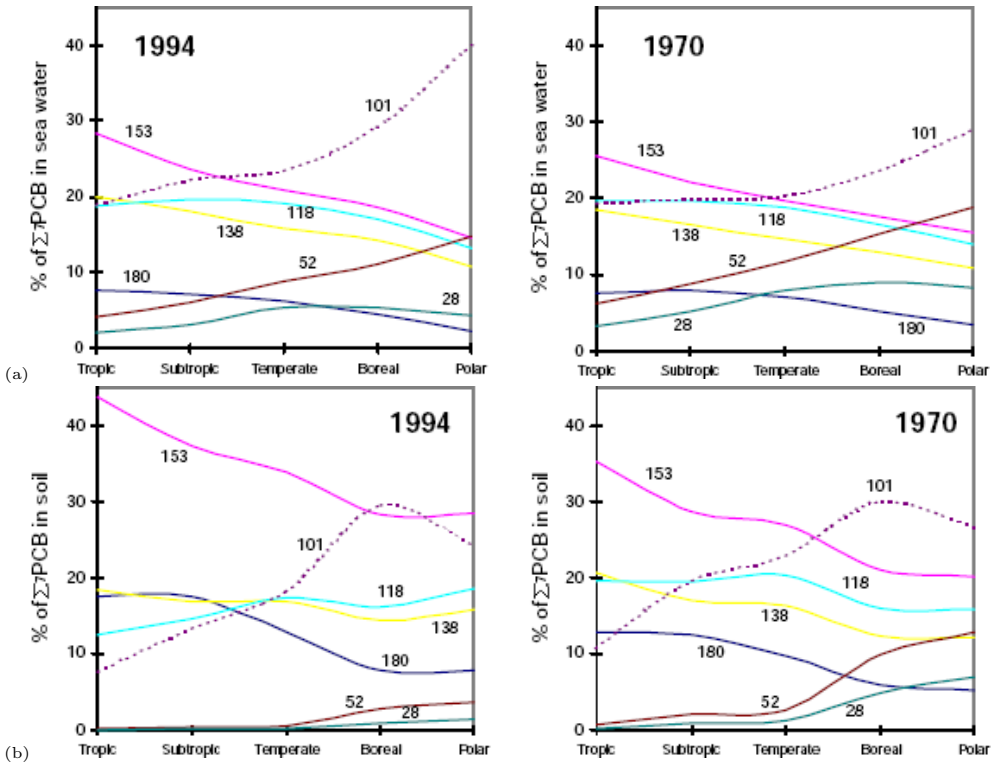

Figure 6.19: Latitudinal comparison of compartment distribution of ocean (a) and soil (b) for several PCBs with the model by *Wania* (1999).

speed causes more turbulence in the lower atmosphere, thus degradation by OH-radicals is more active and the further storage in the ocean compartment declines. The aerosol type has an additional influence for the overall distribution of PCB-52 which depends more on the partitioning factor K_{PA} than on the wind speed. Like in the case of DDT, multi-layer vegetation results can be very ambiguous. The single layer model is a simpler approach, but results achieved with the single layer vegetation setup are likely more reliable.

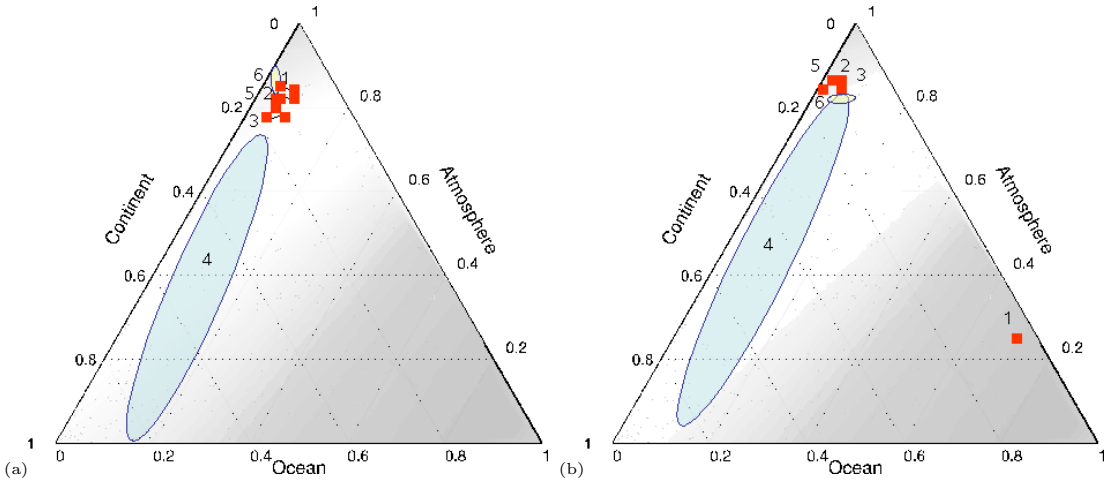

Figure 6.20: Compartment distribution changes over 100 years for PCB-52. a) (temperate) and b) (tropical) are 100 years runs for the uniform vegetation type. No real compartment change is documented. The numbers represent the different processes and setups tested: 1) setup 1 with gas deposition prescribed(I), 2) setup 1 with gas deposition calculated (II), 3) setup 1 with particle deposition, 4) setup 2 with gas diffusion, 5) setup 3 with defoliation single layer 6) setup 4 with multi-layer vegetation. The blue area stands for the uncertainty caused by the choice of K_{PA} parameterization.

Chapter 7

Conclusions and Outlook

The implemented vegetation processes resulted in very different outcomes for PCB-52 and DDT. The properties of the two tested compounds cause large differences in overall behaviour in the environment. Physico-chemical parameters like vapour pressure, K_{OA} and K_{OW}-values, molecular weight are responsible that partitioning between air, bare soil, vegetation (including the subcompartment vegetated soil) and ocean can vary to a remarkable extent for DDT and PCB-52. To conclude this work, the questions addressed in objectives and procedures (see also 2) are discussed again, followed by a brief outlook on potential future research questions concerning the air-vegetation-soil interactions of POPs.

Quantification of vegetation processes relevant for DDT and PCB-52 cycling

The simulated cycling of DDT and PCB-52 show different results for many of the tested processes. Due to different chemical behaviour it is thus not possible to make a general process validation. In a first step we analyse the big leaf deposition parameterizations (setup 1), followed by a quantification of the gas diffusion experiments (setup 2) and the phenology criteria (setup 3 and 4).
Prescribed DDT deposition (setup 1) values (*Lammel et al.* (2007)) cause a higher overall burden b_{tot} than with the implemented gas deposition resistance scheme (setup 1) by *Wesely* (1989). Differences of b_{tot} between the prescribed and calculated gas deposition setups are in the range of about a factor 3 in the higher latitudes and can increase up to one order of magnitude or even more in the mid latitudes (5.1). The introduction of an additional deposition process via the particle settling decreases b_{tot} by a factor 5 to 10. Reasons for this could be either a higher pace of degradation on the continent or the higher ratio volatilization/b_{tot}, which enhances the degradation by OH-radicals. Chemical properties are an evident factor of overall reduction of b_{tot} and will be discussed in a separate section.
PCB-52 shows the exactly opposite behaviour for the overall burden b_{tot}. Prescribed gas deposition (setup 1) causes a much smaller overall burden b_{tot} than calculated gas deposition with the resistance scheme of *Wesely* (1989). Calculated gas deposition results in a higher b_{tot} of even more than one order of magnitude in

some latitudes. Differences of b_{tot} between particle and calculated gas deposition on the other hand are not as large as for DDT. The overall burden b_{tot} of PCB-52 is not affected by this additional deposition process (fig. 6.1).
The influence of vegetation on the overall cycling of both congeners is very different. The land fraction of DDT of the northern hemisphere is much smaller in simulations without vegetation. This is explained by the higher volatilization from bare soil (fig. 5.3). PCB-52 shows the opposite trend concerning the overall fraction of accumulation on land. PCB-52 attaches easier to organic phase in soil and hence has less volatility from this compartment (fig. 6.3).

Chemical properties The influence of partitioning coefficients (K_{OW}, K_{AW}) is shown especially with the process of particle deposition. The meridional cross sections (fig. 5.4) clearly show that particle deposition is strongly depending on K_{OA} and K_{AW}. PCB-52 values of K_{OA} and K_{AW} are higher and thus particle bound deposition is dominant (*McLachlan and Horstmann* (1998)). DDT deposition is even reduced by the additional particle deposition process. The consequence is a higher removal in the atmosphere by OH-radicals, a higher ocean fraction of b_{tot} and a lower overall burden (fig. 5.5). The higher values of K_{OW} also explain the greater affinity of PCB-52 to attach on organic matter in soil, hence a larger continent fraction is the consequence (fig 6.3). The prescribed deposition obviously has the lowest overall land fraction of b_{tot} for DDT while for PCB-52 the exact opposite is the case.

Other factors involved Other factors that can be involved in the meridional differences of overall distribution and b_{tot} are parameters such as different ocean and land surface distribution, temperature regime and the length of day. Relationships between the land fraction and b_{tot} are not linear, however there is a trend to deposit more on land for a larger continent fraction with colder temperature. The prescribed deposition obviously has the lowest overall land fraction of b_{tot} for DDT. The other big leaf deposition scenarios (calculated gas deposition and particle deposition) do not vary to a relevant extent (figure 5.2 and fig. 6.3) (with the exception of the higher northern latitudes) for both chemicals. b_{tot} differences between the two gas deposition schemes show a less strong difference for DDT than for PCB-52. Differences in overall burden b_{tot} between prescribed gas deposition and calculated gas deposition are less strong for DDT than PCB-52. Empirical values of gas deposition are probably more suitable to be included for DDT model studies than for PCB-52.

Gas diffusion The process of gas diffusion (setup 2) is accompanied by a high level of uncertainty for many parameters necessary for an accurate description of this process. We displayed here a 2-compartment approach including a vegetation volume for the gaseous exchange of leaves which has also been used in *Kylin and*

Sjödin (2003), *Tolls and McLachlan* (1994)). This thesis is probably the first attempt to compare different partitioning coefficient K_{PA} parameterizations for the gas diffusion process from literature (see also 3.3.4). Both chemicals show similar behaviour for the implementation of the gas diffusion process, as it strongly depends on the choice of the K_{PA} value. Differences occur in overall burden b_{tot} as well as in the compartmental distribution. The annual mean land fraction of b_{tot} is very sensitive to K_{PA}, while the ocean compartment remains on same the level of the gas plus particle deposition scheme (figure 5.9). Some K_{PA} parameterizations do not show any major differences for the overall burden b_{tot} while others do. K_{PA_3} is the partitioning coefficient leading to by far the highest b_{tot} of both chemicals and overrides all other K_{PA} parameterizations. Depending on the latitude, differences of overall burden b_{tot} caused by K_{PA} parameterizations range between factor 3-15.

Beside the different parameterizations of K_{PA} other factors can have important influence on the gas diffusion. Diffusive air-plant exchange remains a very challenging and not clearly understood topic. Many potentially influential factors are plant type specific (e.g. morphology, lipid content of leaves etc. (*Ockenden et al.* (1998))), others are environmental parameters like humidity, wind speed and light conditions (*Riederer* (1990), *Dalla Valle et al.* (2004)). This work could not test all the possible parameter combinations necessary to understand all the possible influential factors for gas diffusion.

Higher overall storage effects in/on leaves are observed with gas diffusion. This additional pathway leads to higher land compartment fraction and similar or lower overall burden b_{tot} for both chemicals (except for K_{PA_3}). Storage effects of leaves depend on K_{PA} value chosen and can have strong seasonal variations. Previous modelling results (*Tolls and McLachlan* (1994), *Kylin and Sjödin* (2003)) found that the vegetation volume compartment is less prone to concentration seasonality caused by temperature. The present study is not able to confirm this assumption with the global uniform shrub type vegetation setup.

The results show that POPs transfer from vegetation to the vegetated soil are a very important process for the overall cycling. It confirms previous model studies (*Wania and McLachlan* (2001)) which conclude an overall reduction of the total POP concentration by litter fall. Defoliation and the introduction of the vegetated soil (setup 3) as additional compartments have important effects on the distribution. In comparison to the big leaf approach, the setup with inclusion of processes in vegetated soil results in a decrease of b_{tot} of up to one order of magnitude for both chemicals.

Our model does not approve a stronger accumulation in vegetated soil as it is stated in other works (*Wania and McLachlan* (2001), *Brzuzy and Hites* (1996), *Meijer et al.* (2003b)). Annual mean fractions on the land compartment decrease dramatically for both chemicals, which is probably due to the increased ratio of volatilization/b_{tot} after the introduction of litterfall. This effect is caused by the very simple model assumption of immediate POP release after defoliation. Although both chemicals have high K_{OW} and K_{AW} values, sorption on soil organic matter is less strong than volatilization from vegetated soil. However, with such a simple soil model, we cannot ascertain the finding of *Su* (2005) that the forest

hinders the further transport of PCB-52 to the ocean compartment. PCB-52 in our model is rather prone to reside in the atmosphere.
The total disappearance of differences for b_{tot} when using K_{PA} values for both chemicals can be explained by these simplifying assumptions mentioned above. Such an effect is in contradiction to the importance of K_{PA} values for other setups. It is furthermore not clear how this disappearance of cycling differences after the inclusion of litterfall has to be validated. It is evident that a better description of the vegetated soil processes would be a very useful complement for this study. Vegetation removal by phloem transport cannot be considered as a major sink process for POPs. The introduction of a multi-layer vegetation (setup 4) is a further refinement of vegetation canopy processes. Many simplifications are assumed for the display of this process and thus the results should be considered as preliminary. Differences of b_{tot} between the primitive big leaf and two-layer model can reach more than one order of magnitude for some K_{PA} values. K_{PA} is obviously a factor that can change the flux direction to a certain extent as well as the accumulation dynamics depending on wind speed and the temperature. However, this experiment shows that inner-canopy processes need to be studied in more detail for a further improvement of vegetation dynamics of POPs. So far big leaf vegetation model setups are more reliable and further potential improvements are needed to understand the flow of POPs in canopies.
Interception via gas deposition and gas diffusion is probably the more important pathway of deposition for the northern hemisphere. This work confirms previous studies (*Su* (2005), *Wania and McLachlan* (2001)) that vegetation filters POPs from its further atmospheric transport to higher latitudes preferably via gas deposition. However, the mechanism of canopy interception of the two chosen chemicals also depends on other factors (ocean-continent distribution, climatic zone etc.).

Important factors influencing the overall fate for DDT and PCB-52 in vegetation

Meteorological parameters are essential for compartment distribution as well as for b_{tot}. Wind speed is among the most important ones investigated in this work. Air movement is an important factor for deposition as well as for the cycling and overall burden b_{tot} of POPs. *Barber et al.* (2002) found that the plant uptake is enhanced by higher wind speed. Our model shows that differences in vegetation influx between the two wind speeds in absolute values are small (less than one order of magnitude). They are larger for PCB-52 than for DDT. However, wind speed is a very essential factor for the distribution and thus the overall burden b_{tot}. Absolute values for plant uptake of DDT and PCB-52 may be in a similar range, but the compartment distribution can be very different. Another effect which is important for the leaf uptake (and which was not considered here) is the additional turbulence in the leaf canopy caused by higher wind speed. Leaf fluttering would change the laminar leaf boundary layer to a more turbulent one (*Barber et al.* (2004)).

Meteorological impact on POPs is additionally strengthened by the role of aerosols. Aerosols and vegetation influence each other especially for the gas diffusion process, where factors like roughness length and LAI are important. Depending on the type of aerosol, one can distinguish several trends for each vegetation type. Vegetation type testing was performed in only one climatic zone (47^0N) and thus are limited in its statement.
The tested global configuration indicated very different behaviour for the different climatic zones and thus other climatic conditions should be considered as a next subject of investigation. The study has also highlighted a separation of the influence of processes between the two hemispheres. This is mainly due to the different land fractions. Processes at lower temperature in both hemispheres are influenced by different factors (e.g. ocean in the southern hemisphere). It is thus evident that the influence of vegetation is more important in the northern hemisphere. The northern hemisphere is also more polluted due to industrial activities and POP patterns should be studied more intensively. A rough quantification of the importance of certain processes for both chemicals is displayed in table 7.1

Are vegetation types important for the overall cycling of POPs?

The different vegetation types have large effects on the overall burden b_{tot}, compartment distribution and overall persistence τ_{ov}. The simulations show that vegetation characteristic like roughness length, leaf area index LAI of canopies are not negligible, however they also need to be related to the different deposition processes and aerosol types.
Vegetation type differences of overall burden b_{tot} are not too relevant for setup 1 calculations (gas and particle deposition) at high wind speed (5.11). However, the burden distribution is affected by high wind speed where the land fraction of grass is higher than for the other vegetation types (5.12). The influence of the roughness length on the overall distribution of a big leaf canopy (setup 1) is probably less important.
Surface roughness is a more important factor with the introduction of the gas diffusion process (setup 2). It is important to mention that vegetation types react differently for each leaf-air partitioning coefficient K_{PA}. The overall burden b_{tot} depends strongly on vegetation type and the choice of the leaf-air paritioning coefficient K_{PA}. Some K_{PA} runs on the other hand, do not have a strong or any sensitivity at all and the gas diffusion results are similar to the normal gas deposition process of setup 1.

Surface roughness and leaf area index have less effects on the overall burden of the different vegetation types after the inclusion of the vegetation soil. For DDT, the forest vegetation types have a higher fraction of overall burden b_{tot} on the land compartment. However, the higher values of b_{tot} for grass land are caused by the slower pumping of DDT into the ocean compartment (fig. 5.16). For PCB-52 no such effect is observed and neither surface roughness nor the higher LAI con-

	process	DDT					
		WSP	LAI	SRG	TMP	AER	PHE
Setup 1	GDP (I)	++			+	++	
	GDP (II)	++		+	+	+	
	PDP	++		0	+	+	
Setup 2	GDF						
	K_{PA_1}	++	0	-		+	
	K_{PA_3}	++	+++	+++	+	+++	
	K_{PA_6}	++	-	-	+	0	
Setup 3	DEF						
	K_{PA_1}	++	0	-	+	+++	++
	K_{PA_3}	++	0	-	+	+++	++
	K_{PA_6}	++	0	-	+	+++	++
Setup 4	2-LC						
	K_{PA_1}	+	0	-	+	+	++
	K_{PA_3}	+	0	-	+	+	++
	K_{PA_6}	+	0	-	+	+	++
	process	PCB-52					
		WSP	LAI	SRG	TMP	AER	PHE
Setup 1	GDP (I)	+					
	GDP (II)	++	0	+	+	+	
	PDP	+	0	-	0	+	
Setup 2	GDF						
	K_{PA_1}	++	+	+	+	+++	
	K_{PA_3}	+	++	+++	+	+++	
	K_{PA_6}	+	+	+	+	++	
Setup 3	DEF						
	K_{PA_1}	0	0	0	++	++	-
	K_{PA_3}	+	0	0	++	++	-
	K_{PA_6}	++	0	0	+	++	-
Setup 4	2-LC						
	K_{PA_1}	0					-
	K_{PA_3}	+	0	+	0	+	0
	K_{PA_6}	0	0	-	0	0	-

Table 7.1: Rough quantification of the test results for DDT and PCB-52 by estimation of the most important influential factors for the overall cycling. The higher the numbers of + is a more influential a process is; 0 stands for rather neutral effects and - indicates an unexpected effect for the vegetation. GDP(I): big leaf gas deposition prescribed, GDP(II): big leaf gas deposition calculated, PDP: particle deposition, GDF: gas diffusion, DEF: defoliation, 2-LC: 2-layer canopy setup. WSP: wind speed, LAI: leaf area index, SRG: surface roughness, TMP: temperature, AER: aerosols, PHE: phenology

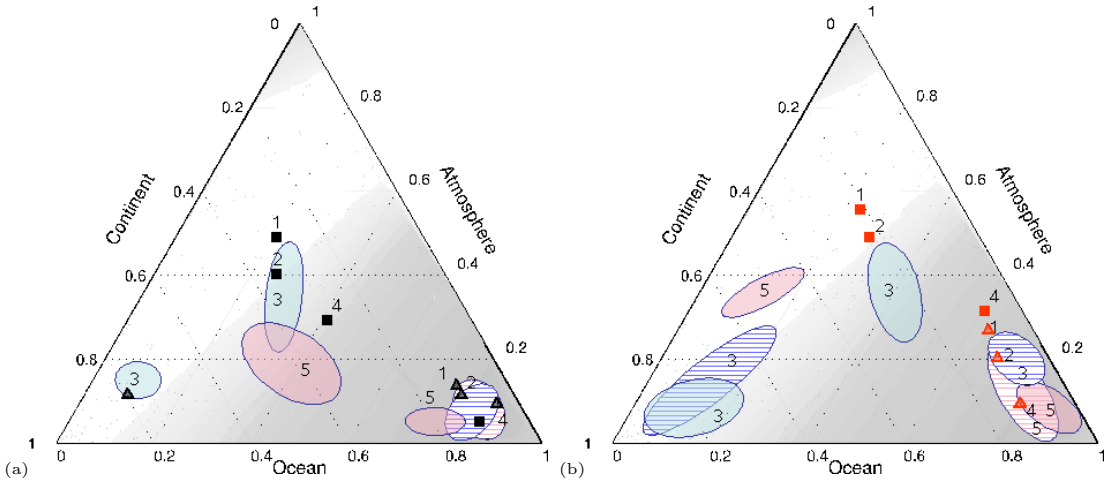

Figure 7.1: Compartment distribution of PCB-52 for grassland (figure a) and coniferous forest (figure b) at the end of the simulation period (2500 days). 1) setup 1 gas deposition (II), 2) setup 1 particle deposition, 3) setup 2 gas diffusion, 4) setup 3 defoliation single layer 5) setup 4 multi-layer vegetation. The triangles represent the low, the square the high wind speed. The blue (setup 3) and red areas (setup 5) represent the uncertainty of K_{PA} calculations. The striped area belongs to low wind speed.

tribute to a larger land fraction of b_{tot} (fig. 6.12). The additional accumulation potential in longer living leaves does not contribute to a higher overall contamination of b_{tot}. For DDT a less strong seasonality with higer wind speed (fig. 5.16) is observed, which could mean that the vegetation volume storage effect already mentioned (*Tolls and McLachlan* (1994), *Kylin and Sjödin* (2003)) is coupled with wind speed.

Wind speed The logarithmic wind profile may be another reason why the overall burden b_{tot} has the highest values with the grassland vegetation. For DDT lower wind speed filters probably more POPs from the atmosphere and re-emission is also coupled with the further transport into the ocean compartment as a final sink. This is also supported by the higher b_{tot} for low wind speed in general and the higher land compartment for grass. Litter fall and leaf area index (LAI) do not have a great influence on the overall burden, although the compartment fractions of b_{tot} can oscillate quite a lot.

7.1 Outlook

Deposition of POPs on the vegetation canopy is a complex process with many factors influencing the further fate and distribution. The vegetation ecosystem is characterized as a very dynamic, multi-causal environment which has the ability to influence the overall cycling of POPs. Uncertainties in the necessary parameters (especially in the case of gas diffusion) though indicate a need for further

exploration. This work has shown that the filter effect of a vegetation canopy in terms of overall cycling of POPs can be modeled to a certain extent. In fact, it is rather an indirect filter effect, because the vegetation recycling via litter fall seems to be very important in this process. Soil storage and leaf decomposition process have been identified as a weak point for the different deposition and phenology processes. The lack of inclusion of different precipitation parameterizations per climate zone is another problem of this box model and should be included in future studies. Air-vegetation-soil interactions remain a challenge to model, especially leaf decomposition processes remain an enigma. Several aspects of improvement should be considered for future studies:

- A more precise test of important parameters like wind speed and temperature or lipid content of leaves should be done in a first step before further model development is needed.

- The large differences in the parameterization of the partitioning coefficients K_{PA} show that there is still a lot of uncertainty left concerning the significance of this process. The POP uptake by vegetation and movement within leaves will still cause difficulties in modelling this process. The movement of POPs through the various leaf cells is far from being understood thus laboratory experiments should provide benchmark values for this process.

- As the 2-layer canopy vegetation test has shown the importance of the canopy architecture, one has to consider that air-vegetation exchange is not only limited to the exchange canopy-atmosphere. The influence of the turbulent eddy fluxes within a canopy could give information about a possible recycling within the air parcel of a forest. Soil-air interactions are represented without a resistance for flux through the canopy. The volatilization from canopy and soil may be inhibited by this leaf barrier. Assuming the natural barrier between the canopy and the open atmosphere as zero is most likely not real (especially not for a forest with a high LAI). Thus a possible interaction between the forest soil and the vegetation canopy should take place. Another process that should be considered is the flux inhibition via snowfall and dew on leaves, which can have effects on the revolatilization of POPs. Especially in the northern hemisphere with its large vegetated continental areas one could expect effects on the overall cycling.

- The soil model under vegetation used here is assuming very simple leaf decomposition, degradation and revolatilization processes. Litter is in various stages of decomposition and certainly can take longer than assumed in our model. Decomposition and microbial biomass activity are to be seen as very important key factors that influence the overall cycling and the compartment change. Residues transfer in soil is unclear and we assumed that POPs do not drain into the deeper layers of the soil due to the affinity to attach on organic matter. *Tinker and Nye* (1980) believed that it is very difficult to distinguish between microbiological and chemical (and perhaps

even anaerobic) decomposition for slowly degrading chemicals like POPs. Measurements between ratios of DDT and its decomposition product DDE and DDD could help to give key values for further model studies.

- POPs in the soil system can react in various ways: absorption to soil or organic matter and leaching to deeper soil layers are only some of the possible processes. Apart from the transport or accumulation, organic soil content and moisture are potentially important process vectors (so far our model was run with only one soil type assuming the same moisture and organic content). Studies in different soil types show a different decomposition and drainage rates for DDT (*Galiulin et al.* (2002)).

- Subsurface flows like river run off to the sea and subsequent sedimentation could be another important soil removal process especially for agrochemical POPs.

- Simulations in our box model are currently performed only with one chemical. DDT metabolites e.g. are also problematic and have similar harm and transport potential. Thus the removal processes in all the compartments could be influenced by the presence of other compounds (metabolites or other POPs). As a possible extention it may be useful to simulate more than one chemical and/or with its decomposition products. This could also help for the other congener where a pool of different PCBs could be calculated.

7.1.1 Final remarks

Future investigations should also include a reasonable discussion about the effects of chemical pollution in relationship with the climate change. Bioclimatic indicators show and predict a migration of many species towards higher latitudes. Malaria for example is probably on the top list of the most dangerous impacts of global warming. Today, public perception considers such a disease as a third world problem. However, the worst outbreak of Malaria in history was the epidemic in the former Soviet Union in the 1920's [1] with a peak incidence of 13 million cases per year and 600 000 deaths. Global warming favours the return of the pathogens to now warmer cold areas

This work has shown that a global increase of temperature would most likely have positive effects on the overall POPs degradation. However, a warmer climate will increase pest populations substantialy, and it is evident that this will imply a higher usage of pesticides. Even discussions about the usage of already banned pesticides like DDT will most likely return to the political agenda of pest control. The conflict area of human health issues and pest control will increase in the next 50 years.

The future agriculture will have to feed more people and produce more crop under

[1] http://commerce.senate.gov/pdf/reiter-042606.pdf

deteriorating climate- and soil conditions. The combined stress of higher temperature and more pest sensitivity might cause unforseeable consequences for the fertility. A higher application of agrochemicals cannot be the longterm answer to this problem. Preventive vegetation stress monitoring will become an important issue for the agriculture of the future. More detailed knowledge about the stress factors a plant is exposed to in the future climate will contribute to the reduction of pesticide usage.

The industrial usage of POPs must be documented and reported. Today more than 8 million chemicals are commercially available and an estimated 240000 of them are to be inventoried [2]. It is evident that this large amount of compounds cannot be screened individually. Preprocessing of POP candidates can be made by collecting data about K_{AW}, K_{OW} and half life values. Production and industrial usage information are pivotal for a further development of model tools. This work may contribute to develop reference chemicals which would help to identify POPs with similar substance properties.

[2] http://www.cas.org/CASFILE/chemlist.html.

Appendix A

Calculations for other compartments than vegetation

Processes that are not related to vegetation or deposition processes are described in the Appendix. They are namely

1. Volatilization from Soil
2. Volatilization from the ocean surface
3. Atmospheric degradation of POPs by OH-radicals cycle
4. Loss to the deep sea compartment as a final sink

A.1 Atmosphere

A.1.0.1 Forcing Atmosphere

The model has a simple one column atmosphere. The model uses a daily and yearly cycle for the mixing layer height, the atmospheric temperature and OH-radicals. All the mentioned variables depend on the length of the day (LOD) and also on the latitude.

Length of the day The length (in seconds)of the day is calculated with the formula

$$L_d = (86400 \cdot acos(-tan\frac{(\psi \cdot \pi)}{180})tan(\frac{23.5 \cdot \pi}{180} \cdot sin(d - 80)\frac{2 \cdot \pi}{365})) \tag{A.1}$$

Mixing layer height cycle Frequently the mixing layer height varies diurnally with low values during the nightime and higher values during the daytime (*Seinfeld and Pandis* (1998)). We prescribed the minimum of the mixing layer height from 2 hours after sunset and until sunrise. At sunrise the boundary layer increases linearly during the first two hours to its maximum. The maximum value is stable until two hours before sunset. Two hours before sunset the mixing height starts to decrease and the linear interpolation is to reach again its minimum 2 hours after the sunset. The maximum values for the mixing layer height are considered with 3000 meters while the minimum value is some 300 meters above the ground (which should represent the stable night layer). Δ_h is the height variability of the boundary layer during the day and is represented with the formula

$$\Delta_h = 3000m - \xi \cdot 2600m \tag{A.2}$$

Cloudiness factor ξ The cloudiness factor ξ is currently set constant with a value of 0.5.

Mixing layer over the ocean The current mixing layer height over the ocean is hold constant since the daily variability of the mixing layer height over water is much smaller.

Atmospheric temperature variation Temperature varies according to the monthly data from LPJ the vegetation canopy and according to the latitude zone. Δ_T is the daily temperature amplitude. It depends on ξ and is set to

$$\Delta_T = 20^\circ C - \xi \cdot 15^\circ C \tag{A.3}$$

Daily temperature variation start at sunrise when the temperature is the lowest, followed by a linear interpolation to 75% of the maximum day temperature. A further interpolation leads to the maximum of the day at 2 pm and from then on the temperature decreases to 75 % at sunset and further decrease to the minimum at sunrise.

Temperatures of other compartments As a simplification, the temperature of the bare soil and on the vegetation are the same like in the atmosphere.

Concentration of OH-radicals Latitude variation of OH-radicals (C_{OH_p}) is prescribed in the model by Spivakovski (*Spivakovsky et al.* (2000)). Additionally it is assumed that C_{OH} is fixed to 100 $\left[\frac{molec}{cm^3}\right]$ at night (sunset to sunrise). It varies with cloudiness factors by

$$C_{OH} = C_{OH_p} \cdot (1 - \xi) \tag{A.4}$$

The day time C_{OH_d}-variability depends on the time of the day t_d and is given as (*Junkermann et al.* (2002)).

$$\begin{aligned} v_t =& 1.02 \cdot 10^7 \cdot (6.10826 \cdot 10^4) \\ &+ 1.13724 \cdot 10^6 \cdot t_d - 1.15095 \cdot 10^6 \cdot t_d^2 \\ &+ 3.09228 \cdot 10^5 \cdot t_d^3 - 3.00476 \cdot 10^4 \cdot t_d^4 \\ &+ 1.22165 \cdot 10^3 \cdot t_d^5 - 1.7793 \cdot 10^1 \cdot t_d^6 \end{aligned} \tag{A.5}$$

$$C_{OH_d} = \frac{C_{OH}}{v_t} \tag{A.6}$$

Partitioning of POPs in the atmosphere In the atmosphere POP can be either in gaseous phase or bound to aerosols and as a further related scavenging process they are also found in rainwater. The aerosol-gas partitioning is a very important ratio since it indicates how much of the pollutant an aerosol is capable to absorb. The aerosol surface A_{aer}, the vapour pressure p_{vap} and the amount of total suspended particulates (TSP) give information about the preferred atmospheric phase of the chemical. Because of the complexity of aerosol processes we apply only a simplified aerosol in the model for which the total aerosol surface is prescribed, hence TSP is already included in those calculations (*Bakan et al.* (1988)). However there is a difference made between several aerosol types.
p_{vap} depends on the temperature and the prescribed substance specific saturated vapour pressure p_{vap_X} at the reference temperature of 298 K and the enthalpy H_{vap} which is formulated as

$$p_{vap} = p_{vap_X} \cdot e^{\left[\frac{H_{vap}}{R} \cdot \left(\frac{1}{T_{at}} - \frac{1}{T_{ref}}\right)\right]} \tag{A.7}$$

Aerosol-gas partitioning The partitioning (θ) of a POP between aerosols and the gas phase is represented with the Junge-Pankow (*Junge* (1977), *Pankow* (1994a), *Pankow* (1994b)) model of adsorption as

$$\theta = \frac{c_x}{c_x \cdot A_{aer} + p_{vap} \cdot e^{6.8 \cdot \frac{T_{ref} - T_{at}}{T_{at}}}} \tag{A.8}$$

with the constant c_x which depends on properties of the substance of interest (*Helm and Bidleman* (2005)) and is usually set to $17.225 Pacm$.

Wet deposition The dimensionless scavenging factor f_{sc} of aerosols by rain rate Z_r are hold constant with ($f_{sc} = 0.8$, $Z_r = \frac{1}{3}\left[\frac{1}{s}\right]$), hence the current wet deposition rate k_w in the model is calculated with the equation

$$k_w = \theta \cdot f_{sc} \cdot Z_r \tag{A.9}$$

The wet deposition in the model is given by

$$D_w = k_w \cdot b_A \tag{A.10}$$

Dry deposition of gas The model uses in setup 1 a substance related prescribed dry deposition velocity $v_{dep_x}\left[\frac{m}{sec}\right]$. The dry deposition rate results in the formulation

$$k_d = \frac{(1-\theta) \cdot v_{dep_x}}{h_{mix}} \tag{A.11}$$

where $h_{mix}[m]$ is the mixing layer height and the ratio $1-\theta$ is the partitioning of dry particles with POP so that the dry deposition of POPs is formulated as

$$D_d = k_d \cdot b_A \tag{A.12}$$

Degradation in the atmosphere The degradation of a POP in the atmosphere is considered only during the daytime. The NO_3 cycle which is mostly active during the nighttime is not included yet. The relevant factors for the degradation are the $OH-$radical concentration in the atmosphere ((C_{OH})), the chemical specific $OH-$degradation constant k_{OH_x}. ϵ_η is the temperature dependent rate of activation energy $\frac{\Delta H^\circ}{R}$ from the Arrhenius equation. The degradation rate k_{OH} is calculated as

$$k_{OH} = C_{OH} \cdot k_{OH}(T^\ominus) \cdot e^{\left(\epsilon_\eta \cdot \frac{1}{T_{at}} - \frac{1}{T^\ominus}\right)} \tag{A.13}$$

and the sink in the atmosphere G_A is calculated by

$$G_A = k_{OH} \cdot b_A \tag{A.14}$$

A.1.1 Ocean surface

As mentioned above the ocean is considered as a 2-dim layer without a deep-sea sink. The oceanic atmosphere has its own boundary layer calculation equal to the one on land with daily cycles etc.

A.1.2 POP related processes in the ocean layer

Three ocean surface processes are considered, namely: degradation on the surface, volatilization from the surface and deposition (which is an atmospheric process and hence will not be described in this subsection).

Oceanic loss to the deep sea We assume a fixed annual rate loss to the deep sea and do not consider a possible return of POPs from the deep sea compartment. There will be no degradation rates included in this additional process. We adopt the annual average deep sea loss of the top ocean layer to the deep sea layer and sediments with a globally averaged rate of 37%, and so is the annual amount of POPs lost to the deep ocean compartment given in $\frac{1}{s}$.

$$k_{lo} = \frac{0.37}{86400 \cdot 365} \tag{A.15}$$

k_{lo} is in $1/s$ and the loss is calculated as

$$L_O = k_{lo} \cdot \frac{b_O}{h_{mix_O}} \tag{A.16}$$

Oceanic degradation The first order ocean degradation coefficient k_o is described in dependence on temperature with a doubling per 10 K increase following the recommendations made by (*Bureau* (1996)). k^o is the degradation coefficient at the reference temperature.

$$k_o = k^o \cdot 2^{\frac{T_o - T_{ref}}{10K}} \tag{A.17}$$

Hence the degradation in the ocean is given as

$$G_o = k_o \cdot b_O \tag{A.18}$$

Volatilization from the ocean surface The air-atmosphere interaction of the model is based on a 2-layer theory (*Liss and Slater* (1974) *Mackay and Leinonen* (1975)). The serial mass transfer coefficients

$$\begin{aligned} U_1 &= 6.5 \cdot 10^{-2} \cdot \sqrt{6.1 + 0.63\mathrm{s/m} \cdot w} \cdot \frac{w}{100} \\ U_2 &= 175 \cdot 10^{-6} \cdot \sqrt{6.1 + 0.63\mathrm{s/m} \cdot w} \cdot \frac{w}{100} \end{aligned}$$

represent the transfer between the top surface layer of the oceanic compartment (U_1) with the marine boundary layer (U_2) as a function of wind speed $\left[\frac{m}{s}\right]$ at ocean surface w (*Mackay and Yeun* (1983)). Volatilization from the ocean surface is based on exchange rate coefficients (*Schwarzenbach et al.* (2003)) which are calculated as

$$\begin{aligned} D_{p_1} &= \frac{1}{\frac{R \cdot T_O}{U_1} + \frac{p_{vap_O}}{U_2 \cdot W_{sol}}} \\ D_{p_3} &= \frac{p_{vap_O} \cdot {M_{POP}}^2}{N_{avo} \cdot h_{mix_O} \cdot W_{sol}} \end{aligned}$$

and the volatilization rate v_O is given by the formulation

$$V_O = \frac{D_{p_1} \cdot D_{p_3} \cdot N_{avo}}{M_{POP} \cdot h_{mix_O}} \tag{A.19}$$

W_{sol} is the water solubility of the substance and the Avogadro number (N_{Avo}) is based on the number of molecules of one mole, namely $6.0221415 \cdot 10^{23} mol^{-1}$. R is the gas constant, T_O the ocean surface temperature and H represents the Henry coefficient. p_{vap_O} is the vapour pressure at ocean surface temperature. The volatilization from the ocean surface is finally calculated by

$$V_O = v_O \cdot b_O \tag{A.20}$$

A.1.3 Deposition on the ocean

The deposition scheme has to be adapted for consistency reasons on the other compartments too. The bare soil and the ocean compartment follow the same scheme of gas deposition mentioned for the vegetation canopy. R_T is also here a combination of serial resistance. R_a is the same like in the vegetation case (see also equation A.1). The ocean boundary layer resistance R_{b_o} is calculated with a different formula and so does the bare soil resistances differ.

A.1.4 Ocean boundary layer resistance for gas

The oceanic deposition scheme has only two main resistances, namely the aerodynamic resistance and the ocean specific boundary layer resistance. For the ocean specific boundary layer resistance, the expression of (*Hicks and Liss*) is used which includes also the molecular diffusivity of the gas κ_{D_g}.

$$R_{b_o} = \frac{1}{\kappa u_*} \cdot ln\left(\frac{z_0}{\kappa_{D_g}} \kappa u_*\right) \tag{A.21}$$

A.1.5 Ocean boundary layer resistance for particles

There are several ways to include the boundary layer over seas. This approach is based on works of *Slinn and Slinn* (1980) and accounts for the effects of wind and the water surface slip.

$$R_{bo_p} = \frac{\kappa \cdot u_h}{u_*^2 \cdot (Sc^{-1/2} + 10^{-3/St})} \tag{A.22}$$

where u_h is the wind speed at the reference height (for the ocean taken as $h = 10m$), u_* is the friction velocity, while St represents the Stokes number calculated by *Seinfeld and Pandis* (1998). Sc is the Schmidt number taken from literature.

$$St = \frac{u_*^2 \cdot v_g}{g \cdot \nu} \tag{A.23}$$

A.1.6 Ocean surface resistance

For the surface resistances over water bodies the expression recommended by (*Sehmel* (1980)) is taken. This expression incorporates wind speed, the surface air temperature T and the air-water partitioning coefficient.

$$R_{c_o} = \frac{2.54 \cdot 10^4}{HTu_*} \tag{A.24}$$

A.2 Bare Soil

A.2.1 Daily cycle of bare soil

Bare soil is the continental surface without vegetation. As in the other compartments temperature has a daily cycle and because there is no other information available also the bare soil is suggested to have the same temperature as the other land compartments. As an additional simplification we suggest a constant soil wetness.

A.2.2 Diffusivity of POPs in soil

Volatilization Several factors influence the POP transfer from the soil compartment back into the atmosphere. Because POPs in soil can reside either in the gaseous or solid phase (attached to the soil matter) one has to incorporate both loss mechanisms. The partitioning between the gaseous and organic (solid) phase of this process is described with a dimensionless capacity fraction F_{pest} (*Smit et al.* (1997)).

$$F_{pest} = \frac{V_{air}}{V_{air} + K_{T_{soil}} \cdot (V_{wat} + Z_{om} \cdot P_{org} \cdot D_{dry})} \tag{A.25}$$

V_{air} and V_{wat} are the volume dimensionless fractions of air and water in soil. The organic matter in soil Z_{om} and the dry bulk density of soil D_{dry} are included in the calculation of F_{pest}. Z_{om} is expressed in $\left[\frac{kg_{om}}{kg_{soil}}\right]$ while the D_{dry} is given with $\left[\frac{kg_s}{m^3}\right]$. Z_{om} is the sorption coefficient on organic matter and , $K_{T_{soil}}$ is the partitioning coefficient which depends on the soil temperature.

F_{pest} parameterizes the cumulative volatilized fraction of applied POP C_v. Two different parameterizations are given for cumulative volatilized fraction C_v both related to the relative soil wetness W_{soil}

$$W_{soil} = \frac{s_{soil}}{s_{soil_{max}}} \tag{A.26}$$

which is the ratio between the soil wetness and the maximum soil wetness. For rather wet-moist conditions C_v is determined as according to Smit (*Smit et al.* (1997)) by

$$C_v = 71.9 + 11.6 \cdot \log\left(100 \cdot F_{pest}\right) \tag{A.27}$$

while for dryer conditions C_v is calculated as

$$C_v = 42.3 + 9.0 \cdot \log\left(100 \cdot F_{pest}\right) \tag{A.28}$$

so that we can formulate the volatilization rate from soil with the equation

$$k_{v_{Bar}} = \frac{-log\left(1 - C_v\right)}{21 \cdot 24 \cdot 3600} \tag{A.29}$$

The volatilization from bare soil then results in

$$V_B = k_{bar} \cdot b_B \tag{A.30}$$

Degradation of POPs on bare soil Degradation of chemicals is not a single process but rather the overall action resulting from biotic and abiotic degradation. We currently adopt a first order degradation kinetics consisting out of a fixed degradation rate coefficient with a temperature dependence that allows the degradation rate to double every $10K$ (*Bureau* (1996)). Again we assume a bare soil degradation coefficient k_b that depends from the prescribed values k_{b_x} at reference temperature. The decay formulation in dependence of temperature is

$$k_b = k_{b_x} \cdot 2^{\frac{T_b - T_{ref}}{10K}} \tag{A.31}$$

POP degradation in soils is a highly complex activity and it is apparent that there is still space for improvement. We use

$$G_B = k_b \cdot b_B \tag{A.32}$$

for our calculations.

A.2.3 Bare soil resistance for gas

The bare soil resistance follows similar rules as for R_T like the vegetation canopy resistance. The boundary layer is the same as in (eq. 3.5) and the surface resistance is calculated like in (eq. 3.15).

A.2.4 Bare soil particle resistance

The same general term which is also used in the calculation of the gas boundary layer resistance of the vegetation (eq. 3.5) is applied for the resistance of a gas to reach the bare soil (smooth surface). For the particle resistance we follow the formulations by *Seinfeld and Pandis* (1998)

$$R_{bs_p} = \frac{1}{u_* \left(Sc^{2/3} + 10^{-3/St}\right)} \tag{A.33}$$

Appendix B

Nomenclature

α	empirical stomata value		κ_{D_g}	diffusivity coefficient	
γ	additional growth rate compensated by the litter fall		ν_i	diffusion coefficients depending on the molecular structure of the gas	
δ_a	fraction of atmospheric application		τ_{ov}	overall residence time	
ΔH_{pa}	vapourisation heat	$\left[\frac{J}{mol}\right]$	π		
θ	aerosol gas partitioning coefficient		ρ_a	densitiy of air	$\frac{kg}{m^3}$
ϑ	leaf longevity	yrs	υ_a	variable for ocean resistance of Schmidt number	
κ	Karman constant		τ_{ph}	The removal rate of POPs within the vegetation volume	$\frac{1}{s}$
κ_D	diffusivity coefficient				

Table B.1: Display of variable process nomenclature

a	attenuation coefficient		D_w	wet deposition	$\frac{molec}{m^2 s}$
A_p	cross section of particle	m	f	fugacity of the chemical	(Pa)
b_A	burden atmosphere	$\frac{molec}{m^2}$	$F_{A \rightarrow V_V}$	gas diffusion atm veg	$\frac{molec}{m^2 s}$
b_{A_g}	burden atmosphere in the gas phase	$\frac{molec}{m^2}$	f_C	interception ratio of canopy	
b_S	burden bare soil	$\frac{molec}{m^2}$	f_D	wet deposition fraction arriving at vegetation soil	
b_O	burden ocean	$\frac{molec}{m^2}$	F_{drg}	drag force	$\frac{kg}{ms^2}$
$a_{S_{tot}}$	area of total soil		f_i	gas reactivity factor	
b_{tot}	total burden	$\frac{molec}{m^2}$	f_L	leaf dripping ratio	
b_{V_C}	burden on vegetaion canopy	$\frac{molec}{m^2}$	f_S	stem flow ratio	
b_{V_V}	burden vegetation volume	$\frac{molec}{m^2}$	f_T	total flow ratio	
b_{V_S}	burden vegetation soil	$\frac{molec}{m^2}$	$F_{V_V \rightarrow A}$	gas diffusion veg atm	$\frac{molec}{m^2 s}$
C_A	concentration in the atmosphere	$\frac{molec}{m^3}$	G_A	degradation atmosphere	$\frac{molec}{m^2 s}$
C_D	drag coefficient		G_B	degradation bare soil	$\frac{molec}{m^2 s}$
C_{D_p}	drag coefficient (particles)		G_O	degradation ocean	$\frac{molec}{m^2 s}$
C_L	concentration in the leaf	$\frac{molec}{m^3}$	G_V	degradation vegetation surface	$\frac{molec}{m^2 s}$
c_{m_l}	annual carbon mass of leaves	$\frac{m^2}{kg}$	G_{V_S}	degradation vegetation soil	$\frac{molec}{m^2 s}$
C_{sto}	number of stomata		H	Henry coefficient	$\frac{m^3 * Pa}{mol}$
D_B	deposition on bare soil	$\frac{molec}{m^2 s}$	H_i	effective Henry coefficient	$\frac{m^3 * Pa}{mol}$
D_g	deposition in the gas phase	$\frac{molec}{m^2 s}$	h_{mix}	mixing layer height	m
D_{g_p}	deposition in the gas phase (prescribed)	$\frac{molec}{m^2 s}$	I_s	ratio of the total light	
D_{g_c}	deposition in the gas phase (calcultated)	$\frac{molec}{m^2 s}$	I_z	fraction of radiation at vegetation surface	
D_O	deposition on ocean	$\frac{molec}{m^2 s}$	I_0	fraction of atmospheric radiation	
D_p	particle deposition	$\frac{molec}{m^2 s}$	K_{AW}	air-water partitioning coefficient	
D_t	total deposition	$\frac{molec}{m^2 s}$	k_b	soil degradation rate	$\frac{1}{s}$
D_V	deposition on vegation (big leaf)	$\frac{molec}{m^2 s}$	K_{CW}	cuticle-water partitioning coefficient	
D_{V_C}	deposition on vegetation canopy	$\frac{molec}{m^2 s}$	k_l	leaf degradation rate	$\frac{1}{s}$
$D_{V_{C_w}}$	wet deposition on vegetation canopy	$\frac{molec}{m^2 s}$	K_{OA}	octanol-air partitioning coefficient	
D_{V_S}	deposition on vegetation soil	$\frac{molec}{m^2 s}$	k_p	plant attenuation factor	
$D_{V_{S_d}}$	deposition on vegetation soil dry	$\frac{molec}{m^2 s}$	K_{PA}	plant air partitioning coefficient	
$D_{V_{S_w}}$	deposition on vegetation soil wet	$\frac{molec}{m^2 s}$	LAI	leaf area index	$\frac{m^2}{m^2}$

Table B.2:

L_O	loss to ocean deep sea	$\frac{molec}{m^2 s}$	a_O	surface fraction ocean	
L_{Sha}	fraction of leaves in the shadow		a_V	surface fraction vegetation	
L_{Sun}	fraction of leaves in the sun		T_{at}	temperature atmosphere	K
L_{V_V}	loss in vegetation volume compartment	$\frac{molec}{m^2 s}$	t_{ph}	phloem removal time	s
M_a	mass of POPs applied	$\frac{molec}{m^2}$	T_{V_C}	litter fall from vegetation canopy	$\frac{molec}{m^2 s}$
M_{H_2O}	molar weight of water	$\frac{kg}{mol}$	T_{veg}	vegetation temperature	K
$M_{mol_{air}}$	molar weight of air	$\frac{kg}{mol}$	T_{V_S}	vegetation soil temperature	K
M_{POP}	molar weight of POP	$\frac{kg}{mol}$	T_{V_V}	litter fall from vegetation volume	$\frac{molec}{m^2 s}$
p_{air}	pressure of air	Pa	u_*	friction velocity	$\frac{m}{s}$
P_r	Prandtl number		u_z	reference wind speed at height z	$\frac{m}{s}$
R	gas constant	$\frac{J}{Kmol}$	u_∞	terminal velocity	$\frac{m}{s}$
R_a	aerodynamic resistance	$\frac{s}{m}$	$u(z)$	wind speed at height z	$\frac{m}{s}$
R_b	boundary layer resistance	$\frac{s}{m}$	u_H	horizontal wind speed at canopy top	$\frac{m}{s}$
R_c	canopy layer resistance	$\frac{s}{m}$	v_a	kinematic viscosity of air	$\frac{m^2}{s}$
R_{cf}	foliar resistance	$\frac{s}{m}$	V_B	volatilization from bare soil	$\frac{molec}{m^2 s}$
R_{cut}	cuticular resistance	$\frac{s}{m}$	V_C	volume fraction of cuticle	
Re	Reynolds number		v_d	deposition velosity	$\frac{m}{s}$
R_{gs}	ground and soil resistance	$\frac{s}{m}$	V_G	volume fraction of glycerine	
$R^i_{g_s}$	seasonal ground and soil resistance	$\frac{s}{m}$	V_L	volume fraction of lipids	
R_{lbl}	leaf boundary layer resistance	$\frac{s}{m}$	V_O	volatilization from bare soil	$\frac{molec}{m^2 s}$
R_{lu}	upper canopy layer resistance	$\frac{s}{m}$	V_P	volume fraction of proteins	
R_m	mesophylic resistance	$\frac{s}{m}$	V_{ph}	volume fraction of phloem	
r_p	radius of particle	m	v_s	settling velocity of particle	$\frac{m}{s}$
R_s	stomatal resistance	$\frac{s}{m}$	V_V	volatilization from vegetation surface	$\frac{molec}{m^2 s}$
$R_{s_{H_2O}}$	stomatal resistance of water	$\frac{s}{m}$	V_{V_S}	volatilization from vegetated soil	$\frac{molec}{m^2 s}$
R_T	total deposition resistance	$\frac{s}{m}$	V_W	volume fraction of water	
a_B	surface fraction of bare soil		x	canopy depth	m
S_c	Schmidt number		z_{ref}	reference height	m
S_L	Leaf area per volume	$\frac{m^2}{m^3}$	z_0	height z zero	m
SLA	specific leaf area index	$\frac{m^2}{m^2}$			

Table B.3: Display of variable vegetation process nomenclature

A_{aer}	aerosol surface	m	T_b	bare soil temperature	K
C_{OH}	concentration of OH radicals	$\frac{molec}{m^3}$	t_d	time of the day	s
C_{OH_d}	daily concentration OH	$\frac{molec}{m^3}$	T_O	ocean temperature	K
C_{OH_p}	prescribed concentration OH	$\frac{molec}{m^3}$	T_{ref}	reference temperature	K
C_v	cumulative volatilized fraction of POPs		U_1	mass transfer coeffitients	
c_x	properties constant for Junge Pankow	Pam	U_2	mass transfer coeffitients	
D_{dry}	dry bulk density of soil	$\frac{kg}{solid/m^3}$	u_h	wind speed ocean at height h	$\frac{m}{s}$
D_{p_1}	exchange rate coefficient (D-value	$\frac{mol}{(Pam^2s}$	V_{air}	volume fraction of air in the soil	
D_{p_3}	fugacity from water into air	$\frac{kg}{m^3}$	v_{dep_x}	prescribed deposition of chemical	$\frac{m}{s}$
F_{pest}	dimensionless 'capacity' fraction in the gas phase		v_O	ocean volatilization rate	$1/s$
f_{sc}	aerosol scavenging factor		v_t	time dependent variability factor of OH	
h_{mix_O}	mixing layer height over ocean	m	$(V_{wat}$	volume fraction of water in soil	
H_{vap}	saturated vapour pressure at 298 K	PaK	w	wind speed at ocean surface	$\frac{m}{s}$
k_b	degradation rate in soil	$1/s$	W_{sol}	water solubility of chemical	$\frac{kg}{m^3}K$
k_{b_x}	degradation rate in soil prescribed	$1/s$	W_{soil}	relative soil wetness	
k_d	dry deposition rate prescribed	$1/s$	Z_{om}	organic matter in soil	$\frac{kg_{om}}{kg_{soil}}$
k_{lo}	loss rate to ocean	$1/s$	Z_r	rain rate	
k^o	degradation coefficient at the reference temperature	$1/s$	δh	difference of atmospheric height	m
k_{OH_x}	chemical specific chemical degradation rate	$1/s$	ϵ_η	temperature dependent rate of activation energy	K
$K_{T_{soil}}$	soil partitioning coefficient		ξ	Cloudiness factor	
$k_{v_{Bar}}$	volatilization rate from bare soil	$1/s$			
k_w	wet deposition rate	$1/s$			
L_d	daylength	s			
lat	latitude	^{0}			
N_{avo}	Avogadro number	$molec/mol$			
P_{org}	fraction in the soil organic phase				
p_{vap}	vapour pressure	PA			
p_{vap_O}	vapour pressure at ocean surface	Pa			
R_{bs_p}	bare soil particle resistance	$\frac{s}{m}$			

Table B.4: Calculation variables used for the other compartmetns

Appendix C

Equations

The change with time of a burden $\frac{db}{dt}$, is given in all calculation in $molecm^{-2}s^{-1}$

C.1 Setup 1

Atmosphere: $\left[\frac{molec}{m^2 \cdot s}\right]$

$$\begin{aligned}\frac{d\,b_A}{dt} =& E_A + V_V\left(b_V\right) \cdot a_V + V_B\left(b_S\right) \cdot a_B \\ &+ V_O\left(b_O\right) \cdot a_O - D_O\left(b_A\right) \cdot a_O \\ &- D_B\left(b_A\right) \cdot a_B - D_V\left(b_A\right) \cdot a_V \\ &- G_A\left(b_A\right)\end{aligned} \tag{C.1}$$

Bare Soil: $\left[\frac{molec}{m^2 \cdot s}\right]$

$$\frac{d\,b_S}{dt} = D_B\left(b_A\right) \cdot a_B - V_B\left(b_S\right) - G_B\left(b_S\right)$$

Vegetation Surface: $\left[\frac{molec}{m^2 \cdot s}\right]$

$$\frac{d\,b_{V_C}}{dt} = D_V\left(b_A\right) \cdot a_V - G_V\left(b_{V_C}\right) - V_V\left(b_V\right)$$

Ocean $\left[\frac{molec}{m^2 \cdot s}\right]$

$$\begin{aligned} \frac{d\, b_O}{dt} = = & D_O\left(b_A\right) \cdot a_O - G_O\left(b_O\right) \\ & - V_O\left(b_O\right) - L_O\left(b_O\right) \end{aligned} \tag{C.2}$$

C.2 Gas or particle deposition

The equations for the particle deposition look like the ones in setup 1 with the exception that the deposition on land D_L and ocean D_O has to include namely the prescribed gas deposition D_g.

$$D_L = D_w + D_g + D_p \tag{C.3}$$

$$D_O = D_w + D_g + D_p \tag{C.4}$$

C.3 Setup 2

For this calculation a vegetation compartment is added which is subdivided into the vegetation surface and the vegetation volume

Atmosphere: $\left[\frac{molec}{m^2 \cdot s}\right]$

$$\begin{aligned}\frac{d\,b_A}{dt} =& E_A + V_V\left(b_V\right) \cdot a_V + V_B\left(b_S\right) \cdot a_B \\ &+ V_O\left(b_O\right) \cdot a_O - D_O\left(b_A\right) \cdot a_O \\ &- D_B\left(b_A\right) \cdot a_B - D_V\left(b_A\right) \cdot a_V \\ &- G_A\left(b_A\right) + F_{V_V \to A} \cdot a_V\end{aligned} \tag{C.5}$$

Bare Soil: $\left[\frac{molec}{m^2 \cdot s}\right]$

$$\frac{d\,b_S}{dt} = D_B\left(b_A\right) \cdot a_B - V_B\left(b_S\right) - G_B\left(b_S\right)$$

Vegetation Surface: $\left[\frac{molec}{m^2 \cdot s}\right]$

$$\frac{d\,b_{V_C}}{dt} = D_V\left(b_A\right) \cdot a_V - G_V\left(b_{V_C}\right) - V_V\left(b_V\right)$$

Vegetation Volume: $\left[\frac{molec}{m^2 \cdot s}\right]$

$$\frac{b_{V_V}}{dt} = F_{A \to V_V} - L_{V_V}\left(b_{V_V}\right)$$

Ocean $\left[\frac{molec}{m^2 \cdot s}\right]$

$$\begin{aligned}\frac{d\,b_O}{dt} =& = D_O\left(b_A\right) \cdot a_O - G_O\left(b_O\right) \\ &- V_O\left(b_O\right) - L_O\left(b_O\right)\end{aligned} \tag{C.6}$$

C.4 Setup 3

One has to add a further compartment, namely vegetation soil (vegetated soil) to calculate the effects caused by litter fall, atmosphere vegetation soil interactions, vegetation soil degradation, and volatilization from litter.

Atmosphere: $\left[\frac{molec}{m^2 \cdot s}\right]$

$$\begin{aligned}\frac{d\,b_A}{dt} =& E_A + V_V\left(b_V\right) \cdot a_V + V_B\left(b_S\right) \cdot a_B \\ &+ V_O\left(b_O\right) \cdot a_O - D_O\left(b_A\right) \cdot a_O \\ &- D_B\left(b_A\right) \cdot a_B - D_V\left(b_A\right) \cdot a_V \\ &- G_A\left(b_A\right) + F_{V_V \to A} \cdot a_V \\ &+ V_{V_S}\left(b_{V_S}\right) \cdot a_V\end{aligned} \tag{C.7}$$

Bare Soil: $\left[\frac{molec}{m^2 \cdot s}\right]$

$$\frac{d\,b_S}{dt} = D_B\left(b_A\right) \cdot a_B - V_B\left(b_S\right) - G_B\left(b_S\right)$$

Vegetation Surface: $\left[\frac{molec}{m^2 \cdot s}\right]$

$$\begin{aligned}\frac{d\,b_{V_C}}{dt} =& = D_{V_C}\left(b_A\right) \cdot a_V - G_V\left(b_{V_C}\right) \\ &- V_V\left(b_V\right) - T_{V_C}\left(b_{V_C}\right)\end{aligned} \tag{C.8}$$

Vegetation Volume: $\left[\frac{molec}{m^2 \cdot s}\right]$

$$\frac{b_{V_V}}{dt} = F_{A \to V_V} - L_{V_V}\left(b_{V_V}\right) - T_{V_V}\left(b_{V_V}\right)$$

Vegetation Soil: $\left[\frac{molec}{m^2 \cdot s}\right]$

$$\begin{aligned}\frac{d\,b_{V_S}}{dt} =& D_{V_S}\left(b_A\right) \cdot a_V - V_{V_S}\left(b_{V_S}\right) \\ &- G_{V_S}\left(b_{V_S}\right) + T_{V_C}\left(b_{V_C}\right) \\ &+ T_{V_V}\left(b_{V_V}\right)\end{aligned} \tag{C.9}$$

Ocean $\left[\frac{molec}{m^2 \cdot s}\right]$

$$\begin{aligned} \frac{d\, b_O}{dt} = = & D_O\left(b_A\right) \cdot a_O - G_O\left(b_O\right) \\ & - V_O\left(b_O\right) - L_O\left(b_O\right) \end{aligned} \tag{C.10}$$

C.5 Setup 4

Atmosphere: $\left[\frac{molec}{m^2 \cdot s}\right]$

$$\begin{aligned}\frac{d\,b_A}{dt} =& E_A + \sum V_V\left(b_V\right) \cdot a_V + V_B\left(b_S\right) \cdot a_B \\ &+ V_O\left(b_O\right) \cdot a_O - D_O\left(b_A\right) \cdot a_O \\ &- D_B\left(b_A\right) \cdot a_B - \sum D_V\left(b_A\right) \cdot a_V \\ &- G_A\left(b_A\right) + \sum F_{V_V \to A} \cdot a_V \\ &+ V_{V_S}\left(b_{V_S}\right) \cdot a_V\end{aligned} \tag{C.11}$$

Bare Soil: $\left[\frac{molec}{m^2 \cdot s}\right]$

$$\frac{d\,b_S}{dt} = D_B\left(b_A\right) \cdot a_B - V_B\left(b_S\right) - G_B\left(b_S\right)$$

Vegetation Surface: $\left[\frac{molec}{m^2 \cdot s}\right]$

$$\begin{aligned}\frac{b_{V_C}}{dt} =& \sum D_{V_C}\left(b_A\right) \cdot a_V - \sum G_V\left(b_{V_C}\right) \\ &- \sum V_V\left(b_V\right) - \sum T_{V_C}\left(b_{V_C}\right)\end{aligned} \tag{C.12}$$

Vegetation Volume: $\left[\frac{molec}{m^2 \cdot s}\right]$

$$\begin{aligned}\frac{b_{V_V}}{dt} =& \sum F_{A \to V_V} - \sum L_{V_V}\left(b_{V_V}\right) \\ &- \sum T_{V_V}\left(b_{V_V}\right)\end{aligned} \tag{C.13}$$

Vegetation Soil: $\left[\frac{molec}{m^2 \cdot s}\right]$

$$\begin{aligned}\frac{d\,b_{V_S}}{dt} =& D_{V_S}\left(b_A\right) - V_{V_S}\left(b_{V_S}\right) - G_{V_S}\left(b_{V_S}\right) \\ &+ \sum T_{V_C}\left(b_{V_C}\right) + \sum T_{V_V}\left(b_{V_V}\right)\end{aligned} \tag{C.14}$$

Ocean $\left[\frac{molec}{m^2 \cdot s}\right]$

$$\begin{aligned} \frac{d\, b_O}{dt} = = & D_O\left(b_A\right) \cdot a_O - G_O\left(b_O\right) \\ & - V_O\left(b_O\right) - L_O\left(b_O\right) \end{aligned} \tag{C.15}$$

Appendix D

Chemicals description

D.1 DDT

Dichloro-Diphenyl-Trichloroethane or abbreviated DDT is one of the most common insecticides used. It was first synthesized in 1874 by the German chemist Othmar Zeidler but was not used for any purpose. In 1939 DDT was produced again by Paul Müller finding that DDT has good effectiveness against insects and its (firstly assumed) low acute toxicity reactions against live stock. First usages of DDT occurred in the 1940's against louse-bourne typhus in Italy and by the US army to kill body lice and crab lice among its soldiers. The chemical showed such an effectiveness that one considered it as a panacea against the malaria vector. At the end of the war the usage rose up to 1350 tons of DDT per month and the US army was spraying DDT in the Asian Pacific regions prior to major military invasion. Every US soldier serving in the South East Pacific was equipped with DDT spray cans.

Based on the success of DDT usage Müller was rewarded for his work by winning the Nobel Prize for Chemistry in 1948. Due to its convenience of production and the chemical stability DDT became the worldwide most common used pesticide. Especially its effectiveness in the fight against the Malaria endemic was the main reason for the huge rise in global production and usage. In 1955 the World Health assembly adopted a Malaria eradication programme and in the next ten years large areas of South Asia and South America managed to massively to reduce the Malaria infection. Europe eradicated Malaria completely in the 1960's. There is

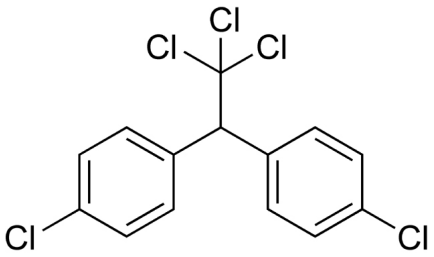

Figure D.1: 4-4'-DDT

no doubt about the efficiency of DDT to fight Malaria and its life saving function for millions of people around the globe. However a total eradication of the Malaria problem was not to be reached. Some mosquito types either developed a resistance against DDT or just avoided areas where DDT was sprayed and efforts from the 1970's onwards were more focused on malaria control or usage of mosquito nets. Today malaria is still one of the biggest causes of death especially on the African continent. Approximately 2.7 million people die every year due to Malaria among them mainly children under five years.

D.1.1 Health impacts

In the early 1960's arguments about the real impact of DDT on humans and the wild life were raised. In humans DDT was suspected to be the cause for cancer and damage to the reproductive cycle; especially breast cancer was correlated with high levels of DDT or its break up products. DDT is a mutagenic chemical and another possible side effect of DDT could be its function as an endocrine disruptor. Endocrine disruptions in mammals can cause impacts similar to hormon dysfunctions. One of the possible effects of such a disruption is a change of the gender ratio, which could lead to a lower fertility and breeding success of a species. In wild life first observations (impairment and eggshell thinning) about the harm of DDT were made for birds in the 1960. Environmental groups raised public awareness.

D.1.2 Global usage and ban

The total amount of DDT used worldwide from 1950 until 1993 is estimated with approximately 2.6 million tons (MT) with peak production level in 1962. The total U.S. production between 1945 and 1972 was estimated with 1.34 MT with a domestic use of 645 kt (*AMAP* (2004)). Other major DDT users were/are the former Soviet Union, China, Mexico, Brazil, India. Sweden was among the first ones to ban DDT in 1970, followed by countries like Switzerland and Germany. The U.S. banned the usage of DDT (or better restricted its usage to very dire situations) after hearings of the EPA in 1972/73, but still allowed to export it. After the ban in the western industrialized countries DDT was still used in countries of the former Eastern block and the developing world. Many of these countries stopped the production or usage in the 1980's or 1990's after changing their Malaria eradication programmes and switching to alternative pesticides. From 1993 onwards the WHO (World Health Organization) considered the usage of DDT as not sustainable and according to recommendation of 1997 DDT should be only used as part of 'integrated programmes'. Today only few countries still produce and use DDT, China and India among them. Although China prohibited the usage in 1983, DDT is still being exported, while India severely cut back the usage in 1995 (*Li* (1999)). Today about 25 countries still use DDT to reduce the thread by Malaria and other diseases (*AMAP* (2004)). In September 2006 the WHO declared that DDT will have to be used again.

D.1.3 Chemical properties

DDT is a very persistent chemical with documented long half life values (depending on the climate zone the reported half life values can vary between 2-15 years (*WHO* (2005b))) over land and its break up products such as DDE[1], DDD[2], are persistent. DDT is rather immobile in soils and can be strongly adsorbed to organic matter and clay minerals, but is not easily soluble in water (*UNEP* (2003a)). DDT is lost via photolytical processes, volatilization to the atmosphere, transport in soils or aerobic or anaerobic biodegradation.. Atmospheric transport of DDT mostly occurs attached to aerosol particles. Due to its lipophilic character DDT ($logK_{OW} = 6.36$), DDE ($logK_{OW} = 5.7$), DDD ($logK_{OW} = 5.5$) have the ability to accumulate in the fatty tissue of humans and animals and biomagnify through the food chain. Particularly damages of liver and kidneys could occur through chronical exposure of DDT. Despite all the known or assumed negative secondary effects a total eradication and replacement of DDT is not foreseeable.

D.2 PCB-52

PCB-52 belongs to the polychlorinated biphenyls (PCBs), class of chlorinated hydrocarbons attached to a biphenyl molecule. There are in total 209 compounds with this chemical structure and for the most general formula one can write $C_{12}H_{10-x}Cl_x$. PCB are very stable chemicals and have been introduced for commercial use in 1929. Especially in the electronic industry used PCBs in transformers and capacitors due to their strong electric insulation. PCBs can be found in paint and were a very common flexibilizer in synthetics or are used as flame retardants or in hydraulic pumps.

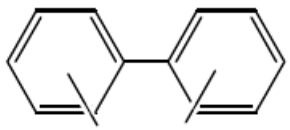

Figure D.2: General structure of PCB molecules

Up to today the accumulated global PCB production reached around 1-1.5 million tons. The peak production of PCBs was in the 1960's especially for extensive usage in the electronic industry where it was used for cooling and isolation. In the mid 1960's health problems became known by a several key events in urbanized areas. In 1968 an accident with the following contamination with PCB and PCDF's [1] in Kyushu (Japan) caused the death of many life stock and more than 2000 people were victims of a severe skin disease (Yusho disease), which later resulted even in cancer or heavy liver damage. PCBs proved to be an ecological problem and they were made responsible for liver and kidneys and other organs damage(making the problem worse by the bioaccumulation and biomagnification processes) in humans and animals. Women and babies are specially endangered

[1] Dichloro-diphenyl-dichloro-ethylene
[2] Dichloro-diphenyl-dichloro-ethane
[1] polychlorinated dibenzofurans

by PCBs. PCBs are correlated with e.g. reduction of mental capacity or reproduction problems (intersex genders) or even cancer. Effects on reproduction have been reported also for the Arctic where e.g. polar bears are affected by endocrine disruptions. PCBs have been detected ubiquitously, and urbanized industrial areas are hot spots of PCB contamination. The U.S. banned the production of PCBs in the late 1970s, followed by the U.K. (1981), West Germany (1983) and other OECD countries in the 1980s [2]. Though the problem of PCBs is still causing public health problems. PCBs are found in many materials and a sustainable disposal is very complex and costly. Especially secondary sources of PCB like construction materials in old houses, cables, or electronic devices need a special treatment for its disposal. PCBs have low water solubility and low vapour pressure but solve well in fatty or organic compounds. Differences among PCBs are based on the amount of chlorinated substitutes, vapour pressure and degradability (*Mackay et al.* (1997)). The chlorination is a driving parameter to the degradability of PCBs. In nature PCBs can be destroyed by microbial dechlorination and in the atmosphere via photochemistry.

D.3 Back ground information of test criteria

D.3.1 Overall burden

The overall burden is the burden per unit area in a compartment multiplied with its surface area. The overall burden thus can be written as

$$B_{ov} = B_{air} \cdot A_{air} + B_{oce} \cdot A_{oce} + B_{land} \cdot A_{land} \tag{D.1}$$

D.3.2 Overall residence time

The total residence time τ_{ov} is considered an important value and indicator for the long range transport potential of a substance. It is an indicator for the degradation, durability and the structured compartment loss processes of a chemical. Similar to the case of overall burden, many parameters are involved in the meridional variability of τ_{ov}. Temperature, OH-radical concentration, land-ocean surface ratio, vegetation fraction and other factors are relevant for τ_{ov}. It also can be used to address the persistence in individual compartments and could be a good indicator for the general behavior of a substance. As we can not display the general spread of POPs in a geographical sense in a box model the most important indicator for substance persistence is based on the overall fate within the diverse compartments. The mass balance equations were based on the overall source Q_{ov} and depletion terms k_{ov} so that the most primitive equation used was

$$\frac{\delta m}{\delta t} = Q_{ov} - k_{ov} \tag{D.2}$$

[2] http://www.umweltlexikon-online.de/fp/archiv/RUBbauenwohnen/PCB.php

The inverse of the ratio of the depletion rate D and the overall burden m is defined as the inverse of the overall residence time τ_{ov}

$$k_{ov} = \frac{D}{m} = \frac{1}{\tau_{ov}} \tag{D.3}$$

Bibliography

Ackerly, D., S. Mulkey, R. Chazdon, and A. Smith (Eds.) (1996), *Tropical forest and plant ecophysiology*, chap. Canopy Structure and Dynamics: Integration of Growth Processes in Tropical Pioneer Tree, pp. 619–658, Chapmann and Hall, New York.

Agrell, C., L. Okla, P. Larsson, C. Backe, and F. Wania (1999), Evidence of Latitudinal Fractionation of Polychlorinated Biphenyl Congeners along the Baltic Sea Region, *Environ. Sci. Technol.*, *33*(8), 1149–1156.

AMAP (1997), Arctic Pollution Issues, *Tech. rep.*, Arctic Monitoring and Assessment Programme, Oslo, Norway.

AMAP (1998), The influence of physical and chemical processes on contamint transport into and within the arctic, *Tech. rep.*, Arctic Monitoring and Assessment Programme, Oslo, Norway.

AMAP (2002), Amap assessment 2002: Persistent Organic Pollutants in the Arctic, *Tech. rep.*, Arctic Monitoring and Assessment Programme, Oslo, Norway.

AMAP (2004), AMAP, 2004. amap Assessment 2004: Persistent Organic Pollutants (POPs) in the arctic., *Tech. rep.*, Arctic Monitoring and Assessment Programme (AMAP), Oslo, Norway.

Bacci, E., D. Calamari, C. Gaggi, and M. Vighi (1990), Bioconcentration of Organic Chemical Vapors in Plant Leaves: Experimental Measurements and Correlation, *Environ. Sci. Technol.*, *24*, 885–889.

Bakan, S., H. Hinzpeter, H. Höller, R. Jaenicke, H. Jeske, H. Volland, P. Warneck, and C. Wurzinger (1988), *Zahlenwerte und Funktionen aus Naturwissenschaften und Technik*, Band 4 Meteorologie, Teilband b, Physikalische und chemische Eigenschaften der Luft, Landolt-Börnstein, Springer Verlag, Berlin.

Barbas, J., M. Sigman, and R. Dabestani (1996), Photochemical Oxidation of Phenanthrene Sorbed on Silica Gel, *Environ. Sci. Technol.*, *30*(5), 1776–1780.

Barber, J., G. O. Thomas, G. Kerstiens, and K. Jones (2002), Air-Side and Plant-Side Resistances Influence the Uptake of Airborne PCBs by Evergreen Plants, *Envi. Sci. Technol.*, *36*(15), 3224–3229.

Barber, J., G. Thomas, G. Kerstiens, and K. C. Jones (2004), Current Issues and Uncertainties in the Measurement and Modelling of Air-Vegetation Exchange and within Plant Processing of POPs, *Environmental pollution*, *128*, 99–138.

Basheer, C., J. P. Obbard, and H. K. Lee (2003), Persistent Organic Pollutants in Singapore's Coastal Marine Environment: Part II, Sediments, *Water, Air, & Soil Pollution*, *149*(1 - 4), 315–325.

Behymer, T. D., and R. A. Hites (1985), Photolysis of Polycyclic Aromatic Hydrocarbons (PAHs) adsorbed on simulated Atmospheric Particulates, *Environ. Sci. Technol.*, *19*, 1004 – 1006.

Beyer, A., F. Wania, T. Gouin, D. Mackay, and M. Matthies (2003), Temperature Dependence of the Characteristic Travel Distance, *Environ. Sci. Technol.*, *37*(4), 766–771.

Blais, J. M., D. W. Schindler, D. C. G. Muir, L. E. Kimpe, D. B. Donald, and B. Rosenberg (1998), Accumulation of Persistent Organochlorine Compounds in Mountains of Western Canada, *Nature*, *395*(6702), 585–588.

Boehme, F., K. Welsch-Pausch, and M. M. S. (1999), Uptake of Airbourne semivolatile organic Compounds in Agricultural plants: Field Measurements of Interspecies Variability, *Environ. Sci. and Technol.*, *33*, 1805–1813.

Brandes, J., H. den Hollander, and D. van de Meent (1996), Simplebox 2.0: A nested multimedia fate Model for Evaluating the Environmental Fate of Chemicals;, Report National Institute of Public Health and the Environment (RIVM) No. 719 101 029, Wageningen, The Netherlands.

Brzuzy, L. P., and R. A. Hites (1996), Global mass balance for polychlorinated dibenzo-p-dioxins and dibenzofurans, *Envi. Sci. Technol.*, *30*(6), 1797–1804, doi:10.1021/es950714n.

Bureau, E. C. (1996), Technical Guidance Document in Support of The Commision's Directive 93/67/EEC on Risk Assessment for the Notified Substances and the Commission's Regulation (EC)1488/94 on Risk Assessment on Existing Substances, *Tech. rep.*, European Chemicals Bureau, Ispra.

Calamari, D., E. Bacci, S. Focardi, C. Gaggi, and M. V. M. Morosini (1991), Role of Plant Biomass in the Global Environmental Partitioning of chlorinated Hydrocarbons, *Environ. Sci. and Technol.*, *25*, 1489–1495.

Carson, R. (1962), *Silent Spring*, Houghton Mifflin Company, 215 Park Avenue South, New York, 10003.

Cionco, R. (1965), A mathematical model for airflow in vegetative canopy, *J Appl Meteorol*, *4*, 517–522.

Cionco, R. (1972), A Wind Profile Index for Canopy Flow, *Boundary-Layer Meteorol*, *3*, 255–263.

Cohen, M., R. Draxler, R. Artz, B. Commoner, P. Bartlett, P. Cooney, K. Couchot, A. Dickar, H. Eisl, C. Hill, J. Quigley, J. Rosenthal, D. Niemi, D. Ratte, M. Deslauriers, R. Laurin, L. Mathewson-Brake, and J. McDonald (2002), Modeling the Atmospheric Transport and Deposition of PCDD/F to the Great Lakes, *Environ. Sci. Technol.*, *36*(22), 4831–4845.

Cotham, W. E. J., and B. T. F. (1991), Estimating the Atmospheric Deposition of Organochlorine Contaminats to the Arctic, *Chemosphere*, *22*, 165–188.

Dabestani, R., K. J. Ellis, and M. E. Sigman (1995), Photodecomposition of Anthracene, *Journal of Photochemistry and Photobiology A*, *86*, 231–239.

Dai, Y., R. Dickinson, and Y. Wang (2004), A two big Leaf Model for Canopy Temperature, Photosynthesis and Stomatal Conductance, *Journal of Climate*, *17*, 2281–2299.

Dalla Valle, M., J. Dachs, A. Sweetmann, and K. Jones (2004), Maximum Reservoir Capacity of vegetation for Persistent Organic Pollutants, *Global Biogeochemical Cycles*, *18*, GB 4032.

de Wit, C., A. Fisk, K. Hobbs, D. Muir, G. Gabrielsen, R. Kallenborn, M. Krahn, R. Norstrom, and J. Skaare (2002), AMAP Assessment 2002: Persistent Organic Pollutants in the Arctic, Arctic Monitoring and Assessment Programme (AMAP), Oslo, *Tech. rep.*, AMAP Secretariat, P.O. Box 8100 Dep, N-0032 Oslo, Norway.

Duyzer, J. H., and R. F. van Oss (1997), Determination of Deposition Parameters of a Number of Persistent Organic Pollutants by Laboratory Experiments, *Tech. rep.*, TNO Institute of Environmental Sciences, Energy Research and Process Inovation.

Eriksson, G., S. Jensen, H. Kylin, and W. Strachan (1989), The pine needle as a monitor of atmospheric pollution, *Nature*, *341*, 42–44.

Faber, R., and H. J.J. (1970), Eggshell Thinning, chlorinated Hydrocarbons, and Mercury in inland aquatic Bird Eggs , 1969 and 1970, *Pesticide Monitoring Journal*, *7*, 27–39.

Faun, A. (1990), *Plant Anatomy*, Pergamon Press.

Fry, D., and C. Toone (1981), DDT-induced Feminization of Gull Embryos, *Science*, *213*, 992–924.

Fuller, E. N., P. D. Schettler, and J. C. Giddings (1966), A new Method for Prediction of binary gas-phase Diffusion Coefficients, *Industrial and engineering chemistry*, *58*(5), 19–27.

Galiulin, R. V., V. N. Bashkin, and R. A. Galiulina (2002), Review: Behavior of Persistent Organic Pollutants in the Air-Plant-Soil system, *Water, Air, & Soil Pollution*, *137*(1 - 4), 179–191.

Ganzeveld, L., and J. Lelieveld (1995), Dry deposition Parameterization in a Chemistry General Circulation Model and its Influence on the Distribution of Reactive trace Gases, *J. Geophys. Res., Vol. 100 , No. D10*, 20,999–21,012.

Glydekaerne, S., B. Secher, and E. Nordbo (1999), Ground Deposit of a Pesticide in Relation to the Cereal Canopy Density, *Pestic. Sci.*, *55*, 1210–1216.

Gustafsson, ., J. Axelman, D. Broman, M. Eriksson, and H. Dahlgaard (2001), Process-diagnostic patterns of chlorobiphenyl congeners in two radiochronologically characterized sediment cores from the northern baffin bay, *Chemosphere*, *45*(6-7), 759–766.

Halsall, C. J., R. Bailey, G. A. Stern, L. A. Barrie, P. Fellin, D. C. G. Muir, B. Rosenberg, F. Y. Rovinsky, E. Y. Kononov, and B. Pastukhov (1998), Multiyear Observations of Organohalogen Pesticides in the Arctic Atmosphere, *Environmental Pollution*, *102*(1), 51–62.

Hellström, A., H. Kylin, W. Strachan, and S. Jensen (2004), Distribution of Organochlorine Compounds in Pine Needles from Central and Northern Europe, *Environmental pollution*, *128*, 24–48.

Helm, P. A., and T. F. Bidleman (2005), Gas-particle Partitioning of Polychlorinated Naphthalenes and non- and mono-ortho-substituted Polychlorinated Biphenyls in Arctic Air, *Science of The Total Environment*, *342*(1-3), 161–173.

Hiatt, M. (1999), Leaves as an Indicator of Exposure to Airborne Volatile Organic Compounds, *Environ. Sci. and Technol.*, *33*, 4126–4133.

Hicks, B., and P. Liss (), Transfer of SO2 and other reactive gases across the air-sea interface.

Hicks, B. B., D. D. Baldocchi, T. P. Meyers, R. P. Hosker, and M. D. R. (1987), A preliminary multiple Resistance Routine for deriving dry Deposition Velocities from measured Quantities, *Water, Air and Soil pollution*, *37*, 311–330.

Hikosaka, K. (2005), Leaf Canopy as a Dynamic System: Ecophysiology and Optimality in Leaf Turnover, *Annals of Botany*, *95*, 521–533.

Hirose, T. (2005), Development of the Monsi-Saeki Theory on Canopy Structure and Function, *Annals of Botany*, *95*, 483–494.

Hollert, H., M. Dürr, H. Olsman, K. Halldin, B. van Bavel, W. Brack, M. Tysklind, M. Engwall, and T. Braunbeck (2002), Biological and Chemical Determination of Dioxin-like Compounds in Sediments by Means of a Sediment Triad Approach in the Catchment Area of the River Neckar, *Ecotoxicology*, *11*(5), 323–336.

Horstmann, M. (1990), Fugazitätsmessungen schwerflüchtiger chlororganischer Verbindungen an Fichtennadeloberflächen, Master's thesis, University Bayreuth.

Horstmann, M., and M. McLachlan (1998), Atmospheric deposition of semivolatile organic compounds to two forest canopies, *Atmospheric Environment*, *32*, 1799–1809.

Hung, H., C. Halsall, P. Blanchard, H. Li, P. Fellin, G. Stern, and B. Rosenberg (2002), Temporal Trends of Organochlorine Pesticides in the Canadian Arctic Atmosphere, *Environ. Sci. Technol.*, *36*(5), 862–868.

Ikonomou, M., S. Rayne, and R. Addison (2002), Exponential Increases of the Brominated Flame Retardants, Polybrominated Diphenyl Ethers, in the Canadian Arctic from 1981 to 2000, *Environ. Sci. Technol.*, *36*(9), 1886–1892.

Jensen, S., G. Eriksson, H. Kylin, and W. Strachan (1992), Atmospheric pollution by Persistent Organic Compounds: Monitoring with Pine Needles, *Chemosphere*, *24*, 229–245.

Junge, C. E. (1977), *Basic Consideration about Trace Constiuents in the Atmosphere as realted to the Fate of Global Pollutants*, in Fate of Pollutants in the Air and Water Environments, ed. Suffet, I. H., Wiley, New York.

Junkermann, W., C. Brühl, D. Perner, E. Eckstein, T. Trautmann, B. Früh, R. Dlugi, B. Gori, A. Ruggaber, J. Reuder, M. Zelger, H. A., A. Kraus, F. Rohrer, D. Brüning, G. Moortgat, A. Horowitz, and J. Tadić (2002), Actinic radiation and photolysis processes in the lower troposphere: Effect of clouds and aerosols, *J. Atmos. Chem.*, *42*, 413–441.

Kallenborn, R., M. Oehme, D. D. Wynn-Williams, M. Schlabach, and J. Harris (1998), Ambient Air Levels and Atmospheric Long-Range Transport of Persistent Organochlorines to Signy Island, Antarctica, *The Science of The Total Environment*, *220*(2-3), 167–180.

Kerler, F., and J. Schönherr (1988), Permeation of Lipophilic Chemicals across Plant Cuticles: Prediction from Partition Coefficients and Molar Volumes, *J. Arch. Environ. Contam. Toxicol.*, *17*, 1–70.

Kikuzawa, K. (2003), Phenological and Morphological Adaptations to the Light Environment in two Woody and two Herbaceous Plant Species, *Functional Ecology*, *17*, 29–38.

Killingbeck, K. T. (1996), Nutrients in senescent Leaves: Keys to the Search for potential Resorption and Resorption Proficiency, *Ecology*, *77*, 1716–1727.

Kömp, P., and M. McLachlan (1997), Influence of Temperature on the Plant/Air Partitioning of Semivolatile Organic Compounds, *Environ. Sci. and Technol.*, *31*, 886–890.

Koziol, A. S., and J. A. Pudykiewicz (2001), Global-scale environmental transport of Persistent Organic Pollutants, *Chemosphere*, *45*, 1181–1200.

Kylin, H., and Sjödin (2003), Accumulation of Airborne Hexachlorocyclohexanes and DDT in Pine Needles, *Environ. Sci. and Technol.*, *37*, 2350–2355.

Kylin, H., K. Söderquist, A. Undeman, and R. A. Franich (2002), Seasonal Variation of Terpene Content, an overlooked Factor in the Determination of Environmental Pollutants in Pine Needles, *Bull. Environ. Contam. Toxicol.*, *68*, 155–160.

Lammel, G., W. Kloepffer, V. Semeena, E. Schmidt, and A. Leip (2007), Multicompartment Fate of Persistent Substances, *Env Sci Pollut Res*, *14 (3)*, 153–165.

Larcher, W. (1994), *Ökophysiologie der Pflanzen, 5. Auflage*, Verlag Eugen Ulmer, Wollgrassweg 41, 70599 Stuttgart (Hohenheim).

Li, Y. F. (1999), Global Technical Hexachlorocyclohexane Usage and its Contamination Consequences in the Environment: from 1948 to 1997, *The Science of The Total Environment*, *232*(3), 121–158.

Liss, P. S., and P. G. Slater (1974), Flux of Gases accross the the Air Sea Interface, *Deep Sea Res.*, *247*, 181–184.

Lohmann, R., W. Ockenden, J. Shears, and K. Jones (2001), Atmospheric Distribution of Polychlorinated Dibenzo-p-dioxins, Dibenzofurans (PCDD/Fs), and Non-Ortho Biphenyls (PCBs) along a North-South Atlantic Transect, *Environ. Sci. and Technol.*, *35*(20), 4046–4053.

Mackay, D., and P. J. Leinonen (1975), Rate of Evaporation of low-Solubility Contaminants from Water Bodies to Atmosphere, *Environ. Sci. and Technol.*, *9*, 1178–1180.

Mackay, D., and A. T. K. Yeun (1983), Mass Transfer Coefficient Correlations for Volatilization of Organic Solutes from Water, *Environ. Sci. and Technol.*, *17(4)*, 211–217.

Mackay, D., S. Paterson, and W. Y. Shiu (1992), Generic Models for Evaluating the Regional Fate of Chemicals, *Chemosphere*, *24*, 695–717.

Mackay, D., W. Y. Shiu, and K.-C. Ma (1997), *Illustrated Handbook of Physical-Chemical Properties and Environmental Fate for Organic Chemicals*, vol. Vol. V, – pp., Ma. Lewis Publishers, 1992.

MacLeod, M., D. Woodfine, D. G. Mackay, T. E. McKone, D. Bennett, and M. R. (2001), BETR North America: A Regionally Segmented Multimedia Contaminant Fate Model for North America, *Environ Sci Pollut. Res.*, *8 (3)*, 156?163.

Matsuzawa, S., L. Nasser-Ali, and P. Garrigues (2001), Photolytic Behavior of Polycyclic Aromatic Hydrocarbons in Diesel Particulate Matter Deposited on the Ground, *Environ. Sci. Technol.*, *35*(15), 3139–3143.

McLachlan, M., and M. Horstmann (1998), Forests as Filters of Airborne Organic Pollutants: a Model, *Environ. Sci. and Technol.*, *32*, 413–420.

McLachlan, M., K. Welsch-Pausch, and J. Tolls (1995), Field validation of a model of the uptake of gaseous SOC in Lolium multiflorum (rye grass), *Environ. Sci. and Technol.*, *29*, 1998–2004.

Meijer, S., E. Steinnes, W. Ockenden, and K. Jones (2002), Influence of Environmental Variables on the Spatial Distribution of PCBs in Norwegian and U.K. Soils: Implications for Global Cycling, *Environ. Sci. Technol.*, *36*(10), 2146–2153.

Meijer, S., W. Ockenden, E. Steinnes, B. Corrigan, and K. Jones (2003a), Spatial and Temporal Trends of POPs in Norwegian and UK Background Air: Implications for Global Cycling, *Environ. Sci. Technol.*, *37*(3), 454–461.

Meijer, S., W. Ockenden, A. Sweetman, K. Breivik, J. Grimalt, and K. Jones (2003b), Global Distribution and Budget of PCBs and HCB in Background Surface Soils: Implications for Sources and Environmental Processes, *Environ. Sci. Technol.*, *37*(4), 667–672.

Meneses, M., M. Schuhmacher, and J. L. Domingo (2002), A Design of two Simple Models to predict PCDD/F Concentrations in Vegetation and Soils, *Chemosphere*, *46*(9-10), 1393–1402.

Mill, T., W. R. Mabey, B. Y. Lan, and A. Baraze (1981), Photolysis of Polycyclic Aromatic Hydrocarbons in Water, *Chemosphere*, *10*(11-12), 1281–1290.

Miller, J. S., and D. Olejnik (2001), Photolysis of Polycyclic Aromatic Hydrocarbons in Water, *Water Research*, *35*(1), 233–243.

Monsi, M., and T. Saeki (1953), Über den Lichtfaktor in den Pflanzengesellschaften seine Bedeutung fuer die Stoffproduktion, *Japanese Journal of Botany*, *14*, 22–52.

Monteith, J., and M. H. Unsworth (1990), *Principles of Environmental Physics, 2nd edition*, Butterworths, London.

Mörner, J., R. Bos, and M. Fredrix (2002), Reducing and Eliminating the use of Persistent Organic Pesticides Guidance on alternative Strategies for Sustainable Pest and Vector Management, *Tech. rep.*, Inter-Organization Programme for the Sound Management of Chemicals (IOMC).

Mortimer, C. E. (1987), *Das Basiswissen der Chemie*, Georg Thieme Verlag, Stuttgart.

Muir, D., A. Omelchenko, N. Grift, D. Savoie, W. Lockhart, P. Wilkinson, and G. Brunskill (1996), Spatial Trends and Historical Deposition of Polychlorinated Biphenyls in Canadian Midlatitude and Arctic Lake Sediments, *Environ. Sci. Technol.*, *30*(12), 3609–3617.

Müller, J. F., D. W. Hawker, and D. W. Connell (1994), Calculation of Bioconcentration Factors of Persistent Hydrophobic Compounds in the Air/Vegetation System, *Chemosphere*, *29*(4), 623–640.

Nhan, D. D., N. M. Am, N. C. Hoi, L. Van Dieu, F. P. Carvalho, J.-P. Villeneuve, and C. Cattini (1998), Organochlorine Pesticides and PCBs in the Red River Delta, North Vietnam, *Marine Pollution Bulletin*, *36*(9), 742–749.

Niu, J., J. Chen, D. Martens, X. Quan, F. Yang, A. Kettrup, and K.-W. Schramm (2003), Photolysis of polycyclic aromatic hydrocarbons adsorbed on spruce [picea abies (l.) karst.] needles under sunlight irradiation, *Environmental Pollution*, *123*(1), 39–45.

Niu, J., J. Chen, D. Martens, B. Henkelmann, X. Quan, F. Yang, H. K. Seidlitz, and K. W. Schramm (2004), The Role of UV-B on the Degradation of PCDD/Fs and PAHs sorbed on Surfaces of Spruce (Picea abies (L.) Karst.) Needles, *Science of The Total Environment*, *322*(1-3), 231–241.

Nizzetto, L., C. Cassani, and A. Di Guardo (2006), Deposition of PCBs in Mountains: The Forest Filter Effect of different Forest Ecosystem Types.; The Role of High Mountains in the Global Transport of Persistent Organic Pollutants, *Ecotoxicology and Environmental Safety*, *63*, 75–83.

Ockenden, W., A. Sweetman, H. Prest, E. Steinnes, and K. Jones (1998), Toward an Understanding of the Global Atmospheric Distribution of Persistent Organic Pollutants: The Use of Semipermeable Membrane Devices as Time-Integrated Passive Samplers, *Environ. Sci. Technol.*, *32*(18), 2795–2803.

OSPAR, . (2000), Commission for the protection of the marine environment of the North-East Atlantic: Quality Status Report 2000. region II Greater North Sea,136 pp, *Tech. rep.*, OSPAR Commission, London.

Pankow, J. F. (1994a), An Absorption Model for the Gas-Aerosol Partitioning involved in the Formation of Secondary Organic Aerosols, *Atmospheric Environment*, *28*, 185–188.

Pankow, J. F. (1994b), An Absorption Model for the Gas-Aerosol Partitioning involved in the Formation of Secondary Organic Aerosols, *Atmospheric Environment*, *28*, 189–193.

Paterson, S., D. Mackay, E. Bacci, and D. Calamari (1991), Correlation of the Equilibrium and Kinetics of Leaf-Air Exchange of Hydrophobic Organic Chemicals, *Environ. Sci. and Technol.*, *25*, 866–871.

Prevedouros, K., K. Jones, and A. Sweetman (2004), European-Scale Modeling of Concentrations and Distribution of Polybrominated Diphenyl Ethers in the Pentabromodiphenyl Ether Product, *Environ. Sci. Technol.*, *38*(22), 5993–6001.

Rasmussen, J., D. Rowan, D. Lean, and J. Carey (1990), Food Chain Structure in Ontario Lakes determines PCB levels in Lake Trout (Salvelinus namaycush) and other Pelagic Fish, *Can. J. Fish.aquat. Sci.*, *47*, 2030–2038.

Reyes, C., M. Medina, C. Crespo-Hernandez, M. Cedeno, R. Arce, O. Rosario, D. Steffenson, I. Ivanov, M. Sigman, and R. Dabestani (2000), Photochemistry of pyrene on unactivated and activated silica surfaces, *Environ. Sci. Technol.*, *34*(3), 415–421.

Riederer, M. (1990), Estimating Partitioning and Transport of Organic Chemicals in the Foliage/Atmosphere System: Discussion of a Fugacity based Model, *Environ. Sci. and Technol.*, *24*, 829–837.

Ritter, L., K. Solomon, and J. Forget (1995), Persistent Organic Pollutants: An Assessment Report on DDT, Aldrin, Dieldrin, Endrin, Chlordane, Heptachlor, Hexachlorobenzene, Mirex and Toxaphene, Polychlorinated Biphenyls, and Dioxins and Furans., *Tech. rep.*, International Programme on Chemical Safety (IPCS) within the framework of the Inter Organization Programme for the Sound Management of Chemicals (IOMC).

Sabate, J., J. M. Bayona, and A. M. Solanas (2001), Photolysis of PAHs in Aqueous phase by UV irradiation, *Chemosphere*, *44*(2), 119–124.

Sabljić, A., H. Güsten, J. Schönherr, and M. Riederer (1990), Modelling Plant Uptake of Airborne Organic Chemicals. Plant Cuticle/Water Partitioning and Molecular Connectivity, *Environ. Sci. and Technol.*, *24*, 1321–1326.

Sapozhnikova, Y., O. Bawardi, and D. Schlenk (2004), Pesticides and PCBs in Sediments and Fish from the Salton Sea, California, USA, *Chemosphere*, *55*(6), 797–809.

Scheringer, M., and F. Wania (2003), *Handbook of Environmental Chemistry Vol. 3/O, Persistent Organic Pollutants*, chap. Multimedia Models for Global Transport and Fate of Persistent Organic Pollutants, pp. 237–269, Springer Verlag Berlin Heidelberg.

Scheringer, M., H. Heldt, and M. Stroebe (2001), Chemrange 1.0 - a Multimedia Transpoort Todel for Calculating Persistence and Spatial Range of Prganic Chemicals. Model - and Sofware Description ETHZ.

Schindler, D., K. Kidd, D. Muir, and W. Lockhart (1995), The Effects of Ecosystem Characteristics on Contaminant Distribution in Northern Freshwater Lakes, *Science of The Total Environment*, *160-161*, 1–17.

Schnock, G., and P. Duvigneaud (Eds.) (1971), *Productivity of forest ecosystems*, chap. Le bilan del l'eau dans l'écosystème forêt. Application à une chênaie mélangée de haute Belgique, pp. 41–42, UNESCO, Paris.

Schönherr, J., and M. Riederer (1989), Foliar Penetration and Accumulation of Organic Chemicals in Plant Cuticles, *M. Rev. Environ. Contam. Toxicol.*, *108*, 1–70.

Schwarzenbach, R. P., P. M. Gschwend, and D. M. Imboden (2003), *Environmental and Organic Chemistry*, 2nd edition, John Wiley, Hoboken, New Jersey.

Sehmel, P. (1980), Particle and Gas Deposition, a Review, *Atmos. Environ.*, *14*, 983–1011.

Seinfeld, J., and S. N. Pandis (1998), *Atmospheric Chemistry and Physics: From Air Pollution to Climate Change*, John Wiley & Sons, New York.

Selin, H., and N. Eckley (2003), Science, Politics, and Persistent Organic Pollutants: The Role of Scientific Assessments in International Environmental Cooperation, *International Environmental Agreements: Politics, Law and Economics*, *3*(1), 17–42.

Semeena, V., and G. Lammel (2005), The Significance of the Grasshopper Effect on the Atmospheric Distribution of Persistent Organic Substances, *Geophys. Res. Lett.*, *Vol. 32, No. 7*, 1–5.

Simonich, S., and R. A. Hites (2003), Organic pollutant accumulation in vegetation, *Environ. Sci. and Technol.*, *37*, 2350–2355.

Simonich, S. L., and R. A. Hites (1995), Global Distribution of Persistent Organochlorine Compounds, *Science*, *269*, 1851–1854.

Slinn, S. A., and W. G. N. Slinn (1980), Prediction for Particle Deposition on Natural Waters, *Atmospheric Environment*, *14*, 1013–1016.

Smit, A. A. M. F. R., F. van den Berg, and M. Leistra (1997), Estimation method for the volatilization of pesticides from fallow soil, *Environmentals planning bureau series Rep. 2*, DLO Winard Staring Centre, Wageningen.

Spivakovsky, C., J. Logan, S. A. Montzka, Y. J. Balkanski, M. Foremann-Fowler, D. B. A. Jones, L. W. Horowitz, A. C. Fusco, C. A. M. Brenninkmeijer, M. J. Prather, S. C. Wofsy, and M. B. McElroy (2000), Three-dimensional Climatological Distribution of Tropospheric OH: Update and Evaluation, *Journal of Geophysical Research*, *vol. 105, No d7*, 8931–8980.

Stern, G., C. Halsall, L. Barrie, D. Muir, P. Fellin, B. Rosenberg, F. Rovinsky, E. Kononov, and B. Pastuhov (1997), Polychlorinated Biphenyls in Arctic Air. 1. Temporal and Spatial Trends: 1992-1994, *Environ. Sci. Technol.*, *31*(12), 3619–3628.

Stow, J. (2005), Best Available Scientific Information on the Effects of Deposition of POPs, *Tech. rep.*, Northern Contaminants Program Indian and Northern Affairs Canada, submitted to the UNECE Convention on Long-range Transboundary Air Pollution Protocol on Persistent Organic Pollutants Task Force on POPs.

Strand, A., and O. Hov (1996), A Model Strategy for the Simulation of Chlorinated Hydrocarbon Distributions in the Global Environment, *Water, Air, & Soil Pollution*, *86*(1), 283–316.

Su, Y. (2005), The Forest Filter Effect for Semi-Volatile Organic Compounds and Implication for Long Range Transport, Ph.D. thesis, University of Toronto, Graduate Department of Chemical Engineering and Applied Chemistry, University of Toronto.

Su, Y., F. Wania, T. Harner, and Y. D. Lei (2007), Deposition of Polybrominated Diphenyl Ethers, Polychlorinated Biphenyls, and Polycyclic Aromatic Hydrocarbons to a Boreal Deciduous Forest, *Environ. Sci. Technol.*, *41*(2), 534–540, doi:10.1021/es0622047.

Tao, Z., and K. C. Hornbuckle (2001), Uptake of Polycyclic Aromatic Hydrocarbons (PAHS) by Broad Leaves: Analysis of Kinetic Limitations, *Water, Air, & Soil Pollution: Focus*, *1*(5 - 6), 275–283.

Theobald, N., H. Gaul, and U. Ziebarth (1996), Verteilung von organischen Schadstoffen in der Nordsee und angrenzenden Seegebieten, *Deutsche Hydrographische Zeitschrift*, *1*, 81–93.

Thomas, G., A. Sweetman, O. A.J., W.A., M. D., and K. Jones (1998), Air-Pasture Transfer of PCBs, *Environ. Sci. Technol.*, *32*, 936–942.

Thurman, E., and A. Cromwell (2000), Atmospheric Transport, Deposition, and Fate of Triazine Herbicides and Their Metabolites in Pristine Areas at Isle Royale National Park, *Environ. Sci. Technol.*, *34*(15), 3079–3085.

Tinker, P., and P. Nye (1980), *Solute Movement in the Soil-Root System*, – pp., Kolos Publishing House.

Tolls, J., and M. McLachlan (1994), Partitioning of Semivolatile Organic Compounds between Air and Lollum multiflorum (Welsh Ray Grass), *Environ. Sci. and Technol.*, *28*, 159–166.

Trapp, S., and M. Matthies (1995), Generic one Compartment Model for Uptake of Organic Chemicals by foliar Vegetation, *Environ. Sci. and Technol.*, *29*, 2333–2338.

Trapp, S., and C. McFarlane (1995), *InPlant Contamination: Modeling and Simulation of Organic Chemical Processes*, Lewis, Boca Raton.

Tremolada, P., D. Calamari, C. Gaggi, and E. Bacci (1993), Fingerprints of some Chlorinated Hydrocarbons in Plant Foliage from Africa, *Chemosphere*, *27*, 2235–2252.

Tremolada, P., D. Calamari, K. C. Jones, and V. Burnett (1996), A study of the spatial Distribution of PCBs in the UK atmosphere using Pine Needles, *Chemosphere*, *32*, 2189–2203.

Ueno, D., S. Takahashi, H. Tanaka, A. N. Subramanian, G. Fillmann, H. Nakata, P. K. S. Lam, J. Zheng, M. Muchtar, M. Prudente, K. H. Chung, and S. Tanabe (2003), Global Pollution Monitoring of PCBs and Organochlorine Pesticides Using Skipjack Tuna as a Bioindicator, *Archives of Environmental Contamination and Toxicology*, *45*(3), 378–389.

UNEP (2003a), Regionally based Assessment of Persistent Toxic Substances, Global Report, *Tech. rep.*, UNEP Chemicals, Geneva, Switzerland.

UNEP (2003b), The Hazardous Chemicals and Wastes Convention, http://www.pops.int/documents/background/hcwc.pdf.

Van Jaarsveld, J. A., W. A. J. Van Pul, and F. A. A. M. De Leeuw (1997), Modelling Transport and Deposition of Persistent Organic Pollutants in the European region, *Atmospheric Environment*, *31*(7), 1011–1024.

Vilanova, R., P. Fernandez, C. Martinez, and J. O. Grimalt (2001), Organochlorine Pollutants in Remote Mountain Lake Waters, *J Environ Qual*, *30*(4), 1286–1295.

Villa, S., M. Vighi, V. Maggi, A. Finizio, and E. Bolzacchini (2003), Historical Trends of Organochlorine Pesticides in an Alpine Glacier, *Journal of Atmospheric Chemistry*, *46*(3), 295–311.

Wang, D., J. Chen, Z. Xu, X. Qiao, and L. Huang (2005), Disappearance of Polycyclic Aromatic Hydrocarbons sorbed on Surfaces of Pine (Pinua thunbergii) Needles under Irradiation of Sunlight: Volatilization and Photolysis, *Atmospheric Environment*, *39*(25), 4583–4591.

Wania, F. (1999), Global Modeling of Polychlorinated Biphenyls (PCBs), *Tech. rep.*, WECC Wania Environmental Chemist Corp., 280, Simcoe Street, Suite 404, Toronto, Ontario, Canada M5T 2Y5.

Wania, F. (2003), Assessing the Potential of Persistent Organic Chemicals for Long-Range Transport and Accumulation in Polar Regions, *Environ. Sci. Technol.*, *37*(7), 1344–1351.

Wania, F., and D. Mackay (1993), Global Fractionation and Cold Condensation of low Volatility Organochlorine Compounds in Polar Regions, *Ambio*, *22*, 10–18.

Wania, F., and D. Mackay (1995), A Global Distribution Model for Persistent Organic Chemicals, *Science of The Total Environment*, *160-161*, 211–232.

Wania, F., and D. Mackay (1996), Tracking the Distribution of Persistent Organic Pollutants, *Environ. Sci. Technol.*, *30*, 390A– 396A.

Wania, F., and M. S. McLachlan (2001), Estimating the Influence of Forests on the Overall Fate of Semivolatile Organic Compounds Using a Multimedia Fate Model, *Environ. Sci. and Technol.*, *35*, 582–590.

Wania, F., D. Mackay, Y.-F. Li, and A. Bidleman, T.F. Strand (1999), Global Chemical Fate of Alpha-Hexachlorohexane, Part 1: Evaluation of a Global Distribution Model, *Environ. Toxicol. Chem.*, *7*, 1390–1399.

Wania, F., J. Persson, A. Di Guardo, and M. S. McLachlan (2000), CoZMo-POP A Fugacity-Based Multi-Compartmental Mass Balance Model of the Fate of Persistent Organic Pollutants in the Coastal Zone, *Tech. rep.*, WECC Wania Environmental Chemists Corp., 27 Wells Street, Toronto, Ontario, Canada M5R 1P1.

Weber, C. (2001), The Stockholm Convention (POPs Convention): An international, legally binding Regulation for the globale Limination of extremly dangerous Pollutants, *Tech. rep.*, Pesticide Action-Network (PAN Germany), Nernstweg 32, D-22765 Hamburg.

Wegmann, F., M. Scheringer, M. Möller, and K. Hungerbühler (2004), Influence of the Vegetation on the Environmental Partitioning of DDT in Two Global Multimedia Models, *Environ. Sci. Technol.*, *38*, 1505–1512.

Welke, B., K. Ettlinger, and M. Riederer (1998), Sorption of volatile organic chemicals in plant surfaces, *Environ. Sci. and Technol.*, *32*, 1099–1104.

Wesely, M. (1989), Parametrizations of Surface Resistance to Gaseous Dry Deposition in Regional Scale Numerical Models, *Atmospheric Environment*, *23*, 1293–1304.

Wesely, M. L., and B. B. Hicks (1977), Some Factors that effect the Deposition Rates of Sulphur Dioxine and similar Gases on Vegetation, *J. Air Pollut. Control. Assoc.*, *27*, 1110–ff.

WHO (2005a), Fourth WHO-Coordinated Survey of Human Milk for Persistent Organic Pollutants A Protocol for Collection, Handling and Analysis of Samples at the Country Level.

WHO (2005b), Fourth WHO-Coordinated Survey of Human Milk for Persistent Organic Pollutants A Protocol for Collection, Handling and Analysis of Samples at the Country Level protocol,WHO, Geneva, Switzerland.

Wild, E., J. Dent, G. Thomas, and K. Jones (2005), Real-Time Visualization and Quantification of PAH Photodegradation on and within Plant Leaves, *Environ. Sci. Technol.*, *39*(1), 268–273.

Wild, E., J. Dent, G. Thomas, and K. Jones (2006), Visualizing the Air-to-Leaf Transfer and Within-Leaf Movement and Distribution of Phenanthrene: Further Studies Utilizing a Two-Photon Excitation Microscopy, *Environ. Sci. Technol.*, *40*(1), 907–916.

Yoda, K., T. Kira, Y. Ono, and T. Hosokawa (Eds.) (1978), *Biological Production in a warm-temperate Evergreen Oak Forest of Japan*, chap. Light climate within the forest, pp. 46–54, JIBP, Tokyo.

Zepp, R. G., P. Schlotzhauer, P. Jones, and P. Leber (Eds.) (1979), *Photoreactivity of selected Aromatic Hydrocarbons in Water*, pp. 141–158, Ann Arbor Science Publishers Inc., Ann Arbor, MI.

Acknowledgements

Several people helped me to save this thesis. First I would like to thank all of my family for their unconditional support in these adventurous years here in Hamburg. Especially during the hard times without any supervisor and no financial backing I stressed their patience to the maximum limit and though they never gave me up. I am gratefull to Prof. Dr. Hartmut Grassl, Dr. Christian Reick, Dr. Thomas Raddatz, Dr. Sebastian Rast and Prof. Dr. Claussen who gave me the scientific and financial support to finish this document in the last nine months. I also would like to mention Dr. Yushan Su (Environment Canada) and Prof. Dr. Frank Wania (University of Toronto, Scarborough) for the short but intensive scientific exchange. I enjoyed being embedded in a relaxed and human climate here in the Land in the Earth System Group at the Max-Planck-Institute and would like to thank all my working colleagues for the encouragement during difficult periods. Last but not least I should mention all my friends who made life beside work agreeable. I especially would like to thank those who harboured me during the constrained times, helped me to finish this work and were there whenever I needed them.

Die gesamten Veröffentlichungen in der Publikationsreihe des MPI-M
„Berichte zur Erdsystemforschung“,
„Reports on Earth System Science“,
ISSN 1614-1199

sind über die Internetseiten des Max-Planck-Instituts für Meteorologie erhältlich:

http://www.mpimet.mpg.de/wissenschaft/publikationen.html



ISSN 1614-1199